STUDY OF THE REACTIVITY AND SPECTROSCOPIC PROPERTIES OF COMPOUNDS WITH METAL-METAL BONDS

A thesis submitted to the

Victoria University of Manchester

for the degree of

DOCTOR OF PHILOSOPHY

in the Faculty of Science

by

GILLIAN PIMBLETT

Department of Chemistry,
University of Manchester,
Manchester,
M13 9PL

September 1986.

To

My Parents

Abstract

The compounds $[M_2(O_2CMe)_2(NCMe)_6][BF_4]_2$ (where M = Mo and Rh) have been prepared from the parent tetra-acetate compounds, and have been fully characterized and their structures determined by X-ray crystallography. Structural and spectroscopic comparisons have been made between these two related compounds. Where M = Mo the corresponding formate complex has been prepared and fully characterized and shows very similar behaviour to its acetate analogue. For both M = Mo and Rh, the chemistry has been extended to replacing the acetonitrile groups with the more bulky trimethylacetonitrile, producing $[M_2(O_2CMe)_2(NCCMe_3)_n][BF_4]_2$ (M = Mo, n = 5; M = Rh, n = 6) compounds. These have been fully characterized and have been shown to resemble their MeCN analogues.

The reactivity of $[Mo_2(O_2CMe)_2(NCMe)_6][BF_4]_2$ and its formate analogue towards Na mhp and dppm have been investigated and the products $[Mo_2(O_2CH)_2(mhp)_2]$ and the new compound $[Mo_2(O_2CMe)_2(NCMe)_2(dppm)][BF_4]_2$ have been characterized. ^{95}Mo n.m.r. spectra have been recorded of the new compounds $[Mo_2(O_2CMe)_2(NCMe)_6][BF_4]_2$, $[Mo_2(O_2CMe)_2(NCCMe_3)_5][BF_4]_2$ and $[Mo_2(O_2CMe)_2(NCMe)_2(dppm)][BF_4]_2$.

The reactivity of $[Rh_2(O_2CMe)_2(NCMe)_6][BF_4]_2$ has also been investigated, producing a number of axially substituted compounds, including the pyridine adduct $[Rh_2(O_2CMe)_2(NCMe)_4(py)_2][BF_4]_2$, which has had its structure determined by X-ray crystallography.

Examples of oxidative and reductive cleavage of the rhodium-rhodium single bond have been shown with the reagents NaS_2CNEt_2 and PPh_3 respectively. With the latter reagent the new compound $[Rh(PPh_3)_3(NCMe)][BF_4]$ has been fully characterized and its structure determined by X-ray crystallography. Catalytic studies have been performed on this rhodium monomer.

BIOGRAPHY

The author obtained a First class honours B.Sc. degree in Chemistry at the University of Manchester in 1982. Since that time she has been engaged in research in the Department of Chemistry under the supervision of Professor C.D. Garner. The results of this research are embodied in this thesis.

No portion of the work referred to in this thesis has been submitted in support of an application for another degree or qualification of this or any other university or other institution of learning.

ACKNOWLEDGEMENTS

I would like to express my thanks to my supervisor, Professor C.D. Garner, for his helpful advice, guidance and encouragement during my time at Manchester.

Thanks are also due to the following:

Mr. M. Hart and staff of the Microanalytical Department of this University.

The staff and technicians of the Chemistry Department, especially Christine.

Dr. D. Waddan and Dr. D. Collison for their advice and helpful discussions.

Dr. W. Clegg for performing the X-ray structure determinations.

Dr. J. Mason, Dr. R.A. Grieves, Dr. E.M. Curzon, and Dr. Haworth for their help in recording the ^{95}Mo n.m.r. spectra.

Mrs. A. Roberts for her patience in typing this thesis.

My colleagues at Manchester University, especially Ian, Tim, Stuart, and Philippe for their friendship during my time at Manchester.

Dr. J.M. Charnock for his patience in the proof reading of this thesis and for being a good friend.

My parents for their support, encouragement and patience during my research and the writing of this thesis.

The S.E.R.C. for their financial support.

CONTENTS

CHAPTER 1

AN INTRODUCTION TO METAL-METAL BONDS

1.1 A general introduction to metal-metal bonds

To scan the history of metal-metal bonds in dimeric systems, it is necessary to go back as far as 1844 when the very first quadruply bonded compound, between a pair of chromium atoms, was reported.[1] The method of preparation, the properties, and the analytical data leave no doubt that the compound Eugene Peligot prepared is $[Cr_2(O_2CMe)_4(H_2O)_2]$. Yet it was 120 years later that the existence of quadruple bonds was first recognized.[2]

However, such non-Wernerian chemistry did not remain at a total standstill during the intervening years. Werner recognized the existence of polynuclear complexes and, indeed, he wrote a number of papers on that subject[3] but the compounds he dealt with were regarded, quite rightly, as simply the result of joining two or more mononuclear complexes through shared ligand atoms. No direct M-M interactions of any type were considered.

In 1907, the compound "$TaCl_2.2H_2O$"[4] (later correctly formulated[5] as $Ta_6Cl_{14}.7H_2O$) was reported which appeared anomalous from a Wernerian point of view. During the 1920's several lower halide compounds of molybdenum were discovered[6] which also did not fit into the established pattern and subsequently were assigned incorrect structures.

It was only with the advent of X-ray crystallography and its evolution into a tool capable of handling reasonably large structures that the existence of non-Wernerian transition metal chemistry could be recognized with certainty. In 1946, C. Brosset provided the first such experimental results[7] showing that the lower chlorides of molybdenum contain octahedral groups of metal atoms with Mo-Mo distances even shorter ($\sim$2.6 Å) than those in metallic molybdenum (2.725 Å).

In 1950 an X-ray diffraction experiment, carried out on aqueous solutions, showed that $Ta_6Cl_{14}.7H_2O$ and its bromide analogue also contain octahedral groups of metal atoms with rather short M-M distances.[8] Neither of these observations led to further research activity. However, it was not until 1963 that attention was effectively focused on non-Wernerian co-ordination compounds. The "$ReCl_4^-$" anion was seen to contain triangular Re_3 groups[9,10] with a Re-Re distance (2.47 Å) much shorter than those in metallic rhenium. A conclusion was reached that the rhenium atoms are joined by a set of three Re-Re double bonds,[9] the first M-M multiple bonds discussed explicitly in the literature.[11] Thus, by the middle of 1963, studies on this triangular Re_3 cluster, now recognised as $[Re_3Cl_{12}]^{3-}$, had led to the recognition that this cluster was the essential stereoelectronic feature of most of the chemistry of rhenium(III). Both the chloride and bromide of Re^{III} had been shown to contain the Re_3 clusters[11,12] but the preparation of these halides, as starting materials, was tedious and time consuming. Reduction in aqueous solution of the common $[ReO_4]^-$ ion was hoped to provide a much more efficient method of production of $[Re_3Cl_{12}]^{3-}$. Using concentrated aqueous HCl as the reaction medium and hypophosphorous acid as the reducing agent, an intense blue solution formed from which a solid of composition $CsReCl_4$ could be isolated.[11] At that same time a report emerged from Russia[13] stating that on reduction of $[ReO_4]^-$ in HCl by hydrogen gas under pressure, a dark blue-green product of formula K_2ReCl_4 was obtained. Eventually it was shown that this substance did not have the composition K_2ReCl_4 but actually it was $KReCl_4.H_2O$,[14] similar to the product $CsReCl_4$ proposed by Cotton *et al*. Crystals of "$KReCl_4$" were obtained and an X-ray diffraction study was initiated. Prior to this Kotel'nikova and

Tronev, in 1958, had observed the formation of a grey-green material,[15] formulated as "(pyH)$HReCl_4$" upon addition of pyridine to an acetone solution of "$H_2ReCl_4.2H_2O$" acidified with concentrated HCl. In 1963 another article was published[16] dealing with the crystal structure determination of "(pyH)$HReCl_4$" which stated:

"Eight chlorine atoms constitute a square prism with two rhenium atoms lying within the prism, whereby each rhenium atom is surrounded by four neighbouring chlorine atoms ... the rhenium atom has for its neighbours one rhenium atom, at a distance of 2.22 Å and four chlorine atoms at a distance of 2.43 Å. As a result, the dimeric ion $[Re_2Cl_8]^{4-}$ is generated."[16]

This was the first crystal structure of the quadruply bonded $[Re_2Cl_8]^{2-}$ ion and a better refinement was later achieved by Cotton and Harris[17] and this structure is shown in Fig.1.1. However, much remained to be discussed, namely the stereochemistry of the anion and the short Re-Re distance. Alongside their crystal structure, Kotel'nikova and Tronev[15] noted that the Re-Re distance (2.22 Å) was less than that in the metal (2.76 Å), indicating that the valence electrons of rhenium take part in the formation of the Re-Re bond, and that this may offer an explanation for the diamagnetism of this compound.

In 1964, Cotton first put forward the proposal of the existence of a quadruple bond.[17] He stated that each rhenium atom uses a set of s, p_x, p_y and $d_{x^2-y^2}$ hybrid orbitals to form its four Re-Cl bonds, leaving the other valence shell orbitals of each rhenium atom to be used for metal-metal bonding

(i) each Re d_{z^2}-p_z orbitals overlap to form a σ-bond

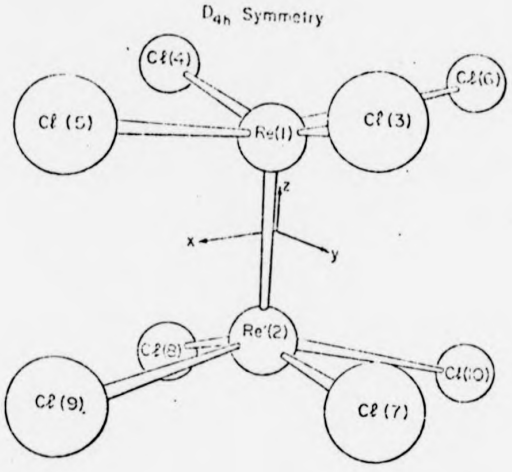

FIG.1.1 Crystal structure of $[Re_2Cl_8]^{2-}$

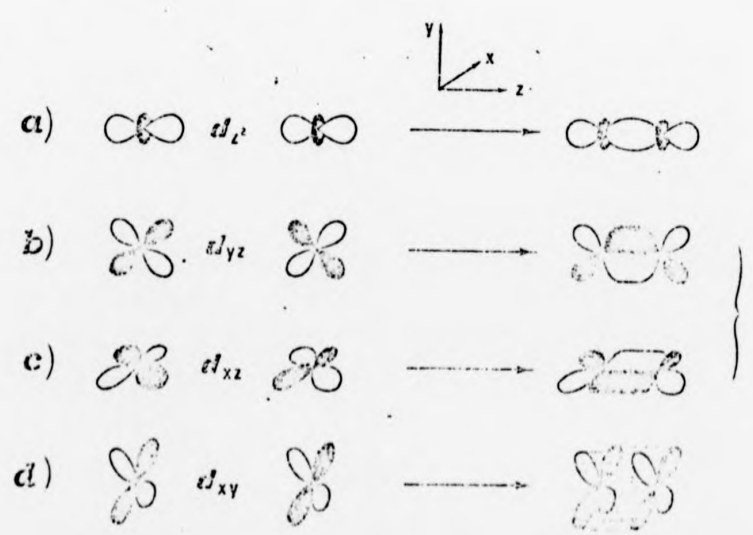

FIG.1.2

(ii) the d_{xz}, d_{yz} orbitals are used to form two π-bonds, and

(iii) the remaining d_{xy} orbitals overlap, in the eclipsed configuration, to give a δ-bond.

The σ-bond was proposed to be the strongest with the π-bond having a reasonable strength. Neither of these bonds imposes any restriction on rotation about Re-Re axis. Only the presence of the δ-bond dictates the eclipsed structure due to the overlap of the d_{xy} orbitals, estimated to be about one third of that of one of the π-overlaps. The electronic configuration of the dirhenium(III) centre results in the metal-metal orbitals filling as $\sigma^2\pi^4\delta^2$, and thus the diamagnetism and molecular conformation can be explained.[17,18] The positive bonding σ, π, and δ overlaps of d orbitals are shown in Fig.1.2. Shortly afterwards a full paper was published[18] to further detail this proposal correlating metal-metal distances with bond orders from < 1 to 4.

This was the start of what was to become an intriguing subject on its own; that of the study of bonds between metal atoms. The metals exhibiting properties within the structural patterns X_5MMX_5, X_4MMX_4, and X_3MMX_3, now extend from rhenium to molybdenum, technetium to chromium, the mystery uncovered after 120 years; tungsten, ruthenium, rhodium, osmium, platinum and vanadium.[11] They constitute bond orders of 1, 2, 2.5, 3, 3.5, and 4, and the metals, with their respective bond orders are shown below.[11]

V	Cr
3	4

Mo	Tc	Ru	Rh
3,3.5,4	3.5*,4	2*,2.5*,3*	1*

W	Re	Os	Pt
3,3.5,4	3,3*,3.5*,4	3*	1*

* denotes bond orders obtained when electrons in excess of eight occupy antibonding orbitals.

1.2 Types of ligands co-ordinated to metals in multiply bonded compounds

Unidentate Ligands

Common unidentate ligands include F^-,[19] Cl^-,[18,20] Br^-,[21] I^-,[22] and SCN^- and the latter is always found co-ordinated through the nitrogen.[23] Neutral unidentate ligands include nitriles,[24,25] water,[26] pyridine and substituted pyridines,[24] and other amines and phosphines,[24,27] both monodentate and bidentate. Organo-groups such

as methyl,[28] ethyl,[29] $Me_3SiCH_2^-$,[29] Me_3SiCH^{2-},[30] and allyl species[28] are also known. Phosphides that can act both as unidentate ligands and as R_2P^- bridging ligands are also known.[31] For the triply bonded species of the type $X_3M{\equiv}MX_3$ (M = Mo, W) the dialkylamido groups Me_2N^- and Et_2N^- [32,33] are of considerable importance. The alkoxide groups, with bulky alkyls, are also important, primarily in these $X_3M{\equiv}MX_3$ compounds,[34,35] but occasionally occur elsewhere, recently being found supporting quadruple bonds.[36]

The type of unidentate ligand that characteristically does not occur in quadruply bonded M-M complexes, and only rarely in conjunction with other M-M multiple bonds, is the strongly π-acid type, such as isocyanides, CO and NO. As a rule, the attempt to introduce such ligands results in M-M bond cleavage,[37,38] although this can be advantageous as a good preparative route to mononuclear complexes of such ligands.[37] However, careful control of reaction conditions has recently provided the first examples of quadruply bonded molybdenum(II)[39] and multiply bonded dirhenium(II) complexes[40,41] with isocyanide ligands.

Bridging Ligands

One of the most common and important ligands for multiply bonded M-M systems is that whose essential stereoelectronic characteristics, which may be represented in the abstract as

are

1. The ligand is bidentate.

2. Its preferred, or only, conformation is such that X and Y have their donor orbitals directed along approximately parallel lines.
3. The distance between X and Y is in the approximate range 2.0-2.5 Å.

These ligands do not favour chelation of a single metal but their ability to bridge two metal atoms connected by a multiple bond makes them especially suitable for promoting the formation and stabilization of M-M bonds of orders 1 to 4.

Dianions such as sulphate,[42] HPO_4^{2-},[43] $P_2O_5H_2^{2-}$,[44] and CO_3^{2-} [45] are the only important representatives to date.

Mono-anionic ligands constitute the most important set of ligands and they include carboxylato or carboxylato-like anions (e.g. dithiocarboxylates and carbamates) A-F, a number of similar anions with RN in place of one oxygen atom G or both oxygen atoms H of the carboxyl groups, and the triazinido ions I.

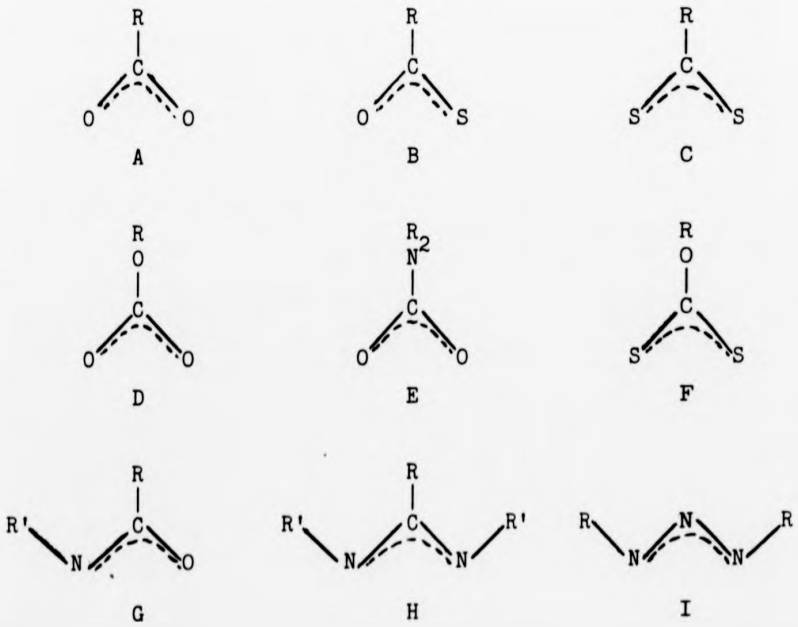

The properties of the carboxylato ligands can be varied in many ways. Its basicity can be altered by changing R from CMe_3 at one extreme to CF_3 at the other. Its steric properties can be changed from those with R=H to those with R = 9-anthracenyl or 2-phenylphenyl. R groups can also be amino acids and peptides, the former giving stable, water-soluble compounds, such as $[Mo_2(glycyl)_4][SO_4]_2$.[11]

A major part of this set of anionic ligands are those containing ring systems. These are shown below. DMP is found in multiply bonded vanadium compounds, bridging not only as a three-atom but also as a five-atom chain. Neutral ligands of this type include diphosphines and arsines.

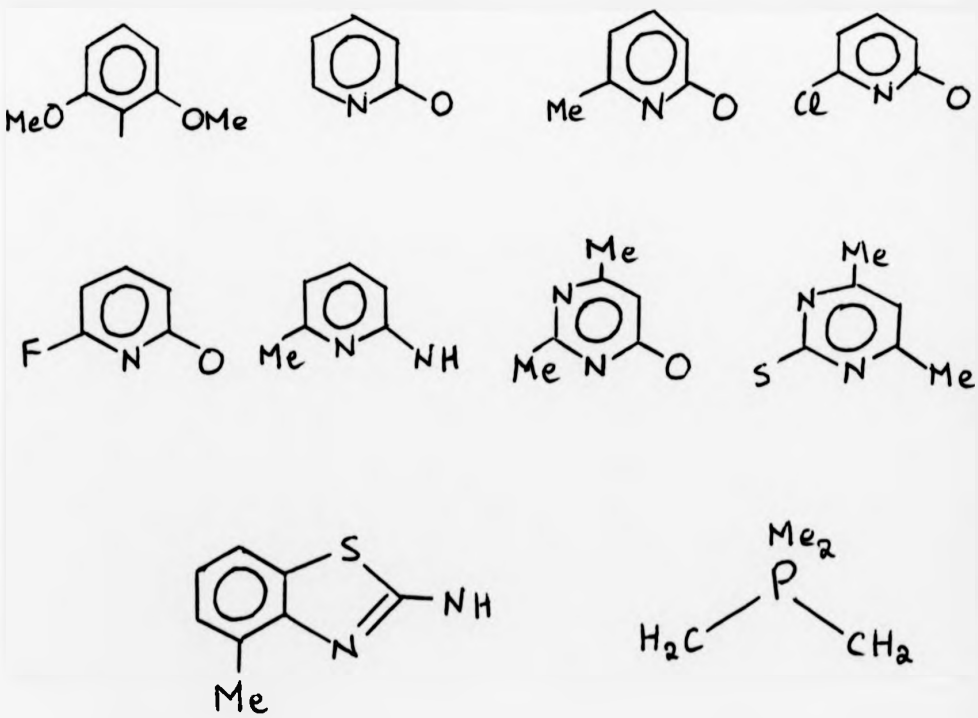

Other Chelating Ligands

A number of chelate ligands have been introduced into the co-ordination spheres of M_2^{n+} species. These include ethylenediamine,[46] 1,2-bis(diphenylphosphino) ethane,[47] pyrazolylborates,[48] β-diketonates,[49] phenanthroline,[50] and pynp.[51] There is also some evidence, although not crystallographic, that ligands such as 1,2-bis(dimethylphosphino) ethane[24] and arphos[47] can act as chelating ligands.

1.3 Quadruple Bonds

The next element, after rhenium, that was shown to form a quadruple bond was molybdenum, in the acetate $[Mo_2(O_2CMe)_4]$, in 1965.[52] It was not until 1969, however, that Mo_2^{4+} chemistry began to develop; the preparation of salts of the $[Mo_2Cl_8]^{4-}$ [53] anion led to a surge of research work[11] so that today several hundred Mo_2^{4+} compounds are known and probably about one hundred have been structurally characterised by X-ray crystallography.

Also, the chemistry of Re-Re quadruple bonds has developed systematically, and several compounds with Tc-Tc quadruple bonds are known, although the small number exemplifies the difficulties in preparation (see later).

The structure of $[Cr_2(C_3H_5)_4]$ was reported in 1967[54] and that of $[Cr_2(Me)_8]^{4-}$ [55] in 1970 but it was only with the determination structure of $[Cr_2(O_2CMe)_4(H_2O)_2]$ in 1970[56] that the nature of the metal-metal bonding was discussed. With the discovery in 1977 of the first "supershort" Cr-Cr bond (<1.9 Å)[57] a new chapter of extensive systematic chemistry of quadruple Cr-Cr bonds was begun.

The quadruply bonded W-W compounds proved the most elusive. While $Mo(CO)_6$ reacted with acetic acid to give $[Mo_2(O_2CMe)_4]$[58] $W(CO)_6$ is much more sensitive to acids, being oxidised to W^{x+} (where $x > 2$) instead of forming W^{II} quadruply bonded W_2^{4+} units.[59] Then in 1977 the first such bond, in $[W_2Me_8]^{4-}$ was reported which was highly unstable.[60] In 1978 the air-stable $[W_2(mhp)_4]$ was produced[61] and the number of such dimers has been growing steadily ever since.

The various compounds containing rhenium, technetium, chromium, molybdenum and tungsten quadruple bonds have been well reviewed[11,62,63] but the more recent and interesting advances will be discussed here for each metal.

1.4 Rhenium

The synthesis of the tetra-n-butylammonium salt $[Bu_4N]_2[Re_2Cl_8]$ by the hypophosphorous acid reaction of $[ReO_4]^-$ in aqueous HCl still remains one of the most convenient routes to this complex,[64] although slight modifications to the original procedure have been recommended.[65] Recently a high yield preparation of $[Bu^n_4N]_2[Re_2Cl_8]$ from perrhenate has been reported. $[Bu^n_4N][ReO_4]$ is refluxed with PhCOCl after which an HCl(g) saturated solution of $[Bu^n_4N]Br$ in ethanol is added to produce analytically pure crystals of $[Re_2Cl_8]^{2-}$ in a 92% yield.[66]

The other three octahalodirhenate(III) anions (F^-, Br^-, I^-) are all known. $[Re_2F_8]^{2-}$ has been prepared by reacting an excess of $[Bu^n_4N]F.3H_2O$ with $[Bu^n_4N]_2[Re_2Cl_8]$ in dichloromethane.[19] $Cs_2[Re_2Br_8]$ can be prepared by the hypophosphorous acid reduction of $K[ReO_4]$ in 48% aqueous HBr with CsBr.[67] A crystal structure determination has shown the anion to have a Re-Re bond length of

2.228(4) Å and the eclipsed rotational configuration.[67]

The reactions of these octahalodirhenate(III) anions fall into three categories:[11]

(a) substitution reactions, where the Re_2^{6+} core remains intact,

(b) redox reactions, where a Re-Re bond remains but of a lower order than four, and

(c) reactions where the Re-Re bond is totally cleaved, and these are well described elsewhere.[11]

During the study in which the preparative routes to the $[Re_2Cl_8]^{2-}$ and $[Re_2Br_8]^{2-}$ anions were first established it was shown that the $[Bu^n_4N]_4[Re_2Cl_8]$ salt could be converted to the orange carboxylate bridged dimers $[Re_2(O_2CR)_4Cl_2]$ (R = Me or Et) on reaction with a mixture of the appropriate carboxylic acid and its anhydride.[68] The carboxylate complexes $[Re_2(O_2CR)_4X_2]$ represent the maximum extent to which substitution of the halide ligands of the parent $[Re_2X_8]^{2-}$ anions may occur. The dihydrates $[Re_2(O_2CMe)_2X_4].2H_2O$ (X = Cl or Br) and the compounds $[Re_2(O_2CR)_3Cl_3]$ are known[69,70] and can be synthesised easily using $[Re_2X_8]^{2-}$ as the starting materials.

Recently, $Re_2Cl_4(O_2CMe)_2L_2$ (L = H_2O or py) has been shown to react with PPh_3 in ethanol to give the quadruply bonded complex $[Re_2Cl_4(OEt)_2(PPh_3)_2]$ (Re-Re = 2.231(1) Å). This, however, is a mixed valence Re^{IV}-Re^{II} dimer with a dative Re≡Re bond.[71] Quantitative theoretical calculations performed by the SCF-Xα-SW method on the $[Re_2Cl_8]^{2-}$ ion confirmed the primacy of metal d orbitals in the formation of quadruple bonds.[72] The pattern of orbitals as the energy decreases from the LUMO is $2b_{1u}(\delta^*) > 2b_{2g}(\delta) > 5e_u(\pi)$

with a considerable gap from the δ^* orbital to the next lowest antibonding orbital. Below the $\pi(e_u)$ orbital is the a_{1g} orbital, a_{1g} being the symmetry required to play a role in M-M σ-bonding. In $[Re_2Cl_8]^{2-}$ the highest filled a_{1g} orbital has 34% metal character being more involved in Re-Cl bonding than Re-Re bonding. The main M-M σ-bonding is the next a_{1g} orbital down, which has 62% metal character.

Recently the electronic structure of $[Re_2Cl_8]^{2-}$ was reinvestigated by the SCF-Xα-SW method which essentially agreed with the earlier calculations but the inclusion of corrections for inner-shell and valence relativistic effects caused appreciable shifts in the energy levels. The single crystal spectrum of $[Re_2Cl_8]^{2-}$ was reassigned on this basis.[73]

For the configuration $\sigma^2\pi^4\delta^2$ the lowest energy electronic transition should be the one in which an electron goes from the δ to δ^* orbital as recent theoretical calculations have indicated.[73] As an optical transition this is electric dipole-allowed in polarization parallel to the metal-metal bond axis. A local symmetry of D_{4h} applies to a number of these dimeric complexes. Under this symmetry the spin-allowed $\delta \rightarrow \delta^*$ transition can be characterized as $^1A_{1g} \rightarrow {}^1A_{2u}$ ($b_{1g} \rightarrow b_{2u}$). However, in all cases the intensities of these transitions is low, considering that the transitions are fully allowed.[11] It has been observed that the d orbital overlap forming the δ bond is quite small and as Mulliken showed, oscillator strength in a transition of this nature is approximately proportional to the square of the overlap integral.[74] Thus, low intensity is a straightforward consequence of the weakness of the δ bond. The transition, also, is always observed at a far higher energy than that calculated and this difficulty is now

recognised to have its origin in the electron correlation phenomenon, the effect of which is enormously increased because of the weakness of the δ bond.[11]

Since, until recently, the reliability of theoretical predictions of the intensities and positions of $\delta \rightarrow \delta^*$ transitions has been somewhat questionable, the assignment of observed bands to this transition has depended on experimental criteria. In several cases studies of the band intensity at room temperature and at ca. 5 K have shown little or no temperature dependence, thus supporting the assignment as an orbitally allowed (as opposed to vibronically activated) transition. Single crystal spectra with polarized light can also determine whether the band exhibits the correct polarization which, for a $\delta \rightarrow \delta^*$ band, should be along the molecular axis only (z polarization) i.e. along the metal-metal bond.[11]

For the $[Re_2Cl_8]^{2-}$ ion, the $\delta \rightarrow \delta^*$ transition contains two progressions, one in the ν(Re-Re) vibration, the other involving the totally symmetric Re-Cl stretching and Re-Re-Cl bending vibration.[75] Recently for both $[Bu^n_4N]_2[Re_2Cl_8]$ and $[Bu^n_4N]_2[Re_2Br_8]$, highly resolved vibrational structure in the polarized crystal spectra were recorded for the first observed electronic band at about 714 nm. The Franck-Condon progressions were resolved for both the major and minor components of each compound with intensities consistent with the $\delta \rightarrow \delta^*$, $^1A_{1g} \rightarrow {}^1A_{2u}$ assignment.[76]

One of the only single crystal polarized absorption spectra reported for tetrakis-(carboxylato)-bridged rhenium(III) complexes recently reported a peak at 485 nm with molecular z polarization assigned as the electric-dipole-allowed $^1A_{1g} \rightarrow {}^1A_{2u}$ ($\delta \rightarrow \delta^*$) transition.[77]

1.5 Technetium

The first compounds containing a Tc-Tc quadruple bond were reported in 1977[78] yet for many years before that, salts of the $[Tc_2Cl_8]^{3-}$ ion, prepared by reduction of Tc(IV) ions with zinc and HCl acid, having the same non-bridged eclipsed M_2Cl_8 structure as $[Re_2Cl_8]^{2-}$ had been studied.[79] The very short Tc-Tc distance of 2.13 Å in $[Tc_2Cl_8]^{3-}$ is indicative of a very strong M-M bond[80] and the paramagnetism is consistent with the anion possessing a $\sigma^2\pi^4\delta^2\delta^*$ electronic configuration.[81] As Re_2^{5+} derivatives were known, for example $[Re_2Cl_5(PR_3)_3]$[82] and $[Re_2Cl_4(PR_3)_4]^+$,[83] the indications were that $[Tc_2Cl_8]^{3-}$ contained a Tc-Tc bond of order 3.5. In 1975 it was shown that in mixtures of HCl and ethanol $[Tc_2Cl_8]^{3-}$ is reversibly oxidised to $[Tc_2Cl_8]^{2-}$ at +0.14 V versus SCE, which was diamagnetic and had a lifetime in solution of at least 5 minutes.[84] However, it was not until 1977 that Schwochau *et al.*[78] reported the isolation of $[Bu_4N]_2[Tc_2Cl_8]$, prepared by the hypophosphorous acid reduction of $[^{99}TcO_4]^-$ in HCl, followed by addition of $[Bu_4N]Cl$.[78]

In 1980, Preetz and Peters reported a procedure for isolation of $[Bu_4N]_2[Tc_2Cl_8]$ by reducing $[NH_4]_2[TcCl_6]$ with zinc in aq.HCl. Both $[Bu_4N]_3[Tc_2Cl_8]$ and $[Bu_4N]_2[Tc_2Cl_8]$ were isolated from this procedure and all the data support the proposal that $[Tc_2X_8]^{2-}$ had been isolated.[85]

In 1981, the crystal structure of $[Bu_4N]_2[Tc_2Cl_8]$[86] was reported and the Tc-Tc bond length shown to be 2.142 Å. The following year a structure determination on $Y[Tc_2Cl_8].9H_2O$ gave the Tc-Tc bond length as 2.105(1) Å.[87] This was certainly not the expected change in bond order on progressing from a quadruple to a triple bond but it was

proposed that the change from $[Tc_2Cl_8]^{3-}$ to $[Tc_2Cl_8]^{2-}$ not only raises the bond order, but also causes a contraction of the valence orbitals of the metal atoms and this has the effect of lengthening the bond because it weakens the σ and π overlaps.[88]

The pivalate structure $[Tc_2(O_2CCMe_3)_4Cl_2]$ has also been obtained with a long Tc-Tc bond length of 2.192(2) Å.[89] This will also be affected by orbital contraction but a further explanation lies in the short Tc-Cl bonds (2.408(4) Å) since the strengths of M-M multiple bonds often show an inverse relationship to the $M-L_{ax}$ bond strengths.[11]

In 1982 Nefedov et al. reported shorter Tc-Tc bond lengths in the compounds $[Tc_2(O_2CMe)_4Cl]$ and $[Tc_2(O_2CMe)_4Cl_2]^-$ than $[Tc_2(O_2CCMe_3)_4Cl_2]$ and postulated the presence of bonds of order 4.5 in the first two compounds.[90] However, no discussion on the relative expansions and contractions of the valence orbitals was presented.

1.6 Chromium

The largest known and the most common quadruply bonded chromium compounds are the tetracarboxylates. Since Peligot prepared the first such compound in 1844,[1] a large number of additional compounds has been made, but the most significant advance has been the structural characterisation of many of these compounds since 1970.[11]

Virtually all of these $[Cr_2(O_2CR)_4L_2]$ and $[Cr_2(O_2CR)_4]$ compounds have the types of structure shown in Fig.1.3. The axial positions are filled either by separate ligands L or by the oxygen atoms of other $[Cr_2(O_2CR)_4]$ molecules.[11]

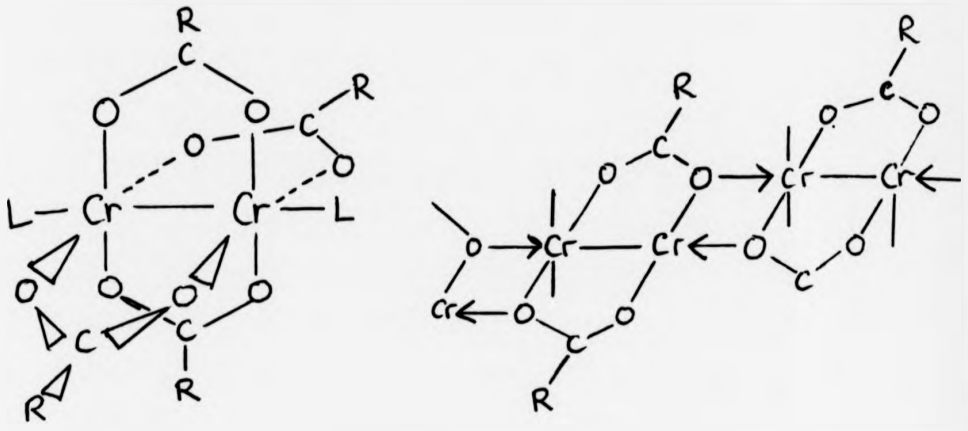

Figure 1.3

The hydrated acetate can be prepared by the addition of $Na[O_2CMe]$ to a fairly dilute aqueous solution of $CrCl_2$, and is isolated immediately as a precipitate[1,91]

$$2Cr^{2+}(aq) + 4MeCO_2^- + 2H_2O \longrightarrow [Cr_2(O_2CMe)_4(H_2O)_2]$$

The tetra-acetate has served as a starting material in the preparation of many other quadruply bonded dichromium compounds. Many of the dichromium tetra-carboxylates have been structurally characterized and the majority show axial co-ordination.[11] Although a number of unsolvated compounds have been reported, only a very few have been studied structurally. The drive to isolate such compounds comes from the desire to know how long the Cr-Cr bond would be in an isolated $[Cr_2(O_2CR)_4]$ molecule. With the R group 2-phenylphenyl, in each of two $[Cr_2(O_2C\,biph)_4]$ molecules, all phenyl groups are orientated to one end and the unencumbered ends of the two $[Cr_2(O_2C\,biph)_4]$ molecules have united to produce a dimer.[92]

The volatility of $[Cr_2(O_2CR)_4L_2]$ compounds and the stability in the vapour phase has allowed the mass spectra of a number of these compounds to be studied.[93]

The range of bond lengths in these compounds progresses from 2.214(1) Å in the $[Cr_2(CO_3)_4(H_2O)_2]^{4-}$ [94] ion to 2.541(1) Å in $[Cr_2(O_2CCF_3)_4(Et_2O)_2]$.[95] Although there is a significant variation in Mo-Mo and Re-Re quadruple bond lengths (quadruple Mo_2^{4+} dimers will be discussed later), the ranges covered by these bonds for all kinds of diverse ligands are much smaller, only about 0.13 and 0.08 Å respectively.[11]

Many studies have been made on the variation of the Cr-Cr distance in $[Cr_2(O_2CR)_4L_2]$ compounds with (a) $Cr\text{-}L_{(axial)}$ distance[96,97,98] and (b) changes in the bridging ligand[99,100,101] but no definite relationship has as yet been established.

Many quadruply bonded chromium dimers that lack axial attachments fall into the "supershort" range, i.e. compounds with Cr-Cr bond lengths $d_{Cr-Cr} < 1.90$ Å and such compounds can generally be characterized as having ligands derived from weak acids having the axial positions blocked as a result of intramolecular hindrance.[11]

A comparison of these "supershort" bonds with other short bonds can be made using the "formal shortness ratio" FSR, defined for a bond A-B

$$FSR_{AB} = \frac{D_{A-B}}{R_1^A + R_1^B}$$

D_{A-B} = length of bond A-B

R_1^X = Pauling's atomic radius for atom X

The FSR of the Cr≡Cr bond in $Cr_2(2\text{-MeO-5-MeC}_6H_3)_4$[102] is 0.767, that of the C≡C bond and N≡N bond in HCCH and N_2, respectively, is 0.783 and 0.786,[11] and that of the Mo≡Mo bond in $[Mo_2[(2\text{-pyridyl})NCMeO]_4]$[103] is 0.807 making the bond in $[Cr_2(2\text{-MeO-5-MeC}_6H_3)_4]$ the shortest homonuclear bond known.

1.7 Molybdenum

The largest group of compounds containing quadruple bonds are those formed by molybdenum. Soon after the anion $[Re_2Cl_8]^{2-}$ was recognised to contain a quadruple bond, the correct structure of $[Mo_2(O_2CMe)_4]$, first reported by Wilkinson *et al.*,[58] was published by Lawton and Mason.[52] The fact that the structure consisted of two eclipsed square planes, as in $[Re_2Cl_8]^{2-}$, a short Mo-Mo distance of 2.11 Å and that Re^{III} is isoelectronic with Mo^{II}, meant that $[Mo_2(O_2CMe)_4]$ must contain a quadruple bond.[11] The structure, later refined to give a Mo-Mo distance of 2.093(1) Å,[104] is shown in Fig.1.4.

The anion analogous with $[Re_2Cl_8]^{2-}$ in $K_4[Mo_2Cl_8].2H_2O$ was identified and structurally characterised (Mo-Mo = 2.139(4) Å), as the product of the reaction between KCl and $[Mo_2(O_2CMe)_4]$ in cold hydrochloric acid.[105]

The molybdenum(II) carboxylates are probably the single most important class of compounds to contain the Mo-Mo quadruple bond because they have traditionally been the starting point for the synthesis of almost all other derivatives of the quadruply bonded Mo_2^{4+} core. Wilkinson's preparative procedure of heating $Mo(CO)_6$ with the carboxylic acid (and the anhydride) either alone or in diglyme is still a general method of production.[58] Generally, they

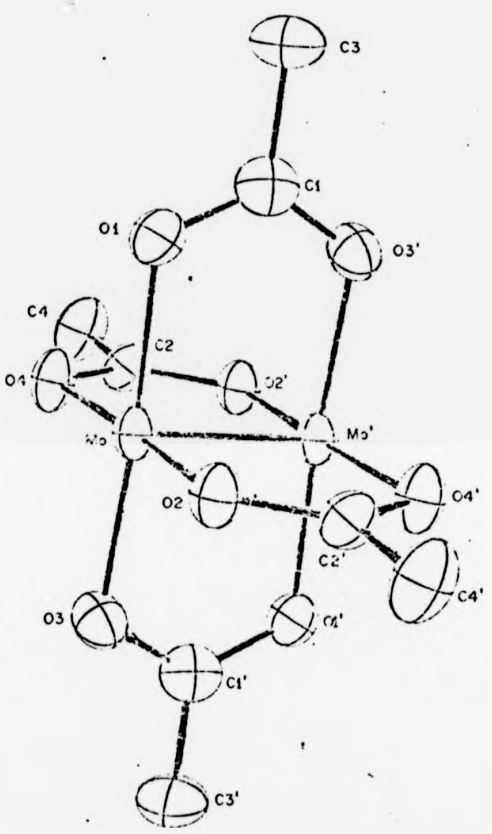

FIG.1.4 Crystal structure of $[Mo_2(O_2CMe)_4]$

can be obtained directly by carboxylate exchange with the acetate $[Mo_2(O_2CMe)_4]$, and the range includes alkyl,[58] haloalkyl,[58,106] and aryl[58,107] monocarboxylic acids plus a variety of dicarboxylic acids.[108]

Several crystal structures have been reported for the tetracarboxylates and there is a reluctance for axial co-ordination.[11] In those compounds with axial ligands that have been studied crystallographically the bonds to the axial ligands are very long. Such adducts include H_2O,[109] diglyme,[110] pyridine,[111] halides,[112] phosphines,[113] and DMSO.[114] The Mo-Mo bond lengths in the $[Mo_2(O_2CR)_4]$ and $[Mo_2(O_2CR)_4L_2]$ compounds structurally characterized appear insensitive to the variation in R group and only slightly sensitive to the nature of the axial co-ordination.[11]

Numerous reactions involve partial displacement of the carboxylate ligands. Reactants affording such removal include dil. HCl,[115] Na acac,[116] and sodium pyrazolylborate.[48] Esterfication and removal of carboxylate groups has been employed using Me_3SiCl[25] and $[Et_3O]BF_4$[117] and products obtained have included halide derivatives with nitrile and phosphine substitution e.g. $[Mo_2(O_2CCF_3)_3(NCEt)Cl]$[25] and $[Mo_2(O_2CCMe_3)_2Cl_2(PEt_3)_2]$.[118] Recently the action of strong non-complexing acids CF_3SO_3H and $HBF_4.Et_2O$ on acetonitrile solutions of $[Mo_2(O_2CMe)_4]$ gave two derivatives $[Mo_2(O_2CMe)_2(NCMe)_4][CF_3SO_3]_2$ and $[Mo_2(O_2CMe)_2(NCMe)_5][BF_3OH]_2$ which were characterized by infrared, UV/visible and ^1H n.m.r. spectroscopy.[119]

A variety of neutral halide complexes have been prepared of general formula $Mo_2X_4L_4$ (X = halide, L = monodentate phosphine or phosphite, ½bidentate phosphine, nitrile).[11,120,121,122] Several of the bidentate phosphines impose internal twists in $Mo_2X_4L_4$ compounds

away from the precisely eclipsed conformation and have led to several studies of their CD and ORD spectra and of the relationship between the energy of the $\delta \rightarrow \delta^*$ transition and the strength of the δ bond.[123,124]

Recently, investigations into the rotational barrier about the metal-metal bond in molybdenum(II) porphyrin dimers using ^1H n.m.r. studies provided evidence for the existence of quadruple bonds and an activation energy for this rotational process of 10.1 ± 0.5 kcal mol^{-1}.[125]

Only a very few cationic dinuclear Mo(II) species are known, excluding those with cationic ligands. Bowen and Taube reported $Mo_2^{4+}(aq)$ from which they made $Mo_2(en)_4^{4+}$ precipitated as its chloride salt.[126] Although it was not structurally characterized they suggested that it was more likely to contain chelating ligands than bridging diamine ligands, a proposal that was recently questioned in a report on the CD spectrum of $[Mo_2(R\text{-}pn)_4]^{4+}$ (which has similar absorption spectra to $[Mo_2(en)_4]^{4+}$ and which was concluded to contain bridging ligands).[127] More recently $[Mo_2(NCMe)_8][TFMS]_4$ was reported,[128] which was believed to be the first isolated tetracation of binuclear Mo(II) with a unidentate ligand. The only other MeCN complex reported was that in $[Mo_2(NCMe)_4Cl_4]$[24] and there was no evidence here for further substitution to a cationic species. However, neither of these two acetonitrile complexes was structurally characterized.

A recent extension into the series of compounds containing the Mo-Mo quadruple bond has been in the preparation of the first Mo_2^{4+} dimers supported by alkoxy ligands.[36] They are prepared by reacting Bu^tCH_2OH and Pr^iOH with 1,2-$MoBu^i_2(NMe_2)_4$ producing $[Mo_2(OCH_2Bu^t)_4(HNMe_2)_4]$ and $[Mo_2(OPr^i)_4(HNMe_2)_4]$, respectively. Solutions containing the latter complex react with neutral donor ligands to give

$[Mo_2(OPr^i)_4L_4]$ (where L = py, H_2NMe and PMe_3) and with excess Pr^iOH $[Mo_2(OPr^i)_4(HOPr^i)_4]$ is produced. The reaction is thought to proceed via reductive elimination, as in the reactions of CO_2 and 1,3-diaryltriazines with $[1,2\text{-}Mo_2R_2(NMe_2)_4]$ (R = Et, $CHMe_2$, and n, sec, and t-C_4H_9) where $[Mo_2(O_2CNMe_2)_4]$ and $[Mo_2(ArN_3Ar)_4]$ are produced.[129]

Theoretical calculations on the $[Mo_2Cl_8]^{4-}$ ion showed a similar pattern of orbitals to those for $[Re_2Cl_8]^{2-}$ mentioned earlier, with $2b_{1u}(\delta^*) > 2b_{2g}(\delta) > 5e_u(\pi) > a_{1g}$ with decreasing energy. The a_{1g} orbital is almost totally responsible for Mo-Mo σ-bonding and has 83% metal d character.[130] The Hartree-Fock LCAO method has been applied to several $[M_2X_8]^{n-}$ species. For $[Mo_2Cl_8]^{4-}$ the energy separations are different from those obtained using the SCF-Xα-SW method but there is a general qualitative correspondence.[131]

Both SCF-Xα-SW[132] and Hartree-Fock[131] calculations have been carried out on the prototype molecule $[Mo_2(O_2CH)_4]$. Basically the bonding picture is the same as above. In the SCF-Xα-SW case eight of the sixteen C-O π and O 2p lone-pair orbitals of the formate ions mix with the metal atom orbitals and thus approximately represent the eight M-O bonds in the complex. Considerable charge transfer from the formate ions to the Mo_2^{4+} unit occurs, reducing the charge on the metal atoms, thereby expanding the metal orbitals and enhancing the Mo-Mo bonding interactions.

The HF treatment of $[Mo_2(O_2CH)_4]$[131] gave similar results to those obtained for $[Mo_2Cl_8]^{2-}$. The major disagreement between the SCF-HF and SCF-Xα-SW results has to do with the placement of the σ-bonding orbitals. The HF calculation puts the σ orbital ($5a_{1g}$) at about the same energy as the π orbital ($6e_u$) whereas these two are separated by

about 1 eV according to the SCF-Xα-SW calculation and the main σ-bonding orbital ($4a_{1g}$) is about 3 eV lower.

One of the experimental techniques with the strongest bearings on the nature of the quadruple metal-metal bond is low-energy photoelectron spectroscopy which in conjunction with theoretical calculations can provide information on the states generated from ionization of electrons out of the σ, π and δ metal-metal bonding orbitals. Different interpretations of the recorded photoelectron spectra of $Mo_2(O_2CR)_4$ systems[133,134] have, however, been provided by the HF ab initio method and the SCF-Xα-SW scheme in connection with theoretical calculations on $Mo_2(O_2CH)_4$. An ab initio calculation by Atha, Hillier, and Guest on $Mo_2(O_2CH)_4$ presented with the photoelectron spectrum gave assignments of the lowest energy peak A (Fig.1.5) to ionization from the $2b_{2g}(\delta)$ metal orbital and peak B to both the $5e_u(\pi)$ and $4a_{1g}(\sigma)$ metal orbitals.[135] These were different from those given by SW-Xα calculations. The latter assign peaks A, B and E to the δ, π and σ ionizations, respectively.[136]

This controversy extended to the binuclear tetracarboxylates of chromium also. For both Cr and Mo, all interpretations[11,135] of their recorded photoelectron spectra[11,133,134,137] agreed in the assignment of the ligand-based orbitals but differed in other interpretations.

The polarized crystal spectra of $K_4[Mo_2(SO_4)_4]$ contain a band at 526 nm and there is no change in the integrated intensity of this peak on going from 300 to 15 K, supporting the assignment as an orbitally allowed transition. The spectra also indicate that this lowest energy band is z polarized.[138] Similar studies on $[Mo_2Cl_8]^{4-}$ have shown that

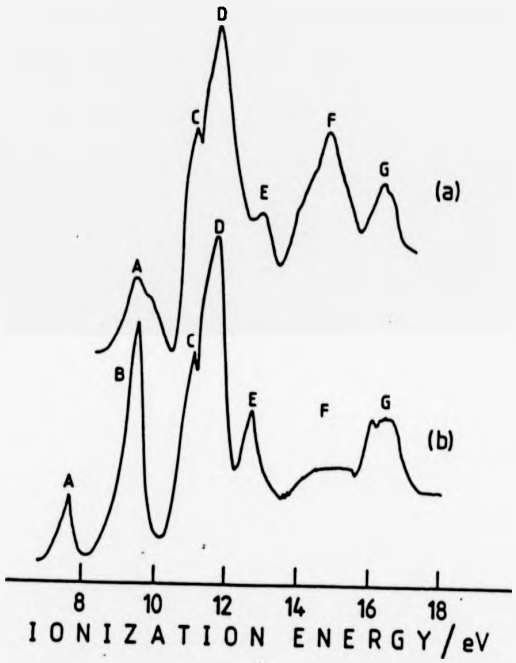

Photoelectron Spectrum of (*a*) $Cr_2(O_2CCH_3)_4$ and (*b*) $Mo_2(O_2CH)_4$.

Figure 1.5

the lowest energy band is z polarized consistent with the $\delta \rightarrow \delta^*$ assignment.[139] However, the absorption band for $K_4[Mo_2(SO_4)_4]$, unlike that for most other cases, shows no vibrational structure, even at 15 K.[138] In $K_4[Mo_2Cl_8].2H_2O$ a single series of equally spaced components is observed at 3.7 K.[139] The electronic transition here is that in which one internal co-ordinate in particular (the M-M distance) is expected to change on going to the excited state and the series of states of vibrational excitation is responsible for the structure of the absorption band.[11]

While the behaviour of the $[M_2X_8]^{n-}$ ions is conventional and easily interpreted, that of the carboxylato species presents examples of complicated vibronic interactions that were previously rare, and it was some time before the true situation was recognised. Dubicki and Martin initially examined several of these compounds, most notably $[Mo_2(O_2CMe)_4]$ by diffuse-reflectance spectroscopy at 77 K.[140] Aided by Hückel MO calculations they assigned the weak structured absorption at ca. 435 nm to a dipole-forbidden transition from the δ-bonding orbital to a σ-type non-bonding level. A subsequent study of the analogous glycinate and formate complexes supported this conclusion that the 435 nm band must arise from a dipole-forbidden transition.[141,138] At this time Norman and Kolari[136,142] suggested a specific $\delta \rightarrow \pi^*(^1A_{1g} \rightarrow {}^1E_g)$ assignment for this transition on the basis of Xα calculations and this was supported by experimental evidence. In 1979 Martin, Newmann, and Fanwick showed that the characteristics of the band in $[Mo_2(O_2CMe)_4]$ at ca. 435 nm and similar bands in other $[Mo_2(O_2CR)_4]$ compounds are not inconsistent with their being assigned to the $\delta \rightarrow \delta^*$ transition.[143] More recently the electronic spectra of

$Mo_2(O_2CMe)_4$ have been the subject of studies,[144] and Martin *et al.* have put forward a further assignment justifying that of the 435 nm band to the $\delta \rightarrow \delta^*$ transition.[145]

Recently the absorption and emission spectra of *cis*-$[Mo_2(mhp)_2Cl_2(PEt_3)_2]$ were reported, the lowest energy band at 540 nm being assigned to the $\delta \rightarrow \delta^*$ transition in the solution spectrum, and the strong fluorescence at 600 nm observed from the $\delta^* \rightarrow \delta$ transition.[146] The electronic spectra of $[Cr_2(mhp)_4]$, $[Mo_2(mhp)_4]$, and $[W_2(mhp)_4]$ have also recently been reported, and the lowest energy transition for all three are assigned to the $\delta \rightarrow \delta^*$ transition.[147,148]

A number of electronic emission spectra of quadruply bonded dimers have also been reported.[11,149,150]

It has been observed that for the three ions $[Cr_2Me_8]^{4-}$, $[Mo_2Me_8]^{4-}$, and $[Re_2Me_8]^{2-}$ the energies of the $\delta \rightarrow \delta^*$ bands plotted against the M-M distance give approximately a straight line with negative slope.[151] Data for $[W_2Me_8]^{4-}$ fits on the same line.[152] Similar data for the two compounds $[M_2Cl_4(PMe_3)_4]$ (M = Mo, W) define a line parallel to that for the $[M_2Me_8]^{n-}$ species but the four $[M_2X_8]^{n-}$ ions (M = Mo, Re; X = Cl, Br) require a line with a different slope.[153] Therefore, it appears that the relationship is quite a general one.[11]

Vibrational Spectra

The most interesting feature of the vibrational spectra of the multiply bonded dimolybdenum species is the vibration that corresponds mainly to Mo≡Mo stretching, ν(Mo-Mo). In most cases this vibration is active in the Raman spectrum only.[11]

The first Raman spectra of M-M quadruply bonded compounds were

reported in 1971.[154,155] Of the ν(M-M) frequencies reported for M_2 compounds, those for Mo_2^{4+} and Re_2^{6+} number the most. The ν(Mo-Mo) values vary over a considerable range (336-425 cm^{-1}).[11] The extent to which these ν(M-M) modes are limited to vibration of that particular bond is somewhat uncertain and may vary from case to case. Nevertheless, the fact that the frequencies of ν(M-M) are fairly constant when ligands are changed from Cl to Br indicates that, in some cases, the localization of the mode in the M-M bond is fairly complete.[11]

In $Mo_2(O_2CMe)_4$ there is direct experimental evidence using isotopic substitution, that the strong Raman band at 406 cm^{-1} is due to a motion that is virtually pure Mo-Mo stretching.[156] However, a recent spectroscopic and theoretical study on $Mo_2(O_2CH)_4$, $Mo_2(O_2CMe)_4$, and $Mo_2(O_2CCF_3)_4$ has assigned the peak due to the M-M stretch to be at 406, 404, and 398 cm^{-1}, respectively.[157]

Useful comparisons can be made within the series of five $MM'(mhp)_4$ molecules, with M and M' representing Cr, Mo, or W. For these homologous molecules it is possible to use only the observed ν(M-M) and the atomic masses to calculate a set of force constants that have considerable significance relative to one another. Similarly, such relative force constants may be compared for the pair of compounds $M_2Cl_4(PBu^n_3)_4$ with M=Mo or W.[11]

Resonance Raman spectra have also been recorded and the resonance Raman effect is useful because it often makes otherwise weak lines measurable.[11,158]

Molybdenum-95 nuclear magnetic resonance spectroscopy

^{95}Mo has a reasonable natural abundance (15.7%), n.m.r. receptivity (better than ^{13}C) and quadrupole moment (-0.019×10^{-28} m^2, smaller than for ^{14}N). ^{95}Mo n.m.r. spectroscopy has, therefore, recently been established as a sensitive probe of both electronic and structural effects in diamagnetic molybdenum complexes. The chemical shift range currently covers ca. 7250 p.p.m. for all molybdenum species. Relatively few quadruply bonded molybdenum dimers have been studied via ^{95}Mo n.m.r. techniques.[159,160,161] Those investigated have been the phosphine/halide complexes $Mo_2X_4L_4$ (X = Cl, Br, or I; L = PMe_3), the tetracarboxylate complexes $Mo_2(O_2CR)_4$ (R = Bu^t, Bu^n, Pr^i, Pr^n, $CHCl_2$, Me, CF_3), Mo_2^{4+}, $K_4[Mo_2(SO_4)_4]$ and $[Mo_2X_8]^{4-}$ (X = Cl or Br) and the chemical shifts are shown in Table 1.1.

Table 1.1

^{95}Mo chemical shifts for Mo≡Mo-bonded compounds

Compound	δ^{95}Mo (p.p.m.)	$\nu_{\frac{1}{2}}$ (Hz)	Ref.
$[Mo_2I_4(PMe_3)_4]$	2927	850	159
$[Mo_2Br_4(PMe_3)_4]$	3008	840	159
$[Mo_2Cl_4(PMe_3)_4]$	3021	800	159
$Cs_4[Mo_2Br_8]$	3227	510	161
$[Mo_2(O_2CBu^n)_4]$	3661	1440	161
$[Mo_2(O_2CBu^t)_4]$	3667	870	159
$[Mo_2(O_2CPr^i)_4]$	3670	950	161
$[Mo_2(O_2CPr^n)_4]$	3682	1320	161
$[Mo_2(O_2CMe)_4]$	3702	520	161
$[Mo_2(O_2CH)_4]$	3768	670	159
$K_4[Mo_2Cl_8]$	3816	1440	161
$[Mo_2(O_2CCHCl_2)_4]$	3911	490	161
$[Mo_2(O_2CCF_3)_4]$	4021	480	159,161
Mo_2^{4+}	4056	430	161
$K_4[Mo_2(SO_4)_4]$	4090	990	161
$[Mo_2(O_2CCF_3)_4(py)_2]$	4199	320	159

1.8 Triple Bonds[162]

Triple bonds between molybdenum atoms may have a variety of electronic configurations, $\sigma^2\pi^4$, $\sigma^2\pi^2\delta^2$, $\pi^4\delta^2$, and $\sigma^2\pi^4\delta^2\delta^{*2}$. The triply bonded dimolybdenum and ditungsten hexa-alkoxides, compounds of formula $M_2(OR)_6$, constitute compounds that are members of an extensive group of d^3-d^3 dimers which adopt a staggered "ethane-like" geometry in the ground state. The triple bond has a configuration $\sigma^2\pi^4$ derived from the metal d^3-d^3 interaction. Taking the M-M axis to be the z axis, the metal atomic d_{z2} orbitals interact to form σ and σ^* orbitals and the degenerate d_{xz}, d_{yz} atomic orbitals form $\pi_{x,y}$ and $\pi_{x,y}^*$ molecular orbitals. The triple bond is cylindrical and these molecules are inorganic analogues of alkynes. He(I) and He(II) photoelectron spectroscopy reveals that the first ionization is from the filled M-M π orbitals; the second ionization comes from the M-M σ orbitals while the third, at still higher ionization energy, is from oxygen lone pairs.

These compounds are co-ordinatively unsaturated and can, if steric factors permit, co-ordinate Lewis bases such as pyridine and PMe_3 to form adducts of formula $M_2(OR)_6L_2$.

1.9 Tungsten

The history of attempts to make stable compounds containing W≡W quadruple bonds covers a period of more than 20 years. In view of the tremendous range of isolable and readily characterizable complexes of Cr_2^{4+} and Mo_2^{4+}, it might be anticipated that W_2^{4+} derivatives would be quite common but this has proved not to be the case.[11] In 1977, compounds containing the $[W_2Me_8]^{4-}$ [60,163] and $[W_2Cl_nMe_{8-n}]^{4-}$ [164]

ions were characterized and were the first authenticated compounds containing W≡W bonds, but they are very unstable, both chemically and thermally. The lithium salts of the above set of compounds were isolated using methyllithium as a ligand source and reductant in reactions with WCl_4 or WCl_5.[60,163,164] The first stable compound was $[W_2(mhp)_4]$ reported in 1978[61] to be produced on refluxing $W(CO)_6$ with Hmhp in diglyme. This complex is isostructural with its chromium and molybdenum analogues.[61] The reaction of $[W_2(mhp)_4]$ with the lithium salt of Hmap leads to the formation of $[W_2(map)_4]$.[165]

The reaction of $W(CO)_6$ with the ligands Hdmhp, and Hchp produces $[W_2(dmhp)_4]$[166] and $[W_2(chp)_4]$[167] respectively. Two of the dmhp ligands of $[W_2(dmhp)_4]$ are replaced on its reaction with the lithium salts of N,N'-diphenylacetamide, $Li[(PhN)_2CMe]$, and 1,3-diphenyltriazine, $Li[(PhN)_2N]$ in THF to give $[W_2(dmhp)_2[(PhN)_2CMe]_2].2THF$[168] and $[W_2(dmhp)_2[(PhN)_2N]_2].THF$[169] that contain a transoid arrangement of bridging ligands.

Recently, the reaction of Na(fhp) with a THF solution of WCl_4 produced $[W_2(fhp)_4(THF)]$[170] and a structure determination showed that the four bridging fhp ligands are all orientated in the same direction

Prior to this there had been no cases for any $[M_2(Xhp)_4]$ molecules where the totally polar arrangement had been observed.[170]

In 1980, Sharp and Schrock prepared a series of $[W_2Cl_4(PR_3)_4]$ complexes.[171] The most general procedure involves the sodium amalgam reduction of a mixture of WCl_4 and phosphine in THF.[171]

$$2WCl_4 + 4Na/Hg + 4PR_3 \xrightarrow{THF} W_2Cl_4(PR_3)_4$$

(PR_3 = PMe_3, PMe_2Ph, $PMePh_2$, or PBu_3^n)

The second method involves the thermal decomposition of mer-$[WCl_3(PMe_3)_3]$ and trans-$[WCl_2(PMe_3)_4]$.[171]

The reactions of toluene solutions of $[W_2Cl_4(PBu^n_3)_4]$ with the bidentate phosphines dmpe and dppe produce green $W_2Cl_4(dmpe)_2$ and a mixture of green (α isomer) and brown (β isomer) complexes of composition $W_2Cl_4(dppe)_2$. The green isomers of $W_2Cl_4(dppe)_2$ and $W_2Cl_4(dmpe)_2$ possess centrosymmetric eclipsed structures with chelating phosphine ligands while the brown β-$W_2Cl_4(dppe)_2$ is structurally similar to β-$Mo_2Cl_4(dppe)_2$.[172]

The successful preparation of $[Mo_2(O_2CMe)_4]$ from $Mo(CO)_6$ by Wilkinson et al.[58] could not be extended to $[W_2(O_2CR)_4]$ systems from $W(CO)_6$ as acidic media lead to oxidation providing trinuclear tungsten(IV) species.[11,173] It was only in 1981 that $[W_2(O_2CCF_3)_4]$ was successfully prepared using NaO_2CCF_3,[174] and soon after $[W_2(O_2C\text{-}Bu^t)_4]$ was isolated using a similar procedure[175] along with a number of other carboxylate compounds.[176,177] The acetate compound $[W_2(O_2CMe)_4]$ was only recently isolated via carboxylate exchange between $[Bu_4N][O_2CMe]$ and $[W_2(O_2CCF_3)_4]$.[175]

A general high yield synthesis for $W_2(O_2CR)_4$ compounds has also been proposed using triply bonded tungsten dimers as starting materials.[178]

Numerous halide,[11,179] phosphine/halide,[180] and phosphine/carboxylate tungsten[181,182] dimers have also been prepared.

The most recent development in W≡W bonds came with the production of $[W_2(CH_2Ph)_2(O_2CEt)_4]$ from the reaction of $W_2(CH_2Ph)_2(NMe_2)_4$ and EtCOOCOEt.[183] A similarly formulated compound $W_2Me_2(O_2CNEt_2)_4$ is known, containing a triply bonded d^3-d^3 dimer,[184] but the geometries of the two compounds differ considerably, and the former compound has been shown by a theoretical study to be considered as a $W_2(O_2CH)_4$ fragment interacting with two CH_3 radicals.[185]

Bancroft et al. have recorded the photoelectron spectrum of $[W_2(O_2CCF_3)_4]$[186] where three bands can be clearly identified. Bancroft et al. assigned δ to A (7.3 eV) and π, σ to B_1 (9.01 eV), B_2 (9.71 eV), respectively, and this assignment is supported by an HFS calculation on $[W_2(O_2CCF_3)_4]$[187] where ionization from δ, π, σ were calculated to be at a lower energy than the first ionization from a ligand based orbital. This HFS study calculated, as in the case of $[W_2(O_2CCF_3)_4]$, the ionization from δ, π, σ to be at lower energy than the ionization from the first ligand based orbital for both $[Cr_2(O_2CMe)_4]$ and $[Mo_2(O_2CH)_4]$ and the same assignment was offered for the photoelectron spectra of the two molecules as given previously based on ab initio calculations on $[Cr_2(O_2CH)_4]$ and $[Mo_2(O_2CH)_4]$.[11,135]

The photoelectron spectra of $[Mo_2Cl_4(PMe_3)_4]$ and $[W_2Cl_4(PMe_3)_4]$ have also been recorded.[188] The low energy region (below that due to ionization from the ligand-based orbitals) has as in the case of the tetracarboxylates, for M=Mo two bands A and B and for M=W three bands A, B_1, and B_2, where the splitting between B_1 and B_2 is 0.4 eV. Cotton et al. have, from SCF-Xα-SW calculations[188] on $M_2Cl_4(PH_3)_4$ (M = Mo, W), found σ to be of lower energy than δ, π and for this reason assigned only δ, π to the contested region. Recent HFS calculations on $M_2(PH_3)_4Cl_4$ (M = Mo, W) show the two orbitals π, σ to be of nearly the same energy and the three ionizations of lowest energy to correspond to δ, π, σ respectively.[187] This calculation offered the assignments A (δ), B (π,σ) and A (δ), B_1 (π), B_2 (σ) for M = Mo, W respectively.[187]

1.10 Reactions of quadruple bonds

Without cleavage

1.10.1 Bond order change from 4 to 3

(i) Addition

Examples of addition reactions causing a reduction in bond order from 4 to 3 are rare. The most important occurs in the reaction between $[Mo_2(O_2CCH_3)_4]$ with aqueous solutions of HX (X = Cl or Br).[188,190] The initial reaction produces $[Mo_2X_8]^{4-}$, with retention of the quadruple bond but, at +60°C, the $[Mo_2X_8H]^{3-}$ Fig.1.6 ion is formed. The structure of the anion is analogous to that of $[Mo_2Cl_9]^{3-}$. Such formation can be regarded as an oxidative addition of HX across the Mo≡Mo quadruple bond.

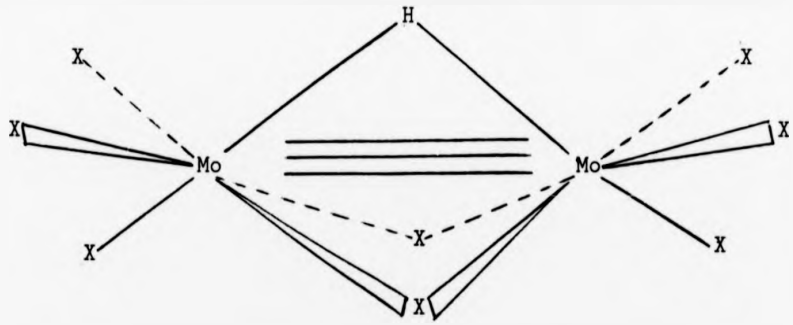

Figure 1.6 $[Mo_2X_8H]^{3-}$ ion

The anion has D_{3h} symmetry. A recent X-ray and neutron diffraction study on $[NMe_4]_3[Mo_2Cl_8H]$ gave an Mo-Mo bond length of 2.376(3) Å.[191]

These complexes have been the subject of numerous structural, spectroscopic and theoretical studies in recent years. An SCF-Xα-SW study of the chloride ion, $[Mo_2Cl_8H]^{3-}$ suggested that the Mo-H-Mo unit

is essentially a three-centre four-electron system with a strong interaction.[192]

Recently the iodo analogue has been prepared $[Mo_2I_8H]^{3-}$ by the reaction of $Mo_2(O_2CMe)_4$ and Et_4NI in an aqueous solution of HI.[193]

A similar reaction occurred following an attempt to prepare a quadruply bonded tungsten benzoate compound. Reaction of benzoic acid with $[W_2Cl_4(PBu_3)_4]$ in a 2:1 molar ratio produced the triply bonded dimer $[W_2(\mu\text{-}H)(\mu\text{-}Cl)Cl_2(PBu^n_3)_2(O_2CPh)_2]$,[194] Fig.1.7. The W-W distance in this complex is 2.429(1) Å and the structure of the central part of the molecule is shown.

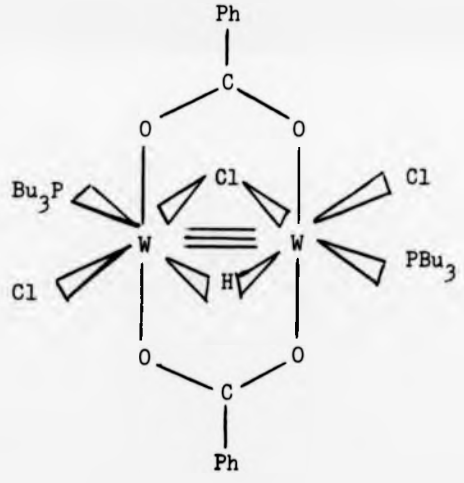

Figure 1.7 Structure of $[W_2(\mu\text{-}H)(\mu\text{-}Cl)Cl_2(PBu^n_3)_2(O_2CPh)_2]$ [194]

This reaction involves oxidative addition of HCl to the quadruply bonded species leading to production of the W^{III} dimer. The process is irreversible, as is the oxidative addition across the Mo≡Mo of $[Mo_2Cl_8]^{4-}$ to produce $[Mo_2X_8H]^{3-}$.

Oxidation of W^{II} in $[W_2(mhp)_4]$ occurs upon reaction with gaseous halide hydrides HX (X = Cl or Br) in methanol or ethanol:[195]

$$[W_2(mhp)_4] \xrightarrow[\text{Methanol or Ethanol}]{HX(g)} [W_2X_4(OR)_2(ROH)_4]$$

Quadruple bonds of the type $Mo_2Cl_4(RSCH_2CH_2SR)_2$ undergo slow decomposition in CH_2Cl_2 to give the compound $Mo_2Cl_6(RSCH_2CH_2SR)_2$. The compound where R = Et has been studied crystallographically and was found to contain a doubly chloro-bridged Mo(III) species with a Mo-Mo triple bond.[196]

(ii) Dimerization

A reduction in the metal-metal bond order can occur upon dimerization. McCarley et al.[197] showed that it was possible to couple Mo-Mo quadruple bonds to form a rectangular Mo_4 cluster by an elimination of four labile methanol ligands. This was achieved by preparing the compound $[Mo_2Cl_4(PPh_3)_2(CH_3OH)_2]$ and, on dissolving in benzene, subsequent self-addition occurred, Fig.1.8. The Mo-Mo distances are 2.211(3) and 2.901(2) Å which may be reasonably taken to represent Mo-Mo triple and single bonds, respectively. McCarley et al. suggested that the electron pairs utilized in the dimers for δ-bonding are recast for forming the long σ-bonds in the tetramer.[197]

Subsequently several synthetic methods were developed for the preparation of $[Mo_4X_8L_4]$ (X = Cl, Br, I; L = neutral donor ligand) compounds.[198] From $[Mo_2Cl_4(PPh_3)_2(CH_3OH)_2]$ the tetramer $[Mo_4Cl_8(CH_3OH)_4]$ has been prepared, which may be converted to $[Mo_4Cl_8(C_2H_5CN)_4]$, $[Mo_4Cl_8(PPh_3)_4]$ and $[Mo_4Cl_8(PR_3)_4]$ by the appropriate ligand substitution. $[Mo_4Cl_8(PR_3)_4]$ may be prepared:

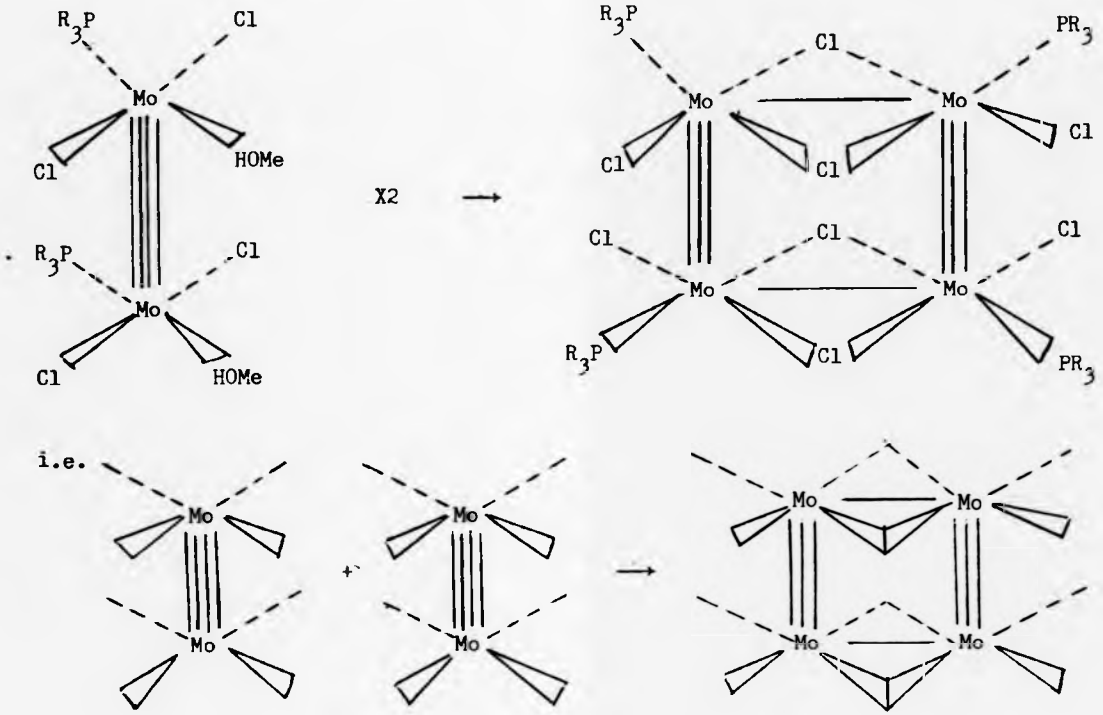

Figure 1.8[197]

(a) by reacting $K_4[Mo_2Cl_8]$ and PR_3 in a 1:2 molar ratio,

(b) by reacting $[Mo_2(O_2CMe)_4]$ and PR_3 and Me_3SiCl in a 1:2:4 molar ratio,

(c) by reacting $[Mo_2(O_2CMe)_4]$ and PR_3 and $AlCl_3$ in a 1:2:2 molar ratio, or

(d) by reacting $[Mo_2Cl_4(PR_3)_4]$ and $Mo(CO)_6$ in a 1:1 molar ratio.

The bromo-analogue $[Mo_4Br_8(PBu^n_3)_4]$ has also been prepared but the iodide $[Mo_4I_8(PBu^n_3)_4]$ was found to consist only of weakly coupled quadruply bonded dimers linked by bridging iodide atoms. Cotton has prepared the tetranuclear complex $[Mo_4Cl_8(P(OMe)_3)_4]$ reacting $K_4[Mo_2Cl_8]$ with $P(OMe)_3$.[199]

Recently, reactions of these tetrameric clusters $Mo_4Cl_8(PR_3)_4$ (PR_3 = PEt_3, PPr^n_3, PBu^n_3 and PMe_2Ph) with $Mo(CO)_4Cl_2$ or $Mo(CO)_6$ has led to phosphine abstraction and formation of the condensation products $[Mo_4Cl_8(PR_3)_2]x$, formulated as dimers of tetramers $[Mo_4Cl_8(PR_3)_2]_2$.[200]

(iii) Reduction

An example of a metal-metal bond order change from 4 to 3, via reduction of the metal, is found in the reaction of phosphines with the $[Re_2X_8]^{2-}$ ions (X = Cl or Br). These $[Re_2X_8]^{2-}$ anions react with alkyl and mixed alkyl-phenyl phosphines giving reduced phases of composition $[Re_2X_5(PR_3)_3]$ or $[Re_2X_4(PR_3)_4]$. The extent of the reduction depends on the degree of phenyl substitution on the phosphine.[201] With an excess of PR_3 (R = alkyl) the reaction is:

$$[Re_2Cl_8]^{2-} \xrightarrow[CCl_4]{PR_3} [Re_2Cl_4(PR_3)_4]$$

i.e. a two-electron reduction of $(Re^{III})_2$ to $(Re^{II})_2$ has occurred, with the conversion of a quadruple to a triple bond since two electrons are added to antibonding orbitals of the metal-metal framework.

However, with mixed alkyl-phenyl phosphines, $PRPh_2$ (R = Me or Et), the compound $[Re_2Cl_5(PRPh_2)_3]$, Fig.1.9, is formed.

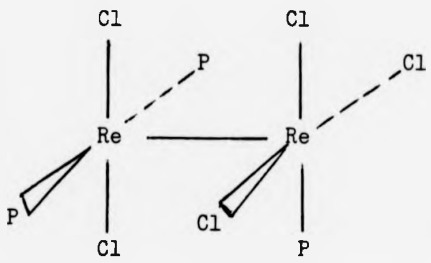

Figure 1.9 The structure of $[Re_2Cl_5(PRPh_2)_3]$[201]

Here, the Re-Re bond order is 3.5 and rhenium is in the +2.5 oxidation state. Reduction of the metal ions by an even number of electrons probably occurs in stepwise reactions, as above, involving the transference of a single electron.[202] The corresponding reduction does not occur with Ph_3P.

Recently, Cotton et al. have achieved reactions between $[Re_2Cl_6(PBu^n{}_3)_2]$ or $[Re_2Cl_8]^{2-}$ and the unsymmetrical Ph_2Ppy molecule[203] which are dominated by the reduction of the Re_2^{6+} core to give complexes derived from the triply bonded Re_2^{4+} core. The course of these reactions is markedly dependent on the choice of solvent, the stoichiometry of the reactants and the reaction time. This is shown in Fig.1.10.[204]

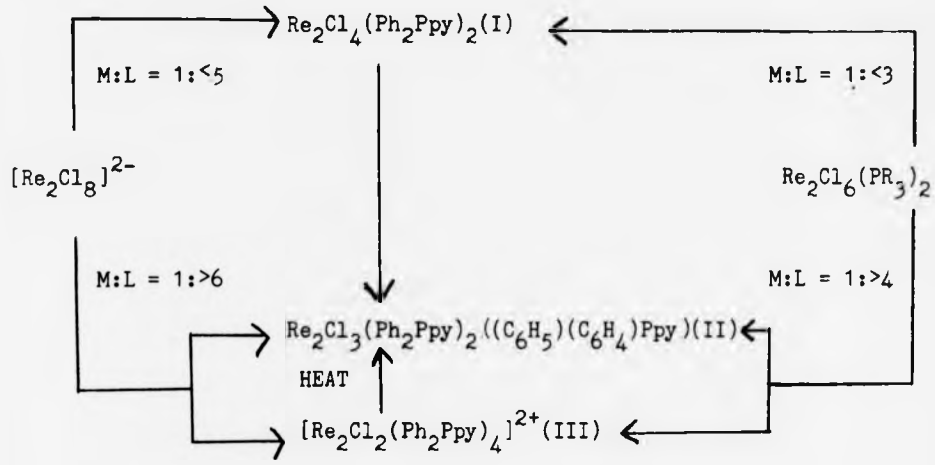

Figure 1.10

The complex $[Re_2Cl_4(Ph_2Ppy)_3]$(I) is formed initially and is found to eliminate HCl to give the ortho-metallated complex $[Re_2Cl_3(Ph_2Ppy)_2((C_6H_5)(C_6H_4)Ppy)]$(II). Complex (III) $[Re_2Cl_2(Ph_2Ppy)_4]^{2+}$ constitutes a rare example of a multiply bonded dimetal unit complexed by four neutral bridging ligands. The structures of complexes (II) and (III) have been solved by X-ray crystallography and all three complexes contain Re-Re triple bonds.[204]

1.10.2 Bond order change from 4 to 2

(i) Addition

This occurs when $[Re_2Cl_8]^{2-}$ is reacted with bis(diphenylphosphino) methane (dppm), a ligand favouring bridging of binuclear compounds. The compound $[Re_2Cl_6(dppm)_2]$ is formed and a recent structure determination showed it to have the structure shown in Fig.1.11.

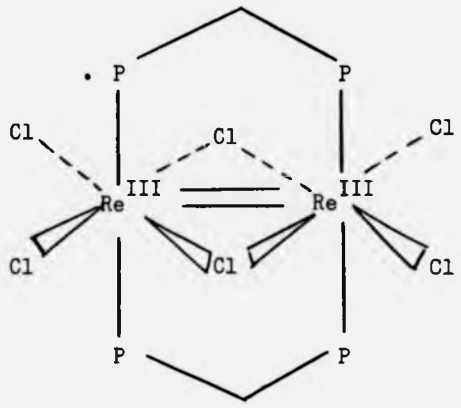

Figure 1.11 Structure of $[Re_2Cl_6(dppm)_2]$[205]

The Re-Re distance is 2.616(1) Å with a net formal double bond of a $\sigma^2\pi^2\delta^2\delta^{*2}$ configuration.[205]

An intriguing conversion of a dinuclear compound, $[Re_2(O_2CMe)_4X_2]$ to a trinuclear compound, $[Re_3X_9]$ by addition of HX (X = Cl, Br or I) has been reported by Walton *et al*. The equation below represents the reorganisation, although the pathway is not known.[206,207]

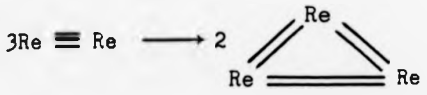

(ii) Oxidative addition

When $[W_2(mhp)_4]$ is reacted with methanol or ethanol, oxidation occurs to give the corresponding ditungsten(IV,IV) alkoxides $[W_2Cl_4(\mu\text{-}OR)_2(OR')_2(R'OH)_2]$,[208] Fig.1.12.

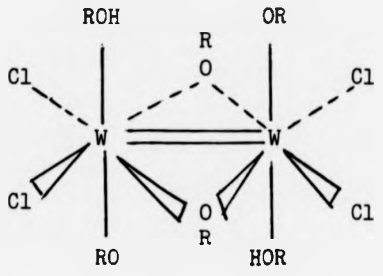

W-W = 2.482 Å

Figure 1.12 Structure of $[W_2Cl_4(\mu\text{-}OR)_2(OR')_2(R'OH)_2]$[208]

Ligand exchange reactions for this compound can produce the above system with R = Et, R' = i-Pr with a symmetrical ROHOR group hydrogen bonded unit bridging the W=W bond.

1.10.3 Bond order change from 4 to 1

This is achieved by reaction of the xanthate compound $[Mo_2(S_2COEt)_4]$ and the halogens X_2 (X = Br or I) which yields $[Mo_2X_2(S_2COEt)_4]$.[209] Structural analyses by X-ray diffraction of both $[Mo_2Br_2(S_2COEt)_4]$ and $[Mo_2I_2(S_2COEt)_4]$ showed that these compounds contain single bonds with Mo-Mo distances of 2.72 Å. This change in bond order results from a rearrangement of the xanthate ligands as shown in Fig.1.13. Two of the xanthate ligands act as four-electron π donors across the Mo-Mo bond. In this way, each molybdenum atom attains a valence shell of 18-electrons by forming a Mo-Mo single bond.

The reaction of $[W_2Cl_4(PBu_3)_4]$ with acetic acid yields a complex consisting of equilateral, triangular clusters of W(IV) atoms of formula $[W_3O_3Cl_5(O_2CMe)(PBu_3)_3]$.[210] Similarly $[Mo_2(O_2CMe)_4]$ reacts with propionic acid and propionic anhydride to produce the triangular

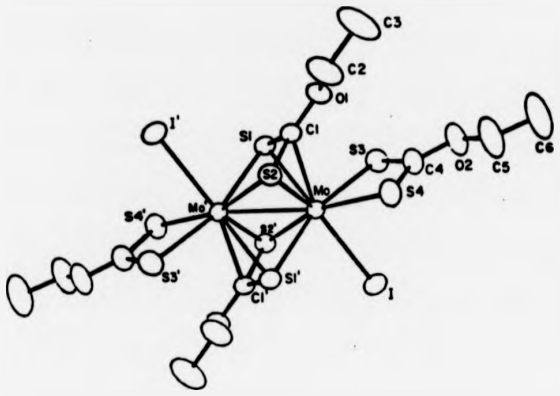

Figure 1.13 An ORTEP view of the $Mo_2(S_2COEt)_4I_2$ molecule showing the unusual bridging xanthate ligands.[209]

Mo(IV) metal cluster $[Mo_3O_2(O_2CEt)_6(H_2O)_3][CF_3SO_3]_2[CF_3SO_3H][H_2O]_4$.[211] The reaction of $[Mo_2(O_2CMe)_4]$ with $Na_2[MoO_4]$ in acetic acid produces the acetate analogue $[Mo_3O_2(O_2CMe)_6(H_2O)_3][CF_3SO_3]_2$[212] and the benzoate complex $[Mo_3O_2(O_2CPh)_6(H_2O)_3]^{2+}$ has also recently been prepared from the parent tetracarboxylate.[213]

The reaction of $[NH_4]_5[Mo_2Cl_9]H_2O$ with 3,6-dithiaoctane (dto) $EtSCH_2CH_2SEt$ and ethyl disulphide has been reported to give the Mo(III) dimer $[Mo_2Cl_4(\mu\text{-}SEt)_2(dto)_2]$. Similarly, $[Mo_2Cl_4(\mu\text{-}SEt)_2(dmpe)_2]$ has been prepared from the reaction of β-$[Mo_2Cl_4(dmpe)_2]$ with EtSSEt. Both dimers have been structurally characterized and are described as edge-sharing bioctahedrons, with M-M distances (ca. 2.7 Å) indicative of a Mo-Mo bond order of at least 1, another example of oxidative addition reactions involving quadruply bonded compounds.[214]

1.10.4 Cleavage

For the three Group 6 metals, metal-metal quadruply bonded compounds are all cleaved by reactions with isonitriles.[215] Phenylisonitrile reacts with $[M_2'(O_2CMe)_4]$ (M' = Cr or Mo) and $[W_2(dmhp)_4]$ (dmhp = 2,4-dimethyl-6-hydroxypyrimidine) to give $[M(CNPh)_6]$ (M = Cr, Mo or W). In the presence of non-co-ordinating anions such as $[PF_6]^-$, addition of alkylisonitriles to $[Mo_2(O_2CMe)_4]$ or $[Mo_2Cl_8]^{4-}$ gives $[Mo(CNR)_7][PF_6]_2$. Similarly, addition of RNC (R = Bu^t or cyclo-C_6H_{11}) and $K[PF_6]$ to an acetone solution of $[W_2(mhp)_4]$ gives, on heating, $[W(CNR)_7]^{2+}$.[216] The π-acceptor ligand NO will also cleave quadruple bonds to produce nitrosyl monomers.[202,216]

The anion $[Re_2(NCS)_8]^{2-}$ reacts with monodentate (L) and bidentate tertiary phosphines (L_2) to produce complexes of formula $[Re_2(NCS)_8L_2]^{2-}$[217] which are dimeric thiocyanate bridged Re(III) centres.

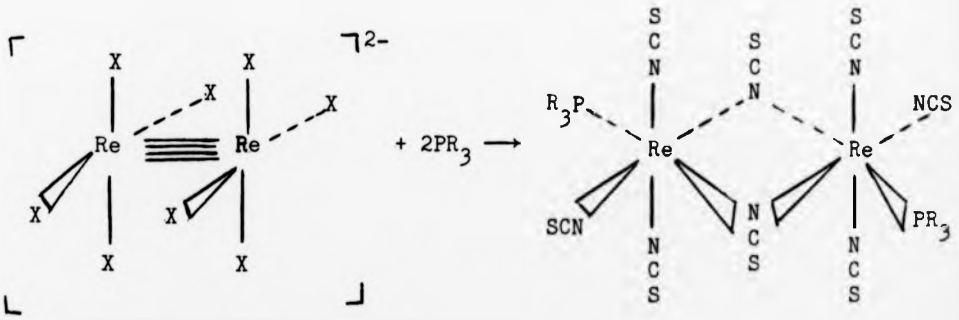

The reactions of the diethylphenylphosphine product thus formed with dppe, bipy, or 1,10-phenanthroline produce cleavage of the thiocyanate bridges and formation of the corresponding six co-ordinate Re(III) monomers $[Re(NCS)_3(PEt_2Ph)B]$ (B = dppe, bipy or phen).[215] Cleavage of the metal-metal quadruple bond typically occurs, possibly due to the weaker bond in $[Re_2(NCS)_8]^{2-}$ with respect to that in the $[Re_2X_8]^{2-}$ (X = halide) ions.[217]

$[Re_2Cl_8]^{2-}$ reacts with diphos to produce a bridged M-M non-bonded dimer.[218]

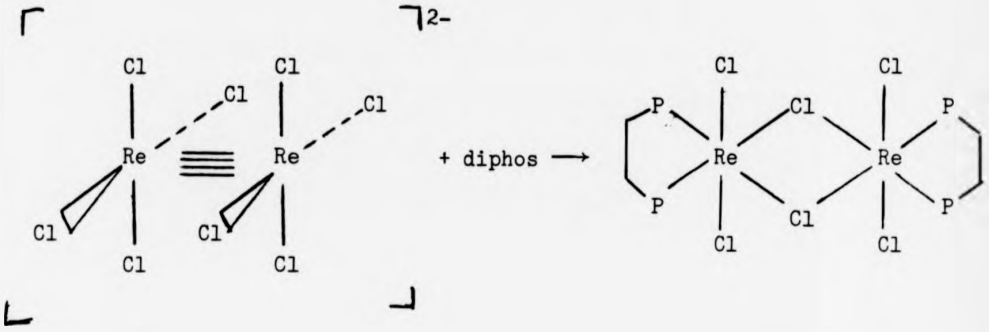

Reductive cleavage of the metal-metal bond occurs upon treatment of the quadruply bonded rhenium complexes $[Re_2(O_2CR)_4Cl_4]$ (R = Me or Ph) with alkyl isocyanides RNC (R = CMe_3 or C_6H_{11}), affording solutions from which salts of the $[Re(CNR)_6]^+$ cations can be isolated.[219] The salts $[Bu^n{}_4N]_2[Re_2X_8]$ (X = Cl or Br) react with tert-butyl isocyanide to give mononuclear seven co-ordinate rhenium(III) species $[Re(CNCMe_3)_5X_2]^+$.[220]

1.10.5 Dimer of dimers

Cotton et al. have recently noted that the reaction of $[Cr_2(O_2CMe)_4]$ with a potentially chelating ligand $Na[OCH_2CH_2NMe_2]$ affords the compound $[Cr_4(O_2CMe)_4(OCH_2CH_2NMe_2)_4]$,[221] Fig.1.14. The Cr^{II}-Cr^{II} bond, still formally a quadruple bond is retained and the local stereochemistry about the Cr_2^{4+} unit is still of the original type, but a more complex overall structure has been formed. The Cr^{II}-Cr^{II} distance, 2.531(2) Å, is just within the previously established range for these interactions and it appears this increase is caused by replacement of two bridging $MeCO_2$ groups by the O_2Cr-CrO_2 unit, Fig.1.14.

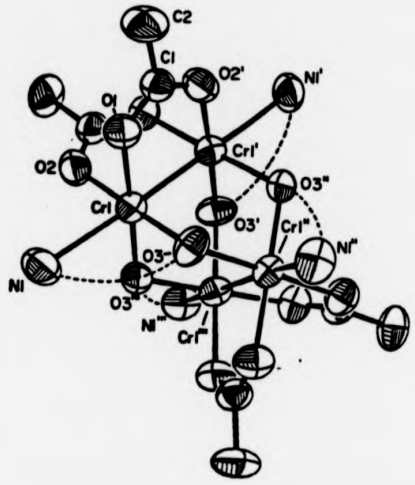

Figure 1.14 Semischematic view of the $Cr_4(O_2CMe)_4(OCH_2CH_2NMe_2)_4$ molecule in which the $-CH_2CH_2-$ and CH_3 groups of the $OCH_2CH_2NMe_2$ ligands have been omitted for clarity. Associated O and N atoms are connected by dashed lines.[221]

1.11 Reactivity of triple bonds[162]

1.11.1 Bond order change from 3 to 2

Whilst the triple bond in compound $W_2(OBu^t)_6$ is cleaved with nitriles R'CN (R' = Ph or Me), and $W_2(OPr^i)_6(py)_2$ reacts with MeCN in the presence of Pr^iOH to form an imido-capped $W_3(\mu_3\text{-}NH)(OPr^i)_{10}$ compound, molybdenum alkoxides form 1:1 adducts with dimethyl- and diethylcyanamide $R'_2N\text{-}C{\equiv}N$ to give $Mo_2(OR)_6(NCNR'_2)$ compounds, one structure of which has shown that the Me_2NCN ligand spans the Mo-Mo bond indicating a Me_2NCN^{2-} ligand bonded to a $(Mo{=}Mo)^{8+}$ centre.

The molybdenum alkoxide compound $Mo_2(OPr^i)_6$ reacts with CO in the presence of pyridine to give the doubly bonded $Mo_2(OPr^i)_6(py)_2(\mu\text{-}CO)$.

1.11.2 Bond order change from 3 to 1

Alkynes react with $M_2(OR)_6$ compounds or their adducts $M_2(OR)_6L_2$ in hydrocarbon solvents at <25°C to give a wide variety of products. Alkyne adducts of formula $M_2(OR)_6(R'CCR')(py)n$ where n = 1 or 2 adopt one of the three structures below which may be regarded as dimetallatetrahedranes having M-M and C-C and four M-C bonds, all of roughly order unity, (Fig.1.15).

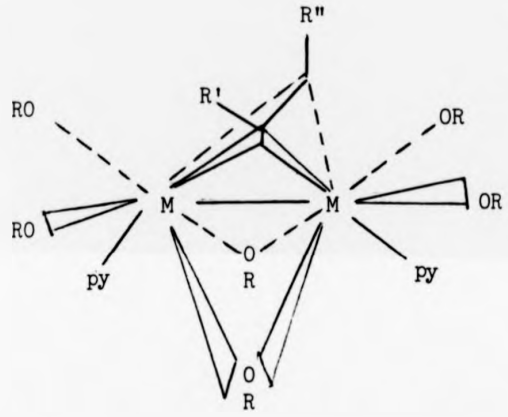

M=Mo or W R=Pr^i R'=R"=H

M = Mo R=Pr^i R'=H R"=Me

R'=R"=Me

M=Mo R=CH_2Bu^t R'=R"=H

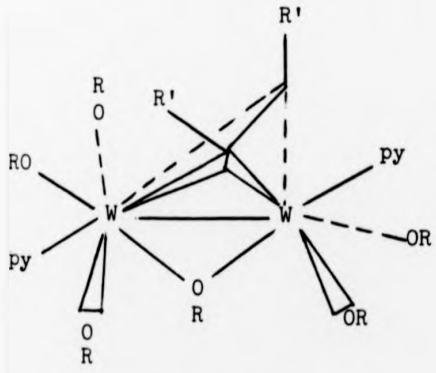

R=CH_2Bu^t R'=H or Me

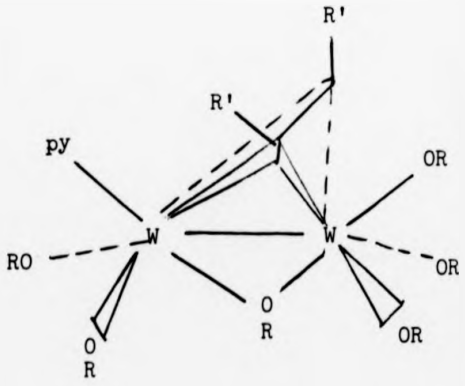

R=Bu^t R'=H

R=CH_2Bu^t R'=Et or Ph

Figure 1.15

1.12 Rhodium

In 1960 Chernyaev et al.[222] reported an extremely stable crystalline green compound, formulated as a rhodium(I) formate, $HRh(O_2CH)_2 . 0.5H_2O$, but this formulation was quickly retracted two years later[223] when the results of a preliminary X-ray diffraction study showed that the analogous acetato complex $[Rh_2(O_2CMe)_4(H_2O)_2]$, had a dimeric composition with four bridging acetate ligands and a Rh-Rh bond.[224] These were the first compounds in what was to become an enormous class of dimeric singly bonded Rh(II) compounds of the "lantern type", structure, (Fig.1.16).[223,225]

A convenient classification of Rh_2^{4+} complexes can be made according to the ligands that co-ordinate to the Rh atoms approximately perpendicular to the Rh-Rh bond. This classification includes three categories:

1. carboxylato-ligand complexes including carbonates and thiocarboxylates,
2. complexes containing bridging ligands other than carboxylates including sulphato, phosphato, 2-oxypyridine anions and bipyridine groups, and
3. complexes with ligands that do not span the Rh-Rh bond.[223,225]

The carboxylate compounds contain most of the shortest Rh-Rh bond lengths[223,225] and these range from 2.37 to 2.49 Å. A closely analogous thiocarboxylate compound has a Rh-Rh bond length of 2.55 Å. Non-carboxylate-ligand complexes, of which there are fewer examples, overlap with the Rh-Rh bond distances found for the carboxylates. The 2-oxypyridine complexes occupy the lower part of the carboxylate range (less than 2.39 Å) while the phosphato complex is found at the upper part of

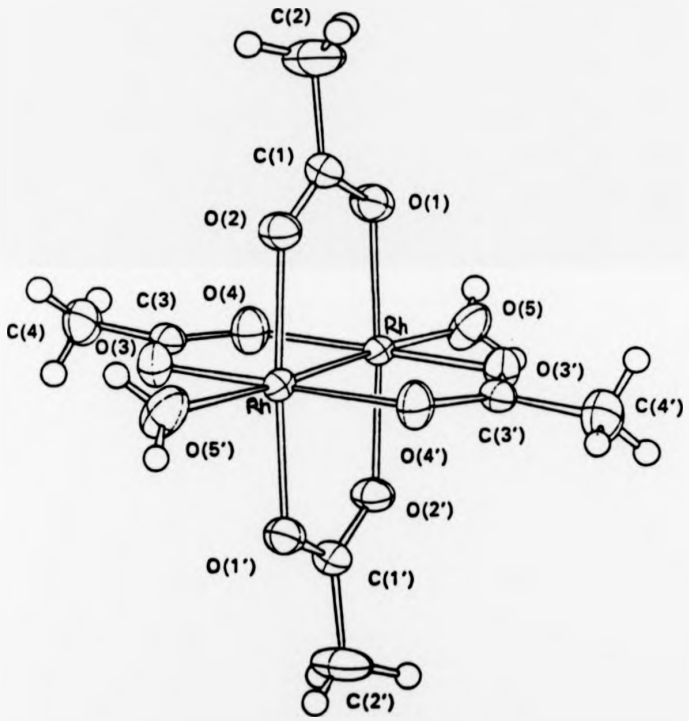

FIG. 1.16 Structure of $[Rh_2(O_2CMe)_4(H_2O)_2]$

the range (2.48 Å). A number of examples of tris- and bis-carboxylato complexes with the other ligands monodentate or bidentate non-bridging have been prepared with a bond length range of 2.47 to 2.64 Å.[223] The unbridged dirhodium complexes all exceed 2.60 Å[223] with the longest Rh-Rh bond distance between divalent ions found to be 2.94 Å in $[Rh_2(dmg)_4(PPh_3)_2]$.[226]

Compounds having the general formula $[Rh_2(O_2CR)_4L_2]$ were first prepared by refluxing salts of $[RhCl_6]^{3-}$ in an aqueous formic acid solution.[222] Dark green crystals of $[Rh_2(O_2CH)_4(H_2O)]$ were obtained.[227] Wilkinson et al. designed a synthesis which has become the standard preparative procedure for rhodium(II) acetate.[228] Refluxing red $RhCl_3$ solution for one hour produces a green solid of $[Rh_2(O_2CMe)_4]$.[228]

$$RhCl_3.3H_2O \xrightarrow[EtOH]{NaO_2CMe/MeCO_2H} Rh_2(O_2CMe)_4$$

Carboxylate exchange using the dirhodium tetraacetate has been used, as with the molybdenum carboxylates to generate other dirhodium tetracarboxylates. This has been well reviewed.[223]

The dimeric rhodium(II) carboxylates are air-stable compounds that, in direct contrast to the corresponding dimolybdenum(II) tetracarboxylates, readily form adducts with suitable donor ligands. Their thermal stability is dependent on both the carboxylate R group substituent and the identity of the axial ligand.[229,230,231] The trifluoroacetate compound sublimes near 350°C and mass spectral data reveal[231] that this dimer remains intact in the gas phase. The Rh_2^+ ion is detected in the mass spectrum at an m/e value of 206.

The initial structural report of $[Rh_2(O_2CMe)_4(H_2O)_2]$ in 1962 claimed a Rh-Rh distance of 2.45 Å[224] but when reinvestigated by Cotton et al. this distance was found to be 2.3855(5) Å.[232]

The "lantern type" structure in Fig.1.16 is isomorphous to the analogous Cr(II) and Cu(II) complexes.

The first trifluoroacetate complex of Rh_2^{4+} to be structurally characterized was $[Rh_2(O_2CCF_3)_4(EtOH)_2]$ in 1979.[233] Drago et al. showed in 1977[234] that the electron-withdrawing CF_3 group in carboxylate complexes could enhance the Lewis acidity of the axial site, enabling co-ordination by weakly basic ligands such as nitroxides. The 1:1 nitroxyl adduct of $[Rh_2(O_2CCF_3)_4]$ could be detected using e.p.r. spectroscopy, while the butyrate complex gave no such adduct in non-co-ordinating solvents. The enhanced acidity of $[Rh_2(O_2CCF_3)_4]$ over that of the alkyl carboxylates was further demonstrated in the first transition metal-sulphone complex $[Rh_2(O_2CCF_3)_4(Me_2SO_2)_2]$.[235] The weakly donating dimethyl sulphone ligand co-ordinates through one of the oxygen atom lone pairs.

Dimethylsulphoxide was one of the first adducts observed in $[Rh_2(O_2CR)_4L_2]$ complexes and has been much studied.[223] The Me_2SO molecule is ambidentate and while early studies[236] produced orange compounds, presumably co-ordinated through the sulphur atom, other work showed a blue complex, indicative of oxygen co-ordination.[230] Recent structural studies on $[Rh_2(O_2CR)_4(Me_2SO)_2]$ (R = Me, Et, CF_3) compounds have confirmed the ambidentate nature.[237,238] The structure of $[Rh_2(O_2CCF_3)_4(d_6\text{-}Me_2SO)_2]$ is not isomorphous to the Me_2SO analogue, differing in the packing arrangement of the binuclear molecules.[239] The axial Rh-O distance is the same but the Rh-Rh distance in the

deutero-molecule is 0.01 Å less than in the Me_2SO complex suggesting that crystal packing forces can account for changes in Rh-Rh distances as well as variation of axial ligands.[223] A recent structural study on $[Rh_2(O_2CMe)_4(HCONMe)_2]$ indicated that the Rh-Rh bond distance could be correlated with the acidity of the ligand L but only within the determined group of donors i.e. ligands co-ordinated by the same atom.[240]

Other sulphur donor axial adducts include alkyl sulphides,[230] thioethers,[237] thiols,[241] various adducts of thiourea,[242] benzothiadiazole,[243] $[SO_3]^{2-}$, $[S_2O_5]^{2-}$, and SO_2.[244]

In their early work, Charnyaev et al.[227,245] found that $Rh_2(O_2CR)_4$ compounds formed green products with alkali metal, ammonium and guanidinium halides in aqueous solution.[246]

Carboxylate compounds of Rh_2^{4+} that incorporate a functional group into the carboxylate side-chain have also been reported. Compounds have been described with $^{-}O_2C(CH_2)_nNH_2$, n = 1(glycinate),[247] 2(β-alaninate)[248] or 3(γ-aminobutyrate),[249] with mandelic,[250] glutaric,[251] α-aminopropionic,[251] and salicylic acid.[252] The vicinal optical activity of dirhodium(II) tetramandelate has been studied by electronic spectroscopy and circular dichroism.[253]

Nitrogen donor adducts of the rhodium(II) carboxylates constitute the largest class of compounds studied. These adducts present a wide range of basicities for bonding to the $Rh_2(O_2CR)_4$ nucleus but only recently have structural data been available from which to draw comparisons.[223] Although a preliminary analysis of the structural data for $NHEt_2$, py and H_2O adducts of $Rh_2(O_2CMe)_4$[254] suggested a linear correlation between the Rh-Rh distance and the pKb of the nitrogen donor adducts, examination of a wider range of $Rh_2(O_2CR)_4L_2$ structures suggests

that a simple correlation between the Rh-Rh bond length and the basicity of the axial ligand does not exist.[255]

Although it has been reported that MeCN interacts with $Rh_2(O_2CR)_4$ compounds to form violet adducts in solution,[256,257] the adducts have been reported to be unstable in the solid state, reverting to the green starting material on evaporation of the MeCN solvent.[256] Recently the first stable MeCN adduct $[Rh_2(2\text{-BPC})_4(NCMe)_2]$,[258] along with the acetonitrile[259] and benzonitrile[223] adducts of $[Rh_2(O_2CMe)_4]$ have been isolated.

Phosphorus donor adducts of $[Rh_2(O_2CR)_4]$ compounds constitute the most effective set of axial ligands in lengthening the Rh-Rh bond.[223] Recent structural evidence has reported adducts of PPh_3,[260,261] PF_3,[254] $P(OPh)_3$,[260,261] and $P(OMe)_3$,[254] with a variation in the Rh-Rh bond length of 2.4215(6) Å in $[Rh_2(O_2CMe)_4(PF_3)_2]$[254] to 2.486(1) Å in $[Rh_2(O_2CCF_3)_4(PPh_3)_2]$.[261]

An obvious way to release the bridging group constraints on the Rh-Rh bond is to reduce the number of bridging groups. Wilkinson *et al.* reported[262] in 1970 that protonation of $[Rh_2(O_2CMe)_4]$ occurs in aqueous and alcoholic media to give $Rh_2^{4+}(aq)$. Wilson and Taube later proposed that cationic species of lesser charge were formed, namely $[Rh_2(O_2CMe)_3]^{3+}(aq)$ and $[Rh_2(O_2CMe)_2]^{2+}(aq)$ in which water molecules occupy the equatorial positions.[263] Recently Telser and Drago investigated the action of strong non-complexing acids CF_3SO_3H and $HBF_4.Et_2O$ on acetonitrile solutions of $[Rh_2(O_2CCH_2CH_2Me)_4]$ and were able to characterize a complex proposed to be $[Rh_2(O_2CCH_2CH_2Me)_2]^{2+}$ in solution by ^1H and ^{13}C n.m.r. spectroscopy.[119] At around the same time Baranovskii *et al.*[264] found that the reaction of $[Rh_2(O_2CMe)_4]$ with trifluoromethanesulphonic acid

leads to $[Rh_2(O_2CMe)_3(CF_3SO_3)].nH_2O$ and $[Rh_2(O_2CMe)_2(CF_3SO_3)_2].nH_2O$ which, on dissolution in pyridine produced the crystalline products $[Rh_2(O_2CMe)_3(py)_4][CF_3SO_3]$ and $[Rh_2(O_2CMe)_2(py)_6][CF_3SO_3]_2$ with Rh-Rh bond lengths of 2.473(1) Å and 2.639(2) Å respectively. The bis-acetate structure possessed a cis-arrangement of acetate groups and was the first such complex with monodentate neutral equatorial groups.[264]

The first complex where one bridging acetate has been replaced by a neutral bridging ligand was that of $[Rh_2(O_2CMe)_3(bpnp)]^+$ prepared by reacting $[Rh_2(O_2CMe)_4]$ with one equivalent of HCl(aq) in the presence of bpnp.[265] Similar results have been achieved with other 1,8-naphthylidine derivatives according to:[266]

$$L + Rh_2(O_2CMe)_4 + HX \longrightarrow [Rh_2(O_2CMe)_3L]^+ + X^- + HO_2CMe$$

L = bpnp, dinp, pynp

$$2L + Rh_2(O_2CMe)_4 + 2HX \longrightarrow [Rh_2(O_2CMe)_2L_2]^{2+} + 2X^- + 2HO_2CMe$$

L = pynp

$$4L + Rh_2(O_2CMe)_4 + 4HX \longrightarrow Rh_2L_4X_4 + 4HO_2CMe$$

L = np

$[Rh_2(O_2CMe)_4(MeOH)_2]$ has been shown to react with PPh_3 in acetic acid leading to replacement of two of the acetate groups by PPh_3 in which ortho-metallation has occurred at one of the phenyl rings on each phosphine.[267] In this complex the dimetal unit is bridged, in a cisoid arrangement, by two acetate groups, and a similar stoichiometry is seen in the complex $[Rh_2(dmg)_2(O_2CMe)_2(PPh_3)_2]$[268] and in $[Rh_2(phen)_2(O_2CH)_2Cl_2]$.[50]

Recently, attention has been placed on amidato complexes of dirhodium, dimers being prepared including $[Rh_2(ONHCCF_3)_4]$,[269] $[Rh_2(ONHCCF_3)_4(py)_2]$[269] and some mixed ligand complexes $[Rh_2(ac)_n(acam)_{4-n}]$ (where ac = O_2CMe^-, acam = $HNOCMe^-$ and n varies between 0 and 4)[270] and their electrochemistry has been investigated (see later).

The first dirhodium(II) compound containing no bridging ligands was reported by Shchepinov in 1967[271] in the complex $[Rh_2(dmg)_4(PPh_3)_2]$ and a very long Rh-Rh bond length (2.936(2) Å) was apparent in the crystal structure.[226] Soon afterwards the aquorhodium(II) ion $Rh_2(H_2O)_{10}^{4+}$ was prepared by Maspero and Taube, characterized on the basis of reaction stoichiometry, similarity of its UV/visible spectrum to that of $[Rh_2(O_2CMe)_4(H_2O)_2]$ and magnetic susceptibility measurements.[272]

Mixed Valence Compounds

Electrolytic oxidation of $[Rh_2(O_2CMe)_4]$ in acid solution to give $[Rh_2(O_2CMe)_4]^+$ was first reported by Cannon *et al.* in 1976.[273] Solid compounds having the composition $[Rh_2(O_2CMe)_5]$ and $Rh_2(O_2CMe)_4Cl$ have been isolated, but these revert to $Rh_2(O_2CMe)_4$ in air.[273] Chemical oxidation of $Rh_2(O_2CMe)_4$ with ceric ion in sulphuric acid affords a crystalline compound after separation on a cation exchange column with $HClO_4$.[274] A structure determination of $[Rh_2(O_2CMe)_4(H_2O)_2][ClO_4]H_2O$ showed[275] it to be similar to that of the neutral compound except the Rh-Rh distance has decreased by 0.069(2) Å on going from the neutral to the oxidised species. Spectroscopic studies suggest a totally delocalised electronic structure with an average +2.5 valence state for each rhodium.[273] A similar reaction of $Rh_2(O_2CMe)_4$ with conc.

HNO_3 produces $[Rh_2(O_2CMe)_4(NO_3)]$ containing rhodium in oxidation states (II) and (III).[276]

Theoretical Calculations

The Rh-Rh bond in $[Rh_2(O_2CMe)_4(H_2O)_2]$ was first proposed to be a single one in the original crystal structure report by Porai-Koshits and Antsyshkina.[224] Later, Dubicki and Martin reported, on the basis of extended Hückel calculation that the electronic configuration for $[Rh_2(O_2CMe)_4(H_2O)_2]$ was $\pi^4\sigma^2\delta^2\delta^{*2}\pi^{*4}$ with a net single Rh-Rh σ-bond arising from this configuration.[277] Cotton et al. at the same time proposed[51,278] multiple Rh-Rh bonding by the filling of low lying non-bonding orbitals, giving the configuration $\sigma^2\pi^4\delta^2\sigma_n^2\sigma_n'^2\delta^{*2}$.

In 1978 Norman and Kolari reported their SCF-Xα-SW calculations on $Rh_2(O_2CH)_4$ and $Rh_2(O_2CH)_4(H_2O)_2$.[279] The energy level scheme is summarised in Fig.1.17. The 14 electrons in these d^7-d^7 dimers occupy all but the σ^* orbitals, giving a $\sigma^2\pi^4\delta^2\pi^{*4}\delta^{*2}$ configuration for $Rh_2(O_2CH)_4$. The non-bonding orbitals remain much higher in energy. The δ^* orbital lies higher in energy than the π^* orbitals apparently because of a strong interaction between the Rh d_{xy} orbitals and the carboxylate oxygen π orbitals that shifts the δ^* level above the π^* level in energy. The photoelectron spectrum of $Rh_2(mhp)_4$ has been recorded[280] and the assignments of the peaks support the $\sigma^2\pi^4\delta^2\pi^{*4}\delta^{*2}$ predicted in the Xα-SW calculations for $[Rh_2(O_2CH)_4]$.

The introduction of two water molecules along the Rh-Rh axis in $Rh_2(O_2CH)_4$ causes a lowering in the effective symmetry from D_{4h} to D_{2h}. Although the two oxygen π lone pairs on the H_2O molecules interact very little with the metal orbitals, the oxygen σ lone pair orbitals of the H_2O molecules perturb the Rh-Rh σ orbitals ($4a_{1g}$ and $5a_{1g}$; and the

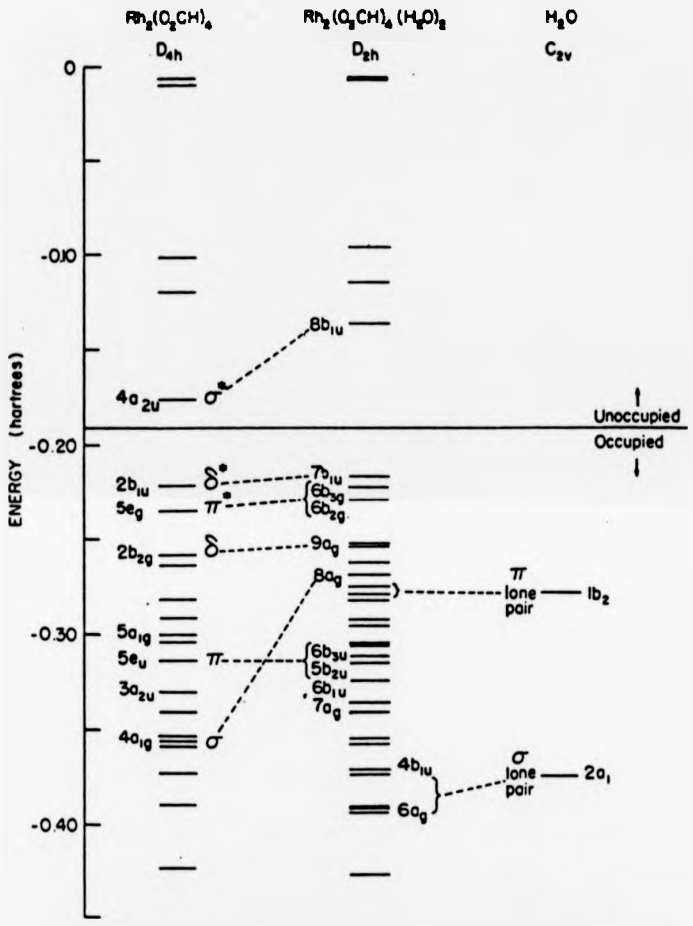

SCF energy levels for $Rh_2(O_2CH)_4$, $Rh_2(O_2CH)_4(H_2O)_2$, and H_2O above −0.49 hartree. The levels which best correlate with the σ, π, δ, δ^*, π^*, and σ^* components of the Rh–Rh bond, and with the in- and out-of-plane water lone pairs, are indicated. Mulliken symbols are given for the Rh-Rh levels, and in addition for all other levels of Rh-Rh and/or Rh-OH_2 σ and σ^* character (a_{1g} and a_{2u} levels for $Rh_2(O_2CH)_4$, a_g and b_{1u} for $Rh_2(O_2CH)_4(H_2O)_2$).

Figure 1.17

Rh-Rh σ^* orbitals ($3a_{2u}$ and the unoccupied $4a_{2u}$), shifting these levels to higher energies as shown in Fig.1.17. The effect of two H_2O σ lone pairs on the overall electronic structure of $[Rh_2(O_2CH)_4(H_2O)_2]$ is a mutual weakening of the Rh-OH_2 and Rh-Rh bonds.[279]

Chemical, electrochemical, and radiochemical oxidation of $[Rh_2(O_2CR)_4L_2]$ molecules produce $[Rh_2(O_2CR)_4L_2]^+$ ions which are paramagnetic with one unpaired electron delocalized over the binuclear cations.[223] Magnetic susceptibility data for $[Rh_2(O_2CMe)_4(H_2O)_2][ClO_4].H_2O$ display Curie Weiss behaviour with an average effective magnetic moment per binuclear complex of 2.18 ± 0.04 μ_B.[274]

E.p.r. studies on $[Rh_2(O_2CR)_4(PY_3)_2]^+$ ions in frozen solution have indicated that a significant amount of spin density is delocalized out onto the phosphine ligands, with the unpaired electron located in an orbital of Rh-Rh σ and Rh-P σ^* symmetry.[281] Ab initio SCF MO calculations on neutral $[Rh_2(O_2CR)_4L_2]$ complexes show the electronic configuration to be $\pi^4\delta^2\pi^{*4}\delta^{*2}\sigma^2$ for L absent, L = OH_2 and NH_3 and $\delta^2\pi^4\pi^{*4}\delta^{*2}\sigma^2$ for L = PH_3.[282]

Recently the electronic structures of $[Rh_2(O_2CH)_4L_2]$ and their cations with L absent and L = OH_2, NH_3 and PH_3 have been calculated by the ab initio, RHF, and UHF methods, the general state being calculated to be $\delta^2\pi^4\pi^{*4}\delta^{*2}\sigma^1$ for the cations with L = OH_2 and PH_3 while for L absent, the δ^* orbital is singly occupied.[283]

Investigations into adduct formation with 2,2,6,6-tetramethylpiperidinyl-1-oxy has provided a probe into the electronic composition of the axial Rh-O (nitroxide) bond via the unpaired spin density associated with the nitroxide adduct.[223] Back donation from the Rh d_{xy} orbital to the π^* orbital of the nitroxide was postulated as

well as ligand-metal σ donation and a comparison between such rhodium and molybdenum dimers illustrated the ability of the Rh-Rh single bond to propagate a sizeable exchange interaction between the co-ordinated nitroxyl groups compared to the inability of any interaction to develop across the Mo-Mo quadruple bond.[284]

Calorimetric studies of rhodium(II) butyrate have shown that there is a bonding interaction occurring between the metals and certain axial bases that could not be accounted for by a σ-only bond.[285] Comparison of the enthalpies of adduct formation with the observed changes in the visible spectrum and the electrochemical behaviour of 1:1 adducts were consistent with the interpretation that the anomalous bonding interaction involved a back-donation of π^*-electron density from high-energy rhodium antibonding molecular orbitals to axial ligands capable of acting as π-acceptors. Later investigations[286] of the $[Mo_2(O_2CC_3H_7)_4]$ dimer which lacks π^* electrons, showed that there was no corresponding bonding stabilisation over and above that predicted for a σ-only bond between acid and base. This differs from the conclusion arrived at concerning the previous e.p.r. results and theoretical calculations. A recent e.p.r. study on the 2:1 base adduct of $[Rh_2(O_2CR)_4]^+$ ions found that when the donor lone pair ionization potential is low and the interaction strong, the σ molecular orbital (arising when the donor lone pair is mixed into the 1:1 adduct) becomes the HOMO and an e.p.r. signal is detected. When the donor ionization potential is high and the interaction weak, the HOMO is π^* and no e.p.r. signal is seen.[287]

well as ligand-metal σ donation and a comparison between such rhodium and molybdenum dimers illustrated the ability of the Rh-Rh single bond to propagate a sizeable exchange interaction between the co-ordinated nitroxyl groups compared to the inability of any interaction to develop across the Mo-Mo quadruple bond.[284]

Calorimetric studies of rhodium(II) butyrate have shown that there is a bonding interaction occurring between the metals and certain axial bases that could not be accounted for by a σ-only bond.[285] Comparison of the enthalpies of adduct formation with the observed changes in the visible spectrum and the electrochemical behaviour of 1:1 adducts were consistent with the interpretation that the anomalous bonding interaction involved a back-donation of π^*-electron density from high-energy rhodium antibonding molecular orbitals to axial ligands capable of acting as π-acceptors. Later investigations[286] of the $[Mo_2(O_2CC_3H_7)_4]$ dimer which lacks π^* electrons, showed that there was no corresponding bonding stabilisation over and above that predicted for a σ-only bond between acid and base. This differs from the conclusion arrived at concerning the previous e.p.r. results and theoretical calculations. A recent e.p.r. study on the 2:1 base adduct of $[Rh_2(O_2CR)_4]^+$ ions found that when the donor lone pair ionization potential is low and the interaction strong, the σ molecular orbital (arising when the donor lone pair is mixed into the 1:1 adduct) becomes the HOMO and an e.p.r. signal is detected. When the donor ionization potential is high and the interaction weak, the HOMO is π^* and no e.p.r. signal is seen.[287]

Electrochemical Reactions

Numerous electrochemical studies have been performed on dirhodium(II) compounds.[223] The oxidation of $[Rh_2(O_2CMe)_4]$ in 0.1 M sulphuric acid occurs at a peak potential of 1.225(5) V versus NHE and is reversible. In contrast $Rh_{2(aq)}^{4+}$ displays no oxidation waves in the cyclic voltammogram.[263]

Das et al. found that $[Rh_2(O_2CR)_4]$ compounds undergo irreversible electroreduction to $[Rh_2(O_2CR)_4]^-$. The monoanion is unstable and is further reduced by at least one electron to the final complex.[256]

The electrochemical behaviour of $[Rh_2(O_2CR)_4L_2]$ complexes have been studied as a function of donor ligand L[256] and carboxylate group R.[256] Oxidation becomes more favourable as L becomes stronger, and high electron donating substituents such as CMe_3 favour oxidation to $[Rh_2(O_2CR)_4]^+$ at lower potentials than electron-withdrawing substituents such as CHClMe.[256]

Recently there have been several electrochemical studies of dimers with acetamidate ligands.[288,289] The dirhodium(II) complexes $[Rh_2(O_2CMe)_n(HNOCMe)_{4-n}]$ (where n = 0-4) have been studied and a uniform variation was observed[290] in the potentials for the first oxidation on increasing the number of acetamidate ligands in the dimer, from 1.17 V versus SCE for $[Rh_2(O_2CMe)_4]$ in MeCN to 0.15 V versus SCE for $[Rh_2(HNOCMe)_4]$ in MeCN.

Vibrational Spectra

Several Raman data have been reported for dimeric rhodium(II) compounds and values reported for the ν(Rh-Rh) stretching frequency in the region of 150-180 cm^{-1} and 288-351 cm^{-1} have been presented.[223,291]

A recent report by Gray et al.[292] assign the vibrations observed in the latter region to Rh-O stretches, preferring the assignment of ν(Rh-Rh) to the 150-170 cm^{-1} range.

UV/visible Spectra

The UV/visible spectra of these complexes have been extensively studied.[223] Martin et al. assigned the low energy band to the Rh-Rh π^* → Rh-Rh σ^* transition[293] on the basis of theoretical calculations performed by Norman and Kolari.[279] A second band at 450 nm was assigned to contain a transition due to that of Rh-Rh π^* → Rh-O σ^*.[293] The low energy band was observed to be dependent on the identity of the axial ligand L which correlates well with a transition to a σ^* orbital located along the L-Rh-Rh-L axis.[293]

Recently the visible spectra were reassigned where the low energy band was attributed to be due to the Rh-Rh π^* → Rh-O(carboxylate) σ^* transition with the 450 nm band assigned to the Rh-O π → Rh-O σ^* transition.[292]

N.m.r. Spectroscopic Studies

Surprisingly little n.m.r. work has been reported on rhodium(II) dimers. A few papers simply record data, others report the application of n.m.r. spectroscopy in the identification of co-ordination sites in ambidentate ligands (i.e. adenine and adenosine),[294,295] the investigation of carboxylate ligand exchange ($MeCO_2^-$, $CF_3CO_2^-$)[296,297] and the determination of magnetic moment in the rhodium(II,III) systems $[Rh_2(O_2CR)_4]^+$.[263]

Recently, a multinuclear (^1H, ^{13}C, ^{31}P and ^{103}Rh) variable-temperature n.m.r. study was reported on $[Rh_2(O_2CR)_4]$-$P(OR')_3$ systems (R = Me, Et, Pr, or Ph; R' = Me, Et or Ph).[298] Ambient temperature

spectra showed broad signals and were consistent with the establishment in solution of dynamic equilibria of the form $[\{(R'O)_3P\}Rh(O_2CR)_4Rh\{P(OR')_3\}] \rightleftharpoons [\{(R'O)_3P\}Rh(O_2CR)_4Rh(solv)] + P(OR')_3$ (solv = solvent). Low temperature (ca. 213 K) spectra of the same solutions show fully resolved resonances indicative of a frozen equilibrium mixture of mono and bis adducts plus free phosphorus-donor ligands. The large ^{31}P chemical shift difference (ca. 50-60 p.p.m.) between the mono and bis adducts points to the operation of a strong trans influence across the binuclear metal centre. This was confirmed by a study of ca. 30 mixed adducts $[\{(MeO)_3P\}Rh(O_2CMe)_4RhL]$ in which ^{31}P chemical shifts and ^2J (RhP) coupling constants have been employed to establish a trans-influence series for the ligands L.[298]

Recently, the ^{103}Rh n.m.r. spectrum of $[(Rh_2(mhp)_4)_2]$ was recorded, where the asymmetrical arrangement of the mhp ligands leads to inequivalent rhodium atoms.[299] The resonances are manifested as a pair of doublets centred at δ = ca. 7644 and 4322 p.p.m. The ^{103}Rh n.m.r. of the symmetrical molecule $Rh_2(mhp)_4$ was also recorded and a single resonance was observed at δ = 5745 p.p.m., a value close to the average of the chemical shifts (5984 p.p.m.) of the first two nuclei. The splitting of the ^{103}Rh resonances is ascribed to $^1J(^{103}Rh, ^{103}Rh)$ coupling, primarily as a result of a direct interaction via a metal-metal single bond and is the largest so far observed.[299]

Antitumour Activity

The discovery by Rosenberg et al. in 1969 that cis-$Pt(NH_3)_2Cl_2$ functions as a potent antitumour drug[300] prompted investigations into the platinum metals. In 1972 a report by Bear et al. showed that rhodium(II) carboxylates in combination with arabinosylcytosine increased survival times in tumour containing mice.[301]

Modifications of the basic structure have been found to give a slightly higher antitumour activity.[302] The poly (adenylic acid) adduct of $[Rh_2(O_2CEt)_4]$ and the singly oxidised $[Rh_2(O_2CEt)_4]^+$ complex both display greater activity than $[Rh_2(O_2CEt)_4]$ alone.[302] Extending the chain length of the R groups from methyl to n-butyl progressively produces compounds having higher antitumour activity but further lengthening decreases the activity.[303] These compounds inhibit DNA and protein synthesis in tumour cells but display little or no effect on RNA synthesis.[304] The mechanism for this inhibition is believed to involve the axial binding ability of the rhodium carboxylates, free amino groups and sulphhydryl groups from cysteine residues providing possible binding sites.[305] Recently, in a study of the reactivity of $Rh_2(O_2CMe)_4$ with selected di- and tripeptides, substituted pyridines and imidazole ligands it was found that, among the nitrogen bases present in proteins, the imidazole nitrogen is the preferred binding site.[306] The interaction of $[Rh_2(O_2CR)_4]$ with nucleic acid bases has been studied and a crystal structure of the rhodium acetate complex of 4-amino-5-(amino-methyl)-2-methylpyrimidine has recently been reported.[307] An EXAFS study of $[Rh_2(O_2CR)_4]$ complexes with five adenine nucleoside systems to elucidate the structural basis of the antineoplastic activity of such complexes had led to the conclusion that rhodium probably binds the purine at N_7 in the adenosine complex and at N_1 in the 8-bromoadenosine complex.[308]

Unfortunately in the rhodium(II) carboxylates the antitumour activity parallels the toxicity, the carboxylate cage structure being degraded on metabolism to give metallic rhodium, free acetate ions and CO_2.[309]

Chemical Reactivity

The reaction products of the interaction of $Rh_2(O_2CR)_4$ with acids depend on the identity of the conjugate base of the acid. Carboxylic, thiocarboxylic, sulphuric and orthophosphoric acids give bridged Rh_2^{4+} complexes.[223] Arenesulphinic acids (RSO_2H) however react with $Rh_2(O_2CMe)_4$ to give rhodium(III) complexes of the form $Rh(RSO_2)_3$.[310] HCl and HBr in the gas phase[311] and in acetone or ethanol solutions[312] decompose $[Rh_2(O_2CMe)_4]$ to produce a mixture of Rh metal and RhX_3 compounds (X = Cl or Br).

Sulphur donor ligands often lead to degradation of the carboxylate framework in $Rh_2(O_2CR)_4$ compounds. DMSO forms blue solutions with $Rh_2(O_2CCF_3)_4$ that eventually turn yellow, indicative of a Rh(III) species.[231] Acidic solutions of $Rh_2(O_2CMe)_4$ react with diethyldithiocarbamate (Et_2dtc) ligands in the presence of PPh_3 to yield $[Rh(Et_2dtc)_2(PPh_3)_2][BF_4]$.[313] Thioacetic acid exchanges with acetate in $[Rh_2(O_2CMe)_4)$ producing $[Rh_2(OSCMe)_4]$ compounds.[314] With dithioacetic acid the Rh-Rh bond is cleaved giving a mixture of products including $Rh(S_2CMe)_3$.[315] $[Rh_2(O_2CMe)_4(H_2O)_2]$ and $[Rh_2(O_2CH)_4]$ react with K_2SO_3, $K_2S_2O_5$ and SO_2 to initially form adducts $K_4[Rh_2(O_2CMe)_4(SO_3)_2].4H_2O$ and $K_2[Rh_2(O_2CH)_4(HSO_3)_2].4H_2O$ but heating or letting the solutions stand for a longer time leads to complete replacement of the carboxylate groups by sulphito groups giving polynuclear Rh(III) compounds $K_4Rh_2(SO_3)_5.6H_2O$, $K_3Rh_2(SO_3)_{4,5}.8H_2O$ and $CsRh(SO_3)_2.2H_2O$.[244]

Phosphine ligands displace carboxylate ligands in $Rh_2(O_2CR)_4$ to afford both Rh(I) and Rh(III) products. HBF_4-MeOH solutions of $Rh_2(O_2CMe)_4$ are reduced by excess PPh_3 to give $Rh(PPh_3)_3BF_4$ which was characterized by analysis and infrared spectroscopy.[313] PMe_3 reacts with $Rh_2(O_2CMe)_4$ in methanol to give fac-$Rh(PMe_3)_3(H)(O_2CMe)_2$.[203]

Reaction of $Rh_2(O_2CCF_3)_4$ with pyridine led to the isolation of 4:1 adducts proposed to contain both axially and equatorially co-ordinated Lewis bases. With N-methylimidazole and piperidine an axial adduct forms followed by decomposition of the dimer. Reaction of t-BuNC with $Rh_2(O_2CMe)_4$ gives the axial adduct $[Rh_2(O_2CMe)_4(t\text{-BuNC})_2]$. Reaction, however, with $Rh_2(O_2CCF_3)_4$ does not yield an axial adduct but a complex formulated as $[Rh_2(O_2CCF_3)_4(t\text{-BuNC})_4]$ with t-BuNC claimed to be equatorially co-ordinated. Reaction of $Rh_2(O_2CCF_3)_4$ with PMe_2Ph, PPh_3 and $P(OMe)_3$ resulted in dimer cleavage and Rh(I) and Rh(III) compounds.[316]

The reactivity of quadruply bonded molybdenum and singly bonded rhodium dimers has been investigated but not to any significant extent. The products have been mainly monomeric resulting from total bond cleavage, in contrast to the reactivity of triple bonds where successive oxidative addition leads to a stepwise reduction in bond order. Replacement of some of the sterically hindering carboxylate groups with more labile, monomeric ligands was sought with a view to investigating the reactivity of these potentially labile compounds and thus extend the reactivity patterns of quadruple and single bonds.

REFERENCES

1. E. Peligot, C.R. Acad.Sci., 1844, 19, 609.
2. F.A. Cotton, N.F. Curtis, C.B. Harris, B.F.G. Johnson, S.J. Lippard, J.T. Mague, W.R. Robinson, and J.S. Wood, Science, 1964, 145, 1305.
3. G.B. Kauffman, Co-ord.Chem.Rev., 1973, 9, 339.
4. M.C. Chabrie, C.R.Acad.Sci., 1907, 144, 804.
5. H.S. Harned, J.Am.Chem.Soc., 1913, 35, 1078.
6. K. Lindner, Zeits.anorg.allg.Chem., 1927, 162, 203.
7. C. Brosset, Ark.Kemi, Miner.Geol., 1946, A20(7).
8. P.A. Vaughan, J.H. Sturdivant, and L. Pauling, J.Am.Chem.Soc., 1950, 72, 5477.
9. J.A. Bertrand, F.A. Cotton, and W.A. Dollase, J.Am.Chem.Soc., 1963, 85, 1349.
10. W.T. Robinson, J.E. Fergusson, and B.R. Penfold, Proc.Chem.Soc., 1963, 116.
11. Multiple Bonds between Metal Atoms, F.A. Cotton and R.A. Walton, Wiley Interscience, 1982.
12. F.A. Cotton, S.J. Lippard, and J.T. Mague, Inorg.Chem., 1965, 4, 508.
13. V.G. Tronev and S.M. Bondin, Khim.Redk.Elem.Akad.Nauk SSSR, 1954, 1, 40.
14. F.A. Cotton and B.F.G. Johnson, Inorg.Chem., 1964, 3, 780.
15. A.S. Kotel'Nikova and V.G. Tronev, Russ.J.Inorg.Chem., 1958, 3, 268.
16. V.G. Kuznetzov and P.A. Koz'Min, J.Struct.Chem., 1963, 4, 49.
17. F.A. Cotton, N.F. Curtis, C.B. Harris, B.F.G. Johnson, S.J. Lippard, J.T. Mague, W.R. Robinson, and J.S. Wood, Science, 1964, 145, 1305.
18. F.A. Cotton, Inorg.Chem., 1965, 4, 334.
19. G. Peters and W. Preetz, Z.Naturforsch., 1979, 34b 1767.
20. J.V. Brencic and F.A. Cotton, Inorg.Chem., 1969, 8, 7.
21. J.V. Brencic, I. Leban, and P. Segedin, Z.anorg.allg.Chem., 1976, 427, 85.

22. W. Preetz and L. Rudzik, Angew.Chem., Int.Ed.Engl., 1979, 18, 150.

23. A. Bino, F.A. Cotton, and P.E. Fanwick, Inorg.Chem., 1979, 18, 3558.

24. J. San Filippo, Jr., H.J. Snaidoch, and R.L. Grayson, Inorg.Chem., 1974, 13, 2121.

25. P. Agaskar and F.A. Cotton, Inorg.Chim.Acta, 1984, 83, 33.

26. J.V. Brencic, L. Golic, and P. Segedin, Inorg.Chim.Acta, 1982, 57, 247.

27. J.A. Potenza, R.J. Johnson and J. San Filippo, Jr., Inorg.Chem., 1976, 15, 2215.

28. F.A. Cotton, J.M. Troup, T.R. Webb, D.H. Williamson, and G. Wilkinson, J.Am.Chem.Soc., 1974, 96, 3824.

29. M.H. Chisholm and D.A. Haitko, J.Am.Chem.Soc., 1979, 101, 6784.

30. K.J. Ahmed, M.H. Chisholm, I.P. Rothwell, and J.C. Hoffman, J.Am.Chem.Soc., 1982, 104, 6453.

31. R.A. Jones, J.G. Lasch, N.C. Norman, B.R. Whittlesey, and T.C. Wright, J.Am.Chem.Soc., 1983, 105, 6184.

32. M.H. Chisholm, F.A. Cotton, B.A. Frenz, W.W. Reichert, L.W. Shive, and B.R. Stults, J.Am.Chem.Soc., 1976, 98, 4469.

33. M.H. Chisholm, F.A. Cotton, M. Extine, and B.R. Stults, J.Am.Chem.Soc., 1976, 98, 4477.

34. M.H. Chisholm, W.W. Reichert, F.A. Cotton, and C.A. Murillo, J.Am.Chem.Soc., 1977, 99, 1652.

35. M. Akiyama, M.H. Chisholm, F.A. Cotton, M.W. Extine, D.A. Haitko, D. Little, and P.E. Fanwick, Inorg.Chem., 1979, 18, 2266.

36. M.H. Chisholm, K. Folting, J.C. Huffman, and R.J. Tatz, J.Am.Chem.Soc., 1984, 106, 1153.

37. R.A. Walton, Reactivity of Metal-Metal Bonds ACS Symp.Ser., 1981, 155, 207.

38. M.H. Chisholm and I.P. Rothwell, Chemical Reactions of Metal-Metal Bonded Compounds of the Transition Metals, Prog.Inorg.Chem., 1982, 29, 1.

39. W.S. Harwood, Ju-Sheng Qi, and R.A. Walton, Polyhedron, 1986, 5, 15.

40. T.J. Barder, F.A. Cotton, L.R. Falvello, and R.A. Walton, Inorg.Chem., 1985, 24, 1258.

41. K.R. Dunbar, D. Powell, and R.A. Walton, Inorg.Chem., 1985, 24, 2842.

22. W. Preetz and L. Rudzik, Angew.Chem., Int.Ed.Engl., 1979, 18, 150.

23. A. Bino, F.A. Cotton, and P.E. Fanwick, Inorg.Chem., 1979, 18, 3558.

24. J. San Filippo, Jr., H.J. Snaidoch, and R.L. Grayson, Inorg.Chem., 1974, 13, 2121.

25. P. Agaskar and F.A. Cotton, Inorg.Chim.Acta, 1984, 83, 33.

26. J.V. Brencic, L. Golic, and P. Segedin, Inorg.Chim.Acta, 1982, 57, 247.

27. J.A. Potenza, R.J. Johnson and J. San Filippo, Jr., Inorg.Chem., 1976, 15, 2215.

28. F.A. Cotton, J.M. Troup, T.R. Webb, D.H. Williamson, and G. Wilkinson, J.Am.Chem.Soc., 1974, 96, 3824.

29. M.H. Chisholm and D.A. Haitko, J.Am.Chem.Soc., 1979, 101, 6784.

30. K.J. Ahmed, M.H. Chisholm, I.P. Rothwell, and J.C. Hoffman, J.Am.Chem.Soc., 1982, 104, 6453.

31. R.A. Jones, J.G. Lasch, N.C. Norman, B.R. Whittlesey, and T.C. Wright, J.Am.Chem.Soc., 1983, 105, 6184.

32. M.H. Chisholm, F.A. Cotton, B.A. Frenz, W.W. Reichert, L.W. Shive, and B.R. Stults, J.Am.Chem.Soc., 1976, 98, 4469.

33. M.H. Chisholm, F.A. Cotton, M. Extine, and B.R. Stults, J.Am.Chem.Soc., 1976, 98, 4477.

34. M.H. Chisholm, W.W. Reichert, F.A. Cotton, and C.A. Murillo, J.Am.Chem.Soc., 1977, 99, 1652.

35. M. Akiyama, M.H. Chisholm, F.A. Cotton, M.W. Extine, D.A. Haitko, D. Little, and P.E. Fanwick, Inorg.Chem., 1979, 18, 2266.

36. M.H. Chisholm, K. Folting, J.C. Huffman, and R.J. Tatz, J.Am.Chem.Soc., 1984, 106, 1153.

37. R.A. Walton, Reactivity of Metal-Metal Bonds ACS Symp.Ser., 1981, 155, 207.

38. M.H. Chisholm and I.P. Rothwell, Chemical Reactions of Metal-Metal Bonded Compounds of the Transition Metals, Prog.Inorg.Chem., 1982, 29, 1.

39. W.S. Harwood, Ju-Sheng Qi, and R.A. Walton, Polyhedron, 1986, 5, 15.

40. T.J. Barder, F.A. Cotton, L.R. Falvello, and R.A. Walton, Inorg.Chem., 1985, 24, 1258.

41. K.R. Dunbar, D. Powell, and R.A. Walton, Inorg.Chem., 1985, 24, 2842.

42. F.A. Cotton, B.A. Frenz, E. Pedersen, and T.R. Webb, Inorg.Chem., 1975, 14, 391.

43. A. Bino and F.A. Cotton, Inorg.Chem., 1979, 18, 3562.

44. K.A. Alexander, S.A. Bryan, F.R. Fronczek, W.C. Fultz, A.L. Rheingold, D.M. Roundhill, P. Stein, and S.F. Watkins, Inorg.Chem., 1985, 24, 2803.

45. F.A. Cotton and T.R. Felthouse, Inorg.Chem., 1980, 19, 320.

46. A.R. Bowen and H. Taube, Inorg.Chem., 1974, 13, 2245.

47. S.A. Best, T.J. Smith, and R.A. Walton, Inorg.Chem., 1978, 17, 99.

48. D.M. Collins, F.A. Cotton, and C.A. Murillo, Inorg.Chem., 1976, 15, 1861.

49. S. Cenini, R. Ugo, and F. Bonati, Inorg.Chim.Acta, 1967, 1, 443.

50. H. Pasternak and F. Pruchnik, Inorg.Nucl.Chem.Lett., 1976, 12, 591.

51. A.T. Baker, W.R. Tikkanen, W.C. Kaska, and P.C. Ford, Inorg.Chem., 1984, 23, 3254.

52. D. Lawton and R. Mason, J.Am.Chem.Soc., 1965, 87, 921.

53. J.V. Brencic and F.A. Cotton, Inorg.Chem., 1969, 8, 2698.

54. G. Albrecht and D. Stock, Z.Chem., 1967, 7, 32.

55. J. Krausse, G. Marx, and G. Schödl, J.Organomet.Chem., 1970, 21, 159.

56. F.A. Cotton, B.G. De Boer, M.D. La Prade, J.R. Pipal, and D.A. Ucko, Acta.Cryst., 1971, B27, 1664.

57. F.A. Cotton, S. Koch, and M. Millar, J.Am.Chem.Soc., 1977, 99, 7372.

58. T.A. Stephenson, E. Bannister, and G. Wilkinson, J.Chem.Soc., 1964, 2538.

59. F.A. Cotton and M. Jeremic, Synth.Inorg.Met.Org.Chem., 1971, 1, 265.

60. F.A. Cotton, S. Koch, K. Mertis, M. Millar, and G. Wilkinson, J.Am.Chem.Soc., 1977, 99, 4989.

61. F.A. Cotton, P.E. Fanwick, R.H. Niswander, and J.C. Sekutowski, J.Am.Chem.Soc., 1978, 100, 4725.

62. I.B. Walton, Ph.D. Thesis, Manchester University, 1979.

63. M.H. Al-Samman, Ph.D. Thesis, Manchester University, 1981.

64. F.A. Cotton, N.F. Curtis, B.F.G. Johnson, and W.R. Robinson, Inorg.Chem., 1965, 4, 326.

65. F.A. Cotton, N.F. Curtis, and W.R. Robinson, Inorg.Chem., 1965, 4, 1696.

66. T.J. Barder and R.A. Walton, Inorg.Chem., 1982, 21, 2510.

67. F.A. Cotton, B.G. De Boer, and M. Jeremic, Inorg.Chem., 1970, 9, 2143.

68. F.A. Cotton, N.F. Curtis, B.F.G. Johnson, and W.R. Robinson, Inorg.Chem., 1965, 4, 326.

69. F.A. Cotton, C. Oldham, and R.A. Walton, Inorg.Chem., 1967, 6, 214.

70. F.A. Cotton, L.D. Gage, and C.E. Rice, Inorg.Chem., 1979, 18, 1138.

71. A.R. Chakravarty, F.A. Cotton, A.R. Cutler, S.M. Tetrick, and R.A. Walton, J.Am.Chem.Soc., 1985, 107, 4795.

72. A.P. Mortola, J.W. Moskowitz, N. Rösch, C.D. Cowman, and H.B. Gray, Chem.Phys.Lett., 1975, 32, 283.

73. B.E. Bursten, F.A. Cotton, P.E. Fanwick, and G.G. Stanley, J.Am.Chem.Soc., 1983, 105, 3082.

74. R.S. Mulliken, J.Chem.Phys., 1939, 7, 20.

75. C.D. Cowman and H.B. Gray, J.Am.Chem.Soc., 1973, 95, 8177.

76. H.W. Huang and D.S. Martin, Inorg.Chem., 1985, 24, 96.

77. D.S. Martin, H.W. Huang, and R.A. Newman, Inorg.Chem., 1984, 23, 699.

78. K. Schwochau, K. Hedwig, H.J. Schenk, and O. Greis, Inorg.Nucl. Chem.Lett., 1977, 13, 77.

79. J.D. Eakins, D.G. Humphreys, and C.E. Mellish, J.Chem.Soc., 1963, 6012.

80. W.K. Bratton and F.A. Cotton, Inorg.Chem., 1970, 9, 789.

81. F.A. Cotton and E. Pedersen, Inorg.Chem., 1975, 14, 383.

82. J.R. Ebner and R.A. Walton, Inorg.Chem., 1975, 14, 1987.

83. F.A. Cotton, B.A. Frenz, J.R. Ebner, and R.A. Walton, Inorg.Chem., 1976, 15, 1630.

84. F.A. Cotton and E. Pedersen, Inorg.Chem., 1975, 14, 383.

85. W. Preetz and G. Peters, Z.Naturforsch, 1980, 35b, 797.

86. F.A. Cotton, L. Daniels, A. Davison, and C. Orvig, Inorg.Chem., 1981, 20, 3051.

87. F.A. Cotton, A. Davison, V.W. Day, M.F. Fredrich, C. Orvig, and R. Swanson, Inorg.Chem., 1982, 21, 1211.

88. F.A. Cotton, K.R. Dunbar, L.R. Falvello, M. Tomas, and R.A. Walton, J.Am.Chem.Soc., 1983, 105, 4950.

89. F.A. Cotton and L.D. Gage, Nouv.J.Chim., 1977, 1, 441.

90. V.I. Nefedov and P.A. Kozmin, Inorg.Chim.Acta, 1982, 64, L177.

91. L.R. Ocone and B.P. Block, "Inorganic Syntheses", Vol.8, McGraw-Hill, New York, 1966, pp.125-130.

92. F.A. Cotton and J.L. Thompson, Inorg.Chem., 1981, 20, 1292.

93. N.V. Gerbeleu, G.A. Popovich, K.M. Indrichan, and G.A. Timko, Russ.J.Inorg.Chem., 1983, 28, 1720.

94. F.A. Cotton and G.W. Rice, Inorg.Chem., 1978, 17, 2004.

95. F.A. Cotton, M.W. Extine, and G.W. Rice, Inorg.Chem., 1978, 17, 176.

96. F.A. Cotton and W. Wang, Nouv.J.Chim., 1984, 5, 331.

97. F.A. Cotton, W.H. Ilsley, and W.J. Kaim, J.Am.Chem.Soc., 1980, 102, 3464.

98. F.A. Cotton and W. Wang, submitted for publication in Nouv.J.Chim., reported in paper by R.A. Kok and M.B. Hall, Inorg.Chem., 1985, 24, 1542.

99. R.A. Kok and M.B. Hall, Inorg.Chem., 1985, 24, 1542.

100. M. Berry, C.D. Garner, I.H. Hillier, A.A. MacDowell, and I.B. Walton, Chem.Phys.Lett., 1980, 70, 350.

101. F.A. Cotton, L.R. Falvello, S. Han, and W. Wang, Inorg.Chem., 1983, 22, 4106.

102. F.A. Cotton, S.A. Koch, and M. Millar, Inorg.Chem., 1978, 17, 2084.

103. F.A. Cotton, W.H. Ilsley, and W. Kaim, Inorg.Chem., 1979, 18, 2717.

104. F.A. Cotton, Z.C. Mester, and T.R. Webb, Acta Cryst., 1974, B30, 2768.

105. J.V. Brencic and F.A. Cotton, Inorg.Chem., 1969, 8, 7.

106. F.A. Cotton and J.G. Norman, Jr., J.Co-ord.Chem., 1971, 1, 161.

107. E. Hochberg, P. Walks, and E.H. Abbott, Inorg.Chem., 1974, 13, 1824.

108. R.J. Mureinik, J.Inorg.Nucl.Chem., 1976, 38, 1275.

109. P.A. Koz'Min, M.D. Surazhskaya, and T.B. Larina, Russ.J.Inorg.Chem., 1980, 25, 702.

110. D.M. Collins, F.A. Cotton, and C.A. Murillo, Inorg.Chem., 1976, 15, 2950.

111. F.A. Cotton and J.G. Norman, Jr., J.Am.Chem.Soc., 1972, 94, 5697.

112. C.D. Garner and R.G. Senior, J.Chem.Soc., Dalton Trans., 1975, 1171.

113. J. San Filippo, Jr., and H.J. Snaidoch, Inorg.Chem., 1976, 15, 2209.

114. G. Holste, Z.anorg.allg.Chem., 1978, 438, 125.

115. W. Clegg, C.D. Garner, S. Parkes, and I.B. Walton, Inorg.Chem., 1979, 18, 2250.

116. C.D. Garner, S. Parkes, I.B. Walton, and W. Clegg, Inorg.Chim.Acta, 1978, 31, L451.

117. C.D. Garner and R.G. Senior, J.Chem.Soc., Dalton Trans., 1976, 1041.

118. J.D. Arenivar, V.V. Mainz, H. Ruben, R.A. Andersen, and A. Zalkin, Inorg.Chem., 1982, 21, 2649.

119. J. Telser and R.S. Drago, Inorg.Chem., 1984, 23, 1798.

120. P.A. Agaskar, F.A. Cotton, D.R. Derringer, G.L. Powell, D.R. Root, and T.J. Smith, Inorg.Chem., 1985, 24, 2786.

121. P.A. Agaskar and F.A. Cotton, I.F. Fraser, and R.D. Peacock, J.Am.Chem.Soc., 1984, 106, 1851.

122. F.L. Campbell, III, F.A. Cotton, and G.L. Powell, Inorg.Chem., 1984, 23, 4222.

123. F.L. Campbell, III, F.A. Cotton, and G.L. Powell, Inorg.Chem., 1985, 24, 177.

124. M.D. Hopkins, T.C. Zietlow, V.M. Miskowski, and H.B. Gray, J.Am.Chem.Soc., 1985, 107, 510.

125. J.P. Collman and L.K. Woo, Proc.Natl.Acad.Sci., USA, 1984, 81, 2592.

126. A.R. Bowen and H. Taube, J.Am.Chem.Soc., 1971, 93, 3287.

127. R.D. Peacock and I.F. Fraser, Inorg.Chem., 1985, 24, 988.

128. J.M. Mayer and E.H. Abbott, Inorg.Chem., 1983, 22, 2774.

129. M.J. Chetcuti, M.H. Chisholm, K. Folting, D.A. Haitko, and J.C. Huffman, J.Am.Chem.Soc., 1982, 104, 2138.

130. J.G. Norman, Jr. and H.J. Kolari, J.Am.Chem.Soc., 1975, 97, 33.

131. M. Benard, J.Am.Chem.Soc., 1978, 100, 2354.

132. J.G. Norman, Jr., H.J. Kolari, H.B. Gray, and W.C. Trogler, Inorg.Chem., 1977, 16, 987.

133. A.W. Coleman, J.C. Green, A.J. Hayes, E.A. Seddon, D.R. Lloyd, and Y. Niwa, J.Chem.Soc., Dalton Trans., 1979, 1057.

134. J.C. Green, A.J. Hayes, Chem.Phys.Lett., 1975, 31, 306.

135. P.M. Atha, I.H. Hillier, and M.F. Guest, Mol.Phys., 1982, 46, 437.

136. J.G. Norman, H.J. Kolari, H.B. Gray, and W.C. Trogler, Inorg.Chem., 1977, 16, 987.

137. D.L. Lichtenberger and C.H. Blevins, II, J.Am.Chem.Soc., 1984, 106, 1636.

138. F.A. Cotton, D.S. Martin, P.E. Fanwick, T.J. Peters, and T.R. Webb, J.Am.Chem.Soc., 1976, 98, 4681.

139. P.E. Fanwick, D.S. Martin, F.A. Cotton, and T.R. Webb, Inorg.Chem., 1977, 16, 2103.

140. L. Dubicki and R.L. Martin, Aust.J.Chem., 1969, 22, 1571.

141. F.A. Cotton, D.S. Martin, T.R. Webb, and T.J. Peters, Inorg.Chem., 1976, 15, 1199.

142. J.G. Norman and H.J. Kolari, J.Chem.Soc., Chem.Comm., 1975, 649.

143. D.S. Martin, R.A. Newman , and P.E. Fanwick, Inorg.Chem., 1979, 18, 2511.

144. M.C. Manning and W.C. Trogler, Inorg.Chem., 1982, 21, 2797.

145. D.S. Martin, R.A. Newman, and P.E. Fanwick, Inorg.Chem., 1982, 21, 3400.

146. P.E. Fanwick, Inorg.Chem., 1985, 24, 258.

147. M.C. Manning and W.C. Trogler, J.Am.Chem.Soc., 1983, 105, 5311.

148. P.E. Fanwick, B.E. Bursten, and G.B. Kaufmann, Inorg.Chem., 1985, 24, 1165.

149. I.F. Fraser and R.D. Peacock, Chem.Phys.Lett., 1983, 98, 620.

150. M.D. Hopkins and H.B. Gray, J.Am.Chem.Soc., 1984, 106, 2468.

151. A.P. Sattelberger and J.P. Fackler, J.Am.Chem.Soc., 1977, 99, 1258.

152. F.A. Cotton, S. Koch, K. Mertis, M. Millar, and G. Wilkinson, J.Am.Chem.Soc., 1977, 99, 4989.

153. R.J.H. Clark and N.R. D'Urso, J.Am.Chem.Soc., 1978, 100, 3088.

154. W.J. Bratton, F.A. Cotton, M. Debeau, and R.A. Walton, J.Co-ord. Chem., 1971, 1, 121.

155. C. Oldham, J.E.D. Davies, and A.P. Ketteringham, J.Chem.Soc., Chem.Comm., 1971, 572.

156. B. Hutchinson, J. Morgan, C.B. Cooper, Y. Mathey, and D.F. Shriver, Inorg.Chem., 1979, 18, 2048.

157. M.C. Manning, G.F. Holland, D.E. Ellis, and W.C. Trogler, J.Phys.Chem., 1983, 87, 3083.

158. R.J.H. Clark and M.J. Stead, Inorg.Chem., 1983, 22, 1214.

159. R.A. Grieves and J. Mason, Polyhedron, 1986, 5, 415.

160. S.F. Gheller, T.W. Hambley, R.T.C. Brownlee, M.J. O'Connor, M.R. Snow, and A.G. Wedd, J.Am.Chem.Soc., 1983, 105, 1527.

161. B.P. Shehan, M. Kony, R.T.C. Brownlee, M.J. O'Connor, and A.G. Wedd, J.Magn.Reson., 1985, 63, 343.

162. M.H. Chisholm, D.M. Hoffman, and J.C. Huffman, Chem.Soc.Rev., 1985, 14, 69.

163. D.M. Collins, F.A. Cotton, S.A. Koch, M. Millar, and C.A. Murillo, J.Am.Chem.Soc., 1977, 99, 1259.

164. D.M. Collins, F.A. Cotton, S.A. Koch, M. Millar, and C.A. Murillo, Inorg.Chem., 1978, 17, 2017.

165. F.A. Cotton, R.H. Niswander, and J.C. Sekutowski, Inorg.Chem., 1978, 17, 3541.

166. F.A. Cotton, R.H. Niswander, and J.C. Sekutowski, Inorg.Chem., 1979, 18, 1152.

167. F.A. Cotton, W.H. Ilsley, and W. Kaim, Inorg.Chem., 1980, 19, 1453.

168. F.A. Cotton, W.H. Ilsley, and W. Kaim, Inorg.Chem., 1979, 18, 3569.

169. F.A. Cotton, W.H. Ilsley, and W. Kaim, Inorg.Chem., 1980, 19, 1450.

170. F.A. Cotton, L.R. Falvello, S. Han, and W. Wang, Inorg.Chem., 1983, 22, 4106.

171. P.R. Sharp and R.R. Schrock, J.Am.Chem.Soc., 1980, 102, 1430.

172. F.A. Cotton and T.R. Felthouse, Inorg.Chem., 1981, 20, 3880.

173. A. Bino, F.A. Cotton, Z. Dori, S. Koch, H. Kippers, M. Millar, and J.C. Sekutowski, Inorg.Chem., 1978, 17, 3245.

174. A.P. Sattelberger, K.W. McLaughlin, and J.C. Huffman, J.Am.Chem.Soc., 1981, 103, 2880.

175. D.J. Santure, J.C. Huffman, and A.P. Sattelberger, Inorg.Chem., 1985, 24, 371.

176. F.A. Cotton and W. Wang, Inorg.Chem., 1982, 21, 3859.

177. F.A. Cotton and W. Wang, Inorg.Chem., 1984, 23, 1604.

178. M.H. Chisholm, H.T. Chiu, and J.C. Huffman, Polyhedron, 1984, 3, 759.

179. F.A. Cotton, G.N. Mott, R.R. Schrock, and L.G. Sturgeoff, J.Am.Chem.Soc., 1982, 104, 6781.

180. R.R. Schrock, L.G. Sturgeoff, and P.R. Sharp, Inorg.Chem., 1983, 22, 2801.

181. D.J. Santure, J.C. Huffman, and A.P. Sattelberger, Inorg.Chem., 1984, 23, 938.

182. D.J. Santure, K.W. McLaughlin, J.C. Huffman, and A.P. Sattelberger, Inorg.Chem., 1983, 22, 1877.

183. M.H. Chisholm, D.M. Hoffman, J.C. Huffman, W.G. Van Der Sluys, and S.Russo, J.Am.Chem.Soc., 1984, 106, 5386.

184. M.H. Chisholm, F.A. Cotton, M.W. Extine, and B.R. Stults, Inorg.Chem., 1978, 17, 603.

185. M.D. Braydich, B.E. Bursten, M.H. Chisholm, and D.L. Clark, J.Am.Chem.Soc., 1985, 107, 4459.

186. G.M. Bancroft, E. Pellach, A.P. Sattelberger, and K.W. McLaughlin, J.Chem.Soc., Chem.Comm., 1982, 752.

187. T. Ziegler, J.Am.Chem.Soc., 1985, 107, 4453.

188. F.A. Cotton, J.L. Hubbard, D.L. Lichtenberger, and I. Shim, J.Am.Chem.Soc., 1982, 104, 679.

189. F.A. Cotton and B.J. Kalbacher, Inorg.Chem., 1976, 15, 522.

190. A. Bino and F.A. Cotton, J.Am.Chem.Soc., 1979, 101, 4150.

191. F.A. Cotton, P.C.W. Leung, W.J. Roth, A.J. Schultz, and J.M. Williams, J.Am.Chem.Soc., 1984, 106, 117.

192. A. Bino, B.E. Bursten, F.A. Cotton, and A. Fang, Inorg.Chem., 1982, 21, 3755.

193. A. Bino and S. Luski, Inorg.Chim.Acta, 1984, 86, L35.

194. F.A. Cotton and G.N. Mott, J.Am.Chem.Soc., 1982, 104, 5978.

195. D. Demarco, T. Nimry, and R.A. Walton, Inorg.Chem., 1980, 19, 575.

196. F.A. Cotton, P.E. Fanwick, and J.W. Fitch, III, Inorg.Chem., 1978, 17, 3254.

197. R.N. McGinnis, T.R. Ryan, and R.E. McCarley, J.Am.Chem.Soc., 1978, 100, 7900.

198. T.R. Ryan and R.E. McCarley, Inorg.Chem., 1982, 21, 2072.

199. F.A. Cotton and G.L. Powell, Inorg.Chem., 1983, 22, 871.

200. W.W. Beers and R.E. McCarley, Inorg.Chem., 1985, 24, 468.

201. J.R. Ebner and R.A. Walton, Inorg.Chem., 1975, 14, 1987.

202. M.H. Chisholm and I.P. Rothwell, Chemical Reactions of Metal-Metal Bonded Compounds of the Transition Metals, Prog.Inorg.Chem., 1982, 29, 1.

203. T.J. Barder, S.M. Tetrick, R.A. Walton, F.A. Cotton, and G.L. Powell, J.Am.Chem.Soc., 1983, 105. 4090.

204. T.J. Barder, F.A. Cotton, G.L. Powell, S.M. Tetrick, and R.A. Walton, J.Am.Chem.Soc., 1984, 106. 1323.

205. T.J. Barder, F.A. Cotton, D. Lewis, W. Schwotzer, S.M. Tetrick, and R.A. Walton, J.Am.Chem.Soc., 1984, 106, 2882.

206. H.D. Glicksman, A.D. Hamer, T.J. Smith, and R.A. Walton, Inorg.Chem., 1976, 9, 2205.

207. H.D. Glicksman and R.A. Walton, Inorg.Chem., 1978, 17. 200.

208. L.B. Anderson, F.A. Cotton, D. Demarco, A. Fang, W.H. Ilsley, B.W.S. Kolthammer, and R.A. Walton, J.Am.Chem.Soc., 1981, 103. 5078.

209. F.A. Cotton, M.W. Extine, and R.H. Niswander, Inorg.Chem., 1978, 17, 692.

210. F.A. Cotton, T.R. Felthouse, and D.G. Lay, Inorg.Chem., 1981, 20, 2219.

211. M. Ardon, A. Bino, F.A. Cotton, Z. Dori, M. Kaftory, and G. Reisner, Inorg.Chem., 1982, 21, 1912.

212. F.A. Cotton, Z. Dori, D.O. Marler, and W. Schwotzer, Inorg.Chem., 1983, 22, 3104.

213. F.A. Cotton, Z. Dori, D.O. Marler, and W. Schwotzer, Inorg.Chem., 1984, 23, 4033.

214. F.A. Cotton and G.L. Powell, J.Am.Chem.Soc., 1984, 106, 3371.

215. M.H. Chisholm and D.A. Haitko, J.Am.Chem.Soc., 1979, 101, 6784.

216. R.A. Walton, Reactivity of Metal-Metal Bonds ACS Symp.Ser., 1981, 155, 207.

217. T. Nimry and R.A. Walton, Inorg.Chem., 1977, 16, 2829.

218. J.R. Ebner, D.R. Tyler, and R.A. Walton, Inorg.Chem., 1976, 15, 833.

219. F.A. Cotton, Acc.Chem.Res., 1978, 11, 225.

220. J.D. Allison, T.E. Wood, R.E. Wild, and R.A. Walton, Inorg.Chem., 1982, 21, 3540.

221. F.A. Cotton and G.N. Mott, Inorg.Chem., 1983, 22, 1136.

222. I.I. Chernyaev, E.V. Shenderetskaya, and A.A. Koryagina, Russ.J.Inorg.Chem., 1960, 5, 559.

223. T.R. Felthouse, Prog.Inorg.Chem., 1982, 29, 73.

224. M.A. Porai-Koshits and A.S. Antsyshkina, Proc.Acad.Sci.USSR, Chem.Sect., 1962, 146, 902.

225. E.B. Boyar and S.D. Robinson, Co-ord.Chem.Rev., 1983, 50, 109.

226. K.G. Caulton and F.A. Cotton, J.Am.Chem.Soc., 1971, 93, 1914.

227. I.I. Chernyaev, E.V. Shenderetskaya, A.G. Maiorova, and A.A. Koryagina, Russ.J.Inorg.Chem., 1966, 11, 1383.

228. G.A. Rempel, P. Legzdins, H. Smith, and G. Wilkinson, Inorg.Synth., 1972, 13, 90.

229. R.A. Howard, A.M. Wynne, J.L. Bear, and W.W. Wendlandt, J.Inorg.Nucl.Chem., 1976, 38, 1015.

230. J. Kitchens and J.L. Bear, J.Inorg.Nucl.Chem., 1970, 32, 49.

231. J. Kitchens and J.L. Bear, Thermochim.Acta., 1970, 1, 537.

232. F.A. Cotton, B.G. DeBoer, M.D. LaPrade, J.R. Pipal, and D.A. Ucko, Acta Cryst., Sect.B, 1971, 27, 1664.

233. M.A. Porai-Koshits, L.M. Dikareva, G.G. Sadikov, and I.B. Baranovskii, Russ.J.Inorg.Chem., 1979, 24, 716.

234. R.M. Richman, T.C.Kuechler, S.P. Tanner, and R.S. Drago, J.Am.Chem.Soc., 1977, 99, 1055.

235. F.A. Cotton and T.R. Felthouse, Inorg.Chem., 1981, 20, 2703.

236. S.A. Johnson, H.R. Hunt, and H.M. Neumann, Inorg.Chem., 1963, 2, 960.

237. F.A. Cotton and T.R. Felthouse, Inorg.Chem., 1980, 19, 323.

238. F.A. Cotton and T.R. Felthouse, Inorg.Chem., 1980, 19, 2347.

239. F.A. Cotton and T.R. Felthouse, Inorg.Chem., 1982, 21, 431.

240. M. Moszner, T. Glowiak, and J.J. Ziolkowski, Polyhedron, 1985, 4,

241. G. Winkhaus and P. Ziegler, Z.Anorg.Allg.Chem., 1967, 350, 51.

242. L.A. Nazarova and A.G. Maiorova, Russ.J.Inorg.Chem., 1976, 21, 583.

243. Yu.N. Kukushkin, S.A. Simanova, V.K. Krylov, S.I. Bakhireva, and I.A. Balen'kaya, J.Gen.Chem.USSR, 1976, 46, 885.

244. I.B. Baranovskii, S.S. Abdullaev, G.Ya. Mazo, and R.N. Shchelokov, Russ.J.Inorg.Chem., 1982, 27, 305.

245. L.A. Nazarova, I.I. Chernyaev, and A.S. Morozova, Russ.J.Inorg. Chem., 1966, 11, 1387.

246. L.M. Dikareva, G.G. Sadikov, I.B. Baranovskii, and M.A. Porai-Koshits, Russ.J.Inorg.Chem., 1980, 25, 1725.

247. V.I. Belova and Z.S. Dergacheva, Russ.J.Inorg.Chem., 1971, 16, 1626.

248. A.M. Dennis, R.A. Howard, J.L. Bear, J.D. Korp, and I. Bernal, Inorg.Chim.Acta, 1979, 37, L561.

249. A.E. Bukanova, I.V. Prokof'eva, J. Salyns, and L.K. Shubockkin, Sov.J.Co-ord.Chem., 1977, 3, 1365.

250. R.N. Shchelokov, A.G. Maiorova, S.S. Abdullaev, O.N. Evstaf'eva, I.F. Golovaneva, and G.N. Emel Yanova, Russ.J.Inorg.Chem., 1981, 26, 1774.

251. M.A. Golubnichaya, I.B. Baranovskii, G.Ya. Mazo, and R.N. Shchelokov, Russ.J.Inorg.Chim., 1981, 26, 1534.

252. D.P. Bancroft, F.A. Cotton, and S. Han, Inorg.Chem., 1984, 23, 2408.

253. I.F. Golovaneva, S.S. Abdullaev, and R.N. Shchelokov, Russ.J.Inorg. Chem., 1982, 27, 1468.

254. G.G. Christoph and Y.-B. Koh, J.Am.Chem.Soc., 1979, 101, 1422.

255. F.A. Cotton and T.R. Felthouse, Inorg.Chem., 1981, 20, 600.

256. K. Das, K.M. Kadish, and J.L. Bear, Inorg.Chem., 1978, 17, 930.

257. R.S. Drago, S.P. Tanner, R.M. Richman, and J.R. Long, J.Am.Chem. Soc., 1979, 101, 2897.

258. F.A. Cotton, T.R. Felthouse, and J.L. Thompson, Inorg.Chem., referenced in ref.223.

259. F.A. Cotton and J.L. Thompson, Acta Cryst., Sect.B, 1981, 37, 2235.

260. G.G. Christoph, J. Halpern, G.P. Khare, Y.-B. Koh, and C. Romanowski, Inorg.Chem., 1981, 20, 3029.

261. F.A. Cotton, T.R. Felthouse, and S. Klein, Inorg.Chem., 1981, 20, 3037.

262. P. Legzdins, R.W. Mitchell, G.L. Rempel, J.D. Ruddick, and G. Wilkinson, J.Chem.Soc., A, 1970, 3322.

263. C.R. Wilson and H. Taube, Inorg.Chem., 1975, 14, 2276.

264. I.B. Baranovskii, M.A. Golubnichaya, L.M. Dikareva, and R.N. Shchelokov, Russ.J.Inorg.Chem., 1984, 29, 872.

265. W.R. Tikkanen, E. Binamira-Soriaga, W.C. Kaska, and P.C. Ford, Inorg.Chem., 1983, 22, 1147.

266. W.R. Tikkanen, E. Binamira-Soriaga, W.C. Kaska, and P.C. Ford, Inorg.Chem., 1984, 23, 141.

267. A.R. Chakravarty, F.A. Cotton, and D.A. Tocher, J.Chem.Soc., Chem.Comm., 1984, 501.

268. J. Halpern, E. Kimura, J. Molin-Case, and C.S. Wong, J.Chem.Soc., Chem.Comm., 1971, 1207.

269. A.M. Dennis, J.D. Korp, I. Bernal, R.A. Howard, and J.L. Bear, Inorg.Chem., 1983, 22, 1522.

270. M.Y. Chavan, T.P. Zhu, X.Q. Lin, M.Q. Ahsan, J.L. Bear, and K.M. Kadish, Inorg.Chem., 1984, 23, 4538.

271. S.A. Shchepinov, E.N. Sal'nikova, and M.L. Khidekel', Bull.Acad. Sci.USSR, Div.Chem.Sci., 1967, 2057.

272. F. Maspero and H. Taube, J.Am.Chem.Soc., 1968, 90, 7361.

273. R.D. Cannon, D.B. Powell, K. Sarawek, and J.S. Stillman, J.Chem.Soc., Chem.Comm., 1976, 31.

274. M. Moszner and J.J. Ziolkowski, Bull.Acad.Pol.Sci., Ser.Sci.Chim., 1976, 24, 433.

275. J.J. Ziółkowski, M. Moszner, and T. Glowiak, J.Chem.Soc., Chem.Comm., 1977, 760.

276. I.B. Baranovskii and M.A. Golubnichaya, Russ.J.Inorg.Chem., 1984, 29, 1558.

277. L. Dubicki and R.L. Martin, Inorg.Chem., 1970, 9, 673.

278. F.A. Cotton, Acc.Chem.Res., 1969, 2, 240.

279. J.G. Norman and H.J. Kolari, J.Am.Chem.Soc., 1978, 100, 791.

280. M. Berry, C.D. Garner, I.H. Hillier, A.A. MacDowell, and W. Clegg, Inorg.Chim.Acta, 1981, 53, L61.

281. T. Kawamura, K. Fukamachi, T. Sowa, S. Hayashida, and T. Yonezawa, J.Am.Chem.Soc., 1981, 103, 364.

282. H. Nakatsiyi, T. Ushio, K. Kanda, Y. Onishi, T. Kawamura, and T. Yonezawa, Chem.Phys.Lett., 1981, 79, 299.

283. H. Nakatsuji, Y. Onishi, J. Ushio, and T. Yonezawa, Inorg.Chem., 1983, 22, 1623, and references therein.

284. T.Y. Dong, D.N. Hendrickson, T.R. Felthouse, and H.S. Shieh, J.Am.Chem.Soc., 1984, 106, 5373.

285. R.S. Drago, Inorg.Chem., 1982, 21, 1697.

286. R.S. Drago, J.R. Long, and R. Cosmano, Inorg.Chem., 1982, 21, 2196.

287. R.S. Drago, R. Cosmano, and J. Telser, Inorg.Chem., 1984, 23, 3120.

288. K.M. Kadish, D. Lançon, A.M. Dennis, and J.L. Bear, Inorg.Chem., 1982, 21, 2987.

289. J.L. Bear, T.P. Zhu, T. Malinski, A.M. Dennis, and K.M. Kadish, Inorg.Chem., 1984, 23, 674.

290. M.Y. Chavan, T.P. Zhu, X.Q. Lin, M.Q. Ahsan, J.L. Bear, and K.M. Kadish, Inorg.Chem., 1984, 23, 4538.

291. R.J.H. Clark, A.J. Hempleman, H.M. Dawes, M.B. Hursthouse, and C.D. Flint, J.Chem.Soc., Dalton Trans., 1985, 1775.

292. V.M. Miskowski, W.P. Schaefer, B. Sadeghi, B.D. Santarsiero, and H.B. Gray, Inorg.Chem., 1984, 23, 1154.

293. D.S. Martin, Jr., T.R. Webb, G.A. Robbins, and P.E. Fanwick, Inorg.Chem., 1979, 18, 475.

294. G. Pneumatikakis and N. Hadjiliadis, J.Chem.Soc., Dalton Trans., 1979, 596.

295. K. Aoki and H. Yamazaki, J.Chem.Soc., Chem.Comm., 1980, 186.

296. J.L. Bear, H.B. Gray, L. Rainer, I.M. Chang, R.A. Howard, G. Serio, and A.P. Kimball, Cancer Chemother.Rep., 1975, 59, 611.

297. J.L. Bear, J. Kitchens, and M.R. Willcott, J.Inorg.Nucl.Chem., 1971, 33, 3479.

298. E.B.Boyar and S.D. Robinson, J.Chem.Soc., Dalton Trans., 1985, 629.

299. C.D. Garner, M. Berry, and B.E. Mann, Inorg.Chem., 1984, 23, 1500.

300. B. Rosenberg, L. Van Camp, J.E. Trosko, and V.H. Mansour, Nature, 1969, 222, 385.

301. R.G. Hughes, J.L. Bear, and A.P. Kimball, Proc.Am.Ass.Cancer Res., 1972, 13, 120.

302. K.M. Kadish, K. Das, R. Howard, A. Dennis, and J.L. Bear, Bioelectrochem.Bioenerg., 1978, 5, 741.

303. R.A. Howard, E. Sherwood, A. Erck, A.P. Kimball, and J.L. Bear, J.Med.Chem., 1977, 20, 943.

304. P.N. Rao, M.L. Smith, S. Pathak, R.A. Howard, and J.L. Bear, Curr.Chemother.Infect.Dis.Proc.Int.Congr.Chemother. 11th Washington, D.C., 1980, 1627.

305. R.A. Howard, T.G. Spring, and J.L. Bear, J.Clin.Hematol.Oncol., 1977, 7, 391.

306. A.M. Dennis, R.A. Howard, and J.L. Bear, Inorg.Chim.Acta, 1982, 66, L31.

307. K. Aoki and H. Yamazaki, J.Am.Chem.Soc., 1984, 106, 3691.

308. N. Alberding, N. Farrell, and E.D. Crozier, J.Am.Chem.Soc., 1985, 107, 384.

309. A. Erck, E. Sherwood, J.L. Bear, and A.P. Kimball, Cancer Res., 1976, 36, 2204.

310. J.G. Norman and E.O. Fey, J.Chem.Soc., Dalton Trans., 1976, 765.

311. H.D. Glicksman, A.D. Hamer, T.J. Smith, and R.A. Walton, Inorg.Chem., 1976, 15, 2205.

312. H.D. Glicksman and R.A. Walton, Inorg.Chim.Acta, 1979, 33, 255.

313. R.W. Mitchell, J.D. Ruddick, and G. Wilkinson, J.Chem.Soc., A, 1971, 3224.

314. L.M. Dikareva, M.A. Porai-Koshits, G.G. Sadikov, I.B. Baranovskii, M.A. Golubnichaya, and R.N. Shchelokov, Russ.J.Inorg.Chem., 1978, 23, 578.

315. I.B. Baranovskii, M.A. Golubnichaya, G.Ya. Mazo, and R.N. Shchelokov, Russ.J.Inorg.Chem., 1977, 22, 308.

316. J. Telser and R.S. Drago, Inorg.Chem., 1984, 23, 2599.

CHAPTER 2

PREPARATION AND CHARACTERIZATION OF $[Mo_2(O_2CMe)_2(NCMe)_6][BF_4]_2$ AND $[Rh_2(O_2CMe)_2(NCMe)_6][BF_4]_2$ AND THEIR DERIVATIVES

2.1 Introduction

Numerous quadruply bonded dimolybdenum and singly bonded dirhodium compounds have been prepared.[1] The reactions of such complexes have been studied extensively,[1] these studies mainly concentrating on ligand exchange rather than reactivity of the metal-metal bonds themselves. Thus a large number of molybdenum dimers have been prepared from the parent compound $[Mo_2(O_2CMe)_4]$; this compound readily undergoes carboxylate exchange leading to the partial and, ultimately, total replacement of the acetate groups. Total replacement of the carboxylates by monodentate ligands leads to $[Mo_2X_8]^{4-}$ (X = halide), $[Mo_2X_4L_4]$ (X = halide; L = neutral monodentate ligands), and $[Mo_2X_4(LL)_2]$ (X = halide; LL = neutral bidentate ligands) compounds.[1] Partial carboxylate replacement has led to the preparation of dimers such as $[Mo_2(O_2CCF_3)_3Cl_3]^{2-}$,[2] $[Mo_2(O_2CMe)_2(acac)_2]$[3] and $[Mo_2(O_2CMe)_2\{PhNC(Me)CHC(Me)O\}]$[4] by reaction of the tetracarboxylate with the respective ligand. Ligand exchange processes are aided by the presence of Lewis acids which react with anionic ligands of dimolybdenum(II) and dirhodium(II) complexes. Protonation of the carboxylates via HCl followed by addition of $[Ph_4As]Cl$ produces <u>trans</u>-$[Mo_2(O_2CMe)_2Cl_4]^{2-}$.[3,5] Ethylation of $[Mo_2(O_2CCF_3)_4]$ using $[Et_3O][BF_4]$, followed by reaction with 2,2'-bipyridyl in CH_2Cl_2 apparently produces $[Mo_2(O_2CCF_3)_2(bipy)_2][BF_4]_2.Et_2O$, although there has been no X-ray crystallographic confirmation of the identity of this cation.[6] Protonation of the carboxylates, leading to their removal, in dirhodium species has also been achieved. Recently, protonation of $[Rh_2(O_2CMe)_4]$, affording acetate removal and replacement by neutral bridging ligands has produced $[Rh_2(O_2CMe)_3L]^+$ (L = bpnp, dinp and pynp),[7] $[Rh_2(O_2CMe)_2(pynp)_2]^{2+}$,[7] $[Rh_2(pynp)_3Cl_2]^{2+}$,[8] and $[Rh_2(np)_4]Cl_4$.[7]

In addition, removal of one or two acetates by trifluoromethanesulphonic acid has afforded $[Rh_2(O_2CMe)_3(O_3SCF_3)].nH_2O$ and $[Rh_2(O_2CMe)_2(O_3SCF_3)_2].nH_2O$. Reaction of the resulting products with pyridine produced $[Rh_2(O_2CMe)_3(py)_4][CF_3SO_3]$ and $[Rh_2(O_2CMe)_2(py)_6][CF_3SO_3]_2$.[9]

Treatment of $[Rh_2(O_2CCH_2CH_2CH_3)_4]$ and $[Mo_2(O_2CMe)_4]$ with the strong non-complexing acids CF_3SO_3H and $HBF_4.Et_2O$ was purported to produce $[Rh_2(O_2CCH_2CH_2CH_3)_2]^{2+}$ and $[Mo_2(O_2CMe)_2]^{2+}$.[10] The rhodium complex was characterized in solution by ^1H and ^{13}C n.m.r. spectroscopy and two derivatives of the dimolybdenum(II) species, $[Mo_2(O_2CMe)_2(NCMe)_4][CF_3SO_3]_2$ and $[Mo_2(O_2CMe)_2(NCMe)_5][BF_3OH]$, were characterized by infrared and UV/visible spectroscopy.[10]

With the view of esterification of the carboxylate groups but replacement by solvent molecules alone, the methylating agent $[Me_3O][BF_4]$ was chosen. It was hoped that successive removal of carboxylates would be achieved to allow a direct attack at the metal-metal bonds yet leave the metals partially bridged by carboxylate ligands to lessen the likelihood of bond cleavage. Thus replacement of the carboxylates by solvent molecules that would allow direct access of reagents to the equatorial sites and the bond itself was anticipated.

2.2 Preparation of $[Mo_2(O_2CMe)_4]$

The procedure described by Cotton *et al.*[11] was followed. A solution of $[Mo(CO)_6]$ (3 g, 11.4 mmol) in acetic acid (150 cm^3) and acetic anhydride (15 cm^3) was refluxed at 140°-150°C for about 20 hours. The solution was then cooled and the yellow crystals that had formed were filtered in air, washed with ethanol (1 x 5 cm^3) and ether (2 x 10 cm^3) and dried *in vacuo* for *ca.* 5 hours. (Yield = 1.31 g, 44%)

Analyses	C	H	Mo
Calc. for $C_8H_{12}Mo_2O_8$	22.4	2.8	44.8 %
Found	22.5	2.9	44.9 %

The infrared and mass spectra of $[Mo_2(O_2CMe)_4]$ were identical to those reported in the literature.[12,13] The infrared spectrum shows bands assigned to the asymmetric (1512 and 1494 cm^{-1}) and symmetric (1409 cm^{-1}) stretching vibrations of the acetate group.

2.3 Preparation of $[Mo_2(O_2CH)_4]$

The procedure described by Cotton et al.[14] was followed. $[Mo_2(O_2CMe)_4]$ (0.8 g, 1.9 mmol) was stirred in formic acid (100 cm^3), while the mixture was heated to boiling, at which point all of the $[Mo_2(O_2CMe)_4]$ had dissolved. The solution was filtered and cooled to 10°C. The yellow crystals thus obtained were filtered in air, washed with ethanol (2 x 3 cm^3) and ether (2 x 10 cm^3) and dried in vacuo for about 6 hours.

The compound prepared in this way was usually analytically and spectroscopically pure but, if necessary, it could be recrystallised from hot formic acid. (Yield = 0.51 g, 73%)

Analyses	C	H	Mo
Calc. for $C_4H_4Mo_2O_8$	12.9	1.1	51.6 %
Found	13.2	0.9	51.1 %

The infrared and mass spectra of $[Mo_2(O_2CH)_4]$ were identical to those reported in the literature.[14,15] The infrared spectrum shows bands assigned to the asymmetric (1525 cm^{-1}) and symmetric (1360, 1350 and 1325 cm^{-1}) stretching vibrations of the formate group.

2.4 Preparation of $[Mo_2(O_2CMe)_2(NCMe)_6][BF_4]_2$

$[Mo_2(O_2CMe)_4]$ (1.12 g, 2.62 mmol) was added to a solution of $[Me_3O][BF_4]$ (1.55 g, 10 mmol) in acetonitrile (50 cm^3). A red solution formed immediately, although much of the $[Mo_2(O_2CMe)_4]$ was still undissolved; however, after stirring for about 30 minutes a clear red solution formed. On reducing the volume of the solvent, a red solid precipitated, the yield of which was increased by the addition of diethyl ether (30 cm^3). The precipitate was collected by filtration and recrystallised from acetonitrile. It was then washed with diethyl ether (10 cm^3) and dried *in vacuo*. (Yield = 1.5 g, 84%)

Analyses	C	H	F	Mo	N
Calc. for $C_{16}H_{24}B_2F_8Mo_2N_6O_4$	26.3	3.3	20.8	26.3	11.5 %
Found	26.3	3.3	19.7	25.7	10.9 %

The compound dissolves in MeCN to produce a deep red solution, and in MeOH and EtOH to afford deep yellow solutions. Crystals of the material were obtained from acetonitrile solution, by reducing the volume to saturation, warming and slow cooling.

2.4.1 Crystal structure of $[Mo_2(O_2CMe)_2(NCMe)_6][BF_4]_2$

The study was accomplished by Dr. W. Clegg of the Anorganisch-Chemisches Institut der Universität Göttingen, Tammanstrasse 4, D3400 Göttingen, F.R.G.

A single crystal, coloured deep red, was sealed in a Lindemann glass capillary. The data were collected on a Stoe-Siemens AED diffractometer using graphite monochromated Mo-K_α radiation (λ = 0.71069 Å) with a ω/θ scan mode with on-line profile[16] fitting at T = 291K; a steady decay, leading to a reduction of *ca*. 18% in intensity, was corrected for in the data reduction; absorption or extinction

corrections were applied; $\underline{D}_m$ was not measured. The structure was solved by Patterson and Fourier techniques, including difference syntheses. Blocked-cascade least squares refinement proceeded to a minimum value of $\Sigma \underline{w}\Delta^2$, where $\underline{w}^{-1} = \sigma^2(\underline{F}) + \underline{g}\underline{F}^2$ and $\underline{g}$ was optimised automatically, with anisotropic thermal parameters but without hydrogen atoms. The $[BF_4]^-$ anions were disordered and F atoms positions with partial occupancy factors were refined to account for the observed electron density with no attempted geometrical interpretation.

Computer programs were written by W.C. (diffractometer control program) and by Professor G.M. Sheldrick (SHELXTL system).[17] Scattering factors were taken from ref.18. A summary of the crystallographic and refinement data is presented in Table 2.1. The atomic co-ordinates are given in Table 2.2, selected bond lengths and bond angles are given in Table 2.3 and the structure of the cation is shown in Fig.2.1.

$[Mo_2(O_2CMe)_2(NCMe)_6][BF_4]_2$ consists of dipositive dimetal cations and (disordered) $[BF_4]^-$ anions, the cation possesses mirror symmetry and approximates to $\underline{C}_{2v}$ symmetry. Each of the mutually cis acetato-groups spans the dimetal centre, which possesses the normal[1] assembly of one axial and four equatorial donor atoms per metal with an eclipsed arrangement of the two sets of equatorial donor atoms within each cation. The structures of two other Mo_2^{4+} complexes involving two μ_2-carboxylato-groups and four monodentate equatorial ligands have been determined; $[Mo_2(O_2CPh)_2Br_2(PBu_3)_2]$[19] and $[Mo_2(O_2CMe)_2Cl_4]^{2-}$ [5] both have a trans-arrangement of bridging ligands. $[Mo_2(O_2CCH(NH_3)R)_2(NCS)_4].\underline{n}H_2O$ (R = H, $\underline{n}$ = 1 Glycinate and R = $CH(CH_3)CH_2CH_3$, $\underline{n}$ = 4.5 L-isoleucinate) have been prepared[20] with the carboxylate groups adopting a cis relationship and four monodentate equatorial thiocyanates, in a "Sawhorse" arrangement.[20] The paucity of structural data for complexes of this type means that the factors which determine whether a cis- or a trans-

Table 2.1 Crystal data and structure determination.

	$[Mo_2(O_2CMe)_2(MeCN)_6][BF_4]_2$	$[Rh_2(O_2CMe)_2(MeCN)_6][BF_4]_2 \cdot 4MeCN$	$[Rh_2(O_2CMe)_2(MeCN)_4(pyridine)_2][BF_4]$
Formula	$C_{16}H_{24}B_2F_8Mo_2N_6O_4$	$C_{24}H_{36}B_2F_8N_{10}O_3Rh_2$	$C_{22}H_{28}B_2F_8N_6O_4Rh_2$
M_r	729.9	908.0	819.9
space group	$P2_1/m$	$C2/c$	$C2/m$
a, Å	7.160(1)	15.749(2)	19.448(3)
b, Å	10.642(1)	18.417(3)	10.476(1)
c, Å	19.402(2)	13.965(2)	18.990(3)
β, °	99.47(1)	91.34(2)	113.25(1)
V, Å	1458.2	4049.4	3554.8
Z	2	4	4
D_{calc}, g cm^{-3}	1.662	1.489	1.532
F(000), electrons	720	1816	1624
μ(MoKα), mm^{-1}	0.919	0.876	0.987
crystal size, mm	0.2 x 0.2 x 0.4	0.4 x 0.4 x 0.75	0.25 x 0.3 x 0.75
$2\theta_{max}$, °	55	50	50
Reflections measured	3753	6549	6617
Unique reflections	3522	3560	2391
Observed [$F>4\sigma(F)$]	2774	2936	2391
R_{int}	0.042	0.038	0.028
Weighting factor g	0.00068	0.00125	0.00100

Table 2.1 (continued)

Number of parameters	214	272	239
$\underline{R}$	0.053	0.040	0.059
$\underline{R}_g = (\Sigma \underline{w}\Delta^2 / \Sigma \underline{w}\underline{F}_o^2)^{1/2}$	0.069	0.057	0.076
Slope of normal probability plot	1.46	1.03	1.36
max. peak in final difference map, e Å^{-3}	0.73	0.45	0.88

Table 2.2 Atomic coordinates ($\times 10^4$) for $[Mo_2(O_2CMe)_2(MeCN)_6][BF_4]_2$

	x	y	z
Mo(1)	466(1)	2500	2256(1)
Mo(2)	2411(1)	2500	1531(1)
O(11)	-1136(5)	1102(4)	1693(2)
O(12)	844(5)	1110(4)	928(2)
C(11)	-620(7)	682(5)	1142(3)
C(12)	-1776(10)	-360(7)	748(3)
N(2)	1575(6)	1102(4)	3012(2)
C(21)	1935(8)	398(6)	3453(3)
C(22)	2321(14)	-524(7)	4025(4)
N(3)	4353(6)	1079(4)	1991(2)
C(31)	5332(7)	325(5)	2264(3)
C(32)	6567(9)	-647(6)	2615(4)
N(4)	-2168(12)	2500	3155(4)
C(41)	-2610(15)	2500	3675(5)
C(42)	-3224(32)	2500	4332(7)
N(5)	4564(12)	2500	484(5)
C(51)	5509(16)	2500	60(6)
C(52)	6695(24)	2500	-454(9)
B(6)	8471(16)	2500	7788(6)
F(61)	10124(15)	2500	7692(10)
F(62)	7233(19)	2500	7204(5)
F(63)	8102(12)	1457(7)	8096(4)
B(7)	2439(21)	2500	5369(8)
F(71)	2127(29)	2500	4668(7)
F(72)	2479(31)	1252(16)	5620(8)
F(73)	1128(30)	2500	5716(15)
F(74)	862(32)	2500	5039(17)
F(75)	3633(63)	2500	5873(17)
F(76)	3802(37)	1878(39)	5299(23)

Table 23 Selected bond lengths (Å) and angles (°)

$[Mo_2(O_2CMe)_2(MeCN)_6][BF_4]_2$

Mo(1)-Mo(2)	2.136(1)		
Mo(1)-O(11)	2.075(4)	Mo(2)-O(12)	2.093(4)
Mo(1)-N(2)	2.148(4)	Mo(2)-N(3)	2.147(4)
Mo(1)-N(4)	2.772(8)	Mo(2)-N(5)	2.745(10)
Mo(2)-Mo(1)-O(11)	91.0(1)	Mo(1)-Mo(2)-O(12)	91.1(1)
Mo(2)-Mo(1)-N(2)	104.0(1)	Mo(1)-Mo(2)-N(3)	100.0(1)
Mo(2)-Mo(1)-N(4)	177.9(2)	Mo(1)-Mo(2)-N(5)	173.6(2)
O(11)-Mo(1)-N(2)	88.5(1)	O(12)-Mo(2)-N(3)	89.2(2)
O(11)-Mo(1)-N(4)	87.5(1)	O(12)-Mo(2)-N(5)	84.4(2)
N(2)-Mo(1)-N(4)	77.5(2)	N(3)-Mo(2)-N(5)	84.5(2)
O(11)-Mo(1)-O(11')	91.5(2)	O(12)-Mo(2)-O(12')	89.9(2)
N(2)-Mo(1)-O(11')	165.0(2)	N(3)-Mo(2)-O(12')	168.8(2)

A prime indicates an atom generated by symmetry (mirror plane or rotation axis).

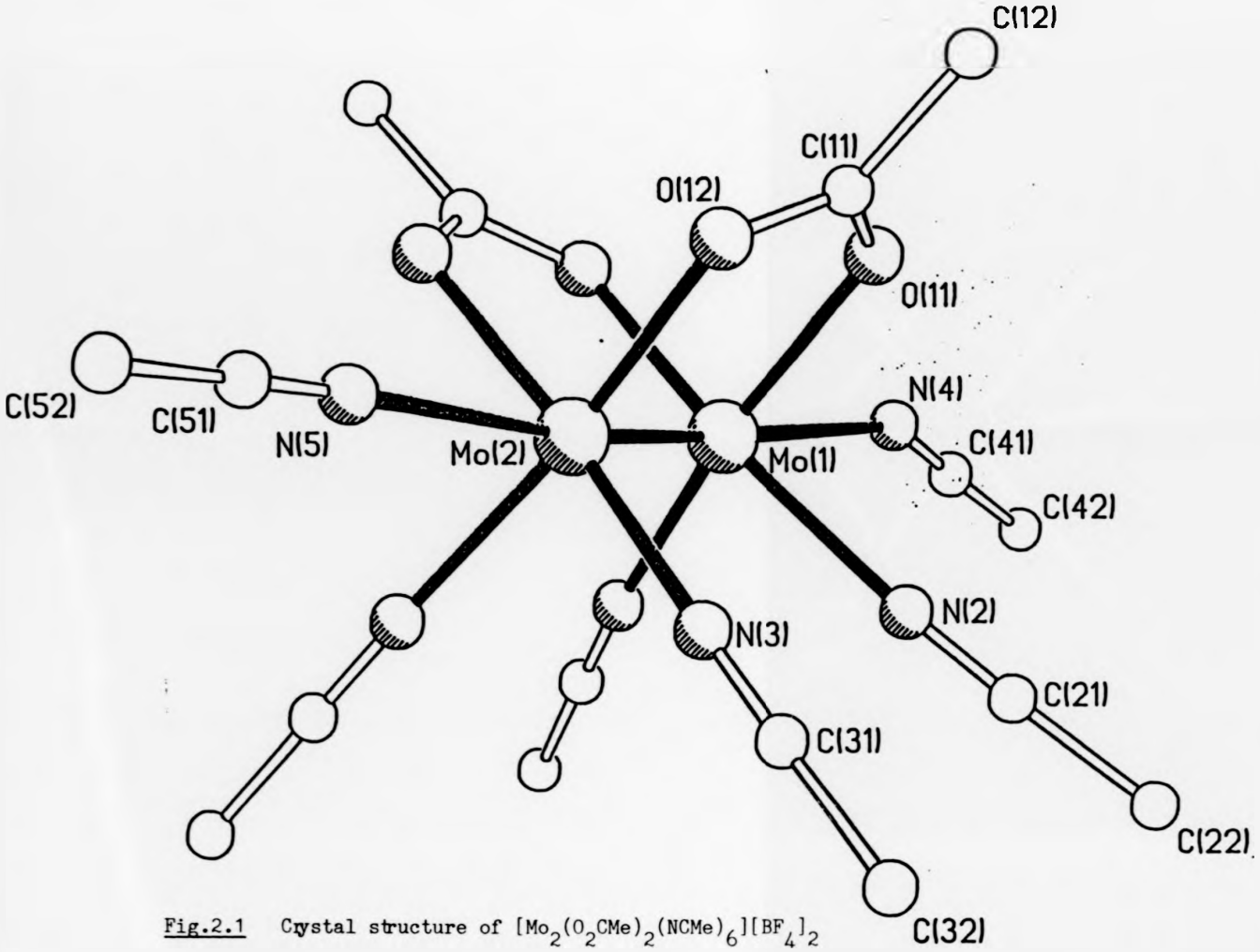

Fig.2.1 Crystal structure of $[Mo_2(O_2CMe)_2(NCMe)_6][BF_4]_2$

arrangement of the two μ_2-carboxylato-groups in $[Mo_2(O_2CR)_2L_n]$ (n = 4 {equatorial ligands} or 6 {4 equatorial + 2 axial ligands}) complexes remain to be established.

With the single exception of Mo(1)-N(4)-C(41), for which the interbond angle is 154.3(8)°, the atoms of the Mo-N-C-C systems of the co-ordinated acetonitrile groups are essentially linear.

The Mo-Mo distance in $[Mo_2(O_2CMe)_2(NCMe)_6][BF_4]_2$ is typical[1] of complexes containing a quadruple bond between two Mo^{II} centres; the particular value (2.136(1)Å) may be compared to that in the parent compound $[Mo_2(O_2CMe)_4]$ (2.0934(8) Å)[21] and other structurally characterized bis(μ_2-carboxylato)dimolybdenum(II) complexes, $[Mo_2(O_2CPh)_2Br_2(PBu_3)_2]$ (2.091(3) Å),[19] $[Mo_2(O_2CMe)_2Cl_4]^{2-}$ (2.086(2) Å),[5] $[Mo_2(glycinate)_2(NCS)_4].H_2O$ (2.132(2) Å) and $[Mo_2(L\text{-leucinate})_2(NCS)_4]4.5H_2O$ (2.154(5) Å).[20] The average bond lengths and bond angles of the $Mo(O_2CR)_2Mo$ framework (Mo-O = 2.084(13), C-O = 1.271(8), C-C = 1.514(9) Å. Mo-Mo-O = 91.1(1), O-Mo-O = 90.7(1.1), Mo-O-C = 118.3(8), O-C-O = 118.3(5)°) are comparable with the corresponding dimensions of $[Mo_2(O_2CMe)_4]$[21] and related structures.[5,19-21] There is a marked distinction in the length of the Mo-N bonds involving the co-ordinated acetonitrile molecules in the equatorial (2.148(4) Å) as compared to the axial (2.759(19) Å) sites. The former are very similar to the lengths of the Mo-N_{eq} bonds in $[Mo_2(glycinate)_2(NCS)_4].H_2O$, $[Mo_2(L\text{-isoleucinate})_2(NCS)_4].4.5H_2O$[20] and $[Mo_2(pyrazolylborate)_2(O_2CMe)_2]$[22] of 2.07(2), 2.11(4), and 2.16(2) Å, respectively, whilst the latter may be compared to the Mo-N_{ax} distances of $[Mo_2(O_2CCF_3)_4(pyridine)_2]$ (2.548(8) Å)[23] and $[Mo_2(pyrazolylborate)_2(O_2CMe)_2]$ (2.45(1) Å).[22] Therefore, the difference between the length of the equatorial and axial Mo-N bonds of $[Mo_2(O_2CMe)_2(NCMe)_6]^{2+}$ has the expected sense

($Mo\text{-}N_{ax}$ > $Mo\text{-}N_{eq}$) and magnitude (0.61 Å). Furthermore, this complex provides an especially clear and quantitative assessment of the static trans-effect of a Mo-Mo quadruple bond.

The structural distinction between axial and equatorial MeCN ligands does not extend to their N-C and C-C bond lengths; the overall average lengths of these bonds are 1.13(2) and 1.44(3) Å, respectively, and are normal for MeCN molecules complexed to other metal centres.[24-26] Also, as generally observed[5,19,20,27] for other complexes of Mo_2^{4+} centres with monodentate ligands, the equatorial MeCN groups make an obtuse angle with the Mo-Mo bond, $Mo\text{-}Mo\text{-}N_{eq}$ = 102(3)°.

2.4.2 Spectroscopic studies of $[Mo_2(O_2CMe)_2(NCMe)_6][BF_4]_2$

2.4.2(i) UV/visible spectrum

The UV/visible spectrum of $[Mo_2(O_2CMe)_2(NCMe)_6][BF_4]_2$ in acetonitrile (Fig.2.2) shows absorption maxima at positions and with extinction coefficients expressed in Table 2.4.

Table 2.4 UV/visible absorption maxima for $[Mo_2(O_2CMe)_2(NCMe)_6][BF_4]_2$ in MeCN

Wavelength λ(nm)	ε(mol.cm^{-1}l^{-1})
531	925
395(sh)	150
262	9,677
222	11,730

The lowest energy band at 531 nm is assigned to the $\delta \rightarrow \delta^*$ transition of the Mo-Mo quadruple bond. This is very similar to the lowest energy band reported for the $[Mo_2Cl_8]^{4-}$ ion species (at 532 nm)[28]

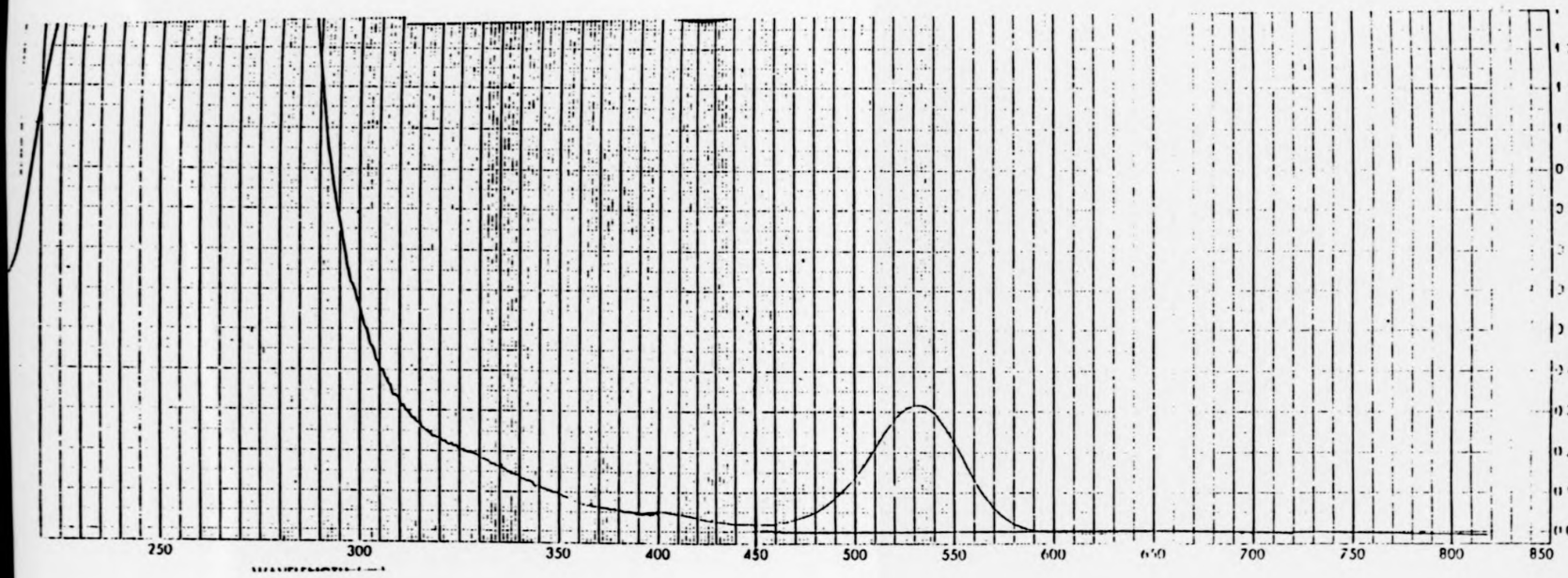

Fig.2.2 UV/visible spectrum of $[Mo_2(O_2CMe)_2(NCMe)_6][BF_4]_2$ in MeCN

which has been assigned to the same transition and indeed it is generally agreed that this lowest energy transition for Mo-Mo quadruply bonded systems is due to the $\delta \rightarrow \delta^*$ transition.[1] Furthermore, there is a general trend that, as the length of a Mo-Mo quadruple bond increases, the $\delta \rightarrow \delta^*$ transition, as expected, decreases in energy, implying a weakening of the Mo-Mo bonds.[1] As shown by Table 2.5, $[Mo_2(O_2CMe)_2(NCMe)_6]^{2+}$ fits into this pattern which also extends to $[Cr_2(Me)_8]^{4-}$, $[Mo_2(Me)_8]^{4-}$ and $[Re_2(Me)_8]^{2-}$ ions.[29]

Table 2.5 Comparison of selected metal-metal bond distances and the position of the lowest energy band in the visible spectrum

Complex	$[Mo_2(O_2CMe)_4]$[1]	$[Mo_2(O_2CMe)_2(NCMe)_6]^{2+}$	$[Mo_2Cl_8]^{4-}$[1,28]	$[Mo_2(NCS)_8]^{4-}$[30]
$\delta \rightarrow \delta^*$ transition (nm)	435	531	532	690
M-M bond distance (Å)	2.0934	2.136	2.139	2.171

The lowest energy visible band for $[Mo_2(NCMe)_8]^{4+}$ occurs at 555 nm;[31] a crystal structure has not yet been determined for this cation but, on the basis of the above data, a Mo-Mo bond length of ca. 2.145 Å would be expected.

2.4.2(ii) Infrared spectrum

The infrared spectrum of a nujol mull of $[Mo_2(O_2CMe)_2(NCMe)_6][BF_4]_2$ (Fig.2.3) was recorded. The broad band at 3500 and the band at 1610 cm^{-1} are assigned to the O-H stretch and O-H bend, respectively, of some absorbed water. The bands at 2340, 2305, and 2275 cm^{-1} are assigned to the CN stretching vibration of the co-ordinated acetonitrile

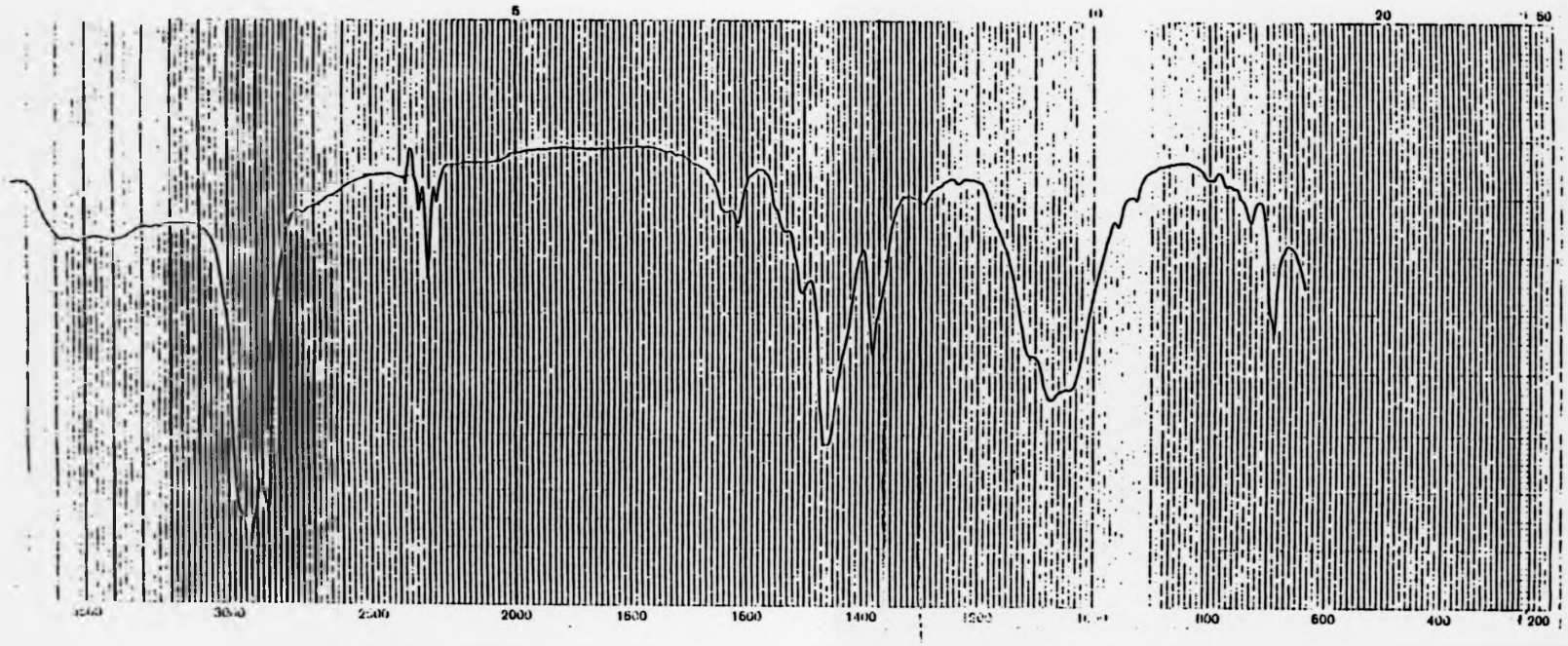

Fig.2.3 Infrared spectrum of $[Mo_2(O_2CMe)_2(NCMe)_6][BF_4]_2$

molecules. The CN stretching vibration ν(CN) in free acetonitrile occurs at 2266 cm^{-1} [32] and the shift of ν(CN) to higher frequency is consistent with the presence of co-ordinated N-bonded acetonitrile[32] providing no indication for π-back bonding from the Mo_2^{4+} centre to the π^* orbitals of the C≡N bond. The bands are further complicated by the fact that, in addition to the ν(C≡N) fundamental, a nearby band is often observed which results from a combination of the symmetrical CH_3 deformation and the C-C stretch.[33]

From site symmetry considerations for this complex five infrared active vibrations and six Raman active vibrations with five coincidences are expected. Observation of only three infrared bands could be due to overlap or simply that the other bands are too weak to be observed.

The band at 1510 cm^{-1} is assigned to the asymmetric carboxylate stretching vibration $\nu_{asym}(OCO)$, with the corresponding symmetric vibration being at 1370 cm^{-1}, which are typical of bidentate or bridging carboxylate groups.[34] The broad band at 1075 cm^{-1} is attributed to the B-F stretching vibration in the $[BF_4]^-$ anion.[34]

Attempts to record the Raman spectrum of this compound were unsuccessful, possibly due to thermal decomposition in the laser source.

2.4.2(iii) N.m.r. spectroscopic studies

The ^1H n.m.r. spectrum of $[Mo_2(O_2CMe)_2(NCMe)_6][BF_4]_2$ (Fig.2.4) was recorded at 300 MHz in deuteroacetonitrile at room temperature. It shows two peaks at 1.90 p.p.m. and 2.82 p.p.m. that integrate in a 3:1 ratio respectively. The resonance at 1.90 p.p.m. is assigned to the acetonitrile ligands and this occurs at the position of (free) CH_3CN. The observation of only one resonance at the position of free acetonitrile leads to the inference that, in solution, all of the acetonitriles,

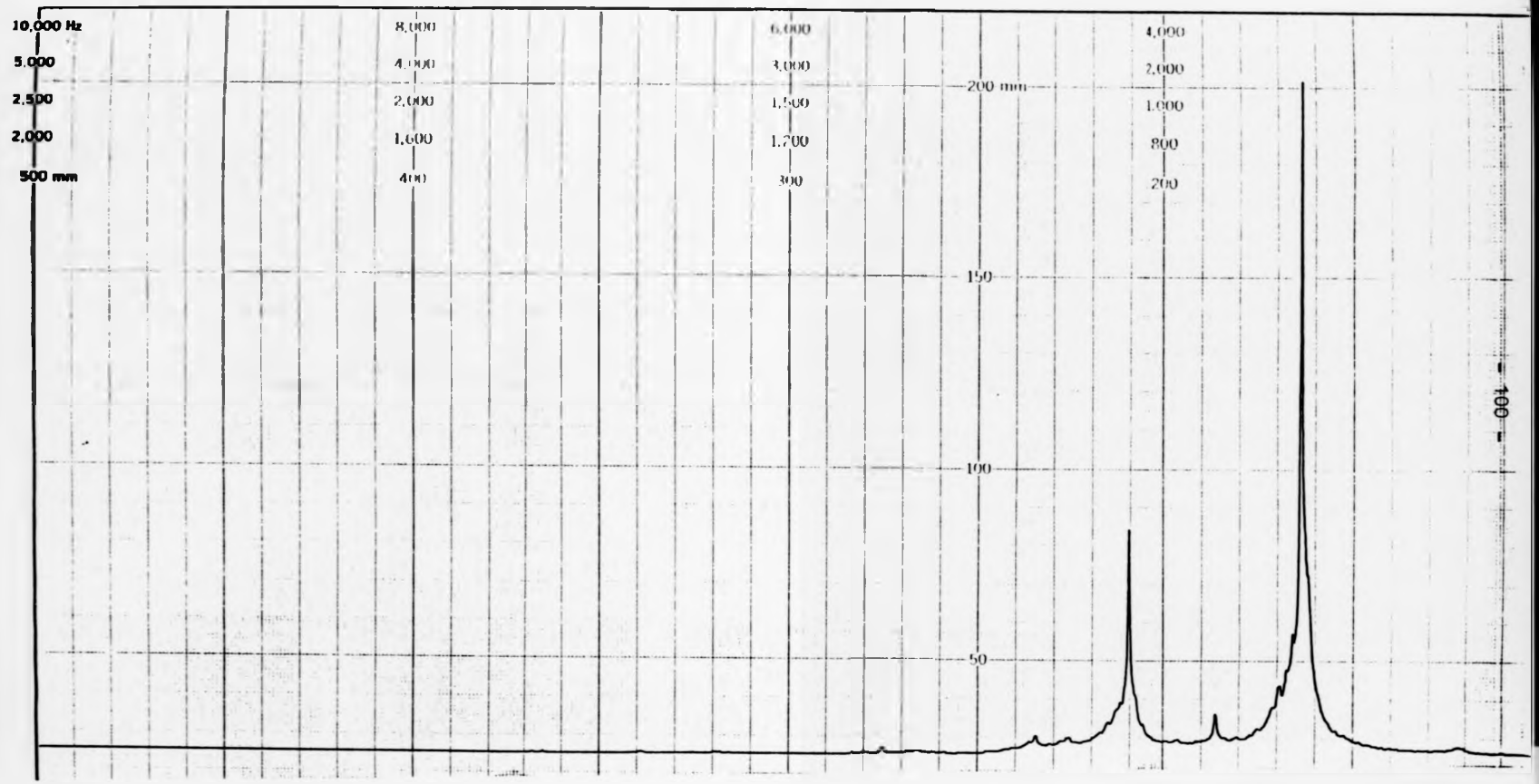

Fig.2.4 300 MHz ^{1}H n.m.r. of $[Mo_2(O_2CMe)_2(NCMe)_6][BF_4]_2$ in CD_3CN

axial and equatorial, are equivalent and labile. The resonance at 2.82 p.p.m. is assigned to the co-ordinated acetate and may be compared with $[Mo_2(O_2CMe)_4]$ which gives a resonance in the ^1H n.m.r. spectrum at 2.63 p.p.m.[13]

The relative integrations are in agreement with the formulation of six acetonitriles to two acetates. Although incompletely deuterated solvent could increase the integration for the acetonitrile resonance, the solvent used was fresh and showed only a very small residual peak when scanned neat.

The ^{13}C n.m.r. spectrum of $[Mo_2(O_2CMe)_2(NCMe)_6][BF_4]_2$ was recorded at 75 MHz (Fig.2.5) in deuteroacetonitrile at room temperature. This spectrum contains peaks at 188.1, 145.6, 117.1, 22.4, and 0 p.p.m. The peaks at 117.1 and 0 p.p.m. are assigned to the nitrile and methyl carbons, respectively, of the solvent CD_3CN and also are considered to contain resonances due to the CH_3CN of the complex. As for the ^1H n.m.r. spectrum, this is consistent with all of the acetonitrile groups of the molecule being labile. The resonances at 188.1 p.p.m. and 22.4 p.p.m. are assigned to the carboxylate and methyl carbons, respectively, of the acetate groups. These are typical of acetate resonances.[35,36] The resonance line at 145.6 p.p.m. appears to a varying extent in all of the ^{13}C n.m.r. spectra recorded for this compound and is assigned to an impurity, the nature of which is unclear. Coming, as it does, in the region for aromatics or heteroaromatics it could be due to some aromatic solvent or a residue from the reaction.

Dissolution of this complex in methanol produced a deep yellow coloured solution with a distinct band in the visible region at 488 nm. Reduction in the volume of solution yielded a yellow oil which was dried in vacuo for ca. 5 hours. A 300 MHz ^1H n.m.r. spectrum of this

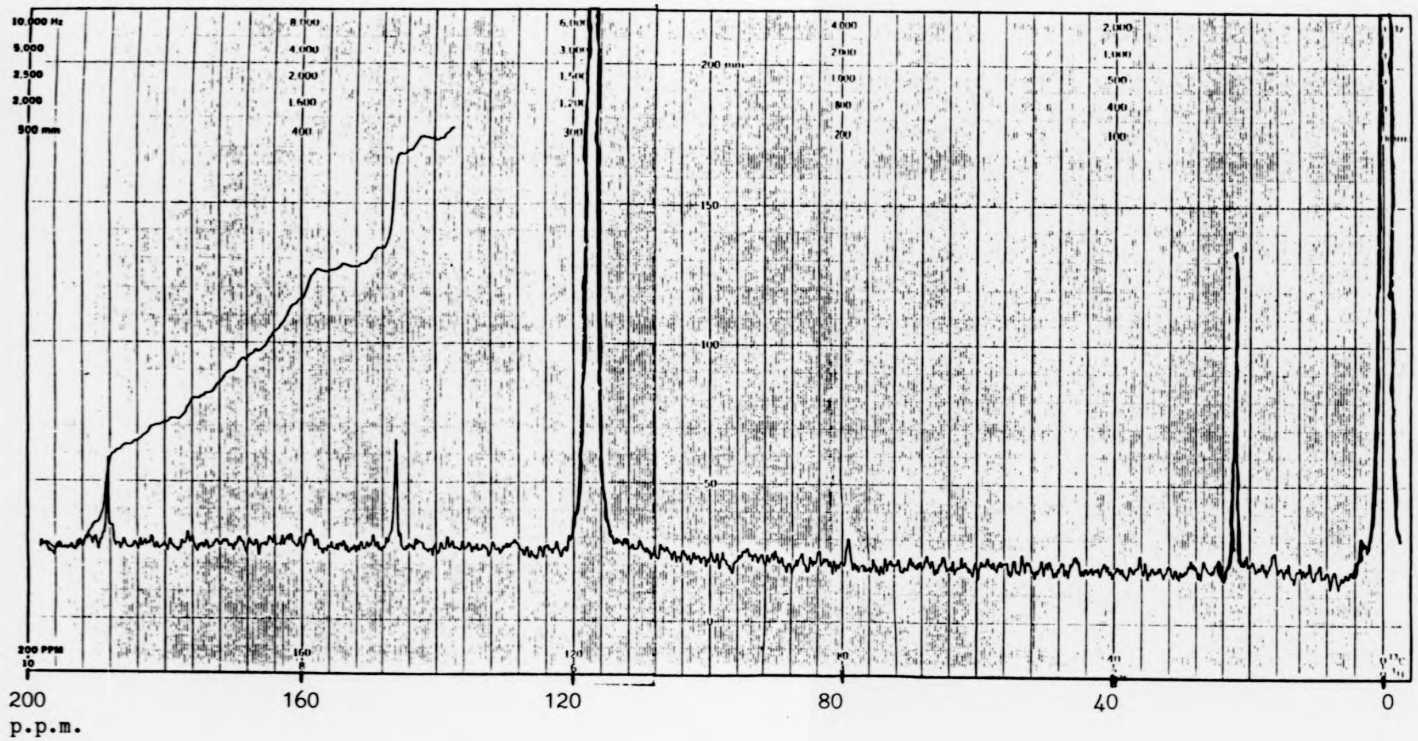

Fig.2.5 75 MHz ^{13}C n.m.r. spectrum of $[Mo_2(O_2CMe)_2(NCMe)_6][BF_4]_2$ in CD_3CN

oil dissolved in deuteromethanol contained resonances at 3.35 and 2.90 p.p.m. due to CH_3OH and acetate respectively but no peaks attributable to CH_3CN were observed. Therefore, it is proposed that methanol will easily and completely displace acetonitrile from the complex, but attempts to isolate this methanol adduct were unsuccessful.

2.5 Preparation of $Mo_2(O_2CH)_2(NCMe)_5(H_2O)_{\frac{1}{2}}(BF_4)_2$

$[Mo_2(O_2CH)_4]$ (0.6 g, 1.6 mmol) was added to a solution of $[Me_3O][BF_4]$ (0.96 g, 6.5 mmol) in acetonitrile (50 cm^3). A pink solution formed immediately although most of the $[Mo_2(O_2CH)_4]$ was undissolved but, after stirring for ca. 30 minutes, a clear pink solution was obtained which deposited a pink solid. A gas was evolved during the reaction. The precipitate was collected by filtration, washed with acetone (2 x 5 cm^3), diethyl ether (2 x 10 cm^3) and dried in vacuo for ca. 5 hours. (Yield = 0.85 g, 80%)

Analyses	C	H	N
Calc. for $C_{12}H_{18}B_2F_8Mo_2N_5O_{4.5}$	21.5	2.7	10.4 %
Found	21.1	3.1	9.7 %

$Mo_2(O_2CH)_2(NCMe)_5(H_2O)_{\frac{1}{2}}(BF_4)_2$ is less soluble in acetonitrile than the analogous acetate complex $[Mo_2(O_2CMe)_2(NCMe)_6][BF_4]_2$. The formate complex appears to be hygroscopic and probably absorbs water from the starting material $[Me_3O][BF_4]$. A somewhat polymeric nature of this formate compound may be indicated by only one axial MeCN, the other axial position being involved in weak bonding to the oxygen of another bridging formate compound as seen in several such carboxylate compounds.[1]

2.5.1 Spectroscopic studies

2.5.1(i) UV/visible spectrum

The UV/visible spectrum of $Mo_2(O_2CH)_2(NCMe)_5(H_2O)_{\frac{1}{2}}(BF_4)_2$ in acetonitrile (Fig.2.6) shows absorption maxima at positions and with extinction coefficients expressed in Table 2.6.

Table 2.6 UV/visible absorption maxima for $Mo_2(O_2CH)_2(NCMe)_5(H_2O)_{\frac{1}{2}}(BF_4)_2$ in acetonitrile

Wavelength λ (nm)	ε (mol.cm^{-1}l^{-1})
526	844
385(sh)	234
265	5910
219	8256

As discussed for the corresponding acetate complex (Section 2.4.2(i)) the lowest energy band at 526 nm is assigned to be due to the $\delta \rightarrow \delta^*$ transition.[1]

2.5.1.(ii) Infrared spectrum

The infrared spectrum of a nujol mull of $Mo_2(O_2CH)_2(NCMe)_5(H_2O)_{\frac{1}{2}}(BF_4)_2$ was recorded (Fig.2.7). The broad peak at 3550 cm^{-1} is assigned to the O-H stretching vibration of water as the powder is hygroscopic. The band at 2290 cm^{-1} is characteristic of a C≡N stretching vibration, shifted to higher frequency as in the corresponding acetate compound and consistent with the presence of co-ordinated acetonitrile.[32] The number of bands expected, from point symmetry considerations, to be active in the infrared is five again for this compound. The observed band appears broadened and most probably

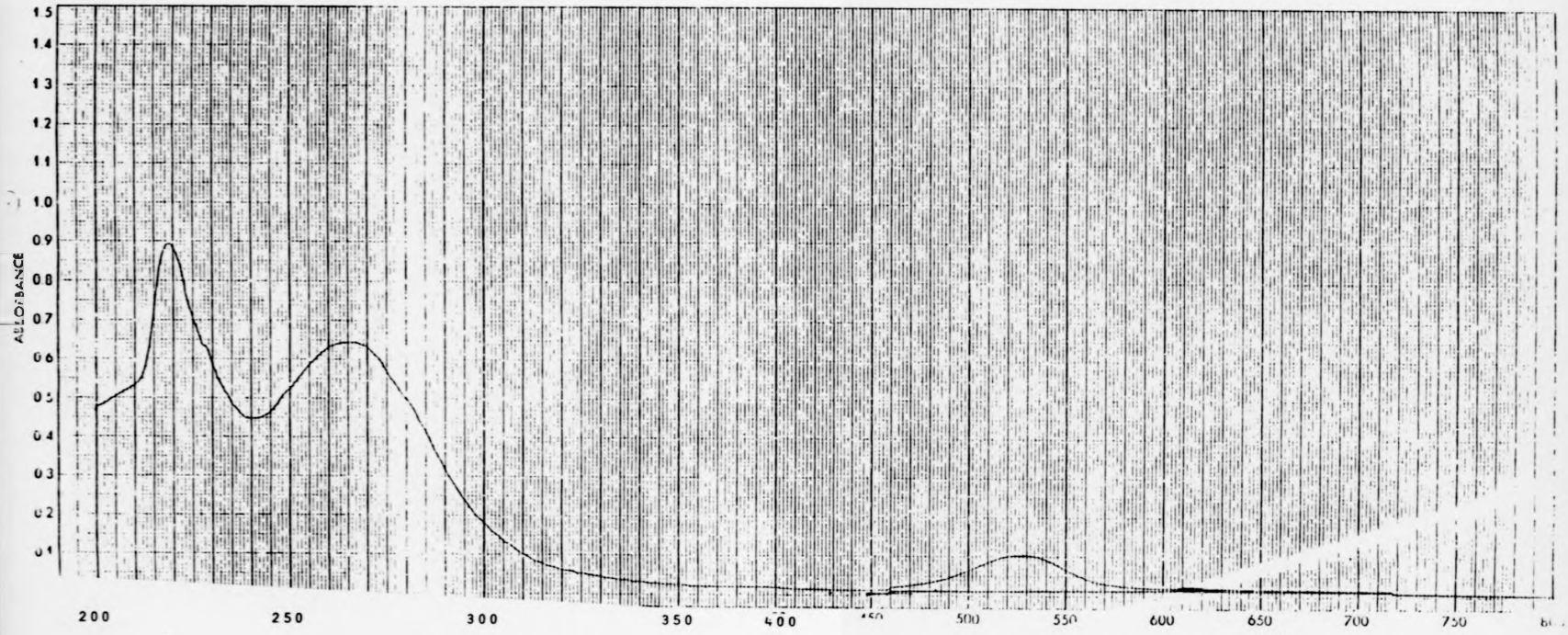

Fig.2.6 UV/visible spectrum of $[Mo_2(O_2CH)_2(NCMe)_5(H_2O)_{\frac{1}{2}}][BF_4]_2$ in MeCN

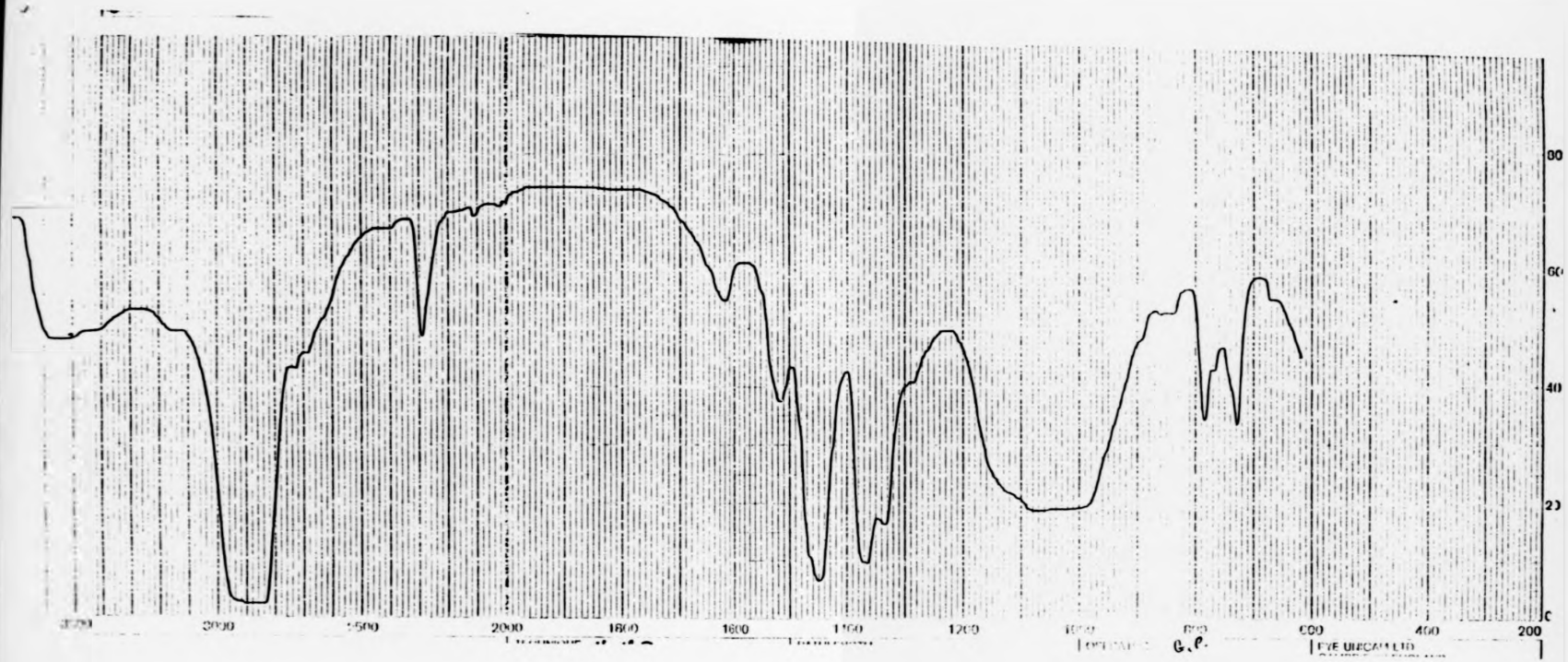

Fig.2.7 Infrared spectrum of $[Mo_2(O_2CH)_2(NCMe)_5(H_2O)_{\frac{1}{2}}][BF_4]_2$

contains more than one vibration. The band at 1515 cm^{-1} is assigned to the asymmetric carboxylate mode of the formate groups with the corresponding symmetric stretching modes occurring at 1365 and 1330 cm^{-1}.[34] The broad band at 1060 cm^{-1} is due to the B-F stretching mode in the $[BF_4]^-$ anion.[34] The band at 1620 cm^{-1} is assigned to the O-H bending vibration of H_2O.

Attempts to record the Raman spectrum were unsuccessful due to thermal decomposition in the laser source.

2.5.1(iii) N.m.r. spectroscopic studies

The ^1H n.m.r. spectrum of $Mo_2(O_2CH)_2(NCMe)_5(H_2O)_{\frac{1}{2}}(BF_4)_2$ in deuteroacetonitrile at room temperature was recorded at 90 MHz (Fig.2.8). This spectrum shows two resonances at 1.96 and 9.38 p.p.m. that integrate in the ratio 10:1, respectively. A resonance at 4.2 p.p.m. was present which integrated at ca. half the value of the peak at 9.38 p.p.m. Additional resonances at ca. 2.5 p.p.m. appeared. The resonance at 1.96 p.p.m. is assigned to the methyl groups of the acetonitrile ligands. Only one resonance for the CH_3CN groups was observed, implying that, as for the corresponding acetate compound, in solution all the acetonitriles are equivalent and labile. The signal at 1.96 p.p.m. is therefore due to free acetonitrile. The peak at 9.38 p.p.m. is assigned to the formate protons. This is in a similar position to the resonance observed for $[Mo_2(O_2CH)_4]$.[13] The integrations are slightly larger than expected from the formulation possibly due to incompletely deuterated solvent. Also when D_2O is added to a solution in CD_3CN, the formate resonance is nearly extinguished suggesting facile exchange between the D_2O and formate protons. Thus, as the compound is hygroscopic evidenced by the water resonance at 4.20 p.p.m.,

Fig.2.8 90 MHz ^1H n.m.r. spectrum of $[Mo_2(O_2CH)_2(NCMe)_5(H_2O)_{\frac{1}{2}}][BF_4]_2$ in CD_3CN

exchange between formate and water could affect the relative integrations. Additional resonances at ca. 2.5 p.p.m. appeared that integrated to ca. 1/9 of the acetonitrile resonance, the amounts varied from spectrum to spectrum for this compound and were observed occasionally in the ^1H n.m.r. spectra of the acetate analogue. These resonances also occurred in the ^1H n.m.r. spectrum of $[Me_3O][BF_4]$ additionally to a water resonance at 4.31 p.p.m. and all are due to impurities in the $[Me_3O][BF_4]$, probably alkyl ethers and esters.

For both $[Mo_2(O_2CMe)_2(NCMe)_6][BF_4]_2$ and $Mo_2(O_2CH)_2(NCMe)_5(H_2O)_{\frac{1}{2}}(BF_4)_2$ in CD_3CN, a shift to higher frequency is seen for the carboxylate protons in the ^1H n.m.r. spectrum from that of their parent tetra-carboxylate compounds (c.f. 2.63[13] to 2.82 p.p.m. for the acetate compounds and 9.20[13] to 9.38 p.p.m. for the formate compounds). The photoelectron spectra of $[Mo_2(O_2CMe)_4]$, $[Mo_2(O_2CMe)_2(O_2CH)_2]$, and $[Mo_2(O_2CH)_4]$ show that, as the number of formate groups increase, the effective positive charge on the molybdenum and oxygen atoms on the Mo_2O_8 centre also increases.[13] Furthermore the formate resonance also shifts to higher frequency on going from $[Mo_2(O_2CMe)_2(O_2CH)_2]$ to $[Mo_2(O_2CH)_4]$.[13] Therefore, since two negatively charged carboxylate groups have been removed, in this instance, and replaced by neutral MeCN molecules, it seems likely that the positive charge on the Mo_2O_4 centre will increase, accounting for the shift to higher frequency of the ^1H resonances of the carboxylate groups.

The ^{13}C n.m.r. spectrum of $Mo_2(O_2CH)_2(NCMe)_5(H_2O)_{\frac{1}{2}}(BF_4)_2$ in CD_3CN at room temperature was recorded at 25.1 MHz (Fig.2.9). This spectrum contains peaks at 1.2, 118.2, and 178.2 p.p.m. The peaks at 118.2 and 1.2 p.p.m. are assigned to the nitrile and methyl carbons, respectively, of the solvent; resonances due to CH_3CN of the compound are also

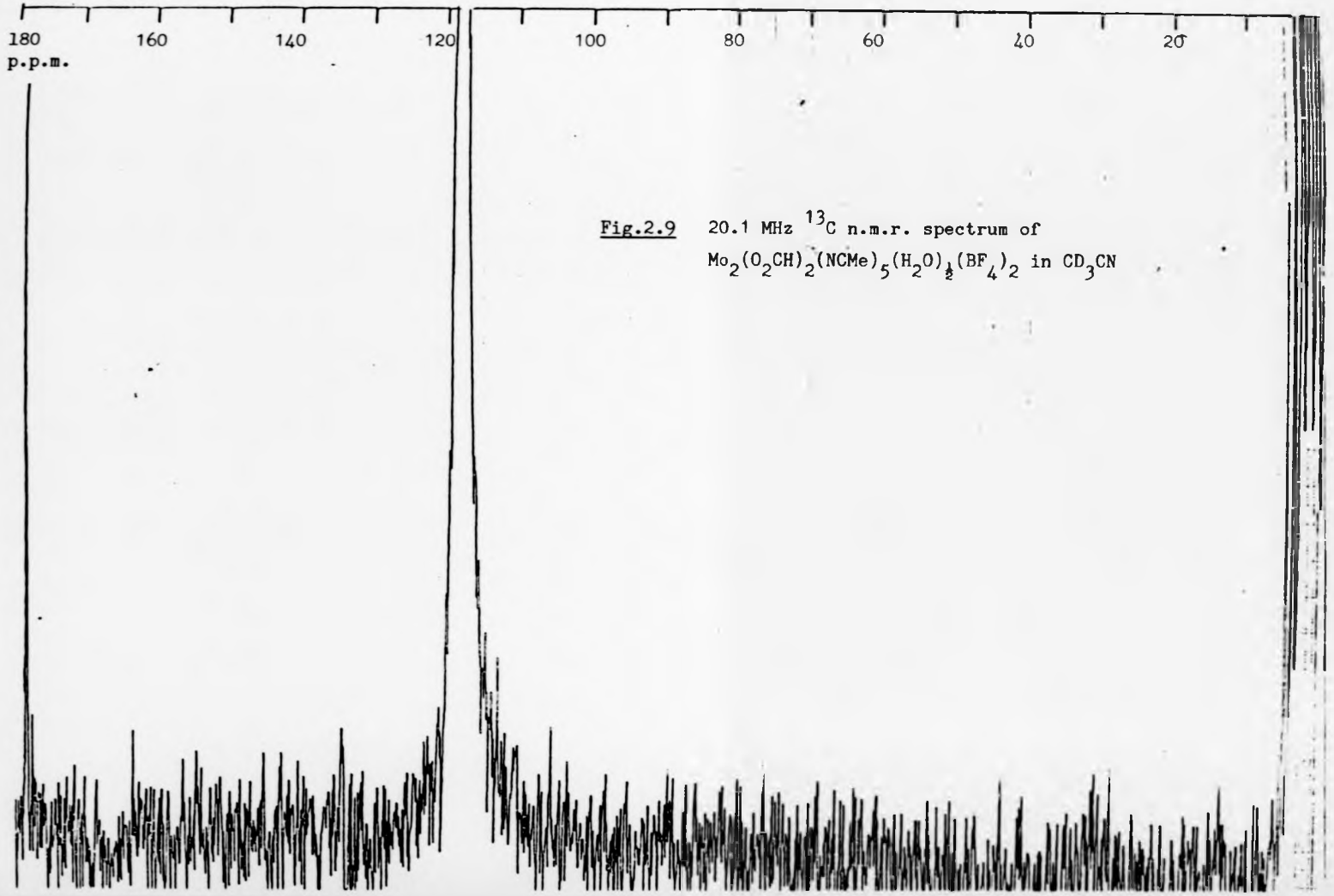

Fig.2.9 20.1 MHz ^{13}C n.m.r. spectrum of $Mo_2(O_2CH)_2(NCMe)_5(H_2O)_{\frac{1}{2}}(BF_4)_2$ in CD_3CN

considered to occur at these positions. The resonance at 178.2 p.p.m. is assigned to the carboxylate carbon of the formate ligands. This is typical of formate resonances.[35]

Following these studies of dimolybdenum systems an attempt was made to investigate similar reactions and characterisations for corresponding singly bonded dirhodium systems.

2.6 Preparation of $[Rh_2(O_2CMe)_4.2MeOH]$

The procedure adopted was that described by G.A. Rempel et al.[37] $RhCl_3$ (3 g, 11.4 mmol) and NaO_2CMe (6.11 g, 74.5 mmol) were refluxed in acetic acid (60 cm^3, glacial), and ethanol (60 cm^3). After 1 hour, the initial red solution had turned blue-green and a blue-green solid formed. The reaction mixture was allowed to cool for 1 hour and was then filtered. The blue-green powder was recrystallised in air from methanol. (Yield = 1.95 g, 70%)

Analyses	C	H
Calc. for $C_{10}H_{20}O_{10}Rh_2$	23.7	3.9 %
Found	23.6	4.0 %

The UV/visible and infrared spectra were recorded and were found to be identical to those reported in the literature.[37,38]

2.7 Preparation of $[Rh_2(O_2CMe)_2(NCMe)_6][BF_4]_2$

A solution of $[Me_3O][BF_4]$ (1.17 g, 7.9 mmol) in acetonitrile (20 cm^3) was added to a suspension of $[Rh_2(O_2CMe)_4(MeOH)_2]$ (1 g, 2 mmol) in acetonitrile (25 cm^3). This mixture was stirred for ca. 8 hours, until a deep purple clear solution had formed. The solution was then reduced to a purple oil under vacuum, methanol was added (20 cm^3), and

the solution was filtered. The filtrate was evaporated to dryness *in vacuo* and acetonitrile (20 cm^3) added to produce a purple solution. Diethyl ether (20 cm^3) was added carefully to this solution, producing a purple powder which was collected by filtration, washed with diethyl ether (2 x 5 cm^3), and dried *in vacuo* for *ca.* 1 hour. (Yield = 1.11 g, 75%) Crystals of this compound were obtained by concentrating an acetonitrile solution to saturation, warming and slow cooling.

Analyses	C	H	F	N	Rh
Calc. for $C_{16}H_{24}B_2F_8N_6O_4Rh_2$	25.8	3.2	20.4	11.3	27.7 %
Found	25.7	3.2	20.1	11.3	28.2 %

2.7.1 Crystal structure of $[Rh_2(O_2CMe)_2(NCMe)_6][BF_4]_2$

The crystal structure was accomplished by Dr. W. Clegg of the Anorganisch-Chemisches Institut der Universität Göttingen, Tammanstrasse 4, D3400 Göttingen, F.R.G.

A single crystal, coloured magenta, was sealed in a Lindemann glass capillary. The data were collected on a Stoe-Siemens AED diffractometer using graphite monochromated Mo-K_α radiation (λ = 0.71069 Å) with a ω/θ scan mode with on-line profile[16] fitting at T = 291K; no significant variation in standard reflection intensities was observed; absorption or extinction corrections were applied; D_m was not measured. The structure was solved by Patterson and Fourier techniques, including difference syntheses. Blocked-cascade least squares refinement proceeded to a minimum value of $\Sigma w\Delta^2$, where $w^{-1} = \sigma^2(F) + gF^2$ and g was optimised automatically, with anisotropic thermal parameters but without hydrogen atoms. The $[BF_4]^-$ anions were disordered and F atoms positions with partial occupancy factors were refined to account for the observed electron density with no attempted geometrical interpretation.

Computer programs were written by W.C. (diffractometer control program) and by Professor G.M. Sheldrick (SHELXTL system).[17] Scattering factors were taken from ref.18. A summary of the crystallographic and refinement data is presented in Table 2.1. The atomic co-ordinates are given in Table 2.7, selected bond lengths and bond angles are given in Table 2.8, and the structure of the cation is shown in Fig.2.10.

$[Rh_2(O_2CMe)_2(NCMe)_6][BF_4]_2.4MeCN$ consists of dipositive dimetal cations and (disordered) $[BF_4]^-$ anions; it contains extra MeCN molecules in the structure which are readily lost upon drying. $[Rh_2(O_2CMe)_2(NCMe)_6]^{2+}$ is located on a 2-fold axis and approximates to C_{2v} symmetry. Each of the mutually *cis* acetato-groups spans the dimetal centre, which possesses the normal[1] assembly of one axial and four equatorial ligands per metal with an eclipsed arrangement of the two sets of equatorial donor atoms within each cation. This structure is the second $Rh_2(O_2CR)_2L_6$ (L = a monodentate ligand) complex to be structurally characterised. The first was very recently achieved by Baranovskii *et al.*[9] of the *cis* acetato $[Rh_2(O_2CMe)_2(py)_6]^{2+}$ cation. The paucity of structural data for complexes of this type means that the factors which determine whether a *cis* or a *trans* arrangement of the two μ-carboxylato-groups in $[Rh_2(O_2CR)_2L_6]$ complexes remain to be established.

The Rh-Rh distance is 2.534(1) Å and this lies in the middle of the range for singly bonded rhodium dimers in which the shortest Rh-Rh distance (2.359(1) Å) is found in the tetra-bridged complex $[Rh_2(mhp)_4]$[39] and the longest Rh-Rh distance (2.936(2) Å) in the unbridged complex $[Rh_2(dmg)_4(PPh_3)_2]$.[40] The structures of the dibridged systems $[Rh_2(O_2CMe)_2(dmg)_2(PPh_3)_2].H_2O$,[41] $[Rh_2(O_2CH)_2(phen)_2Cl_2]$[42] and $[Rh_2(O_2CMe)_2(py)_6][CF_3SO_3]_2$[9] have been determined. The Rh-Rh bond lengths are 2.618(5) Å, 2.576 Å and 2.639(2) Å respectively,

Table 2.7 Atomic coordinates (x10⁴) for $[Rh_2(O_2CMe)_2(MeCN)_6][BF_4]_2 \cdot 4MeCN$

	x	y	z
Rh	4628(1)	2934(1)	1685(1)
O(11)	5480(2)	2168(1)	1328(2)
O(12)	6115(2)	2152(1)	2776(2)
C(11)	6024(3)	1930(2)	1938(3)
C(12)	6599(3)	1323(3)	1609(4)
N(2)	5330(2)	3696(2)	1085(2)
C(21)	5692(3)	4125(3)	681(3)
C(22)	6159(4)	4676(4)	147(5)
N(3)	3768(2)	3672(2)	2011(2)
C(31)	3260(3)	4090(2)	2149(3)
C(32)	2615(4)	4641(3)	2346(5)
N(4)	3978(2)	2753(2)	268(3)
C(41)	3659(3)	2700(3)	-452(3)
C(42)	3267(4)	2619(5)	-1408(4)
N(5)	2678(4)	867(5)	173(8)
C(51)	3375(5)	810(4)	295(6)
C(52)	4313(4)	792(4)	446(6)
N(6)	7540(4)	3252(5)	966(5)
C(61)	8169(4)	2957(4)	979(5)
C(62)	8953(4)	2583(5)	945(5)
B(7)	0	853(7)	2500
F(71)	12(19)	1454(7)	2866(15)
F(72)	249(15)	909(17)	1619(11)
F(73)	-846(10)	936(12)	2290(18)
F(74)	-221(47)	460(27)	1856(32)
F(75)	502(29)	368(20)	2293(49)
B(8)	0	4315(9)	2500
F(81)	564(9)	3811(10)	2032(14)
F(82)	-639(6)	4267(7)	1677(8)
F(83)	389(8)	4921(8)	2309(13)
F(84)	357(17)	4257(18)	1886(20)

Table 2.8 Selected bond lengths (Å) and angles (°)

$[Rh_2(O_2CMe)_2(MeCN)_6][BF_4]_2.4MeCN$

Rh-Rh'	2.534(1)		
Rh-O(11)	2.017(3)	Rh-O(12')	2.012(3)
Rh-N(2)	1.985(4)	Rh-N(3)	1.980(3)
Rh-N(4)	2.232(4)		
Rh'-Rh-O(11)	85.7(1)	Rh'-Rh-N(2)	97.4(1)
Rh'-Rh-N(3)	95.7(1)	Rh'-Rh-O(12')	85.7(1)
Rh'-Rh-N(4)	171.4(1)	O(11)-Rh-O(12')	89.3(1)
O(11)-Rh-N(2)	90.6(1)	O(11)-Rh-N(3)	178.4(1)
O(11)-Rh-N(4)	88.3(1)	O(12')-Rh-N(2)	176.9(1)
O(12')-Rh-N(3)	90.0(1)	O(12')-Rh-N(4)	88.1(1)
N(2)-Rh-N(3)	90.1(1)	N(2)-Rh-N(4)	88.8(1)
N(3)-Rh-N(4)	90.2(1)		

$[Rh_2(O_2CMe)_2(MeCN)_4(pyridine)_2][BF_4]_2$

Rh(1)-Rh(2)	2.548(2)		
Rh(1)-O(11)	2.024(4)	Rh(2)-O(12)	2.014(5)
Rh(1)-N(21)	1.973(5)	Rh(2)-N(31)	1.984(6)
Rh(1)-N(41)	2.231(9)	Rh(2)-N(51)	2.238(9)
Rh(2)-Rh(1)-O(11)	85.6(1)	Rh(1)-Rh(2)-O(12)	85.3(2)
Rh(2)-Rh(1)-N(21)	96.9(2)	Rh(1)-Rh(2)-N(31)	97.6(2)
Rh(2)-Rh(1)-N(41)	170.9(2)	Rh(1)-Rh(2)-N(51)	167.6(2)
O(11)-Rh(1)-N(21)	90.5(2)	O(12)-Rh(2)-N(31)	90.4(2)
O(11)-Rh(1)-N(41)	88.0(2)	O(12)-Rh(2)-N(51)	86.0(2)
O(11')-Rh(1)-N(21)	177.5(3)	O(12')-Rh(2)-N(31)	177.1(2)
N(21)-Rh(1)-N(41)	89.6(2)	N(31)-Rh(2)-N(51)	91.2(2)
O(11)-Rh(1)-O(11')	89.7(2)	O(12)-Rh(2)-O(12')	89.9(3)
N(21)-Rh(1)-N(21')	89.2(3)	N(31)-Rh(2)-N(31')	89.2(3)

A prime indicates an atom generated by symmetry (mirror plane or rotation axis).

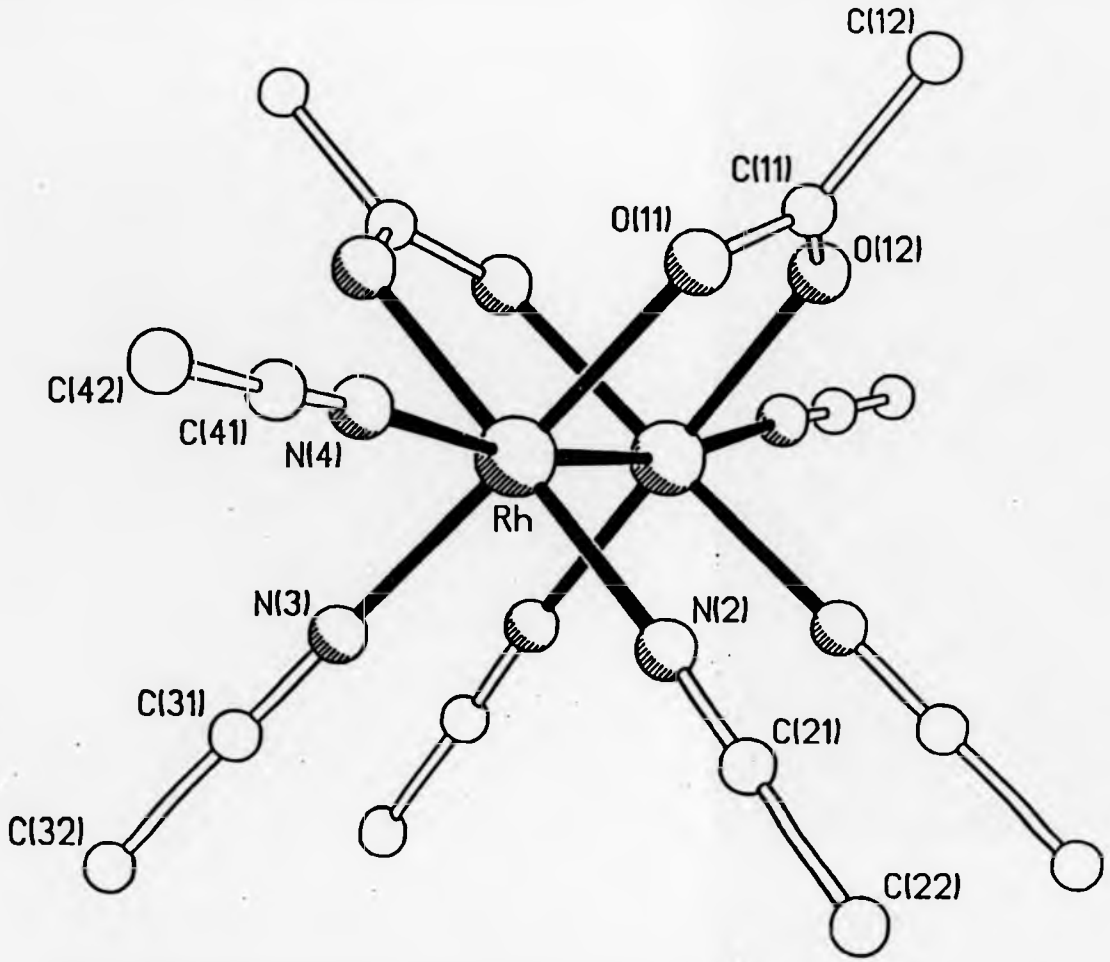

Fig.2.10 Crystal structure of $[Rh_2(O_2CMe)_2(NCMe)_6][BF_4]_2$

all three being longer than the value for the corresponding tetracarboxylate compounds (2.4505(2) Å for $[Rh_2(O_2CMe)_4(PPh_3)_2]$,[43] 2.38 Å for $[Rh_2(O_2CH)_4(H_2O)]$[44] and 2.3963(2) Å for $[Rh_2(O_2CMe)_4(py)_2]$[45]). Steric repulsions between chelating ligands and the effect of "contraction" by the bridging groups (O_2CR), have been proposed to account for the bond lengthening as the number of bridging ligands decreases.[46] This effect was also seen for Mo_2^{4+} systems but was not so dramatic.[1] In $[Rh_2(O_2CMe)_2(dmg)_2(PPh_3)_2]$[41] the dmg ligands are staggered by 20° and bent away from one another and in $[Rh_2(O_2CMe)_2(py)_6][CF_3SO_3]_2$[9] the equatorial planes containing the four pyridines and the two neighbouring rhodium atoms are turned away from one another. Similarly the Rh-Rh bond length of 2.534(1) Å in $[Rh_2(O_2CMe)_2(NCMe)_6][BF_4]_2$ is greater than that in $[Rh_2(O_2CMe)_4(NCMe)_2]$ (2.384(1) Å).[47] There is no staggering of the MeCN ligands but they are bent away from one another; the Rh-Rh'-O angles are 85.7(1) Å, the Rh-Rh'-N (for MeCN equatorial) are 96.6(1)° (average), and the Rh'-Rh-N angle is 171.4(1)° . The equatorial Rh-N bond distance of 1.982(4) Å is normal for Rh-NCMe bond distances e.g. Rh-N distances in $[Rh(PPh_3)_2(NCMe)_2NO][PF_6]_2$[48] are 2.030(7), 2.104(7) and 2.308(5) Å and in $[Rh(PPh_3)_3(NCMe)][BF_4]$ the value is 2.015(10) Å.[26] The Rh-N_{eq} bonds in $[Rh_2(O_2CMe)_2(mhp)_2(imidazole)]$,[49] $[Rh_2(O_2CMe)_2(dmg)_2(PPh_3)_2]$[40] and $[Rh_2(O_2CH)_2(phen)_2Cl_2]$[42] (range 1.952(4)-2.054(9) Å) are very similar to that (1.983(4) Å) observed for $[Rh_2(O_2CMe)_2(NCMe)_6]^{2+}$.

The Rh-N_{ax} bond length of 2.232(4) Å is comparable with those observed for other Rh_2^{4+} complexes containing axially bonded MeCN molecules; $[Rh_2(O_2CMe)_4(NCMe)_2]$,[47] $[Rh_2(mhp)_4(NCMe)]$,[49] and $[Rh_2(O_2CMe)_2(O_2CCPh_3)_2(NCMe)_2]$[50] involve Rh-$N_{ax}$ distances of 2.254(7), 2.152(7), and 2.19(1) Å respectively. The difference in bond length between the Rh-N_{eq} and Rh-N_{ax} is 0.25 Å and this is similar to the observed difference (0.2 Å) in $[Rh_2(O_2CMe)_2(py)_6][CF_3SO_3]_2$.[9]

The Rh-O bond length of 2.015(4) Å is similar but slightly shorter than the length of the corresponding bonds in $[Rh_2(O_2CMe)_4(H_2O)_2]$,[51] $[Rh_2(O_2CMe)_2(mhp)_2(imidazole)]$[49] and $[Rh_2(O_2CMe)_2(dmg)_2(PPh_3)_2]$[40] (range 1.952(4)-2.054(9) Å).

The internal bond lengths and angles within the acetate and acetonitrile ligands are normal.[1,24-26]

2.7.2 Crystal structure of $[Rh_2(O_2CMe)_2(NCMe)_4(py)_2][BF_4]_2$

The compound was prepared from $[Rh_2(O_2CMe)_2(NCMe)_6][BF_4]_2$. $[Rh_2(O_2CMe)_2(NCMe)_6][BF_4]_2$ (0.19 g, 0.25 mmol) was dissolved in pyridine (20 cm^3) to give an orange solution. Reduction of the volume of this solution by evaporation under reduced pressure, and the addition of diethyl ether (5 cm^3) precipitated an orange powder. This material was collected by filtration and recrystallised from methanol to yield ca. 0.18 g (85% yield) of a crystalline product.

Analyses	C	H	F	N	Rh
Calc. for $C_{22}H_{28}B_2F_8N_6O_4Rh_2$	32.2	3.4	18.5	10.2	25.1 %
Found	32.2	3.5	17.5	10.2	24.6 %

The spectroscopic properties of this compound will be discussed in Chapter 4.

The crystal structure was accomplished by Dr. W. Clegg of the Anorganisch-Chemisches Institut der Universität Göttingen, Tammanstrasse 4, D3400 Göttingen, F.R.G.

A single crystal, coloured yellow orange, was sealed in a Lindemann glass capillary. The data were collected and the structure solved as for $[Rh_2(O_2CMe)_2(NCMe)_6][BF_4]_2$. For the pyridine complex, it was necessary to restrain all B-F distances within the anion to be equal

(refined value 1.246(6) Å). A summary of the crystallographic and refinement data is presented in Table 2.1. The atomic co-ordinates are given in Table 2.9, selected bond lengths and bond angles are given in Table 2.8, and the structure of the cation is shown in Fig.2.11.

$[Rh_2(O_2CMe)_2(NCMe)_4(py)_2][BF_4]_2$ consists of dipositive dimetal cations and (disordered) $[BF_4]^-$ anions. The cation has mirror symmetry and the orientation of the planes of the pyridine rings means that $[Rh_2(O_2CMe)_2(NCMe)_4(py)_2]^{2+}$ corresponds to $\underline{C_s}$ symmetry. Each of the mutually cis acetato-groups spans the dimetal centre, which possesses the normal[1] assembly of one axial and four equatorial ligands per metal with an eclipsed arrangement of the two sets of equatorial donor atoms within each cation. The MeCN groups occupy the equatorial positions while the two pyridine molecules are located along the Rh-Rh axis. The comments concerning the structure of $[Rh_2(O_2CMe)_2(NCMe)_6]^{2+}$ apply to $[Rh_2(O_2CMe)_2(NCMe)_4(py)_2]^{2+}$. Inspection of the corresponding bond lengths and angles in Table 2.8 and Table 2.9 reveals that corresponding aspects of these two $Rh_2O_4N_6$ cores have virtually identical dimensions. The Rh-Rh bond length in $[Rh_2(O_2CMe)_2(NCMe)_4(py)_2]^{2+}$ is 2.548(2) Å, in the range of bond lengths for such rhodium dimers (2.359(1)-2.936(2) Å).[46] The Rh-Rh bond length is longer than that in the corresponding tetra-acetate compound $[Rh_2(O_2CMe)_4(py)_2]$[45] (2.3963(2) Å) and the Rh-N py bond distance of 2.233(9) Å (average) in $[Rh_2(O_2CMe)_2(NCMe)_4(py)_2]^{2+}$ is similar to the value (2.227(3) Å) in $[Rh_2(O_2CMe)_4(py)_2]$.[45] However, these values are still 0.1-0.2 Å longer than Rh-N(sp^2) bonds in mononuclear Rh(III) complexes.[52,53] Bond lengths and angles of the ligands are normal.[1,24-26] The orthogonal orientation of the two pyridine rings within the cation $[Rh_2(O_2CMe)_2(NCMe)_4(py)_2]^{2+}$ could be taken[45] as evidence in favour of significant Rh-pyridine π-back bonding.[54,55]

Table 2.9 Atomic coordinates (x10⁴) for $[Rh_2(O_2CMe)_2(MeCN)_4(pyridine)_2][BF_4]_2$

	x	y	z
Rh(1)	5571(1)	5000	6887(1)
Rh(2)	4317(1)	5000	7018(1)
O(11)	5115(2)	6363(4)	6080(2)
O(12)	4022(2)	6357(4)	6201(2)
C(13)	4457(4)	6766(6)	5922(3)
C(14)	4183(5)	7826(8)	5334(4)
N(21)	6057(3)	6322(5)	7665(3)
C(22)	6389(4)	7031(8)	8101(4)
C(23)	6859(6)	8014(10)	8673(6)
N(31)	4557(3)	6330(6)	7824(3)
C(32)	4653(4)	7061(8)	8280(4)
C(33)	4789(7)	8027(10)	8911(5)
N(41)	6562(4)	5000	6572(4)
C(42)	6471(6)	5000	5821(6)
C(43)	7033(5)	5000	5582(6)
C(44)	7747(8)	5000	6142(8)
C(45)	7881(7)	5000	6950(7)
C(46)	7247(5)	5000	7112(6)
N(51)	3113(5)	5000	6856(4)
C(52)	2767(5)	6215(10)	6797(4)
C(53)	1979(7)	6160(17)	6653(7)
C(54)	1615(14)	5000	6614(13)
B(1)	4970(7)	0	2721(8)
F(11)	5433(17)	792(24)	3137(13)
F(12)	4755(12)	926(21)	3007(21)
F(13)	4405(9)	501(13)	2206(9)
F(14)	5386(11)	-672(18)	2513(17)
B(2)	6757(8)	0	460(8)
F(21)	7374(8)	0	417(11)
F(22)	6815(8)	0	1122(6)
F(23)	6390(7)	997(13)	203(8)

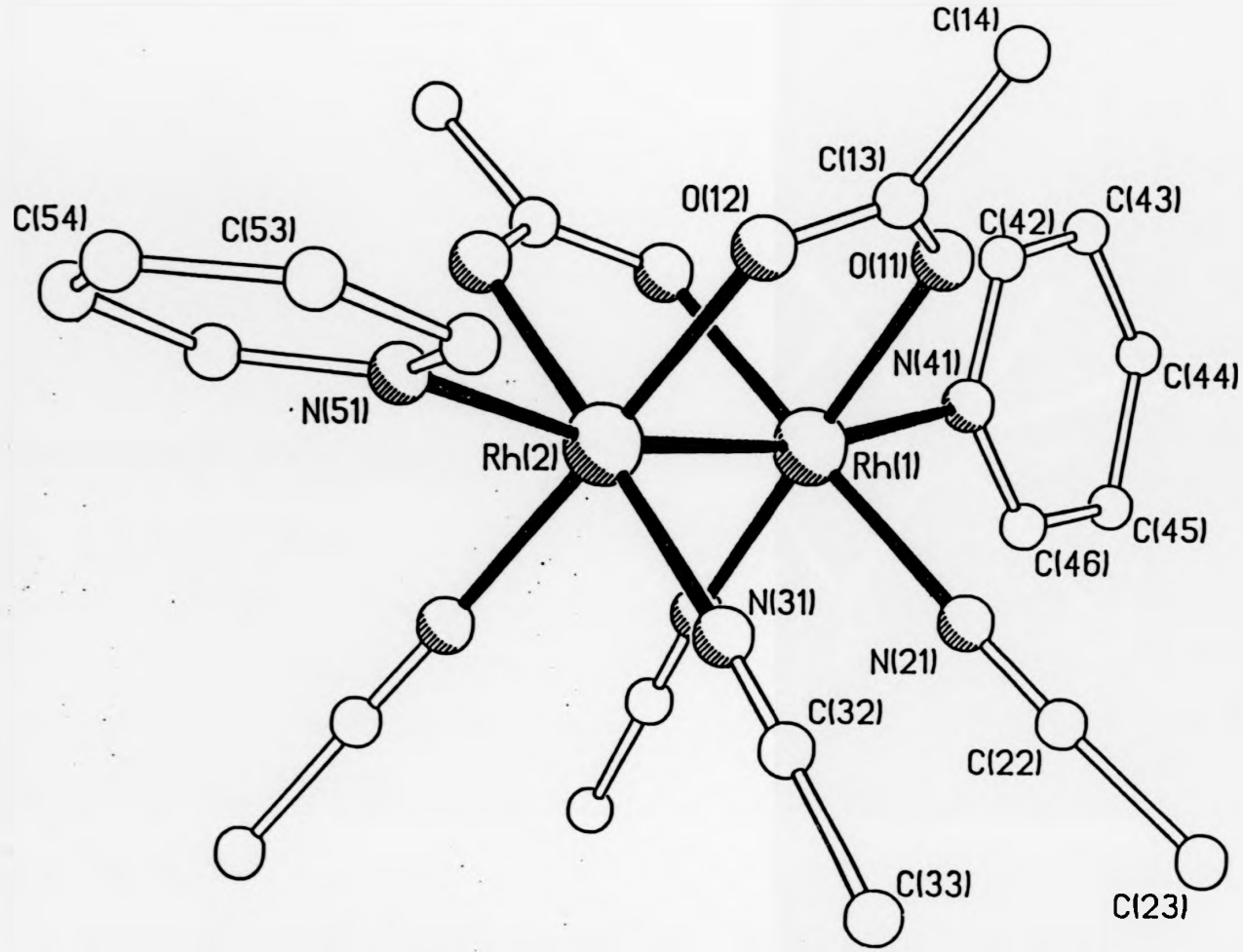

Fig.2.11 Crystal structure of $[Rh_2(O_2CMe)_2(NCMe)_4(py)_2][BF_4]_2$

However, given that the Rh-N_{py} distance in this cation is not significantly different from that in the tetra-acetate compound,[45] in which the pyridine rings manifest a lack of a preferred orientation with respect to each other, it seems unwise to conclude that the new structural data provides clear evidence for Rh→pyridine π-interactions.

Replacement of the axially ligated MeCN molecules by pyridine leads to a lengthening in the Rh-Rh bond length (from 2.534(1) Å to 2.548(2) Å). A similar increase is observed in going from $[Rh_2(O_2CMe)_4(NCMe)_2]$[47] (Rh-Rh = 2.384(1) Å) to $[Rh_2(O_2CMe)_4(py)_2]$[45] (Rh-Rh = 2.3963(2) Å).

2.7.3 Spectroscopic studies of $[Rh_2(O_2CMe)_2(NCMe)_6][BF_4]_2$

2,7.3(i) UV/visible spectrum

The UV/visible spectrum of $[Rh_2(O_2CMe)_2(NCMe)_6][BF_4]_2$ in acetonitrile (Fig.2.12) showed absorption maxima with extinction coefficients as expressed in Table 2.10.

Table 2.10 UV/visible bands for $[Rh_2(O_2CMe)_2(NCMe)_6][BF_4]_2$ in acetonitrile

Wavelength λ(nm)	ε(mol.cm^{-1}l^{-1})
520	202
355(sh)	478
270	23,959
218	9,396

The band at 520 nm is in a similar position to the lowest energy band observed for the $[Rh_2(O_2CR)_4L_2]$ compounds.[46] This band has been assigned by one set of workers to the $\pi^* \rightarrow \sigma^*$ transition of the Rh-Rh bond,[56] and by another to the $\pi^*,\delta^*(Rh_2) \rightarrow \sigma^*$(Rh-O(carboxylate))

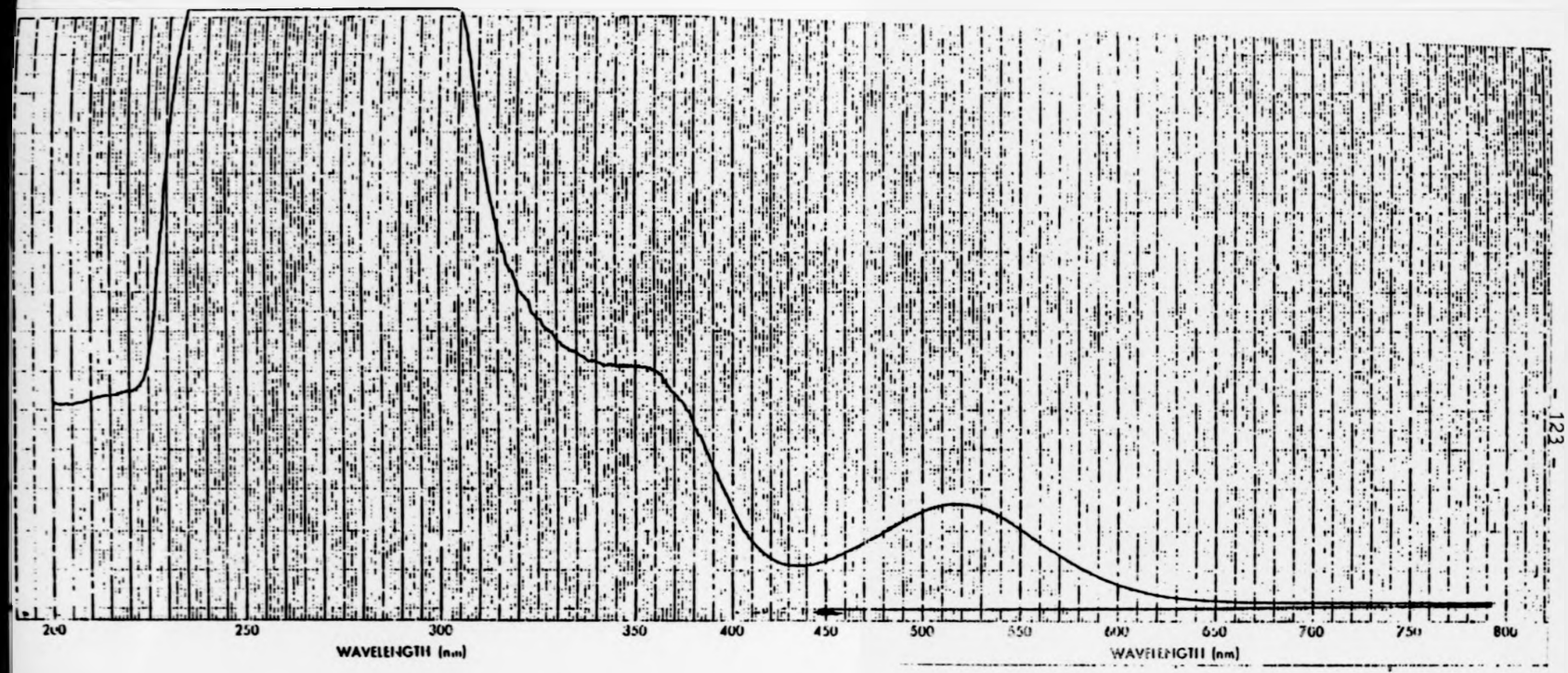

Fig.2.12 UV/visible spectrum of $[Rh_2(O_2CMe)_2(NCMe)_6][BF_4]_2$

transition.[57] The band is at a higher energy than that observed for the parent compound $[Rh_2(O_2CMe)_4]$, where the lowest energy band occurs at 552 nm in acetonitrile, although the molar extinction coefficients for the two bands are very similar. This is a similar observation to that seen for the compounds $[Rh_2(O_2CMe)_n(HNOCMe)_{4-n}]$ (where n = 0-4).[58] The band at 552 nm for $[Rh_2(O_2CMe)_4(NCMe)_2]$ undergoes a stepwise shift toward shorter wavelengths with the sequential replacement of acetate bridging ligands with a band at 528 nm for $[Rh_2(O_2CMe)_2(HNOCMe)_2(NCMe)_2]$. The nature of this band, it was stated, appeared independent of the number of acetamidates in the dirhodium complex. In the compound $[Rh_2(O_2CMe)_2(NCMe)_6][BF_4]_2$ and in the tetracarboxylate systems this band is very sensitive to changes in the nature of the axial ligands. The original assignment of the lowest energy band to $\pi^*(Rh_2) \rightarrow \sigma^*(Rh_2)$[56] was based on observations that its position is highly sensitive to axial-ligand variations since it is associated with a transition to the σ^* orbital which is located along the L-Rh-Rh-L axis. However, it has been pointed out that π-donor/-acceptor interactions of axial ligands also could affect the $\pi^*(Rh_2)$ orbital energy making the second assignment[57] not inconsistent with the observed spectral shifts.

The dependence of the lowest energy band on the identity of the axial ligand L has been described and discussed.[1,46,59,60] $[Rh_2(O_2CMe)_2(NCMe)_6][BF_4]_2$ appears to follow a similar pattern to the dirhodium tetracarboxylates,[1] in respect of the colours displayed in different solvents. The suggestion is that the axial ligands are replaced. Oxygen donors such as picoline-N-oxide, methanol, THF and water produce deep blue solutions with the lowest energy transition moving to lower energy (λ_{max} being at 559 nm, 585 nm, 596 nm and 580 nm respectively). Nitrogen, phosphorus and sulphur donors give yellow, red or orange complexes (for L = py, NH_3, $[NO_2]^-$, PPh_3 and DMSO λ_{max}

occurs at 470 nm, 501 nm, 506 nm, 410 nm and 487 nm respectively). More information about several of these complexes will be presented in Chapter 4.

The shoulder at 355 nm in the UV/visible spectrum of $[Rh_2(O_2CMe)_2(NCMe)_4L_2][BF_4]_2$ is rather insensitive to changes in the axial ligands, as is the corresponding band at around 440 nm in $[Rh_2(O_2CMe)_4L_2]$ complexes. This band, for the latter systems, has been interpreted as containing more than one transition. Martin et al. have assigned one of the transitions to the $\pi^*(Rh\text{-}Rh) \rightarrow \sigma^*(Rh\text{-}O)$ transition.[56] Recent workers have suggested a possible assignment as being the $\pi(Rh\text{-}O) \rightarrow \sigma^*(Rh\text{-}O)$ transition.[57]

The band at 270 nm is possibly a ligand to metal charge transfer band.

2.7.3(ii) Infrared spectrum

The infrared spectrum of a nujol mull of $[Rh_2(O_2CMe)_2(NCMe)_6][BF_4]_2$ is shown in Fig.2.13. The band at 3520 cm^{-1} is assigned to absorbed water from the plates; the compound is hygroscopic and, as discussed in the previous section, undergoes exchange of axial ligands. The bands at 2320, 2295 and 2270 cm^{-1} are assigned to the C≡N stretching vibrations[32,34] of the co-ordinated acetonitrile molecules. This shift to higher frequency of $\nu(C{\equiv}N)$ from that of free acetonitrile (2266 cm^{-1})[32] is consistent with the simple σ-co-ordination of the acetonitrile molecules. The bands can be further complicated by the fact that, in addition to the $\nu(C{\equiv}N)$ fundamental, a nearby band is often observed which results from a combination of the symmetrical CH_3 deformation and the C-C stretch.[33] Point group considerations point to five infrared and six Raman active C≡N vibrations with five coinci-

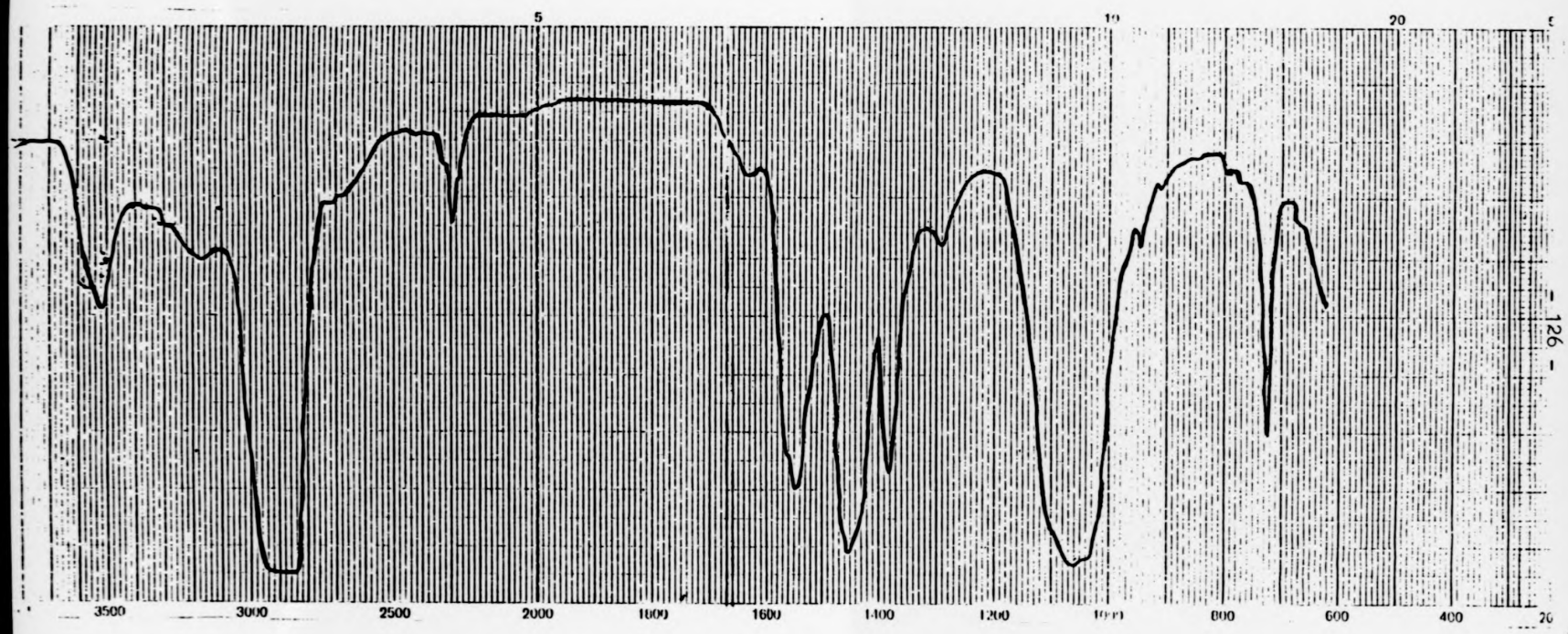

Fig.2.13 Infrared spectrum of $[Rh_2(O_2CMe)_2(NCMe)_6][BF_4]_2$

dences. Observation of fewer bands in the infrared spectrum than expected from symmetry considerations is possibly due to overlap of bands.

The bands in the infrared at 1545 cm^{-1} is assigned to the asymmetric carboxylate stretching frequency with the corresponding symmetric frequency occurring at 1370 cm^{-1}.[34] The broad band at 1070 cm^{-1} is assigned to the B-F stretching vibration of the $[BF_4]^-$ anion.[34]

The peak at 940 cm^{-1} is assigned to the C-C stretching vibration for the acetonitrile molecules.[32]

An attempt was made to record the Raman spectrum but the compound decomposed probably due to thermal decomposition by the laser source.

2.7.3(iii) N.m.r. spectroscopic studies

The 300 and 220 MHz ^1H n.m.r. spectra of $[Rh_2(O_2CMe)_2(NCMe)_6][BF_4]_2$ in deuteroacetonitrile and deuteromethanol at ambient temperature have been recorded and these are shown in Figs.2.14 and 2.15, respectively. In deuteroacetonitrile resonances were observed at 2.00, 2.10, and 2.59 p.p.m. the relative integrations being 3:2:4. The resonance at 2.10 p.p.m. is assigned to the acetate protons, in agreement with that for $[Rh_2(O_2CMe)_4]$ (2.12 p.p.m.)[7] and $[Rh_2(O_2CMe)_4(P(OMe)_3)]$(1.9 p.p.m.).[61] The resonance at 2.00 p.p.m. is assigned to the methyl group of the axial acetonitrile groups. The peak for free acetonitrile is at 1.95-2.00 p.p.m. which suggests that the axial sites are labile. This conclusion agrees with the observations of the UV/visible spectra (Section 2.7.3(i)) of $[Rh_2(O_2CMe)_2(NCMe)_6][BF_4]_2$ in various solvents and the conclusions of Boyar and Robinson.[61]

$$[Rh_2(O_2CMe)_2(NCMe)_6]^{2+} \xrightarrow{\text{SOLVENT L}} [Rh_2(O_2CMe)_2(NCMe)_4L_2]^{2+} + MeCN$$

VERY

TIGHTLY

BOUND

COPY

FIG. 2.14 300 MHz ^1H n.m.r. of $[Rh_2(O_2CMe)_2(NCMe)_6][BF_4]_2$ in CD_3CN

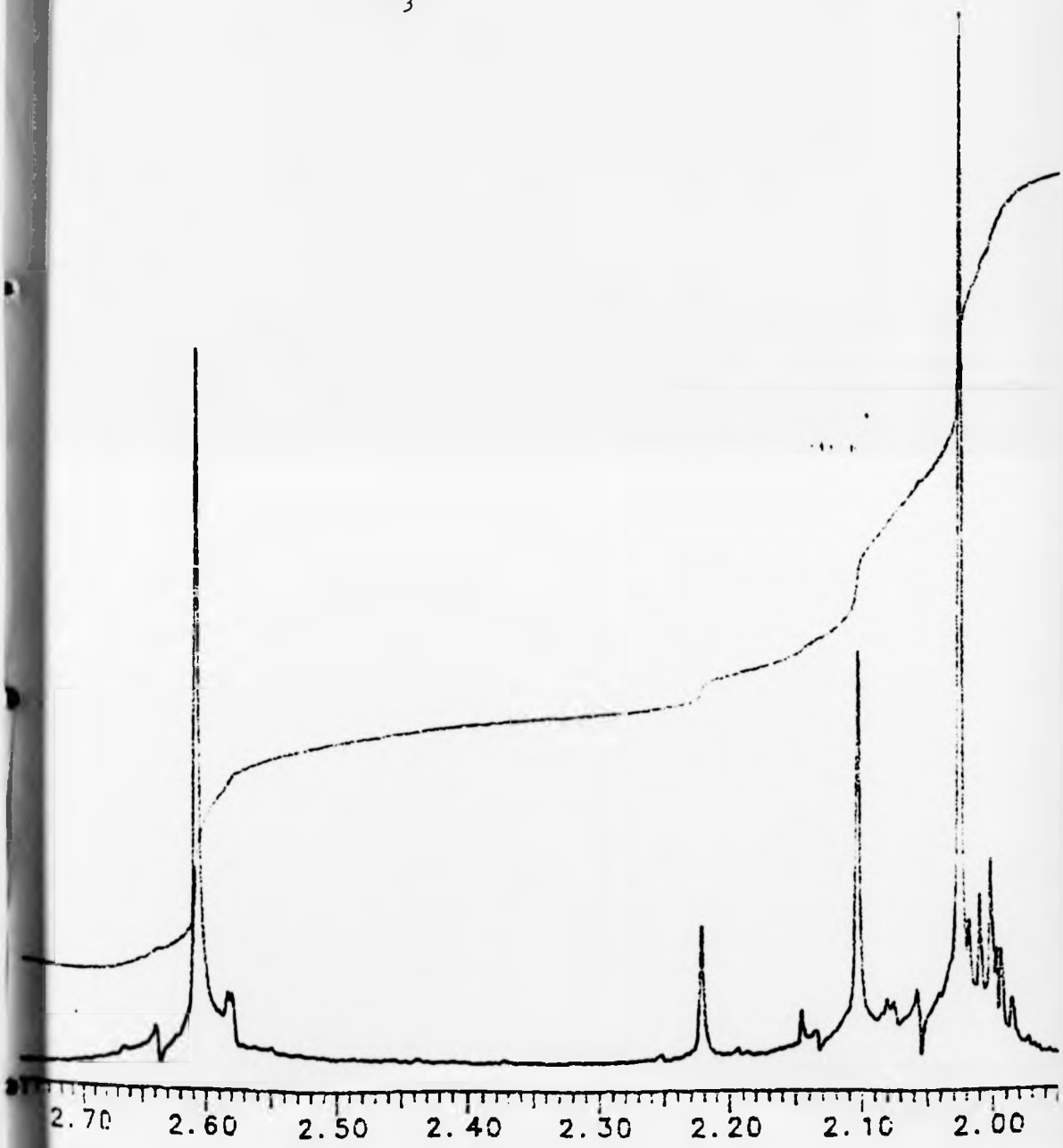

Fig.2.15 300 MHz ^{1}H n.m.r. of $[Rh_2(O_2CMe)_2(NCMe)_6][BF_4]_2$ in d_4-MeOH

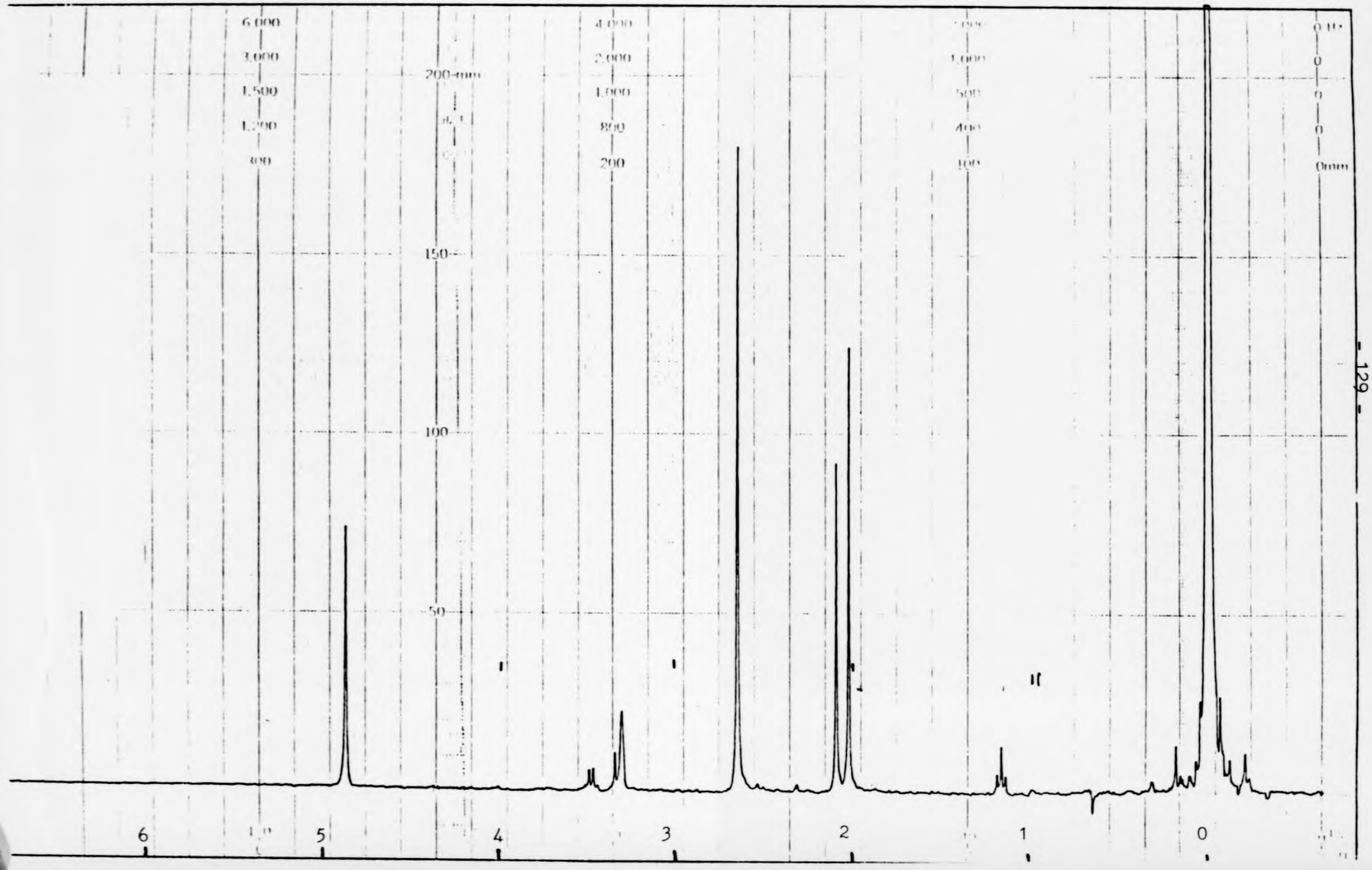

The resonance at 2.59 p.p.m. is assigned to the methyl groups of the equatorially co-ordinated acetonitrile molecules, which, therefore, experience a substantial shift from that of free ligand. There are at least two possible reasons for this large shift; co-ordination and/or the effect of ring currents in the Rh-Rh single bond. Similar shifts to higher frequency are seen in mononuclear Rh(III)NCMe complexes[62,63] (2.54 p.p.m. in $[Rh(NH_3)_5(NCMe)]^{3+}$ and 2.61 p.p.m. in $[Et_4N][RhBr_4(NCMe)_2]$) and are expected for co-ordination to a transition metal cation. Such a shift suggests reduced electron density at the acetonitrile methyl protons after co-ordination. This contrasts with the position of the methyl protons (2.10 p.p.m.) on acetonitrile co-ordinated to the rhodium(I) monomer $[Rh(PPh_3)_3(NCMe)][BF_4]$[26] (See Chapter 5). From this it is concluded that Rh_2^{4+} co-ordinates NCMe like monomeric Rh^{III}. The relative magnitudes of the integrations for these resonances agree for the equatorial acetonitrile and acetate protons, but the integration of the resonance due to axial acetonitrile is slightly too large. This could be due to some incompletely deuterated solvent but it is more likely that the reason is some solvent of crystallisation remaining in the sample.

The ^1H n.m.r. spectrum of $[Rh_2(O_2CMe)_2(NCMe)_6][BF_4]_2$ in deuteromethanol (Fig.2.15) contains resonances at 2.02, 2.09, and 2.65 p.p.m. The resonance at 2.65 p.p.m. is assigned to the methyl groups of the equatorial acetonitrile molecules, that at 2.09 p.p.m. to the acetate protons, and that at 2.02 p.p.m. to the protons of the axial/free acetonitrile. The relative integrations are 2:1:1, for the 2.65, 2.09, and 2.02 p.p.m. resonances, respectively, in agreement with these assignments. The 300 MHz ^1H n.m.r. spectrum of $[Rh_2(O_2CMe)_2(NCMe)_6][BF_4]_2$ in deuteroacetonitrile was recorded at 60°C to investigate if

exchange processes were occurring. However, no line broadening or coalescence was observed and therefore there is no significant exchange between equatorially co-ordinated and free acetonitrile at 60°C.

The 75 MHz ^{13}C n.m.r. spectrum of $[Rh_2(O_2CMe)_2(NCMe)_6][BF_4]_2$ in deuteroacetonitrile (Fig.2.16) shows resonances at 194, 127, 118, 23, 3, and 0 p.p.m. The resonances at 194 and 23 p.p.m. are assigned to the carboxylate and methyl carbons, respectively, of the acetate groups. These are typical of such resonances and are similar to those observed for $[Mo_2(O_2CMe)_2(NCMe)_6][BF_4]_2$ and $[Rh_2(O_2CMe)_4(P(OMe)_3)_2]$.[61] The resonances at 127 and 3 p.p.m. are assigned to the nitrile and methyl carbons, respectively, of the acetonitrile groups that are situated in the equatorially ligated positions. These are shifted to higher frequency from the positions in free acetonitrile (118 and 0 p.p.m. for nitrile and methyl carbons, respectively) by 9 p.p.m. and 3 p.p.m. respectively. Thus shifts to higher frequency on co-ordination are observed in both the ^1H and ^{13}C n.m.r. spectra for the acetonitrile molecules. In the ^{13}C n.m.r. spectra the shift on co-ordination is greater for the nitrile carbon than that for the methyl carbon which is to be expected since the nitrile carbon is closer to the co-ordination site. The peaks at 118 and 0 p.p.m. are assigned to the solvent and are considered to contain the signals of the axially co-ordinated acetonitrile groups. The 75 MHz ^{13}C n.m.r. spectrum of $[Rh_2(O_2CMe)_2(NCMe)_6][BF_4]_2$ was recorded at 60°C but, as in the ^1H n.m.r. spectrum, no change from that recorded at room temperature was observed.

The 300 MHz ^1H n.m.r. spectrum of the bis-pyridine adduct $[Rh_2(O_2CMe)_2(NCMe)_4(py)_2][BF_4]_2$ in deuterodimethylsulphoxide was recorded and contains resonances at 2.07 p.p.m. assigned to the methyl protons on the acetate groups, 2.77 p.p.m. assigned to the protons on

FIG. 2.16 75 MHz ^{13}C n.m.r. spectrum of $[Rh_2(O_2CMe)_2(NCMe)_6][BF_4]_2$ in CD_3CN

the equatorial acetonitrile groups and features at 7.87, 8.29, and 8.92 p.p.m. assigned to the protons on the co-ordinated pyridine. The 20.1 MHz ^{13}C n.m.r. spectrum of $[Rh_2(O_2CMe)_2(NCMe)_4(py)_2][BF_4]_2$ in deuterodimethylsulphoxide was recorded and contains resonances at 3, 23, 126, 127, 139, 150, and 192 p.p.m. As with the compound $[Rh_2(O_2CMe)_2(NCMe)_6][BF_4]_2$, the resonances at 23 and 192 p.p.m. are assigned to the methyl and carboxylate carbon, respectively, on the acetate groups whilst those at 3 and 127 p.p.m. are assigned to the methyl and nitrile carbon, respectively, on the equatorial acetonitrile molecules. The resonances at 126, 139, and 150 p.p.m. are assigned to the pyridine carbons. The n.m.r. spectra of $[Rh_2(O_2CMe)_2(NCMe)_4(py)_2][BF_4]_2$ will be discussed in more detail in Chapter 4 but the interpretations are consistent with those given for the spectra of $[Rh_2(O_2CMe)_2(NCMe)_6][BF_4]_2$.

2.8 Comparison of the properties of $[Mo_2(O_2CMe)_2(NCMe)_6][BF_4]_2$ and $[Rh_2(O_2CMe)_2(NCMe)_6][BF_4]_2$

$[Mo_2(O_2CMe)_2(NCMe)_6][BF_4]_2$ and $[Rh_2(O_2CMe)_2(NCMe)_6][BF_4]_2$ are isostructural. Both have <u>two</u> bridging acetate groups in a <u>cis</u>-arrangement and <u>six</u> acetonitrile groups attached to the metal via the nitrogen, <u>four</u> in the equatorial and <u>two</u> in the axial position. A comparison of the various pertinent bond lengths and bond angles is given in Table 2.11.

Table 2.11 Comparison of selected bond lengths and bond angles in $[Mo_2(O_2CMe)_2(NCMe)_6][BF_4]_2$ and $[Rh_2(O_2CMe)_2(NCMe)_6][BF_4]_2$

Bond length (Å)	$[Mo_2(O_2CMe)_2(NCMe)_6][BF_4]_2$	$[Rh_2(O_2CMe)_2(NCMe)_6][BF_4]_2$
M-M	2.136(1)	2.534(1)
$M-N_{eq}$	2.148(4)	1.982(4)
$M-N_{ax}$	2.758(10)	2.232(4)
M-O	2.084(4)	2.014(3)
Bond angles		
M-M-O	91.0(1)	85.7(1)
$M-M-N_{eq}$	102.0(1)	96.5(1)
$M-M-N_{ax}$	175.7(2)	171.4(1)

The increase in the length of the metal-metalbond, from 2.136(1) Å in the case of molybdenum to 2.534(1) Å in the case of rhodium is consistent with a change from a quadruple[1] to a single bond.[46]

The $Rh-N_{ax}$ bond is significantly shorter than that of its molybdenum counterpart, consistent with previous observations[1] that the structural trans-effect of a Rh-Rh single bond is much less than that of a Mo-Mo quadruple bond. These $[M_2(O_2CMe)_2(NCMe)_6]^{2+}$ (M = Mo or Rh) cations are ideal for a quantitative assessment of the trans effects of these metal-metal bonds; the difference $(M-N_{ax}) - (M-N_{eq})$ is 0.61 Å for M = Mo and 0.25 Å for M = Rh.

Both the Rh-O and Rh-N equatorial bond lengths are shorter than their molybdenum counterparts, consistent with the smaller covalent radius of rhodium as compared to molybdenum.[64] It is of interest to note that, in these $[M_2(O_2CMe)_2(NCMe)_6]^{2+}$ cations, the $M-N_{eq}$ bond

Table 2.11 Comparison of selected bond lengths and bond angles in $[Mo_2(O_2CMe)_2(NCMe)_6][BF_4]_2$ and $[Rh_2(O_2CMe)_2(NCMe)_6][BF_4]_2$

Bond length (Å)	$[Mo_2(O_2CMe)_2(NCMe)_6][BF_4]_2$	$[Rh_2(O_2CMe)_2(NCMe)_6][BF_4]_2$
M-M	2.136(1)	2.534(1)
$M-N_{eq}$	2.148(4)	1.982(4)
$M-N_{ax}$	2.758(10)	2.232(4)
M-O	2.084(4)	2.014(3)
Bond angles		
M-M-O	91.0(1)	85.7(1)
$M-M-N_{eq}$	102.0(1)	96.5(1)
$M-M-N_{ax}$	175.7(2)	171.4(1)

The increase in the length of the metal-metalbond, from 2.136(1) Å in the case of molybdenum to 2.534(1) Å in the case of rhodium is consistent with a change from a quadruple[1] to a single bond.[46]

The $Rh-N_{ax}$ bond is significantly shorter than that of its molybdenum counterpart, consistent with previous observations[1] that the structural *trans*-effect of a Rh-Rh single bond is much less than that of a Mo-Mo quadruple bond. These $[M_2(O_2CMe)_2(NCMe)_6]^{2+}$ (M = Mo or Rh) cations are ideal for a quantitative assessment of the *trans* effects of these metal-metal bonds; the difference $(M-N_{ax}) - (M-N_{eq})$ is 0.61 Å for M = Mo and 0.25 Å for M = Rh.

Both the Rh-O and Rh-N equatorial bond lengths are shorter than their molybdenum counterparts, consistent with the smaller covalent radius of rhodium as compared to molybdenum.[64] It is of interest to note that, in these $[M_2(O_2CMe)_2(NCMe)_6]^{2+}$ cations, the $M-N_{eq}$ bond

undergoes a significantly greater reduction in length than the M-O_{eq} bond, on proceeding from M = Mo to M = Rh; the changes are 0.17 and 0.07 Å, respectively. This parallels the situation observed for the corresponding $[M_2(mhp)_4]$ molecules,[39,65,66] where the corresponding changes are 0.12 and 0.07 Å.

As expected, especially because of the increased length of the M-M separation,[67] the value of the interbond angle M-M-O_{eq} is greater for M = Mo (91.0(1)°) than for M = Rh (85.7(1)°). Also M-M-N_{eq}, at 96.5(1)°, is smaller for $[Rh_2(O_2CMe)_2(NCMe)_6]^{2+}$ than for its molybdenum analogue (102.0(1)°).

The ^1H n.m.r. spectra of both $[Mo_2(O_2CMe)_2(NCMe)_6][BF_4]_2$ and $[Rh_2(O_2CMe)_2(NCMe)_6][BF_4]_2$ in deuteroacetonitrile at ambient temperatures show single peaks at 2.82 p.p.m. and 2.10 p.p.m., respectively, due to the methyl groups on the acetate giving a shift of 0.73 p.p.m. to lower frequency on moving from the dimolybdenum to the dirhodium centre.

Such a shift could arise from

(a) a variation in the distance of the methyl protons from the metal atoms in the two compounds,

or

(b) the effect of the diamagnetic anisotropy of the M-M bond (M = Mo and Rh).

The above two factors will now be discussed.

(a) Distance of the methyl protons from the metal atoms

On the assumption that C-H = 0.96 Å and H-C-H = 109.5° and, with the equivalence of the methyl protons, which suggests an average hydrogen atom position would be appropriate, an assessment of the relative proximity of the methyl hydrogen to the metal by considering the position of the corresponding carbon atoms was made. Taking the average position of the methyl hydrogen atoms to be ca. 0.32 Å from the carbon atom along the projection of the O_2C-C(Me) bond, and using bond lengths and bond angles from the two crystal structures, values of 4.65 Å and 4.62 Å were calculated for the Mo...H and Rh...H distances, respectively. Thus, there is no immediate correlation between the M...H(acetate) distances and the ^{1}H n.m.r. position of these protons.

(b) Effect of the diamagnetic anisotropy of the M-M bond

It has long been recognised[68] that the anomalous shielding observed in the ^{1}H n.m.r. spectra of certain organic compounds which contain a hydrogen nucleus in the vicinity of a carbon-carbon multiple bond is a direct consequence of the diamagnetic anisotropy that results when the circulating electrons within this multiple bond are subjected to an external field. The theoretical aspects of such long range shielding have been treated by McConnell,[69] the approximate relationship for an axially symmetrical group of electrons being

$$\sigma_{av} = \frac{(3\cos^2\theta - 1)(\chi_L - \chi_T)}{3r^3}$$

where r is the distance between the proton and the electrical centre of gravity of the multiple bond, θ is the acute angle between r and the symmetry axis, and χ_L and χ_T are the longitudinal and transverse

magnetic susceptibilities, respectively, of the bond in question. The subscript "av" is included to indicate that the shielding, σ, has been averaged over all orientations of the system. From the angular dependence of this relationship it is noted that the value of the function changes sign at 55°44' so that an axially symmetrical bond can either shield or deshield a neighbouring proton depending on their relative orientations. The sign of the shielding is also seen to be further dependent on the value of the difference $(\chi_L - \chi_T)$ while the magnitude of the shielding increases towards the symmetry axis and towards the electrical centre of gravity.

The shift of the ^1H resonance of ligands due to their proximity to multiple M-M bonds has been considered previously[70] and diamagnetic anisotropy values χ_{M-M} for Mo≡Mo and Rh-Rh bonds determined.[70] Using these values (326 x 10^{-36} m^3 $molecule^{-1}$ for Mo≡Mo and 112 x 10^{-36} m^3 $molecule^{-1}$ for Rh-Rh) and the bond lengths and bond angles from the two crystal structures, again assuming an average position for the methyl protons 0.32 Å from the carbon atom along the projection of the O_2C-C(Me) bond, σ_{av} values of 1.17 p.p.m. and 0.42 p.p.m. are obtained for $[Mo_2(O_2CMe)_2(NCMe)_6][BF_4]_2$ and $[Rh_2(O_2CMe)_2(NCMe)_6][BF_4]_2$, respectively. (Calculation of the actual resonance positions is difficult since there are complications due to the effects of C-O and M-O bonds and the problem of a suitable reference point.) The difference in these σ_{av} values, 0.75 p.p.m., is very close to that observed experimentally, 0.73 p.p.m. (2.83-2.1 p.p.m.). Therefore, the difference in the methyl resonances of these two compounds clearly reflects the different metal-metal bond orders.

The major difference in the solution ^1H n.m.r. spectra of the two complexes concerns the lability of the acetonitrile ligands.

In $[Mo_2(O_2CMe)_2(NCMe)_6][BF_4]_2$, the acetonitriles are all equivalent on the n.m.r. time scale and appear to be labile. In $[Rh_2(O_2CMe)_2(NCMe)_6][BF_4]_2$, the axial and equatorial acetonitriles are inequivalent. The resonance position of the axial acetonitriles indicates that these are labile but the resonance of the equatorial acetonitrile molecules indicates that these are tightly bound to the Rh_2^{4+} core.

2.9 Attempted extensions of this chemistry

Attempts were made to use labile solvent molecules other than MeCN, in the basic reaction of $[Me_3O][BF_4]$ with $[Rh_2(O_2CMe)_4]$. As UV/visible and n.m.r. spectra indicated, the equatorial acetonitriles of this system are not labile and reactivity of $[Rh_2(O_2CMe)_2(NCMe)_6][BF_4]_2$ (see Chapter 4) indicated that only the axial ligands were easily replaced. Thus, a potentially more labile solvent molecule, methanol, was chosen, as a substitute for acetonitrile. Schrock and Osborn observed that methanol and acetone are readily exchanged on a monomer Rh centre while MeCN is more strongly bound.[71] However, no reaction was observed, either because of the instability of the analogous methanol complex of dirhodium or because of the lack of solubility of $[Me_3O][BF_4]$ in methanol.

As the reaction of $[Me_3O][BF_4]$ with $[Mo_2(O_2CMe)_4]$ could be extended to the dirhodium system $[Rh_2(O_2CMe)_4]$ to produce isostructural compounds, containing quadruple and single bonds respectively, an attempt to remove two acetates from $[Cu_2(O_2CMe)_4]$ and replace them with MeCN molecules, was undertaken. Although $[Cu_2(O_2CMe)_4]$ and $[Me_3O][BF_4]$ were stirred in acetonitrile for ca. 3 days, no reaction was observed.

An attempt was made to remove all of the acetates of $[Mo_2(O_2CMe)_4]$ by refluxing $[Mo_2(O_2CMe)_4]$ and $[Me_3O][BF_4]$ (in a 1:8 stoichiometric ratio) in acetonitrile for ca. 4 hours. The crystals isolated from this reaction were shown by UV/visible spectroscopy and ^1H n.m.r. spectroscopy to be $[Mo_2(O_2CMe)_2(NCMe)_6][BF_4]_2$.

The ease of acetate removal and replacement, by acetonitrile ligands, suggested that a change in the nature of the nitrile ligands would be worthwhile, investigating the effects on the properties of the dimolybdenum or dirhodium centre. Nitriles with more bulky substituents were chosen in a hope to impose strains in the arrangement about the dimetal centres, which may be tolerated or may lead to different reactivity.

Steric effects introduced by the ligands have been observed to have important consequences for dimolybdenum and dirhodium complexes. Several dimolybdenum compounds have been studied structurally, to examine the relationship between the energy of the $\delta \rightarrow \delta^*$ electronic transition and the strength of the δ-bond.[72] The latter is taken to be a linear function of $\cos(2\chi)$, where χ is the angle of internal rotation away from the fully eclipsed conformation. The fact that the strength of the δ-bond is greatest for $\chi = 0$ does not mean that this will always be the preferred angle when other factors are taken into account. Thus the δ-bond is the weakest component of the quadruple bond and the minimization of non-bonded repulsions between ligands around the quadruple bond can favour a rotation away from the eclipsed conformation.[1] Steric interactions between ligands may affect the length of the Rh-Rh bond in Rh_2^{4+} complexes. $[Rh_2(dmg)_2(O_2CMe)_2(PPh_3)_2]$[41] contains 2 bridging acetate groups in a cis-arrangement, 2 chelating dmg ligands, and 2 axial PPh_3 molecules. The Rh-Rh distance is 2.618(5) Å, 0.17 Å longer than that in $[Rh_2(O_2CMe)_4(PPh_3)_2]$, and this lengthening is

assumed to arise from steric interactions between dmg ligands that are staggered by 20° and bent away from one another.

Therefore, for both Mo_2^{4+} and Rh_2^{4+} centres the use of the more bulky nitrile ligand, trimethyl acetonitrile Me_3CCN, was investigated. The construction of molecular models for both the proposed molybdenum and rhodium compounds $[M_2(O_2CMe)_2(NCC(Me)_3)_6][BF_4]_2$ (M = Mo or Rh) showed a considerable amount of twist necessary in the solid state to accommodate the bulky methyl groups.

2.9.1 Preparation of $[Mo_2(O_2CMe)_2(NCCMe_3)_5][BF_4]_2$

$[Mo_2(O_2CMe)_4]$ (0.63 g, 1.5 mmol) was added to a solution of $[Me_3O][BF_4]$ (0.87 g, 5.9 mmol) in trimethyl acetonitrile (30 cm^3). A pink solution formed after ca. 3 hours, above some undissolved $[Mo_2(O_2CMe)_4]$ and some undissolved pink powder. After stirring the mixture for 3 days, a pink precipitate and a pink solution were obtained. The powder was collected by filtration. The product was washed with diethyl ether (ca. 20 cm^3) and dried in vacuo for ca. 5 hours. (Yield = 0.11 g, 80%)

Analyses	C	H	F	N
Calc. for $C_{29}H_{45}B_2F_8Mo_2N_5$	37.7	6.1	16.9	7.7 %
Found	36.6	5.7	17.2	7.4 %

The powder was not very soluble in trimethylacetonitrile and it is proposed that it forms chains of dimers with weak axial attachments through the carboxylate oxygen atoms of adjacent Mo_2^{4+} units. The compound is also very hygroscopic, the fine powder absorbing so much water on a few seconds exposure to air that it rapidly becomes a pink oil.

2.9.2 Spectroscopic studies

2.9.2(i) UV/visible spectrum

The UV/visible spectrum of $[Mo_2(O_2CMe)_2(NCCMe_3)_5][BF_4]_2$ in trimethylacetonitrile and acetonitrile are shown in Figs.2.17 and 2.18, respectively. The values for λ_{max}(nm) and molar extinction coefficients in MeCN are listed in Table 2. .

Table 2.12 UV/visible absorptions for $[Mo_2(O_2CMe)_2(NCCMe_3)_5][BF_4]_2$ in MeCN

λ_{max}(nm)	$\varepsilon(mol^{-1}cm^{-1}dm^3)$
532	1085
380(sh)	511
261	9312

The UV/visible spectrum of $[Mo_2(O_2CMe)_2(NCCMe_3)_5][BF_4]_2$ in Me_3CCN contains absorption bands at 513, 380(sh), and 276 nm. As discussed in Section 2.4.2(i) the bands at 532 and 513 nm are assigned to be due to the $\delta \rightarrow \delta^*$ transition[1] as in the analogous acetonitrile complex.

The spectrum of $[Mo_2(O_2CMe)_2(NCCMe_3)_5][BF_4]_2$ in MeCN is identical to that observed for $[Mo_2(O_2CMe)_2(NCMe)_6][BF_4]_2$ in MeCN, suggesting that the trimethylacetonitrile molecules are being replaced by acetonitrile, as would be expected from the lability of all of the RCN molecules of Mo_2^{4+} complexes (Sections 2.4.2(iii), 2.5.2(iii) and 2.8).

The UV/visible spectrum of $[Mo_2(O_2CMe)_2(NCCMe_3)_5][BF_4]_2$ in Me_3CCN exhibits a band at 513 nm. The UV/visible spectrum of the analogous MeCN compound $[Mo_2(O_2CMe)_2(NCMe)_6][BF_4]_2$ in MeCN exhibits a band at 532 nm. This, from the earlier discussion on the correlation of the $\delta \rightarrow \delta^*$ transition vs M-M bond distance, should indicate a shorter

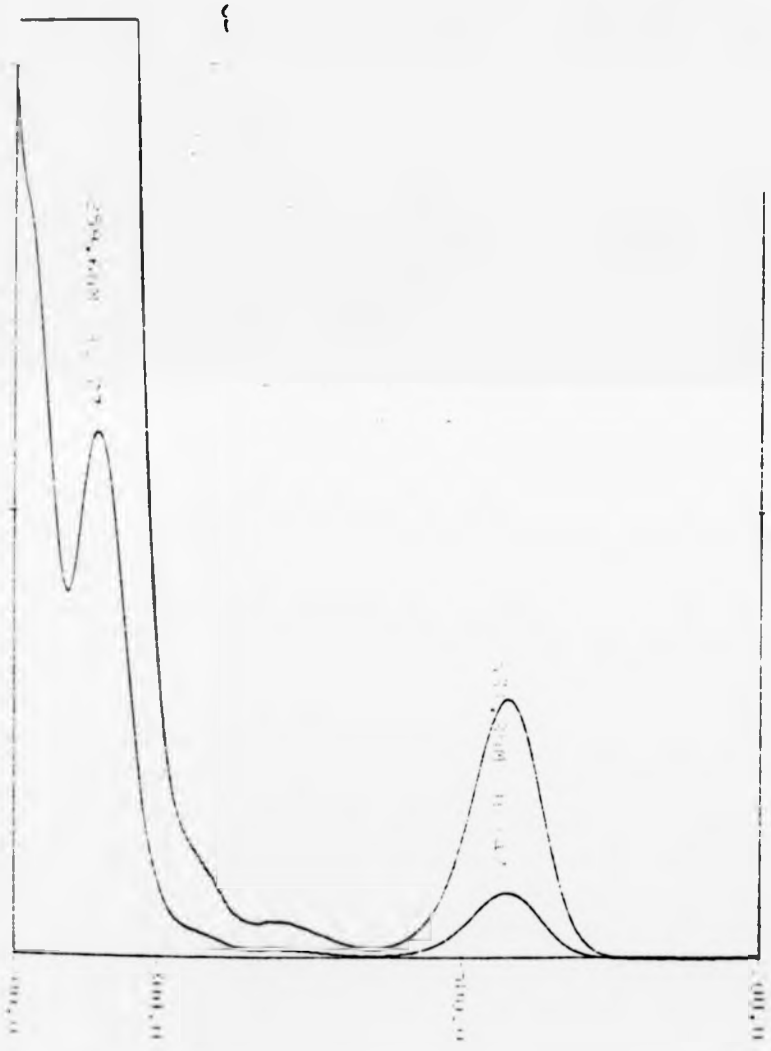

FIG. 2.17 UV/visible spectrum of $[Mo_2(O_2CMe)_2(NCCMe_3)_5][BF_4]_2$ in MeCN

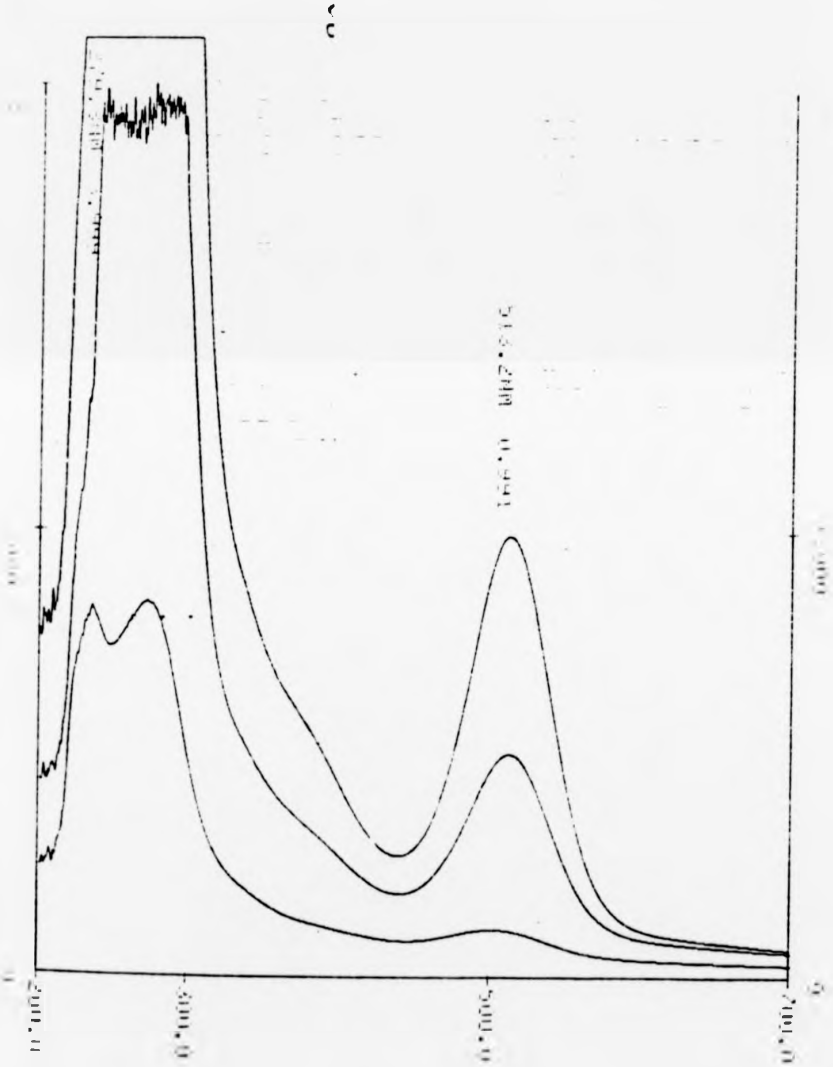

Fig.2.18 UV/visible spectrum of $[Mo_2(O_2CMe)_2(NCCMe_3)_5][BF_4]_2$ in Me_3CCN

Mo-Mo bond in the Me_3CCN complex than in the MeCN complex, which is a result contrary to that expected on steric grounds. However, the electron donating properties of the methyl groups could lead to a more effective reduction in the positive charge at the metal centres and hence a closer approach and stronger Mo-Mo bond.

2.9.2(ii) Infrared spectrum

The infrared spectrum of a nujol mull of $[Mo_2(O_2CMe)_2(NCCMe_3)_5][BF_4]_2$ is shown in Fig.2.19. The broad band at 3400 cm^{-1} is probably due to absorbed water, as the compound is hygroscopic and can become very oily, even when the mull was prepared under nitrogen. The band at 2270 cm^{-1} is assigned to the C≡N stretching vibrations of Me_3CCN. The C≡N stretching vibration in free Me_3CCN is at 2240 cm^{-1} and the shift to higher frequency implies co-ordination via the N atom. The band at 1475 cm^{-1} is assigned to the asymmetric carboxylate stretching frequency with the corresponding symmetric frequency occurring at 1360 cm^{-1}. The broad band at 1240 cm^{-1} will contain vibrations due to the C-H bending of the Me_3CCN molecules and the acetate groups. The band at 1050 cm^{-1} is assigned to the B-F stretching vibrations of the $[BF_4]^-$ anion and that at 1620 cm^{-1} is assigned to the O-H bending vibration of the absorbed water.

2.9.2(iii) N.m.r. spectroscopic studies

The 300 MHz ^1H n.m.r. spectrum of $[Mo_2(O_2CMe)_2(NCCMe_3)_5][BF_4]_2$ in deuteroacetonitrile at ambient temperatures is shown in Fig.2.20. This shows two sharp resonances at 1.39 p.p.m. and 2.95 p.p.m. that integrate in a 15:2 ratio, respectively. A very small multiplet is visible at 2.00 p.p.m. due to incompletely deuterated solvent.

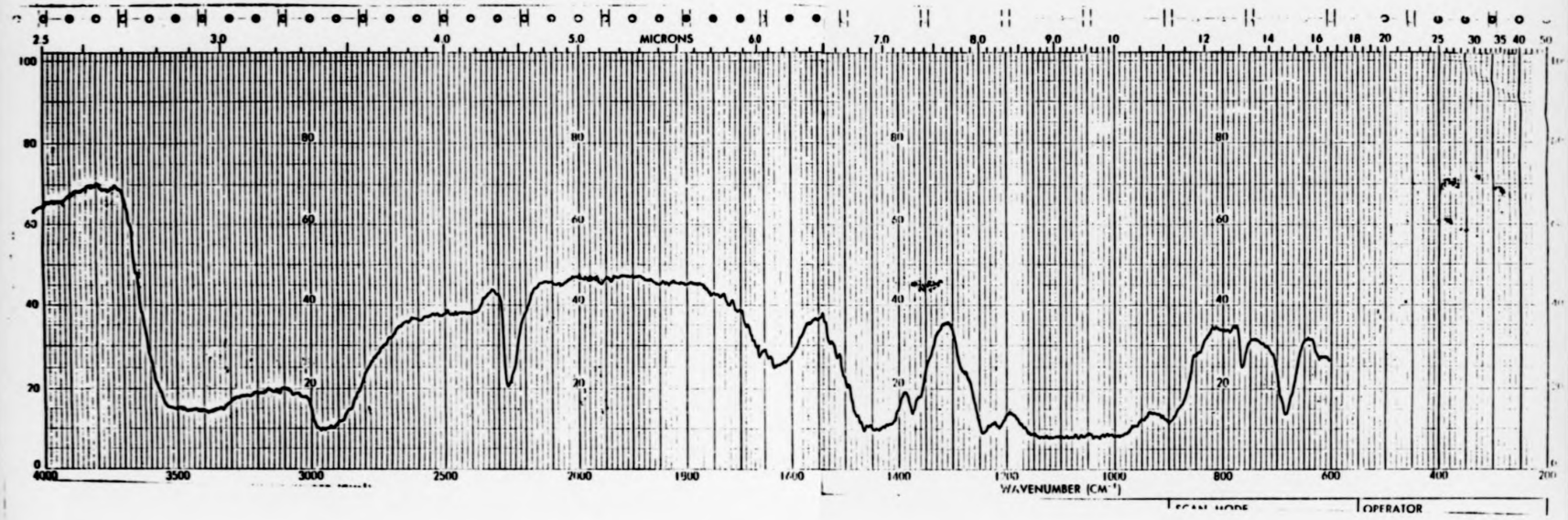

FIG. 2.19 Infrared spectrum of $[Mo_2(O_2CMe)_2(NCCMe_3)_5][BF_4]_2$

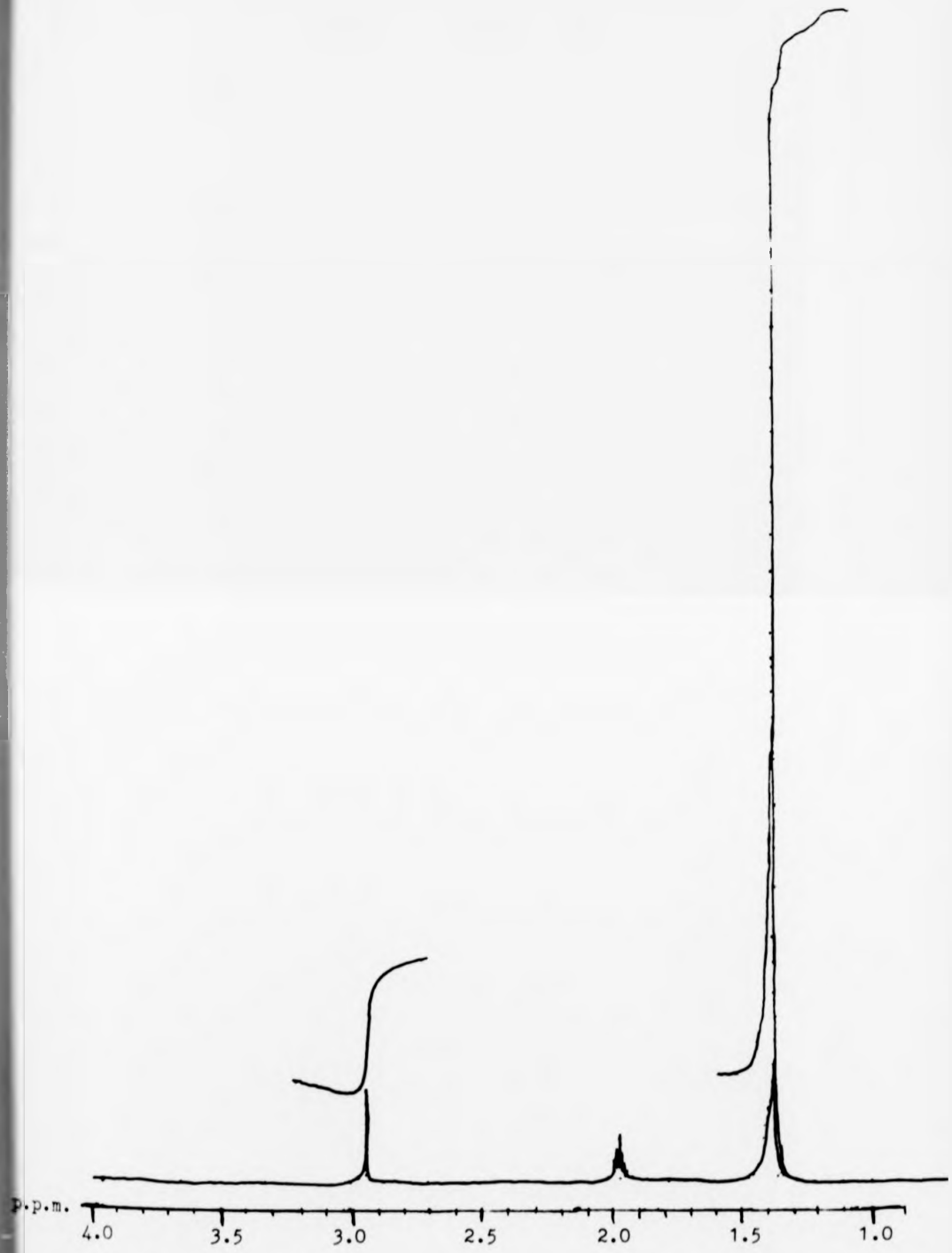

FIG. 2.20 300 MHz ^1H n.m.r. spectrum of $[Mo_2(O_2CMe)_2(NCCMe_3)_5][BF_4]_2$ in CD_3CN

The resonance at 1.39 p.p.m. is assigned to the methyl protons in trimethylacetonitrile and that at 2.95 p.p.m. to the methyl protons in the acetate groups, in agreement with the relative integrations. The position of the Me_3CCN protons is in the position for free Me_3CCN[73] consistent with the proposal that the nitriles in these compounds are labile, and the acetate resonance is shifted further downfield than in the corresponding MeCN adduct suggesting that the acetate resonance shows some dependence on axial and equatorial ligands.

The 75 MHz ^{13}C n.m.r. spectrum of $[Mo_2(O_2CMe)_2(NCCMe_3)_5][BF_4]_2$ in deuteroacetonitrile at ambient temperatures is shown in Fig.2.21. This shows resonances at 189.3, 146.8, 127.1, 119.3, 29.0, 28.4, 23.7, and 0.7 p.p.m. The resonances at 189.3 and 23.7 p.p.m. are assigned to the carboxylate and methyl carbons, respectively, of the acetate group and those at 127.1, 29.0, and 28.4 p.p.m. are assigned to the nitrile, butyl, and methyl carbons, respectively, of Me_3CCN. These are the resonance positions of free Me_3CCN (Fig.2.22). The resonances at 119.3 and 0.7 p.p.m. are assigned to solvent resonances and that at 146.8 p.p.m. is assigned to the same impurity as that observed in the ^{13}C n.m.r. spectrum of $[Mo_2(O_2CMe)_2(NCMe)_6][BF_4]_2$ which could be aromatic solvent.

The ^{95}Mo n.m.r. was recorded and is discussed in Chapter 3.

2.9.3 Preparation of $[Rh_2(O_2CMe)_2(NCCMe_3)_6][BF_4]_2$

A solution of $[Me_3O][BF_4]$ (0.32 g, 2.2 mmol) in trimethylacetonitrile (10 cm^3) was added to a suspension of $[Rh_2(O_2CMe)_4(MeOH)_2]$ (0.27 g, 0.55 mmol) in trimethylacetonitrile (10 cm^3). This mixture was stirred overnight, filtered and diethyl ether (ca. 20 cm^3) added

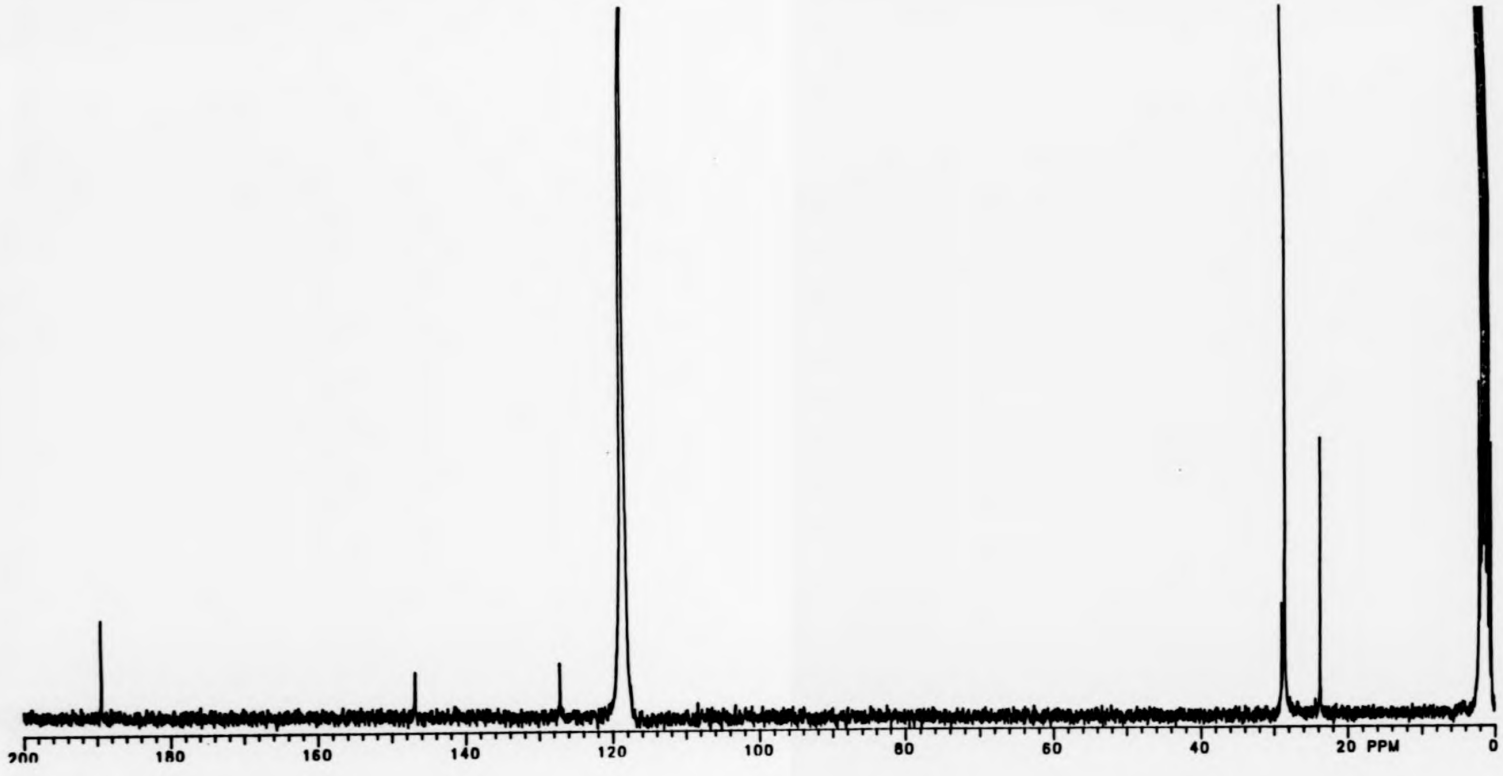

Fig.2.21 75 MHz ^{13}C n.m.r. spectrum of $[Mo_2(O_2CMe)_2(NCCMe_3)_5][BF_4]_2$ in CD_3CN

FIG. 2.22 75 MHz ^{13}C n.m.r. spectrum of Me_3CCN in CD_3CN

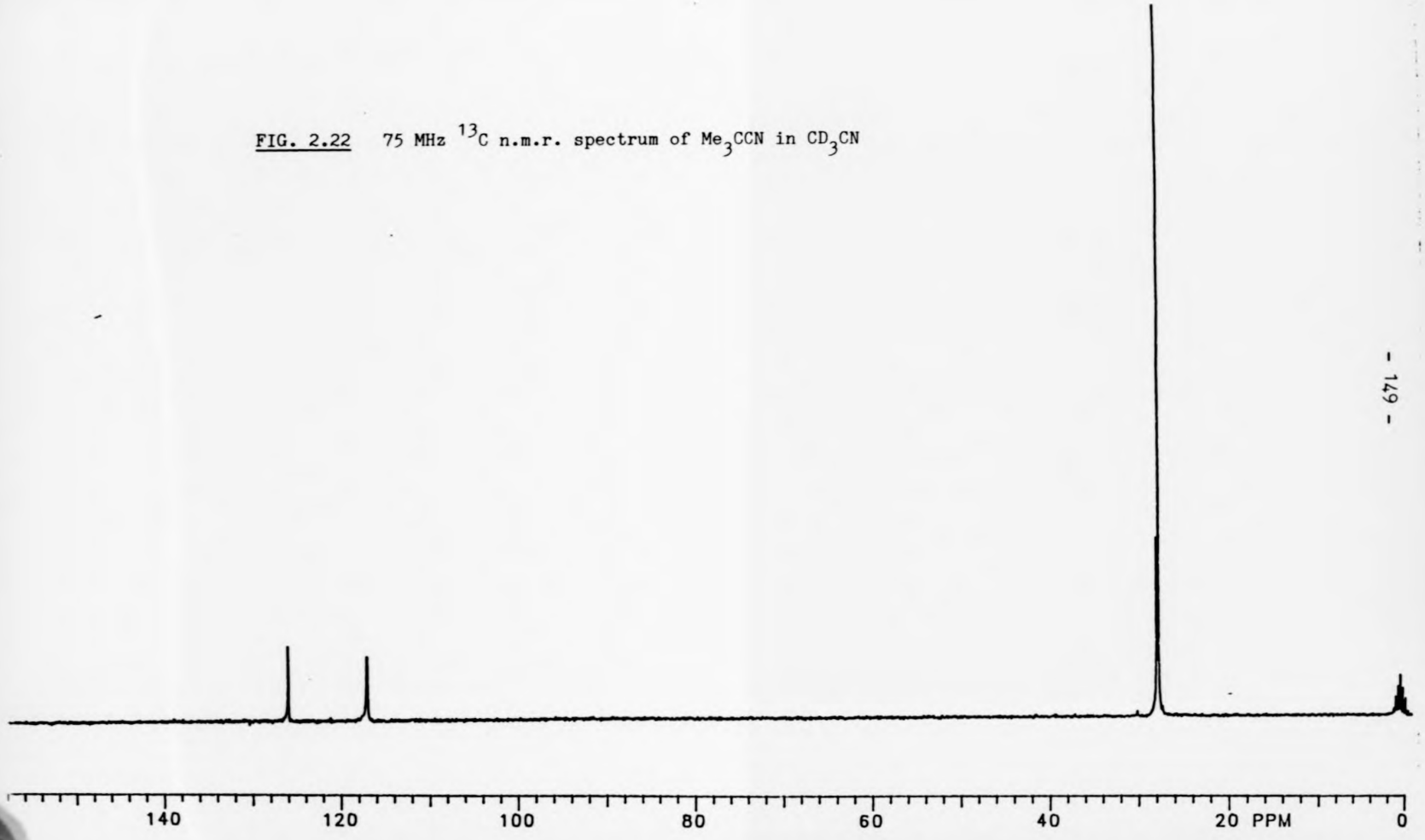

to precipitate out a purple microcrystalline powder. This was collected by filtration, recrystallised from trimethylacetonitrile and dried in vacuo for ca. 3 hours. (Yield = 0.38 g, 70%)

Analyses	C	H	F	N	Rh
Calc. for $C_{34}H_{60}B_2F_8N_6O_4Rh_2$	41.0	6.1	15.2	8.4	20.6 %
Found	41.4	6.2	14.4	8.3	20.3 %

2.9.4 Spectroscopic studies

2.9.4(i) UV/visible spectrum

The UV/visible spectrum of $[Rh_2(O_2CMe)_2(NCCMe_3)_6][BF_4]_2$ in acetonitrile is shown in Fig.2.23 and the absorption maxima and corresponding molar extinction coefficients are given in Table 2.13.

Table 2.13 Absorption maxima and molar extinction coefficients for $[Rh_2(O_2CMe)_2(NCCMe_3)_6][BF_4]_2$ in MeCN

λ_{max}(nm)	$\varepsilon(mol^{-1}cm^{-1}dm^3)$
502	340
360(sh)	997
270	21678
207	16362

The band at 502 nm is assigned to the $\pi^* \rightarrow \sigma^*$ transition of the Rh-Rh bond[56] or the $\pi^*, \delta^*(Rh_2) \rightarrow \sigma^*(Rh\text{-}O)$[57] as for the analogous acetonitrile complex (Section 2.7.3(i)). This band is shifted to higher energy to that observed for $[Rh_2(O_2CMe)_2(NCMe)_6][BF_4]_2$.

FIG. 2.23 UV/visible spectrum of $[Rh_2(O_2CMe)_2(NCCMe_3)_6][BF_4]_2$ in MeCN

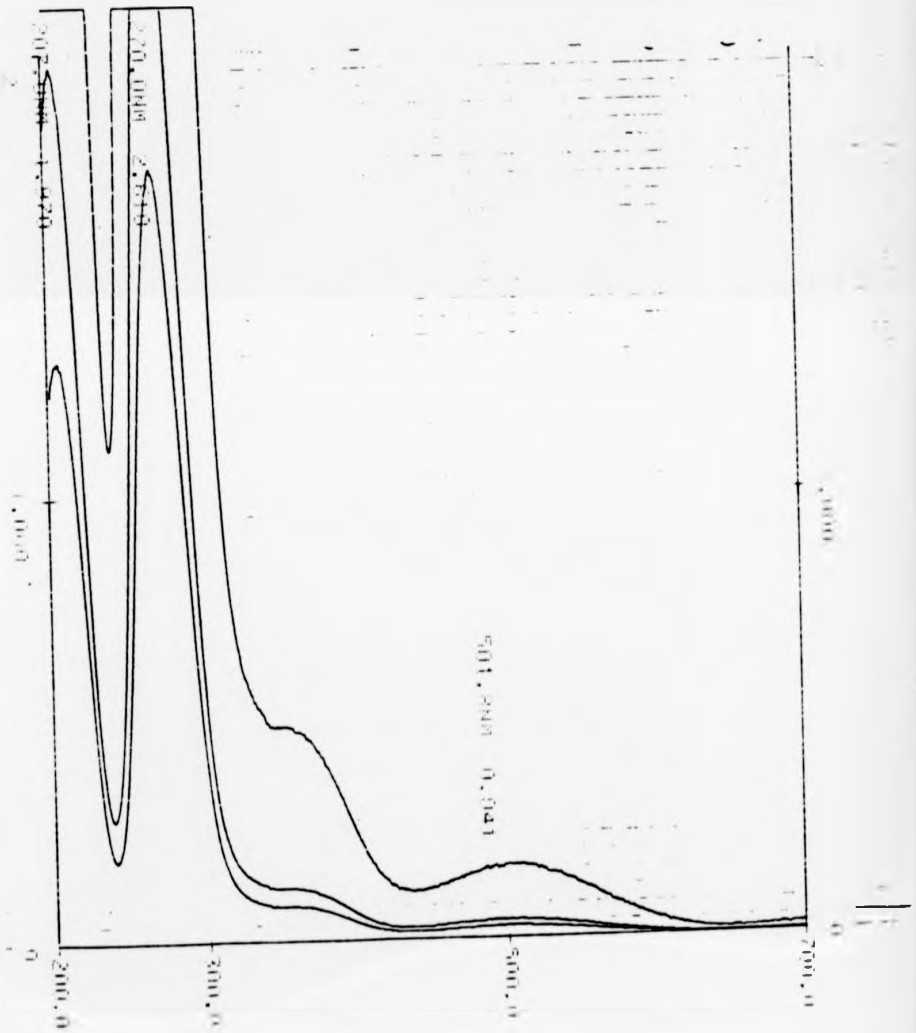

The UV/visible spectrum of $[Rh_2(O_2CMe)_2(NCCMe_3)_6][BF_4]_2$ in methanol shows absorption maxima at 555, 378, 275, and 212 nm. The lowest energy band shifts by 53 nm to lower energy on changing solvents from acetonitrile to methanol and this is very similar to the shift observed for $[Rh_2(O_2CMe)_2(NCMe)_6][BF_4]_2$. Thus, the indications are that for the Me_3CCN complex, the axial ligands have a lability similar to that observed for $[Rh_2(O_2CMe)_2(NCMe)_6][BF_4]_2$ and the dirhodium tetracarboxylates.

2.9.4(ii) Infrared spectrum

The infrared spectrum of a nujol mull of $[Rh_2(O_2CMe)_2(NCCMe_3)_6][BF_4]_2$ is shown in Fig.2.24. The bands at 2290 and 2265 cm^{-1} are assigned to the C≡N stretching vibrations of Me_3CCN. It is possible that these also contain combination bands due to symmetrical CH_3 deformation and C-C stretch. The C≡N stretching vibration in free Me_3CCN is at 2240 cm^{-1} (Fig.2.25) and the shift to higher frequency, as with the MeCN complex, implies co-ordination via the N atom.

The band at 1550 cm^{-1} is assigned to the asymmetric carboxylate stretching frequency with the corresponding symmetric frequency occurring at 1460 and 1355 cm^{-1}. The band at 1245 cm^{-1} is assigned to the C-H bending vibration of the Me_3CCN molecules; that at 1215 cm^{-1} being assigned to the C-H bending vibration of the acetate groups. The broad band at 1060 cm^{-1} is attributed to the B-F stretching vibration in the $[BF_4]^-$ anion.

2.9.4(iii) N.m.r. spectroscopic studies

The 300 MHz ^1H n.m.r. spectrum of $[Rh_2(O_2CMe)_2(NCCMe_3)_6][BF_4]_2$ in deuteromethanol is shown in Fig.2.26. Apart from resonances due to incompletely deuterated solvent, three resonances were observed at

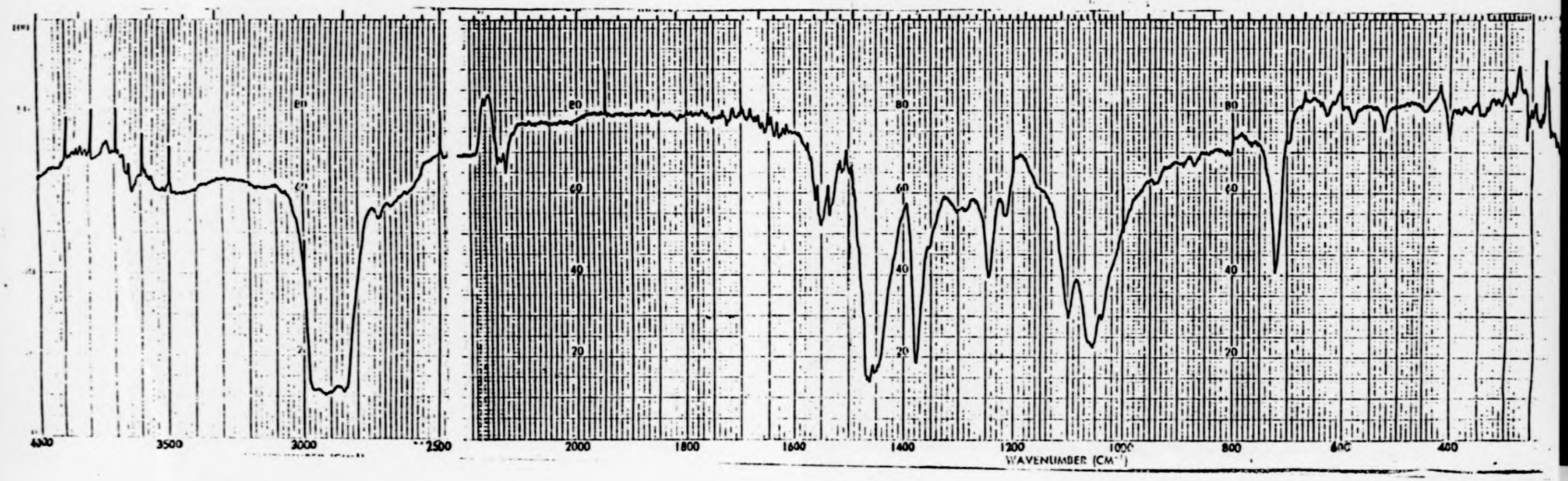

FIG. 2.24 Infrared spectrum of $[Rh_2(O_2CMe)_2(NCCMe_3)_6][BF_4]_2$ as a nujol mull.

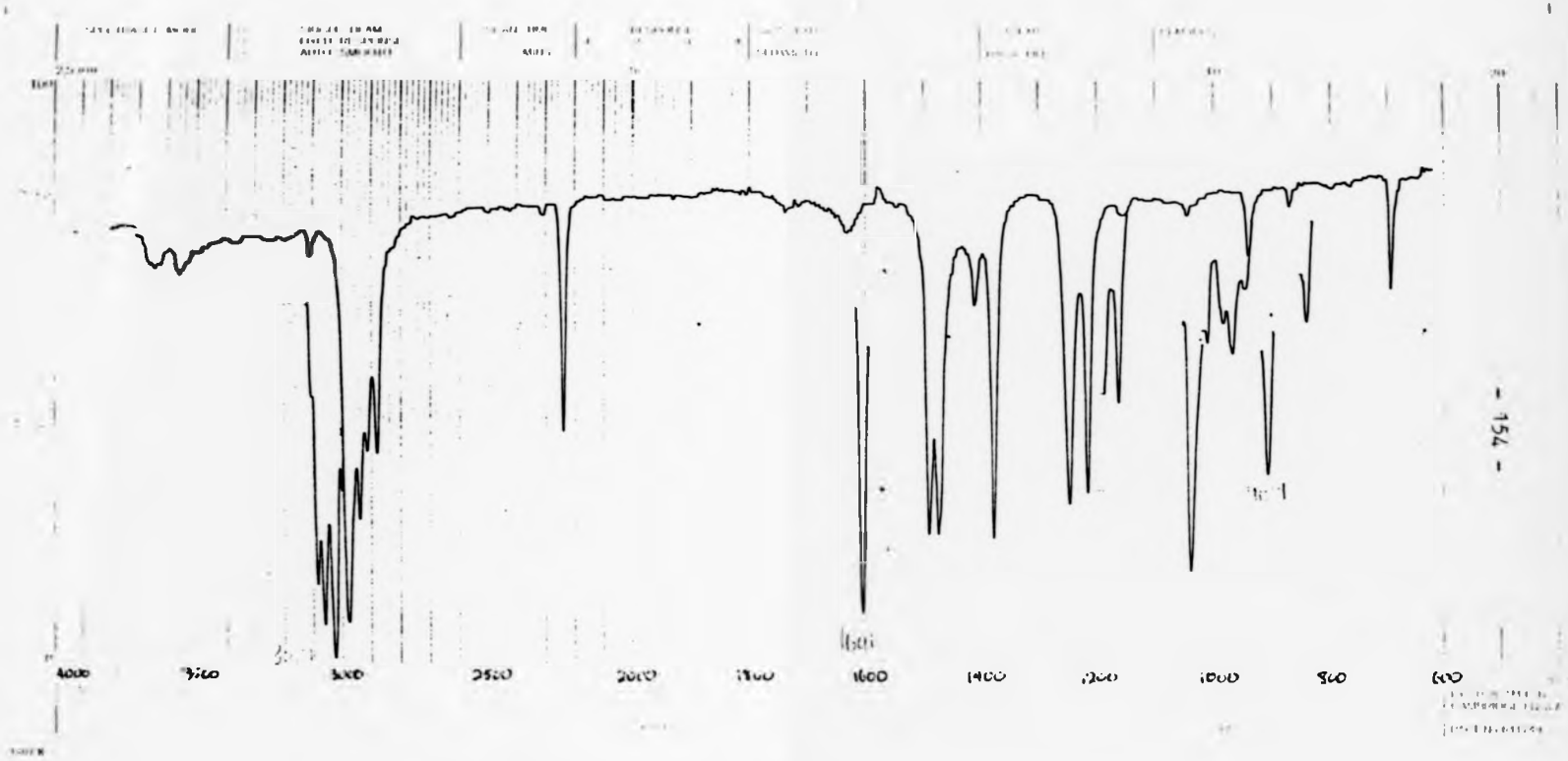

FIG. 2.25 Infrared spectrum of Me_3CCN

Fig.2.26 300 MHz ^1H n.m.r. spectrum of $[Rh_2(O_2CMe)_2(NCCMe_3)_6][BF_4]_2$ in d_4-Methanol

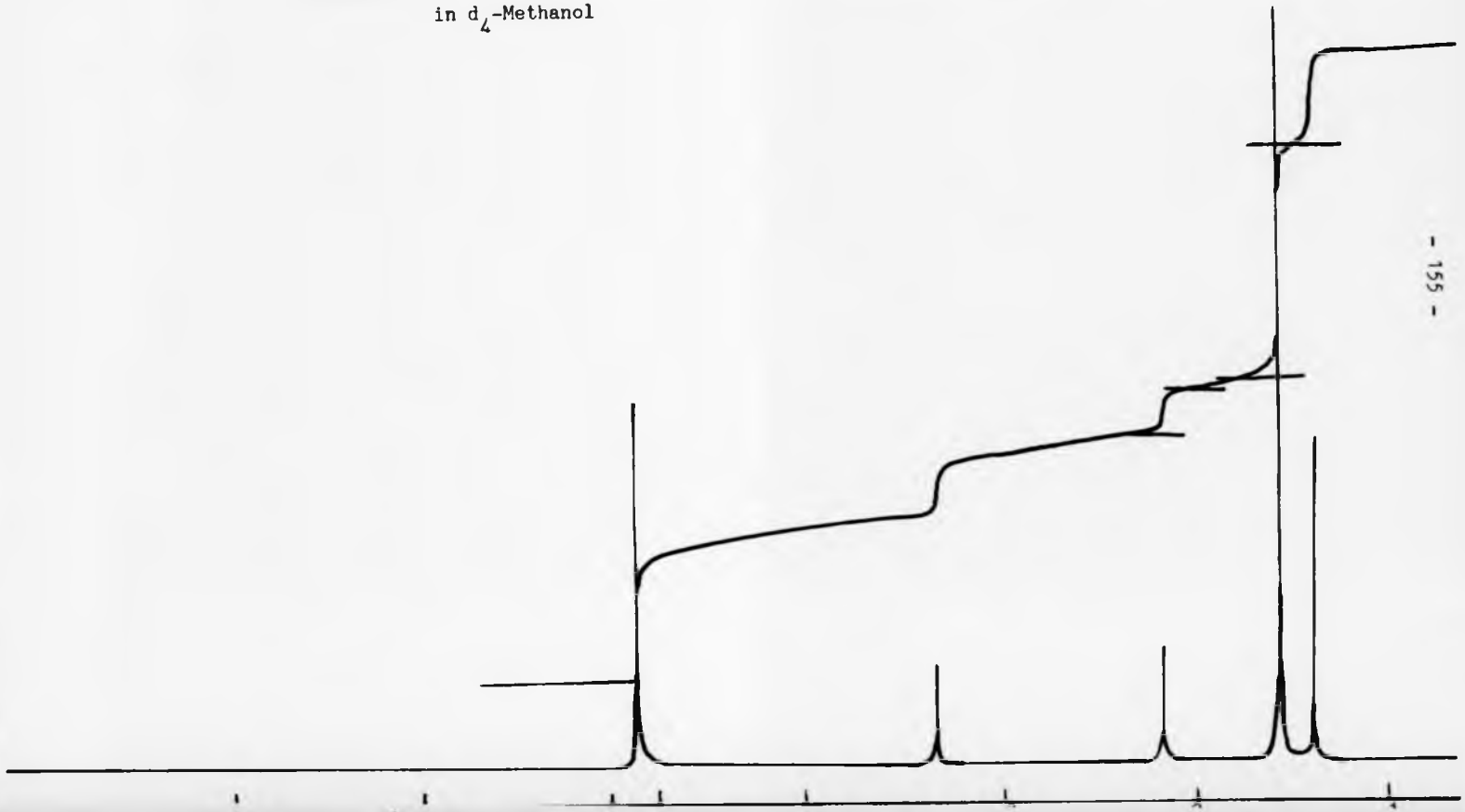

1.41, 1.59, and 2.19 p.p.m. with integrals in a 3:6:1 ratio, respectively. The resonance at 1.41 p.p.m. is assigned to protons on the axial/free nitrile groups, that at 1.59 p.p.m. to protons on the equatorial nitrile ligands and the acetate protons to the resonance at 2.19 p.p.m. The acetate resonance is at a similar chemical shift to that for the MeCN analogue $[Rh_2(O_2CMe)_2(NCMe)_6][BF_4]_2$ (2.09 p.p.m.), the shift of ca. 0.1 p.p.m. to higher frequency for the Me_3CCN compound suggesting that the acetate resonance shows some dependence on the equatorial ligands. The protons of free Me_3CCN have a chemical shift of 1.39-1.40 p.p.m. and, thus, the axial nitrile groups appear to have been displaced by the solvents. The difference in the chemical shift of the protons for axial/free and equatorially co-ordinated Me_3CCN groups is 0.18 p.p.m., which is significantly less than the difference for the corresponding MeCN groups (0.59 p.p.m. in $[Rh_2(O_2CMe)_2(NCMe)_6][BF_4]_2$). This is expected, since the methyl protons in Me_3CCN will be further away from the Rh-Rh dimetal centre and will be that much less affected by co-ordination.

The 75 MHz ^{13}C n.m.r. spectrum of $[Rh_2(O_2CMe)_2(NCCMe_3)_6][BF_4]_2$ in deuteromethanol at ambient temperature is shown in Fig.2.27. Resonances were observed at 21.4, 26.8, 27.0, 30.1, 132.7, and 192.4 p.p.m. The peak at 21.4 p.p.m. and that at 192.4 p.p.m. are assigned to the methyl and carboxylate carbons, respectively, of the acetate groups. This agrees with the assignment of similar peaks in the ^{13}C n.m.r. spectrum of $[Rh_2(O_2CMe)_2(NCMe)_6][BF_4]_2$. The resonance at 132.7 p.p.m. is assigned to the nitrile carbon of the co-ordinated Me_3CCN molecules, a shift of ca. 6 p.p.m. to higher frequency from that of free ligand (127 p.p.m. in deuteromethanol). This compares to a similar shift (9 p.p.m.) to higher frequency for the nitrile

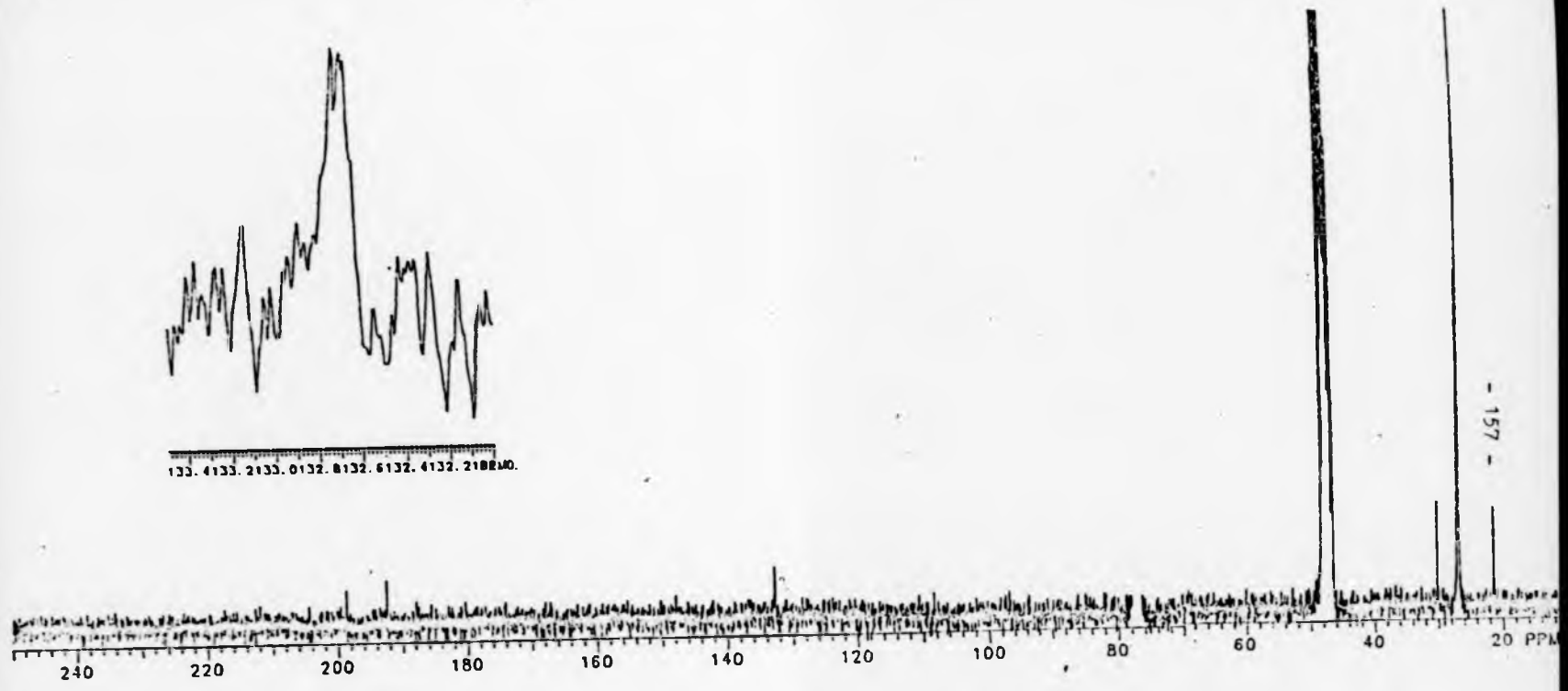

FIG.2.27 75 MHz ^{13}C n.m.r. spectrum of $[Rh_2(O_2CMe)_2(NCCMe_3)_6][BF_4]_2$ in CD_3OD

carbon of MeCN on co-ordination at the equatorial positions in $[Rh_2(O_2CMe)_2(NCMe)_6][BF_4]_2$. The resonance at 26.8 p.p.m. occurs at the position for the methyl carbon of free Me_3CCN and that at 27.0 p.p.m. at the position for the butyl carbon of free Me_3CCN. It is proposed that these resonances contain peaks due to the methyl and butyl carbons of free Me_3CCN and to the methyl carbon of co-ordinated Me_3CCN. One reason for this proposal is that the relative integrations do not agree for solely free Me_3CCN (see Fig.2.28) and may well contain a third resonance. The methyl carbon on the equatorially co-ordinated Me_3CCN may well not be shifted at all on co-ordination as it is 4 bonds away from the Rh_2^{4+} centre. Considering the ^{13}C n.m.r. spectrum for the analogous MeCN compound, the shifts of the carbons on co-ordination are as below:

$$H_3C - C \equiv N \rightarrow Rh_2^{4+}$$

SHIFTS 2.3 9 p.p.m.

The magnitude of the shift on co-ordination attenuates rapidly with the distance from the metal centre, on proceeding from the nitrile carbon to the methyl carbon.

Thus, the signal at 30.1 p.p.m. is assigned to the butyl carbon on the equatorially co-ordinated Me_3CCN molecules, giving a shift of 1.1 p.p.m. (the butyl carbon of free Me_3CCN in deuteromethanol, Fig.2.27, is assigned to the resonance at 29 p.p.m.) on co-ordination. Therefore, the shifts of the carbons on co-ordination for Me_3CCN are postulated as

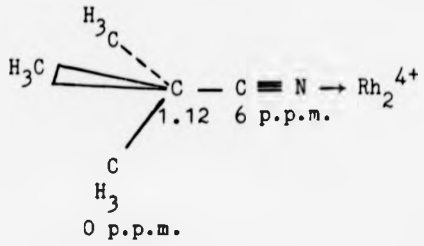

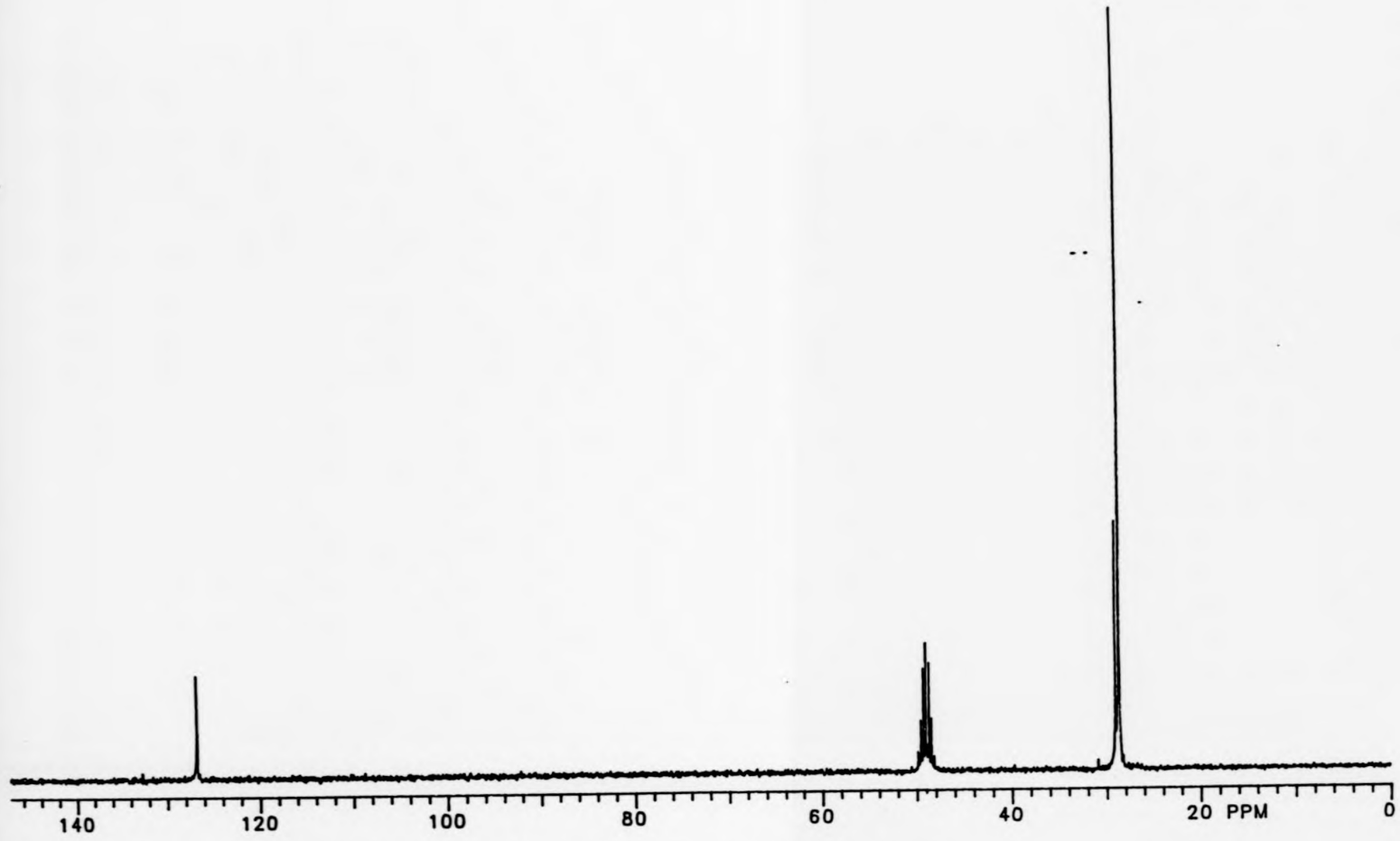

FIG.2.28 75 MHz ^{13}C n.m.r. spectrum of Me_3CCN in CD_3OD

2.9.5 Summary and Conclusions

The compounds $[M_2(O_2CMe)_2(NCMe)_6][BF_4]_2$ (M = Mo or Rh) have been prepared by the reaction of the corresponding tetra-acetate compounds $[M_2(O_2CMe)_4]$ with $[Me_3O][BF_4]$ in MeCN. Both of these compounds have been fully characterised and the structures confirmed by X-ray crystallography. In each case the cation involves a cis-arrangement of the two bridging acetate groups and four equatorial and two axial N-bonded MeCN molecules co-ordinated to the dimetal(II) centre. Comparisons within and between values for the $[M_2(O_2CMe)_2(NCMe)_6][BF_4]_2$ (M = Mo or Rh) provide a clear indication of the static trans effect of a Mo-Mo quadruple bond and a Rh-Rh single bond, together with a clear documentation of the structural similarities and differences for analogous Mo_2^{4+} and Rh_2^{4+} complexes.

^1H and ^{13}C n.m.r. studies have shown that, at ambient temperatures, both the axial and equatorial MeCN molecules of $[Mo_2(O_2CMe)_2(NCMe)_6]^{2+}$ undergo rapid exchange with CD_3CN whereas, for the corresponding rhodium complex, both at ambient temperatures and at 60°C, only the axial molecules undergo such exchange.

The preparation and crystal structure of $[Rh_2(O_2CMe)_2(NCMe)_4(py)_2][BF_4]_2$ has been achieved. The dimension of this $Rh_2O_4N_6$ core is virtually identical to that of $[Rh_2(O_2CMe)_2(NCMe)_6]^{2+}$ and the pyridine complex involves an orthogonal arrangement of the two pyridine rings.

Also, $[Mo_2(O_2CH)_4]$ has been treated with $[Me_3O][BF_4]$ in MeCN to produce $[Mo_2(O_2CH)_2(NCMe)_5(H_2O)][BF_4]_2$, which has been shown by analysis and spectroscopy to be very similar to the corresponding acetate compound $[Mo_2(O_2CMe)_2(NCMe)_6][BF_4]_2$, with two bridging formate groups and MeCN molecules which exchange rapidly on the n.m.r. time scale.

Extension of this chemistry using the more bulky nitrile ligand trimethylacetonitrile has been achieved to produce the $[M_2(O_2CMe)_2(NCCMe_3)_n][BF_4]_2$ (M = Mo, n=5; M = Rh, n=6) compounds, which have been characterised by UV/visible, infrared, and n.m.r. spectroscopy. These compounds have been shown to be very similar to their MeCN analogues.

The lability of the nitrile molecules in the complex $[Mo_2(O_2CMe)_2(NCMe)_6][BF_4]_2$ has proved a fruitful area of study with phosphine ligands (Chapter 3) and this lability of MeCN and Me_3CCN with the Mo_2^{4+} centre, along with the wide choice of nitrile ligands for potential co-ordination on both the Mo_2^{4+} and Rh_2^{4+} centres, should provide a wealth of study for future work.

REFERENCES

1. F.A. Cotton and R.A. Walton, Multiple Bonds Between Metal Atoms, Wiley-Interscience Publication.

2. C.D. Garner and R.G. Senior, J.Chem.Soc., Dalton Trans., 1975, 1171.

3. C.D. Garner, S. Parkes, I.B. Walton, and W. Clegg, Inorg.Chim.Acta., 1978, 31, L451.

4. F.A. Cotton, W.H. Ilsley, and W. Kaim, Inorg.Chim.Acta., 1979, 37, 267.

5. W. Clegg, C.D. Garner, S. Parkes, and I.B. Walton, Inorg.Chem., 1979, 18, 2250.

6. C.D. Garner and R.G. Senior, J.Chem.Soc., Dalton Trans., 1976, 1041.

7. W.R. Tikkanen, E. Binamira-Soriaga, W.C. Kaska, and P.C. Ford, Inorg.Chem., 1984, 23, 141.

8. A.T. Baker, W.R. Tikkanen, W.C. Kaska, and P.C. Ford, Inorg.Chem., 1984, 23, 3254.

9. I.B. Baranovskii, M.A. Golubnichaya, L.M. Dickareva, and R.N. Shchelokov, Russ.J.Inorg.Chem., 1984, 29, 872.

10. J. Telser and R.S. Drago, Inorg.Chem., 1984, 23, 1798.

11. F.A. Cotton, Inorg.Synth., Vol.XIII, p.88.

12. T.A. Stephenson, E. Bannister, and G. Wilkinson, J.Chem.Soc., 1964, 2538.

13. I.B. Walton, Ph.D. Thesis, 1979.

14. F.A. Cotton, J.G. Norman, Jr., B.R. Stults, and T.R. Webb, J.Coord.Chem., 1976, 5, 217.

15. E. Hochberg, P. Walks, and E.H. Abbott, Inorg.Chem., 1974, 13, 1824.

16. W. Clegg, Acta Crystallogr., 1981, A37, 22.

17. G.M. Sheldrick, SHELXTL: an integrated system for solving, refining, and displaying crystal structures from diffraction date, University of Göttingen, 1978.

18. International Tables for X-ray Crystallography, Vol.IV, Kynoch Press, Birmingham, UK, 1974, pp.99, 149.

19. J.A. Potenza, R.J. Johnson, and J. San Filippo, Jr., Inorg.Chem., 1976, 15, 2215.

20. A. Bino and F.A. Cotton, Inorg.Chem., 1979, 18, 1381.

21. F.A. Cotton, Z.C. Mester, and T.R. Webb, Acta Crystallogr., Sect.B, 1974, 30, 2768.

22. D.M. Collins, F.A. Cotton, and C.A. Murillo, Inorg.Chem., 1976, 15, 1861.

23. F.A. Cotton and J.G. Norman, Jr., J.Am.Chem.Soc., 1972, 94, 5697.

24. L.F. Rhodes, J.D. Zubkowski, K. Folting, J.C. Huffman, and K.G. Caulton, Inorg.Chem., 1982, 21, 4185.

25. F.D. Rochon, R. Melanson, H.E. Howard-Lock, C.J.L. Lock, and G. Turner, Can.J.Chem., 1984, 62, 860.

26. G. Pimblett, C.D. Garner,and W. Clegg, J.Chem.Soc., Dalton Trans., 1985, 1977.

27. R.N. McGinnis, T.R. Ryan, and R.E. McCarley, J.Am.Chem.Soc., 1978, 100, 7900.

28. P.E. Fanwick, D.S. Martin, F.A. Cotton, and T.R. Webb, Inorg.Chem., 1977, 16, 2103.

29. A.P. Sattelberger and J.P. Fackler, J.Am.Chem.Soc., 1977, 99, 1259.

30. A. Bino, F.A. Cotton, and P.E. Fanwick, Inorg.Chem., 1979, 18, 3558.

31. J.M. Mayer and E.H. Abbott, Inorg.Chem., 1983, 22, 2774.

32. K.F. Purcell and R.S. Drago, J.Am.Chem.Soc., 1966, 88, 919.

33. J. Zarembowitch and R. Maleki, Spectrochim.Acta, Part A, 1983, 39A, 43.

34. K. Nakamoto, "Infrared and Raman Spectra of INorganic and Co-ordination Compounds", Third Edt., Wiley-Interscience, New York, 1978.

35. R. Hagen and J.D. Roberts, J.Am.Chem.Soc., 1969, 91, 4504.

36. D.E. Cane, T-C. Liang, and H. Hasler, J.Am.Chem.Soc., 1982, 104, 7274.

37. G.L. Rempel, P. Legzdins, H. Smith, and G. Wilkinson, Inorg.Synth., 1971, 13, 90.

38. S.A. Johnson, H.R. Hunt, and H.M. Neumann, Inorg.Chem., 1963, 2, 960.

39. M. Berry, C.D. Garner, I.H. Hillier, A.A. MacDowell, and W. Clegg, J.Chem.Soc., Chem.Comm., 1980, 494.

40. K.G. Caulton and F.A. Cotton, J.Am.Chem.Soc., 1969, 91, 6517.

41. J. Halpern, E. Kimura, J. Molin-Case, and C.S. Wong, J.Chem.Soc., Chem.Comm., 1971, 1207.

42. H. Pasternak and F. Pruchnik, Inorg.Nucl.Chem.Lett., 1976, 12, 591.

43. G.G. Christoph, J. Halpern, G.P. Khare, Y.B. Koh, and C. Romanowski, Inorg.Chem., 1981, 20, 3029.

44. E.M. Shustorovich, M.A. Porai-Koshits, and Yu.A. Buslaev, Co-ord.Chem.Rev., 1975, 17, 1.

45. Y.B. Koh and G.G. Christoph, Inorg.Chem., 1978, 17, 2590.

46. T.R. Felthouse, Prog.Inorg.Chem., 1982, 39, pp.73-166.

47. F.A. Cotton and J.L. Thompson, Acta Crystallogr., Sect. B, 1981, 37, 2235.

48. B.A. Kelly, A.J. Welch, and P. Woodward, J.Chem.Soc., Dalton Trans., 1977, 2237.

49. F.A. Cotton and T.R. Felthouse, Inorg.Chem., 1981, 20, 584.

50. F.A. Cotton, T.R. Felthouse, and J.L. Thompson, cited in ref.46.

51. F.A. Cotton, B.G. De Boer, M.D. La Prade, J.R. Pipal, and D.A. Ucko, Acta Crystallogr., Sect. B, 1971, 27, 1664.

52. G.C. Dobinson, R. Mason, and D.R. Russell, J.Chem.Soc., Chem.Comm., 1967, 62.

53. P. Colamarino and P. Orioli, J.Chem.Soc., Dalton Trans., 1976, 845.

54. R.S. Drago, S.P. Tanner, R.M. Richman, and J.R. Long, J.Am.Chem.Soc., 1979, 101, 2897.

55. J. Telser and R.S. Drago, Inorg.Chem., 1984, 23, 2599.

56. D.S. Martin, Jr., T.R. Webb, G.A. Robbins, and P.E. Fanwick, Inorg.Chem., 1979, 18, 475.

57. V.M. Miskowski, W.P. Schaefer, B. Sadeghi, B.D. Santarsiero, and H.B. Gray, Inorg.Chem., 1984, 23, 1154.

58. M.Y. Chavan, T.P. Zhu, X.Q. Lin, M.Q. Ahsan, J.L. Bear, and K.M. Kadish, Inorg.Chem., 1984, 23, 4538.

59. R.S. Drago, S.P. Tanner, R.M. Richman, and J.R. Long, J.Am.Chem.Soc., 1979, 101, 2897.

60. R.S. Drago, J.R. Long, and R. Cosmano, Inorg.Chem., 1981, 20, 2920.

61. E.B. Boyar and S.D. Robinson, J.Chem.Soc., Dalton Trans., 1985, 629.

62. B.D. Catsikis and M.L. Good, Inorg.Chem., 1971, 10, 1522.

63. R.D. Foust and P.C. Ford, J.Am.Chem.Soc., 1972, 94, 5686.

64. L. Pauling, Proc.Natl.Acad.Sci. U.S.A., 1975, 72, 3799.

65. W. Clegg, Acta Crystallogr., Sect. B, 1980, 36, 2437.

66. W. Clegg, C.D. Garner, L. Akhter, and M.H. Al-Samman, Inorg.Chem., 1983, 22, 2466.

67. Y.B. Koh and G.G. Christoph, Inorg.Chem., 1979, 18, 1122.

68. J.W. Emsley, J. Feeney, and L.H. Sutcliffe, "High Resolution Nuclear Magnetic Resonance Spectroscopy", Vol.1, Pergamon Press, 1965.

69. H.M. McConnell, J.Chem.Phys., 1957, 27, 226.

70. M.H. Al-Samman, Ph.D. Thesis, 1981.

71. R.P. Schrock and J.A. Osborn, J.Am.Chem.Soc., 1976, 98, 2134.

72. F.L. Campbell, III, F.A. Cotton, and G.L. Powell, Inorg.Chem., 1985, 24, 177.

73. The Aldrich Library of N.m.r. Spectra, Volume 1, Edn.11, C.J. Pouchert, p.697-A.

CHAPTER 3

STUDY OF THE REACTIVITY OF $[Mo_2(O_2CMe)_2(NCMe)_6][BF_4]_2$ AND $[Mo_2(O_2CH)_2(NCMe)_5(H_2O)_1][BF_4]_2$

3.1 Introduction

This chapter will deal with some reactions involving $[Mo_2(O_2CMe)_2(NCMe)_6][BF_4]_2$ and $[Mo_2(O_2CH)_2(NCMe)_5(H_2O)_{\frac{1}{2}}][BF_4]_2$. In Chapter 2, it was shown how two carboxylate groups could be removed from the parent tetracarboxylate compounds of dimolybdenum(II) (and dirhodium(II)) centres and replaced by labile acetonitrile groups. The extent to which this lability relates to the reactivity has been investigated through a number of reactions. Thus, the ease with which bridging groups, such as mhp and dppm, could be co-ordinated to the Mo_2^{4+} core has been determined to see if mixed ligand dimers could be prepared showing that the dppm ligand can have some interaction with the M-M core.[1] In this context it is relevant to note that reactions of quadruply bonded dirhenium(III) species with dppm have shown them to be reduced to triply bonded dimers. Phosphine ligands have led to some very interesting reactions[3] with quadruply bonded species and it was thought relevant to undertake such a study here. Monodentate phosphines, e.g. PPh_3 and $P(OMe)_3$, were chosen to investigate if they could easily replace MeCN in the equatorial positions. The ligand dppe was also chosen, as this has been shown to adopt both bridging and bidentate modes of attachment around Mo_2^{4+} centres. The presence of the cis-acetate groups would be helpful for bidentate phosphine systems in determining, via ^1H n.m.r. spectroscopy, whether or not the structure was a bridged or bidentate dimer.[2] N.m.r. spectroscopy has seldom been used to characterize these systems since the complexes are usually of the type $[Mo_2Cl_4(LL)_2]$[2,3] (LL = bidentate phosphine) and the data would not yield much information on the structure of the complex.

3.2 Preparation of $[Mo_2(O_2CH)_2(mhp)_2]$

$[Mo_2(O_2CH)_2(NCMe)_5(H_2O)_{\frac{1}{2}}][BF_4]_2$ (0.4 g, 0.57 mmol) (Chapter 2) was dissolved in methanol (30 cm^3) and to this solution Na[mhp] (0.15 g, 1.14 mmol) was added. Immediately, a yellow solid formed which was washed with dichloromethane (2 x 10 cm^3) and acetonitrile (2 x 10 cm^3) and dried *in vacuo* for *ca*. 6 hours. (Yield = 0.21 g, 75%)

Analyses	C	H	N
Calc. for $C_{14}H_{14}Mo_2N_2O_6$	33.7	2.8	5.6 %
Found	33.7	3.0	5.4 %

The mass spectrum of the material showed a parent ion at m/e 498 corresponding to $[Mo_2(O_2CH)_2(mhp)_2]^+$ plus minor peaks at 424 m/e $[Mo_2(mhp)_2O]^+$ (see mass spectrum of $Mo_2(O_2CH)_4$, ref.4) and 372 m/e $[Mo_2(O_2CH)_4]^+$.

The UV/visible spectrum of $[Mo_2(O_2CH)_2(mhp)_2]$ in methanol shows absorption bands at 475 nm, 397 nm, 286 nm, and 213 nm. The lower energy bands at 475 and 397 nm are identical to those reported for $[Mo_2(mhp)_2(O_2CH)_2]$, the band at 397 nm being ascribed due to a $\pi \rightarrow \pi^*$ transition on the ligand and/or ligand-metal charge transfer transition and that at 475 nm to the $\delta \rightarrow \delta^*$ transition within the quadruple bond orbitals.

Mixed carboxylate/mhp compounds have been synthesised previously.[5] This new route serves to illustrate that all of the acetonitrile ligands of $[Mo_2(O_2CH)_2(NCMe)_5(H_2O)_{\frac{1}{2}}]^{2+}$ are readily replaced by bridging mhp units.

3.3 Preparation of $[Mo_2(O_2CMe)_2(NCMe)_2(dppm)][BF_4]_2$

$[Mo_2(O_2CMe)_2(NCMe)_6][BF_4]_2$ (0.3 g, 0.41 mmol) was dissolved in acetonitrile (30 cm^3) and dppm (0.16 g, 0.42 mmol) was added to this solution. After stirring for ca. 5 minutes the solution had changed colour from a deep pink to a deep purple. The solution was stirred for a further 24 hours, after which time it was filtered. The volume of solution was reduced to ca. 15 cm^3 and a deep purple powder precipitated. Addition of diethyl ether (10 cm^3) produced further precipitation of this purple product which was collected by filtration and recrystallised from acetonitrile. The product was washed with diethyl ether (10 cm^3) and dried in vacuo. (Yield = 0.29 g, 75%)

Analyses	C	H	F	Mo	N	P
Calc. for $C_{33}H_{34}B_2F_8Mo_2N_2O_4P_2$	41.5	3.6	15.9	20.1	2.9	6.5 %
Found	40.6	3.8	15.3	18.6	2.8	6.0 %

3.3.1 Spectroscopic studies

3.3.1(i) UV/visible spectrum

The UV/visible spectrum of $[Mo_2(O_2CMe)_2(NCMe)_2(dppm)][BF_4]_2$ in acetonitrile is shown in Fig.3.1. This exhibits a lowest energy transition at 541 nm (ε = 980 $dm^3mol^{-1}cm^{-1}$) and a shoulder at 387 nm (ε = 227 $dm^3mol^{-1}cm^{-1}$). As for the dimolybdenum compounds in Chapter 2 and similar complexes involving the Mo_2^{4+} centre, the lowest energy band is assigned to the metal-metal $\delta \rightarrow \delta^*$ promotion.[3]

3.3.1(ii) Infrared spectrum

The infrared spectrum of $[Mo_2(O_2CMe)_2(NCMe)_2(dppm)][BF_4]_2$ is shown in Fig.3.2. The bands at 2310 and 2280 cm^{-1} are assigned to

Fig.3.1 UV/visible spectrum of $[Mo_2(O_2CMe)_2(NCMe)_2(dppm)][BF_4]_2$ in MeCN

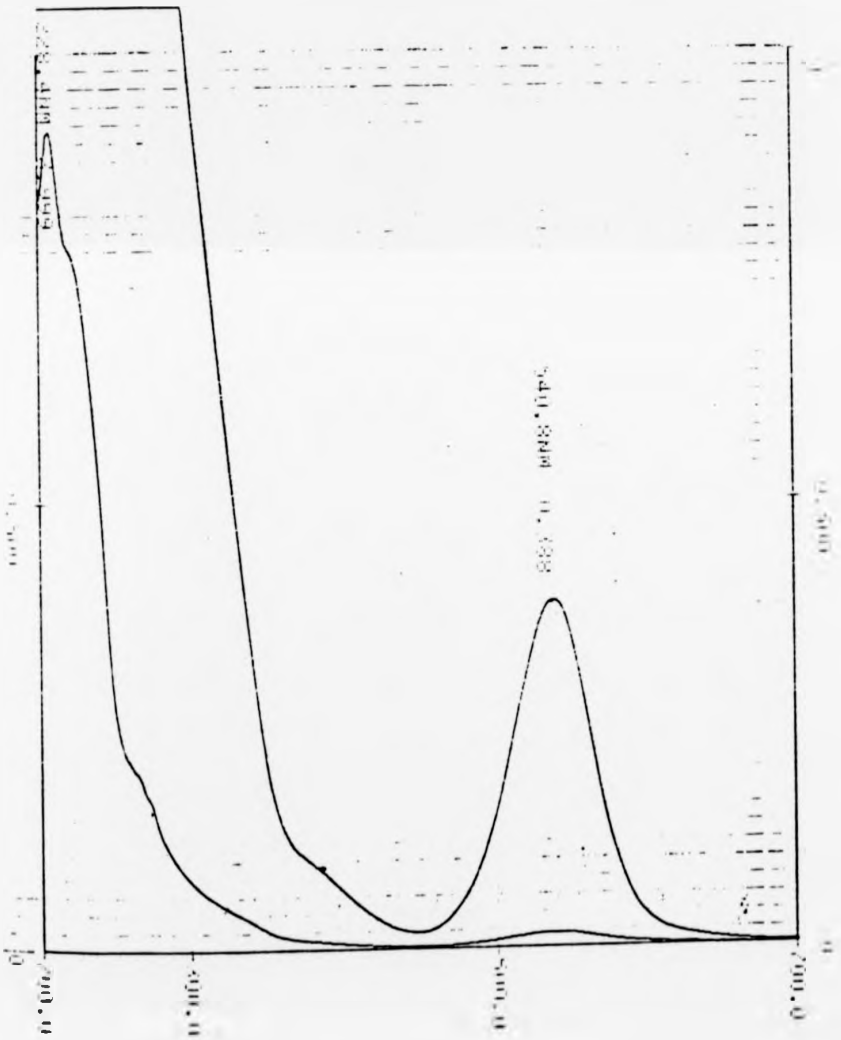

FIG.3.2 Infrared spectrum of $[Mo_2(O_2CMe)_2(NCMe)_2(dppm)][BF_4]_2$ as a nujol mull

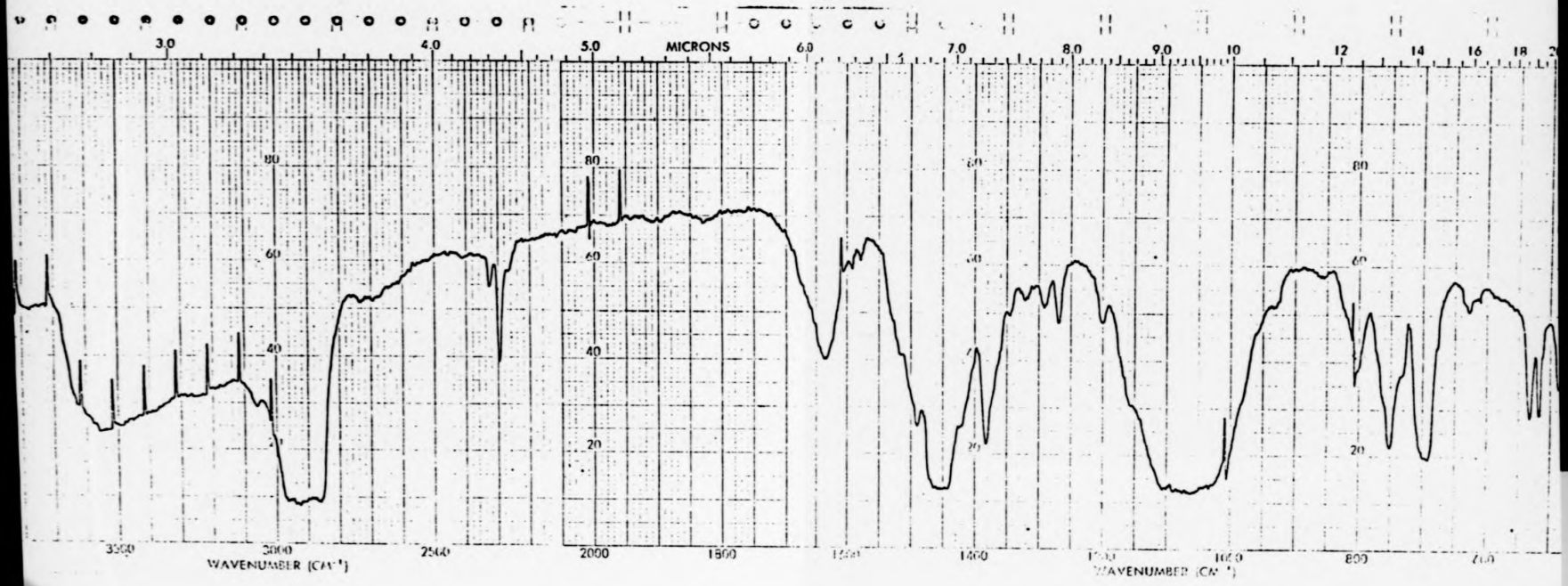

the C≡N stretching vibrations of the co-ordinated acetonitrile molecules. Those at 1625 and 1480 cm^{-1} are assigned to the asymmetric carboxylate stretching vibrations with the corresponding symmetric vibration at 1410 cm^{-1}. The broad band at 1050 cm^{-1} is assigned to the B-F stretching vibration of the $[BF_4]^-$ anion. The bands at 800, 740, and 680 cm^{-1} are due to the dppm ligand, involving the out-of-plane C-H bending vibrations of the phenyl rings.

3.3.1(iii) N.m.r. spectroscopic studies

The ^1H n.m.r. spectrum (Fig.3.3) of $[Mo_2(O_2CMe)_2(NCMe)_2(dppm)][BF_4]_2$ in deuteroacetonitrile was recorded at 300 MHz. This shows single peaks at 1.95, 2.76, and 2.97 p.p.m., two doublets of triplets centred at 4.97 and 5.29 p.p.m. and a broad peak at 7.42 p.p.m. They integrate in a 12:3:3:1:1:20 ratio respectively. The peak at 1.95 p.p.m. is assigned to the equatorial acetonitrile ligands (i.e. to free CH_3CN formed via exchange of the ligated CH_3CN with the CD_3CN solvent), indicating that, as with the parent complex $[Mo_2(O_2CMe)_2(NCMe)_6][BF_4]_2$, the acetonitriles are labile. The peaks at 2.76 and 2.97 p.p.m. are assigned to the two inequivalent acetate groups bridging the metal dimer, one trans to dppm, the other trans to two acetonitrile groups. The two doublets of triplets are due to the two inequivalent protons on the CH_2 group bridging the phosphorus atoms in dppm. In the proposed structure, based on the fact that there are two inequivalent acetate groups, the dppm is bridging the Mo≡Mo centre rather than acting as a bidentate ligand, i.e. as in Fig.3.4.

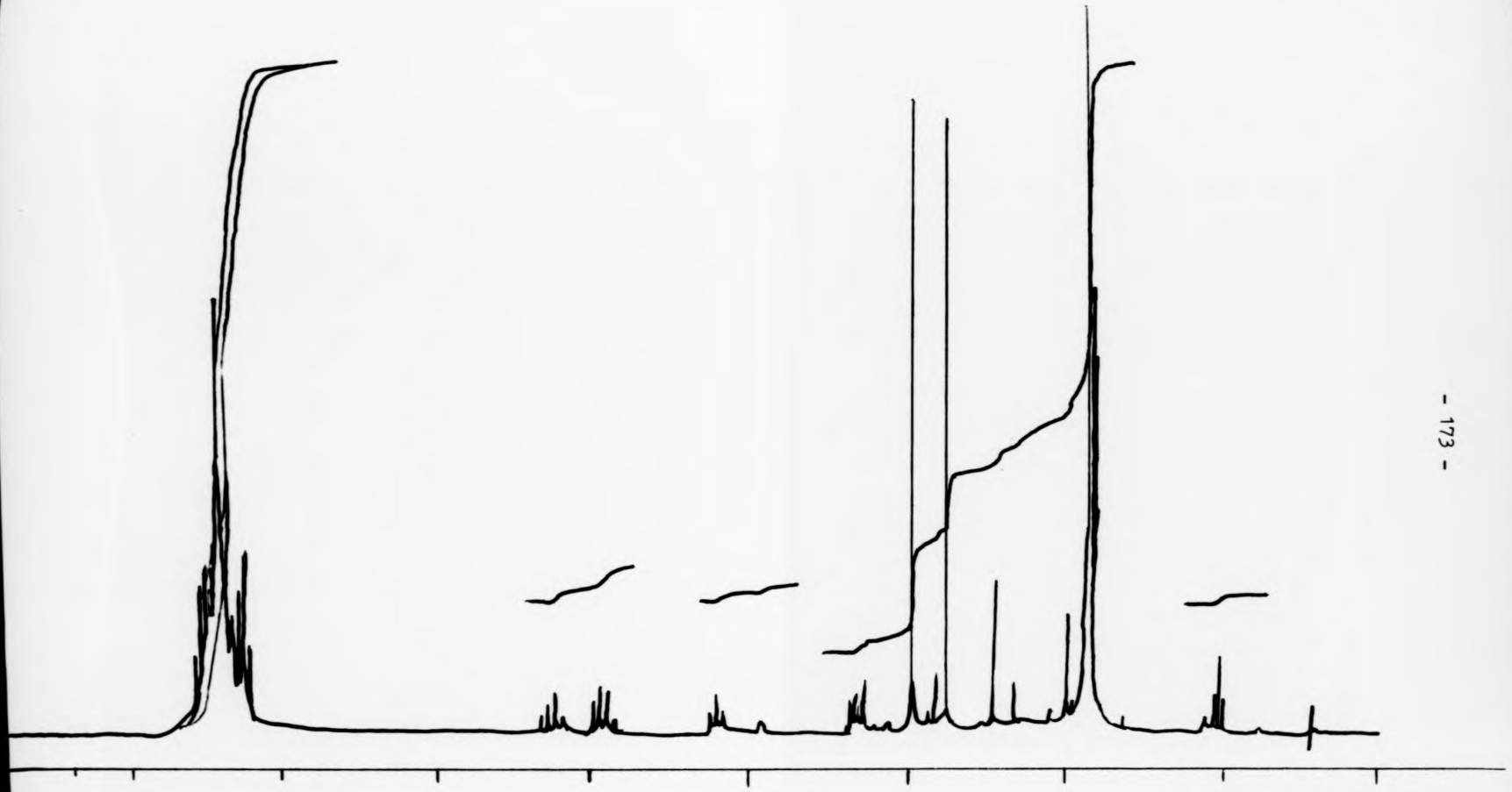

Fig.3.3 300 MHz ^1H n.m.r. of $[Mo_2(O_2CMe)_2(NCMe)_2(dppm)][BF_4]_2$ in CD_3CN

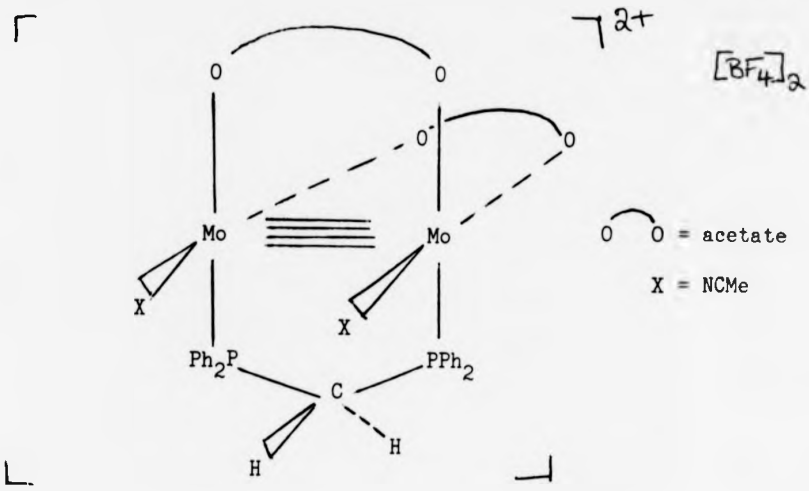

Figure 3.4 Proposed structure of $[Mo_2(O_2CMe)_2(NCMe)_2(dppm)][BF_4]_2$

The ^1H n.m.r. spectrum of dppm itself contains a triplet at 2.77 p.p.m., assigned to the two equivalent $-CH_2-$ protons split into a triplet by coupling to the two equivalent phosphorus atoms. The coupling constant $^2J_{P-H}$ is *ca.* 1.8 Hz. However, when dppm bridges the Mo_2 centre as in Fig.3.4, the two CH_2 protons become inequivalent. Thus, each proton will exhibit a resonance, initially split into a triplet, as for free dppm, due to coupling to the two equivalent phosphorus atoms but which will then be split into a doublet by coupling to the other proton. Thus, for each methylene proton, a doublet of triplets will be observed. The coupling constants measured were $^2J_{P-H}$ *ca.* 12 Hz and $^2J_{H-H}$ *ca.* 15 Hz, taken directly from the spectra. The value of the coupling constant of the geminal protons (15 Hz) is within the range of observed geminal coupling constants.[5] The value of the two bond phosphorus-proton coupling constant has increased from *ca.* 1.8 Hz to 12 Hz. This increase is most likely due to the change in the chemical environment of the phosphorus nuclei and geminal protons on going from free to co-ordinated dppm. The values

$^2J_{P-H}$ = 12 Hz and $^2J_{H-H}$ = 15 Hz are very similar to other phosphorus-proton and proton-proton coupling constants observed for co-ordinated dppm metal complexes.[6] The shift in the resonance position of the geminal protons, here from 2.77 p.p.m. to 4.97 and 5.29 p.p.m., is also similar to that observed for [CpCo(dppm)I]I, where the geminal protons resonate at 4.55 and 5.30 p.p.m. In this cobalt complex the dppm is in a chelating mode.[6]

The broad multiplet at 7.42 p.p.m. is assigned to the phenyl protons and this is shifted by 0.2 p.p.m. from that of free dppm. The integrations for dppm and acetate agree with the formulation. However, the peak due to acetonitrile is larger than expected. When the ^1H n.m.r. spectrum of a similar quantity of CD_3CN alone was recorded at the same sensitivity, a peak at 1.95 p.p.m. was observed, the intensity of which, if subtracted from the value obtained for the complex, gives an integration for acetonitrile in agreement with the formulation.

The shift in position of the geminal protons will partly be due to co-ordination of the dppm ligand and partly due to the diamagnetic anisotropy of the quadruple bond, as discussed in Chapter 2. The difference of 0.3 p.p.m. in the chemical shift of each geminal proton is probably due to the magnetic anisotropy of the Mo-N and Mo-O bonds.[6]

It appears that a small (*ca*. 5%) amount of decomposition of $[Mo_2(O_2CMe)_2(NCMe)_2(dppm)][BF_4]_2$ has occurred prior to recording the ^1H n.m.r. spectrum, as a triplet at 7.22 p.p.m. and a singlet at 2.83 p.p.m. were observed to be present in relatively small amounts. These resonances probably arise from the phenyl protons of free dppm and the methyl protons of the acetate groups in $[Mo_2(O_2CMe)_2(NCMe)_6][BF_4]_2$.

The $^{31}P\{^{1}H\}$ n.m.r. spectra of this compound and of dppm were recorded at 32.4 MHz in CD_3CN solution (Figs. 3.5 and 3.6). The ^{31}P n.m.r. spectrum of $[Mo_2(O_2CMe)_2(NCMe)_2(dppm)][BF_4]_2$ shows a single resonance at 21.3 p.p.m. while that of dppm shows a single resonance at -21.8 p.p.m. Thus, the shift on co-ordination from free ligand is +43.1 p.p.m., i.e. a shift to higher frequency. Such shifts on co-ordination of phosphines to Mo_2^{4+} centres have been observed by Anderson et al. on reaction of phosphines with $[Mo_2(O_2CCF_3)_4]$ and were assumed indicative of strongly bound phosphine.[7,8] Al-Samman[9] attributed this shift to be additionally affected by the diamagnetic anisotropy of the quadruple bond and the Mo-X (X = O, N, P etc.) bonds. On the basis of this latter view, a consideration of the angular relationships, involved for phosphorus binding (i) axially or (ii) equatorially, allowed a proposal of the difference in chemical shifts for the different binding sites. Calculations showed that, for phosphorus bound axially, the net effect would be a slight shift to higher frequency of the ^{31}P resonance (from that of free ligand) while phosphorus bound equatorially would give a ^{31}P resonance at a significantly higher frequency to that of free ligand.[9] This is in agreement with the values of the ^{31}P chemical shifts observed for various molybdenum phosphine complexes, Table 3.1.

The large shift to higher frequency of the ^{31}P resonance of the dppm ligands on co-ordination adds weight to the proposal that dppm is co-ordinated in the equatorial rather than the axial position.

FIG.3.5 32.4 MHz ^{31}P n.m.r. spectrum of $[Mo_2(O_2CMe)_2(NCMe)_2(dppm)][BF_4]_2$ in $CD_3C^{\prime\prime}$

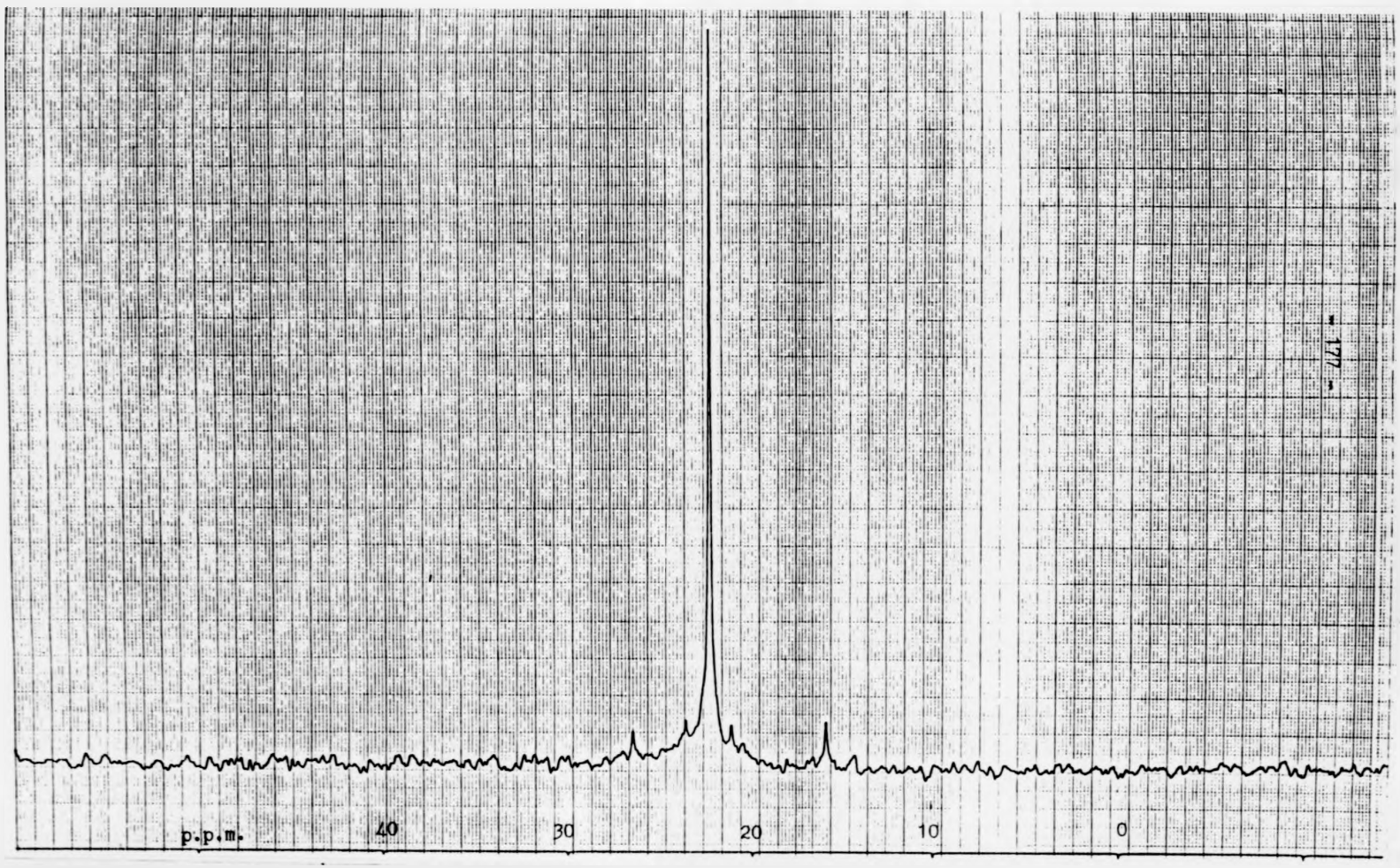

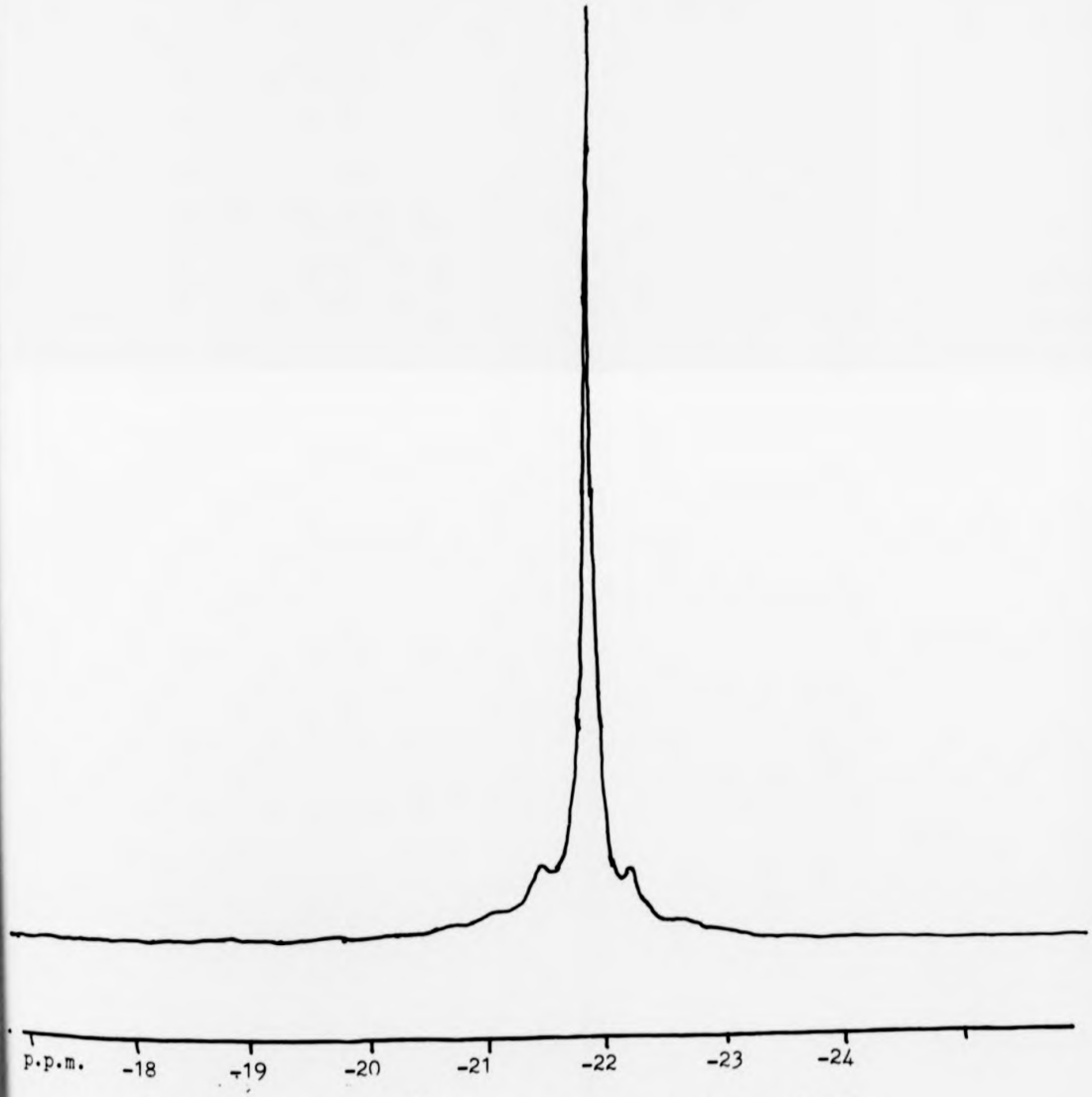

FIG.3.6 32.4 MHz ^{31}P n.m.r. spectrum of dppm in CD_3CN

Table 3.1 The ^{31}P n.m.r. resonances of some molybdenum phosphine complexes

Complex	δ(p.p.m.)[a] complex	δ(p.p.m.) free ligand	Δ(p.p.m.) chemical shift difference	Ref.
$[Mo_2(O_2CCF_3)_4(PPh_3)_2]$	-1.0	-5.8	4.8	
$[Mo_2(O_2CCF_3)_4(PMePh_2)_2]$	-29.6	-28.1	1.5	
$[Mo_2(O_2CCF_3)_4(PPhMe_2)_2]$	4.3,2.2	-46.9	51.2,49.1	
$[Mo_2(mhp)_3Cl(PPh_3)]$	31.9	-5.8	37.4	9
$[Mo_2(mhp)Cl_3(PPh_3)_2(MeOH)]$	32.6	-5.8	38.1	9
$[Mo_2(O_2CMe)_2(NCMe)_2(dppm)]$	21.3	-21.8	43.1	This work

[a] expressed in δ units relative to 85% H_3PO_4 (δ = 0)

3.4 Reaction of $[Mo_2(O_2CMe)_2(NCMe)_6][BF_4]_2$ with PPh_3 and $P(OMe)_3$

$[Mo_2(O_2CMe)_2(NCMe)_6][BF_4]_2$ (0.3 g, 0.4 mmol) was dissolved in acetonitrile (*ca*. 20 cm^3) and PPh_3 (0.21 g, 0.8 mmol) added. The reaction solution was stirred for *ca*. 4 hours and a small change in the UV/visible spectrum of the solution was observed. However, on reduction of the volume of solution *in vacuo* to *ca*. 10 cm^3 and addition of diethylether (*ca*. 10 cm^3), a pink precipitate formed which had identical analyses and spectroscopic properties to those of the starting material.

A similar observation was made on reaction with the phosphine ligand $P(OMe)_3$, which was employed to see if oxidation of the Mo_2^{4+} centre could be achieved by a better π-acceptor ligand. A change in the UV/visible spectrum was seen on addition of a 24:1 molar ratio of

$P(OMe)_3$ to the metal dimer but, on reduction of the volume of solution and addition of diethyl ether, starting material, again, was formed.

It seems reasonable to assume that the chelating effect favoured the formation of the complex $[Mo_2(O_2CMe)_2(NCMe)_2(dppm)][BF_4]_2$ on a simple 1:1 ratio of reactants which does not favour production of a species containing monodentate phosphines, even if present in great excess. This led to an attempt to place the chelating ligand dppe around this dimolybdenum centre.

3.5.1 Reaction of $[Mo_2(O_2CMe)_2(NCMe)_6][BF_4]_2$ with dppe

$[Mo_2(O_2CMe)_2(NCMe)_6][BF_4]_2$ (0.4 g, 0.54 mmol) was dissolved in acetonitrile (*ca.* 30 cm^3) and dppe (0.21g, 0.52 mmol) was added to this solution. A colour change occurred from deep pink to deep purple and the reaction mixture was stirred overnight. The volume of solution was reduced to *ca.* 15 cm^3 *in vacuo* and sufficient diethyl ether was added (*ca.* 10 cm^3) to precipitate a purple solid. This solid was collected by filtration and dried *in vacuo*. Analyses and spectroscopic measurements showed this solid to be $[Mo_2(O_2CMe)_2(NCMe)_6][BF_4]_2$.

An equilibrium could be occurring in the reaction solution of

$$[Mo_2(O_2CMe)_2(NCMe)_6][BF_4]_2 \underset{MeCN}{\overset{dppe}{\rightleftharpoons}} [Mo_2(O_2CMe)_2(NCMe)_x(dppe)][BF_4]_2$$

and, as dppe is slightly soluble in diethyl ether, addition to aid precipitation could shift the equilibrium to the left to produce starting material.

Therefore, an alternative procedure was attempted.

3.5.2 Reaction of $[Mo_2(O_2CMe)_2(NCMe)_6][BF_4]_2$ with dppe

$[Mo_2(O_2CMe)_2(NCMe)_6][BF_4]_2$ (0.3 g, 0.4 mmol) was dissolved in acetonitrile (ca. 20 cm^3) and dppe (0.16 g, 0.4 mmol) was added. An immediate colour change, from deep pink to deep purple occurred and the reaction mixture was stirred overnight. The solvent was subsequently completely removed in vacuo to afford a glassy deep purple compound. This was washed with diethyl ether (3 x 10 cm^3) and dried in vacuo.

Analyses	C	H	Mo	N	P
Calc. for $C_{34}H_{36}B_2F_8Mo_2N_2O_4P_2$	42.3	3.8	19.9	2.9	6.4 %
Found	39.5	4.2	19.5	2.9	6.3 %

Although the product approached analytical purity, the ^1H and ^{31}P n.m.r. spectra showed a large number of peaks which suggested a mixture of products. The mixture was very air sensitive and had a low solubility in non-polar solvents. It dissolved in acetonitrile but showed a tendency to decompose readily to an insoluble black powder. Thus, no new compound involving dppe co-ordinated to a Mo_2^{4+} centre was obtained from these studies.

3.6 Molybdenum-95 n.m.r. spectroscopic studies on some quadruply bonded dimers

Molybdenum-95 n.m.r. spectroscopy has recently been established as a sensitive probe of both electronic and structural effects in diamagnetic molybdenum complexes. Despite the electric quadrupole moment associated with this nucleus ($I = 5/2$, $Q \simeq 0.011 \times 10^{-28}$ m^2, 15.72 atom %), line widths are acceptably narrow in a large number of compounds. The chemical shift range currently covers ca. 7250 p.p.m.

for all molybdenum species (see Table 3.2) and high oxidation numbers for the molybdenum species are present at both extremes of the shift range.[10]

Relatively few quadruply bonded molybdenum dimers have been studied via ^{95}Mo n.m.r. techniques. Typical values are between ~3000 p.p.m. found in phosphine halide systems ($\delta^{95}Mo$ for $[Mo_2I_4(PMe_3)_4]$ at 2927 p.p.m.) to just over 4000 p.p.m. ($\delta^{95}Mo$ for $[Mo_2(O_2CCF_3)_4(py)_2]$ at 4199 p.p.m.). With such a small number of reported values, the ^{95}Mo n.m.r. spectra of the compounds $[Mo_2(O_2CMe)_2(NCMe)_6][BF_4]_2$, $[Mo_2(O_2CMe)_2(NCCMe_3)_5][BF_4]_2$ (reported in Chapter 2) and $[Mo_2(O_2CMe)_2(NCMe)_2(dppm)][BF_4]_2$ were recorded to provide an extension to the results previously obtained.

The author wishes to thank Dr. Haworth and Dr. E. Curzon (S.E.R.C. Service, Warwick) and Dr. J. Mason and Dr. R. Grieves for obtaining the spectra and for helpful discussions in recording of the ^{95}Mo n.m.r. spectra.

The 26 MHz ^{95}Mo n.m.r. spectra of $[Mo_2(O_2CMe)_2(NCMe)_6][BF_4]_2$, $[Mo_2(O_2CMe)_2(NCCMe_3)_6][BF_4]_2$ and $[Mo_2(O_2CMe)_2(NCMe)_2(dppm)][BF_4]_2$ in deuteroacetonitrile were recorded on a Bruker WH400 spectrometer at ambient temperature. Chemical shifts in parts per million were referenced to external aqueous 2M Na_2MoO_4 at apparent pH 11.

These values, as well as some ^{95}Mo n.m.r. shifts previously recorded, are given, along with line widths, in Table 3.2.

Table 3.2 ^{95}Mo n.m.r. shifts of some quadruply bonded Mo dimers

Compound	δ^{95}Mo (p.p.m.)	$\nu_{\frac{1}{2}}$[a] (Hz)	Ref.
$[Mo_2I_4(PMe_3)_4]$	2927	850	10
$[Mo_2Br_4(PMe_3)_4]$	2996	800	10
$[Mo_2Cl_4(PMe_3)_4]$	3008	800	10
$Cs_4[Mo_2Br_8]$	3227	510	11
$[Mo_2(O_2CMe)_2(NCMe)_2(dppm)][BF_4]_2$	3633	450	This work
$[Mo_2(O_2CBu^n)_4]$	3661	1440	11
$[Mo_2(O_2CPr^n)_4]$	3682	1320	11
$[Mo_2(O_2CMe)_4]$	3702	520	11
$[Mo_2(O_2CH)_4]$	3768	670	10
$[Mo_2(O_2CMe)_2(NCMe)_6][BF_4]_2$	3874	950	This work
$[Mo_2(O_2CMe)_2(NCCMe_3)_5][BF_4]_2$	3874	950	This work
$K_4[Mo_2Cl_8]$	3816	1440	11
$[Mo_2(O_2CCF_3)_4]$	4021	480	11
Mo_2^{4+}	4056	430	11
$K_4[Mo_2(SO_4)_4]$	4090	990	11
$[Mo_2(O_2CCF_3)_4(py)_2]$	4199	320	10

[a] line-width at half height

3.7 Discussion

The trend on going from the general small chain aliphatic tetracarboxylates ($[Mo_2(O_2CH)_4]$ and $[Mo_2(O_2CPr^n)_4]$) to the hemi-bridged dimer $[Mo_2(O_2CMe)_2(NCMe)_6][BF_4]_2$, is a downfield (high frequency) shift from ca. 3730-3768 p.p.m. to 3874 p.p.m. The indication is that, although the NCMe and O_2CMe substituents have rather similar effects on the ^{95}Mo shift, the presence of the axial NCMe ligands deshields the molybdenum. A similar effect is found on the addition of pyridine to $[Mo_2(O_2CCF_3)_4]$ in the axial position (Table 3.2). The identical ^{95}Mo n.m.r. shifts found for both $[Mo_2(O_2CMe)_2(NCMe)_6][BF_4]_2$ and $[Mo_2(O_2CMe)_2(NCCMe_3)_5][BF_4]_2$ in CD_3CN agrees with the observations noted in Chapter 2 with respect to the lability of the nitrile ligands when the complex is dissolved in CD_3CN. UV/visible, ^1H and ^{95}Mo n.m.r. spectroscopy each show the solution species observed for $[Mo_2(O_2CMe)_2(NCCMe_3)_5][BF_4]_2$ in acetonitrile to be identical to that for $[Mo_2(O_2CMe)_2(NCMe)_6][BF_4]_2$. Low temperature studies may freeze out the exchange of the nitrile ligands.

The shift of 3633 p.p.m. for the complex $[Mo_2(O_2CMe)_2(NCMe)_2(dppm)][BF_4]_2$ falls between the shifts observed for $[Mo_2X_4(phos)_4]$ (X = halide; phos = phosphine) and $[Mo_2(O_2CR)_4]$ (R = H, Pr^n) in Table 3.2. This is one of the first acetate bridged/dppm bridged dimer to have been prepared and therefore the first to be studied by ^{95}Mo n.m.r. spectroscopy. The trend observed in the ^{95}Mo chemical shifts of these three types of complex is of the expected form.

3.8 Summary and Conclusions

The complexes prepared in Chapter 2 $[Mo_2(O_2CMe)_2(NCMe)_6][BF_4]_2$ and $[Mo_2(O_2CH)_2(NCMe)_5(H_2O)][BF_4]_2$ were shown to react with some ligands to produce mixed ligand dimers. The product $[Mo_2(O_2CH)_2(mhp)_2]$ could be prepared very easily and quickly. The mixed acetate/dppm dimer $[Mo_2(O_2CMe)_2(NCMe)_2(dppm)][BF_4]_2$ has been prepared and fully characterised. This is one of the first bridged acetate/dppm dimers to be prepared and the presence of the acetate groups easily enables the conformation of the dppm molecule, either bridged or bidentate, to be determined by ^1H n.m.r. spectroscopy. The dimer prepared here has a bridging dppm ligand. Also, it has been shown that, on addition of sodium acetate to $[Mo_2(O_2CMe)_2(NCMe)_6][BF_4]_2$, the parent dimer $[Mo_2(O_2CMe)_4]$ is readily produced. Work-up of reaction solutions containing the $[Mo_2(O_2CMe)_2(NCMe)_6]^{2+}$ ion and PPh_3 or $P(OMe)_3$ did not produce the phosphine or phosphite dimer but rather led to reformation of starting material. The increased stability of complexes with bidentate phosphines was attributed to this observation. Attempts to isolate a product of the reaction between $[Mo_2(O_2CMe)_2(NCMe)_6][BF_4]_2$ and dppe gave either starting materials or a mixture of a number of products that were impossible to separate.

The range of ^{95}Mo chemical shifts reported on Mo_2^{4+} dimers, presently covering only a very small number of compounds, has been extended to include $[Mo_2(O_2CMe)_2(NCMe)_6][BF_4]_2$, $[Mo_2(O_2CMe)_2(NCCMe_3)_5][BF_4]_2$, and $[Mo_2(O_2CMe)_2(NCMe)_2(dppm)][BF_4]_2$. Previously only tetracarboxylate compounds and mixed halide/phosphine complexes have been reported and the chemical shift value for $[Mo_2(O_2CMe)_2(NCMe)_2(dppm)][BF_4]_2$ nicely bridges the ranges shown by the above classes.

REFERENCES

1. T.J. Barder, F.A. Cotton, K.R. Dunbar, G.L. Powell, W. Schwotzer, and R.A. Walton, Inorg.Chem., 1985, 24, 2550.

2. P.A. Agaskar, F.A. Cotton, D.R. Derringer, G.L. Powell, D.R. Root, and T.J. Smith, Inorg.Chem., 1985, 24, 2786.

3. F.A. Cotton and R.A. Walton, Multiple Bonds Between Metal Atoms, Wiley-Interscience, 1982.

4. E. Hochberg, P. Walks, and E.H. Abbot, Inorg.Chem., 1974, 13, 1824.

5. J.W. Emsley, J. Feeney, and L.H. Sutcliffe, "High Resolution Nuclear Magnetic Resonance Spectroscopy", Vol.1, Pergamon Press, 1965.

6. Q.-B. Bao, S.J. Landon, A.L. Rheingold, T.M. Haller, and T.B. Brill, Inorg Chem., 1985, 24, 900.

7. G.S. Girolami, V.V. Mainz, and R.A. Anderson, Inorg.Chem., 1980, 19, 805.

8. V.V. Mainz and R.A. Anderson, Inorg.Chem., 1980, 19, 2165.

9. M.H. Al-Samman, Ph.D. Thesis, 1981.

10. R.A. Grieves and J. Mason, Private Communication.

11. B.P. Shehan, M. Kony, R.T.C. Brownlee, M.J. O'Connor, and A.G. Wedd, J.Magn.Reson., 1985, 63, 343.

CHAPTER 4

STUDY OF THE REACTIVITY OF

$[Rh_2(O_2CMe)_2(NCMe)_6][BF_4]_2$

4.1 Introduction

The preparation of $[Rh_2(O_2CMe)_2(NCMe)_6][BF_4]_2$, described in Chapter 2, provided a compound sufficiently different from the dirhodium tetracarboxylates to make a study of its reactivity interesting. Possibilities arise in that the replacement of the bridging anionic carboxylate groups of the parent compound by monodentate neutral acetonitrile may:

(a) expose the metal-metal bond to direct attack,

(b) enable relatively easy replacement of the solvent acetonitrile molecules, in both axial and equatorial positions, to produce new mixed-ligand rhodium dimers,

and/or

(c) increase the susceptibility of attack by anion ligands on the cationic dimer.

The reactivity of the dirhodium(II) carboxylates has been explored by other workers as discussed in Chapter 1. The reaction of pyridine with $[Rh_2(O_2CMe)_2(NCMe)_6]^{2+}$ was used in an attempt to obtain equatorially ligated pyridine complexes, similar to those recently reported,[1-4] or to achieve axial substitution, the new complex perhaps then being more susceptible to equatorial substitution. Reactions with PPh_3 and dppm were investigated, to see whether phosphine donors could be placed equatorially in these complexes and, thus, to investigate the effects of such relatively strong σ-donors on the rhodium-rhodium bond.[5] Reactions with $[NO_2]^-$ were studied, to see if a new bridging ligand could be coordinated to the Rh_2^{4+} centre. Also, reactions with picoline-N-oxide were studied in an attempt to oxidise the dimetal system by initial cleavage of the N-O bond with oxo-transfer;[6]

this oxidation would be expected to remove electrons from the anti-bonding orbitals involved in the Rh-Rh bond, thereby strengthening the bond. Sulphur donors lead to oxidation of dirhodium(II) systems,[7-10] and compounds of dimeric rhodium centres bridged by sulphur ligands are rare.[11,12] Therefore, an attempt was made, via sodium dithiocarbamate, to produce a mixed carboxylate/thiocarbamate bridged system.

Mononuclear carbonylate anions react with polynuclear carbonyl compounds with the expulsion of CO[13,14] and subsequent protonation of the product has led to the synthesis of a range of hydrido-carbonyl mixed-metal cluster compounds:

$$[Ru_3(CO)_{12}] + [Fe(CO)_4]^{2-} \xrightarrow{\Delta, H^+} [H_2FeRu_3(CO)_{13}]$$

$$[Ru_2Os(CO)_{12}] + [Fe(CO)_4]^{2-} \xrightarrow{\Delta} \xrightarrow{H^+} [H_2FeRu_2Os(CO)_{13}]$$

$$[RuOs_2(CO)_{12}] + [Fe(CO)_4]^{2-} \xrightarrow{\Delta} \xrightarrow{H^+} [H_2FeRuOs_2(CO)_{13}]$$

Therefore, the reactivity of $[Fe(CO)_4]^{2-}$ with $[Rh_2(O_2CMe)_2(NCMe)_6][BF_4]_2$ was explored.

Dialkyl or diaryl phosphides have been shown to bridge metal-metal bonds forming a M-P-M arrangement.[15] This type of reaction could occur for $[Rh_2(O_2CMe)_2(NCMe)_6]^{2+}$, i.e. the Rh-Rh bond could be exposed to attack and a dimeric singly bonded Rh-Rh phosphide complex could be formed.

4.2 Preparation of $[Rh_2(O_2CMe)_2(NCMe)_4(pyridine)_2][BF_4]_2$

$[Rh_2(O_2CMe)_2(NCMe)_6][BF_4]_2$ (0.19 g, 0.25 mmol), prepared as described in Chapter 2, was dissolved in pyridine (20 cm^3) to give an orange solution. Reduction of the volume of this solution by evaporation under reduced pressure and the addition of diethyl ether (5 cm^3) precipitated an orange powder. This material was collected by filtration and recrystallised from methanol to produce an orange crystalline product. (Yield = 0.18 g, 85%)

Analyses	C	H	F	N	Rh
Calc. for $C_{22}H_{28}B_2F_8N_6O_4Rh_2$	32.2	3.4	18.5	10.2	25.1 %
Found	32.2	3.5	17.5	10.2	24.6 %

The crystal structure of this compound has been described in Chapter 2.

4.2.1 Spectroscopic Studies

4.2.1(i) UV/visible spectrum

The UV/visible spectrum of $[Rh_2(O_2CMe)_2(NCMe)_4(pyridine)_2][BF_4]_2$ in methanol is shown in Fig.4.1 and the details are summarised in Table 4.1, together with the corresponding data for $[Rh_2(O_2CMe)_2(NCMe)_6][BF_4]_2$

Table 4.1 Comparison of absorption bands of $[Rh_2(O_2CMe)_2(NCMe)_6][BF_4]_2$ and $[Rh_2(O_2CMe)_2(NCMe)_4(py)_2][BF_4]_2$

	λ_{max} (ε $mol^{-1}cm^{-1}dm^3$)
$[Rh_2(O_2CMe)_2(NCMe)_4(py)_2][BF_4]_2$ [a]	470(273) , 350(1600)
$[Rh_2(O_2CMe)_2(NCMe)_6][BF_4]_2$ [b]	520(202) , 355(478)
$[Rh_2(O_2CMe)_2(NCMe)_4(MeOH)_2][BF_4]_2$ [c]	576 , 374

[a] in MeOH [b] in MeCN

[c] $[Rh_2(O_2CMe)_2(NCMe)_6][BF_4]_2$ in MeOH

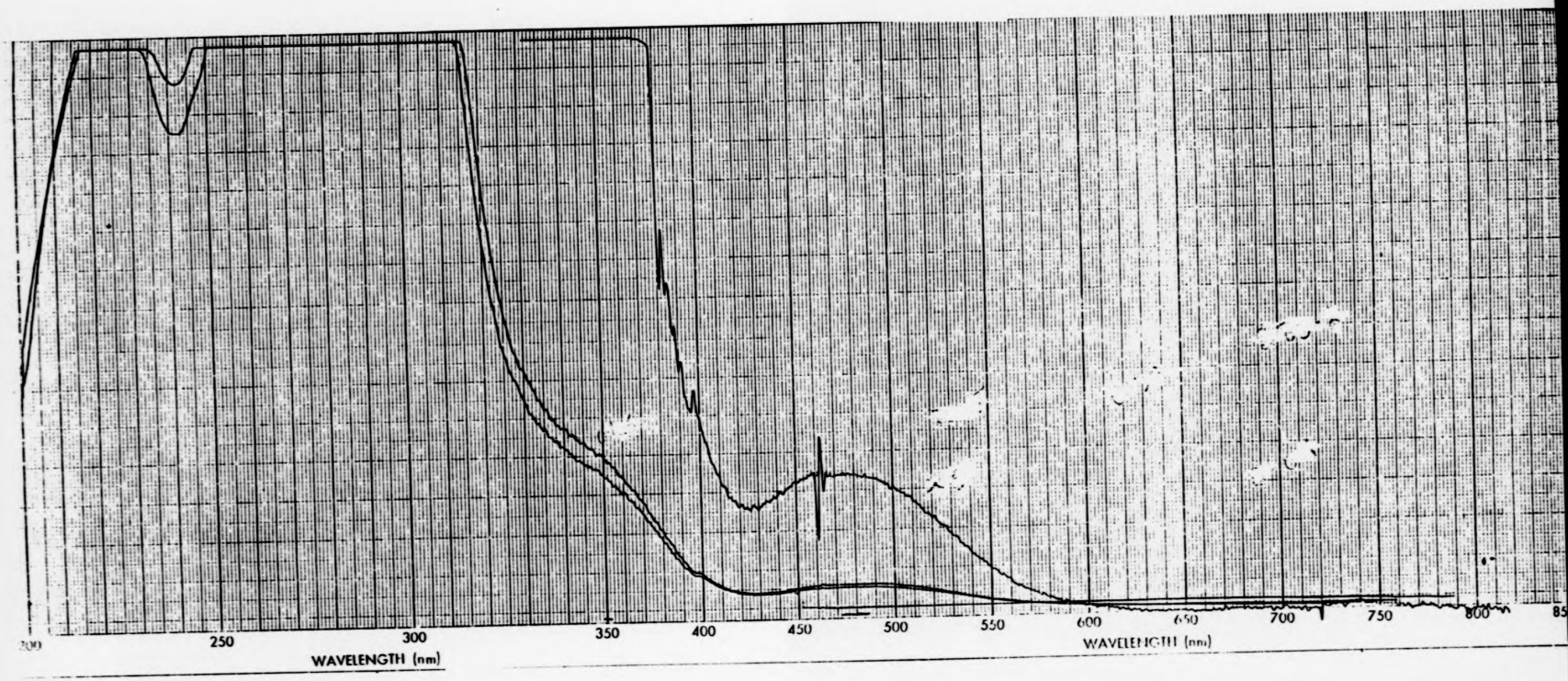

FIG. 4.1 UV/visible spectrum of $[Rh_2(O_2CMe)_2(NCMe)_4(py)_2][BF_4]_2$ in MeOH

A comparison of the two lower energy absorption bands for $[Rh_2(O_2CMe)_2(NCMe)_6][BF_4]_2$ and $[Rh_2(O_2CMe)_2(NCMe)_4(pyridine)_2][BF_4]_2$ shows that, on going from $[Rh_2(O_2CMe)_2(NCMe)_6][BF_4]_2$(I) to $[Rh_2(O_2CMe)_2(NCMe)_4(pyridine)_2][BF_4]_2$(II) the lower energy band shifts from 520 nm to 470 nm. A similar shift is seen in the lowest energy band in moving from $[Rh_2(O_2CMe)_4(NCMe)_2]$ to $[Rh_2(O_2CMe)_4(pyridine)_2]$ (552 nm to 518 nm)[16,17] and this absorption has been assigned to the Rh-Rh π^* → Rh-Rh σ^* transition.[18] Since the σ^* orbital is located along the L-Rh-Rh-L axis, a shift in this band on changes of the axial co-ordination from MeCN to pyridine is understandable. However, other workers have assigned the lowest energy band to the Rh-Rh π^* → Rh-O σ^* and Rh-Rh δ^* → Rh-O σ^* transitions and state that changes in axial ligation will affect the lowest energy transition[19] (i.e. *ca*. 520-560 nm).

The second band at 350 nm in II and 355 nm in I remains relatively constant for this change in axial ligation, and a similar situation occurs for the dirhodium(II) tetracarboxylates. This band may involve two transitions, one has been attributed[20,11] to Rh-Rh π^* → Rh-O σ^* transition and another to Rh-O π → Rh-O σ^*.[19] This band in the tetracarboxylates has a lower molar extinction coefficient than in the $[Rh_2(O_2CMe)_2(NCMe)_4)(L)_2][BF_4]_2$ complexes.[11] For the bis-pyridine adduct(II) the ε value is *ca*. 4 times greater than that for the acetonitrile adduct(I). This sensitivity of ε value to axial and equatorial ligands could be due to a mixing of metal-to-ligand charge-transfer transitions with transitions of the Rh_2^{4+} core.

4.2.1(ii) Infrared spectrum

The infrared spectrum of $[Rh_2(O_2CMe)_2(NCMe)_4(pyridine)_2][BF_4]_2$ in a nujol mull is shown in Fig.4.2, and in a HCBD mull is shown in Fig.4.3. Assignments of the prominent bands of these spectra are given in Table 4.2. The spectra are similar to that obtained for $[Rh_2(O_2CMe)_4(pyridine)_2]$[17] with the addition of bands due to $\nu(C\equiv N)$ stretches at 2290 cm^{-1}.

4.2.1(iii) N.m.r. spectroscopic studies

The ^1H n.m.r. spectrum (Fig.4.4) of $[Rh_2(O_2CMe)_2(NCMe)_4(pyridine)_2][BF_4]_2$ in d_6-dmso was recorded at 300 MHz. This contains two sharp resonances at 2.77 and 2.07 p.p.m. and three broader features centred at 7.87, 8.29, and 8.92 p.p.m. The peaks at 2.07 and 2.77 p.p.m. are assigned to the acetate and equatorial MeCN, respectively, and those at 7.87, 8.29, and 8.92 p.p.m. to the 3-py, 4-py, and 2-py protons, respectively.[22,23] The integrations of the peaks at 2.07, 2.77, 7.87, 8.29, and 8.92 are 4:8:2:1:2 which is in close agreement (expected 3:6:2:1:2) with the molecular formula.

The position of the resonance due to equatorial MeCN is shifted from that of the parent compound (from 2.59 to 2.77 p.p.m.). This could be due to solvent effects although, for the parent compound, changing from d_3-MeCN to d_4-MeOH causes no change in this resonance position. Also, the acetate resonance position hardly changes from d_3-MeCN to d_6-dmso (2.09-2.07 p.p.m.). Therefore, the shift in the resonance position of the nitrile protons to higher frequency could indicate slightly stronger MeCN co-ordination in the bis-pyridine adduct than that of the parent compound with concomitant deshielding of the methyl protons. The $Rh-N_{eq}$ bond length decrease of 0.004 Å

Table 4.2

Assignment of infrared spectra of $[Rh_2(O_2CMe)_2(NCMe)_4(pyridine)_2][BF_4]_2$

Nujol mull (cm^{-1})	HCBD mull (cm^{-1})	Assignment
3550	3550	ν(OH) symmetric and asymmetric[a]
3110		
3080		ν(CH) (nujol)
3019		
2940		
2290		ν(CN) MeCN(Ch.2 and Ref.21)
1605	1605	ν(C=C) pyridine[22]
1550	1560	ν_{asym}(OCO) acetate[21]
1450	1455	
	1435	ν_{sym}(OCO) acetate[21]
	1360	
1290		
1220	1220	pyridine
1060	1060	ν(B-F)[21]
775	770	ν(B-F)[21]
730	720	δ(C-H) pyridine[22]
720	710	

[a] ν(OH) from absorbed water from infrared cells.

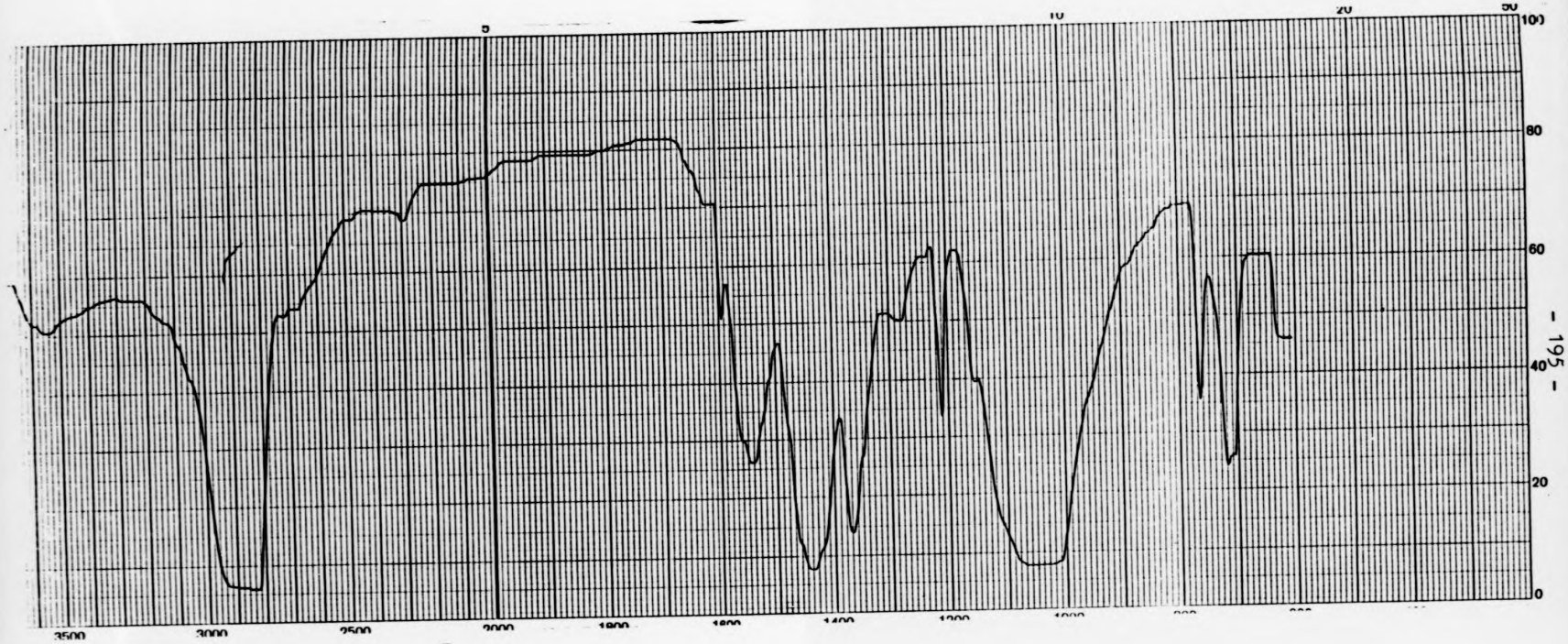

FIG. 4.2 Infrared spectrum of $[Rh_2(O_2CMe)_2(NCMe)_4(py)_2][BF_4]_2$ in a nujol mull.

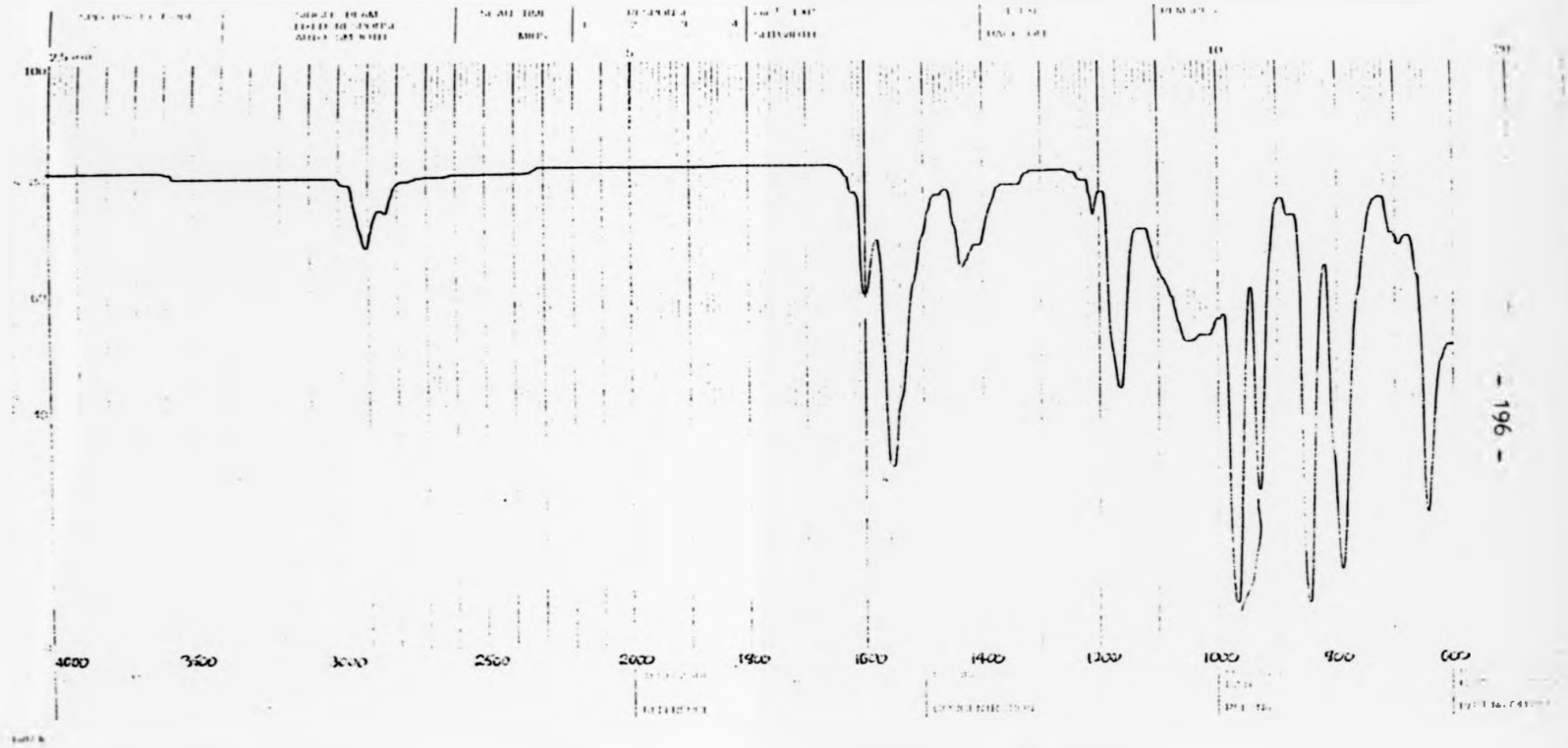

FIG. 4.3 Infrared spectrum of $[Rh_2(O_2CMe)_2(NCMe)_4(py)_2][BF_4]_2$

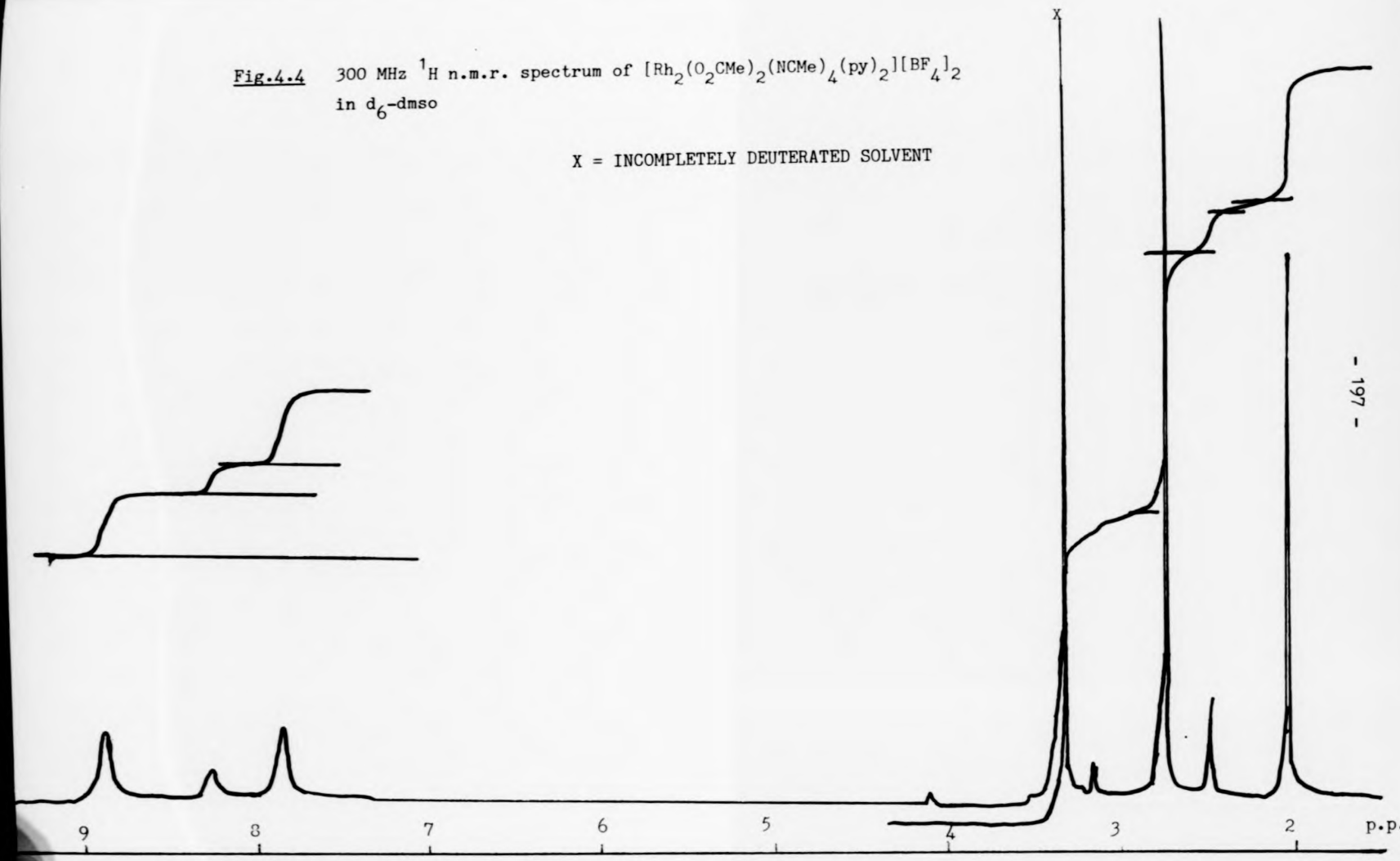

Fig.4.4 300 MHz ^{1}H n.m.r. spectrum of $[Rh_2(O_2CMe)_2(NCMe)_4(py)_2][BF_4]_2$ in d_6-dmso

X = INCOMPLETELY DEUTERATED SOLVENT

on going from $[Rh_2(O_2CMe)_2(NCMe)_6][BF_4]_2$ to $[Rh_2(O_2CMe)_2(NCMe)_4(py)_2][BF_4]_2$ may support this, although the change is rather small.

The ^{13}C n.m.r. spectrum of $[Rh_2(O_2CMe)_2(NCMe)_4(pyridine)_2][BF_4]_2$ in d_6-dmso and d_4-MeOH was recorded at 20.1 MHz and 75 MHz, respectively. The two spectra are very similar, apart from the absence of the peak due to the carboxylate carbon of the acetate group in the 75 MHz spectrum, most probably due to incorrect pulsing to observe a quaternary carbon. The spectrum of the compound in d_6-dmso is shown in Fig.4.5. Apart from the peaks due to solvent, ^{13}C resonances were observed at 192.1, 149.8, 138.9, 126.9, 125.6, 22.8, and 3.4 p.p.m. These are assigned as: 192.1 and 22.8 due to the carboxylate and methyl carbons, respectively, of the acetate groups; those at 149.8, 138.9, and 125.6 p.p.m. due to the 2-C, the 4-C, and the 3-C, respectively, of the pyridine;[24] and those at 126.9 and 3.4 p.p.m. due to the nitrile and methyl carbon, respectively, of the acetonitrile ligands. These peak positions agree closely with the corresponding peaks for the parent $[Rh_2(O_2CMe)_2(NCMe)_6][BF_4]_2$ compound (Chapter 2). In d_4-MeOH peaks were observed at 150, 138.9, 126.4, 125.3, 22.5, and 3.1 p.p.m. and are assigned as above.

As the MeCN (axial) in the parent compound $[Rh_2(O_2CMe)_2(NCMe)_6][BF_4]_2$ appears to be very weakly co-ordinated, and can be replaced by other solvent molecules such as MeOH, thf (as evidenced by the changes in the UV/visible spectra, Chapter 2), it was interesting to determine whether the axial pyridine molecules are more strongly bound. Indeed it appears to be so, since in MeOH the UV/visible spectrum of $[Rh_2(O_2CMe)_2(NCMe)_4(pyridine)_2][BF_4]_2$ does not take on the appearance of that of $[Rh_2(O_2CMe)_2(NCMe)_6][BF_4]_2$ in MeOH and the pyridine adduct can be recrystallised unchanged from MeOH. The ^1H n.m.r. spectrum of

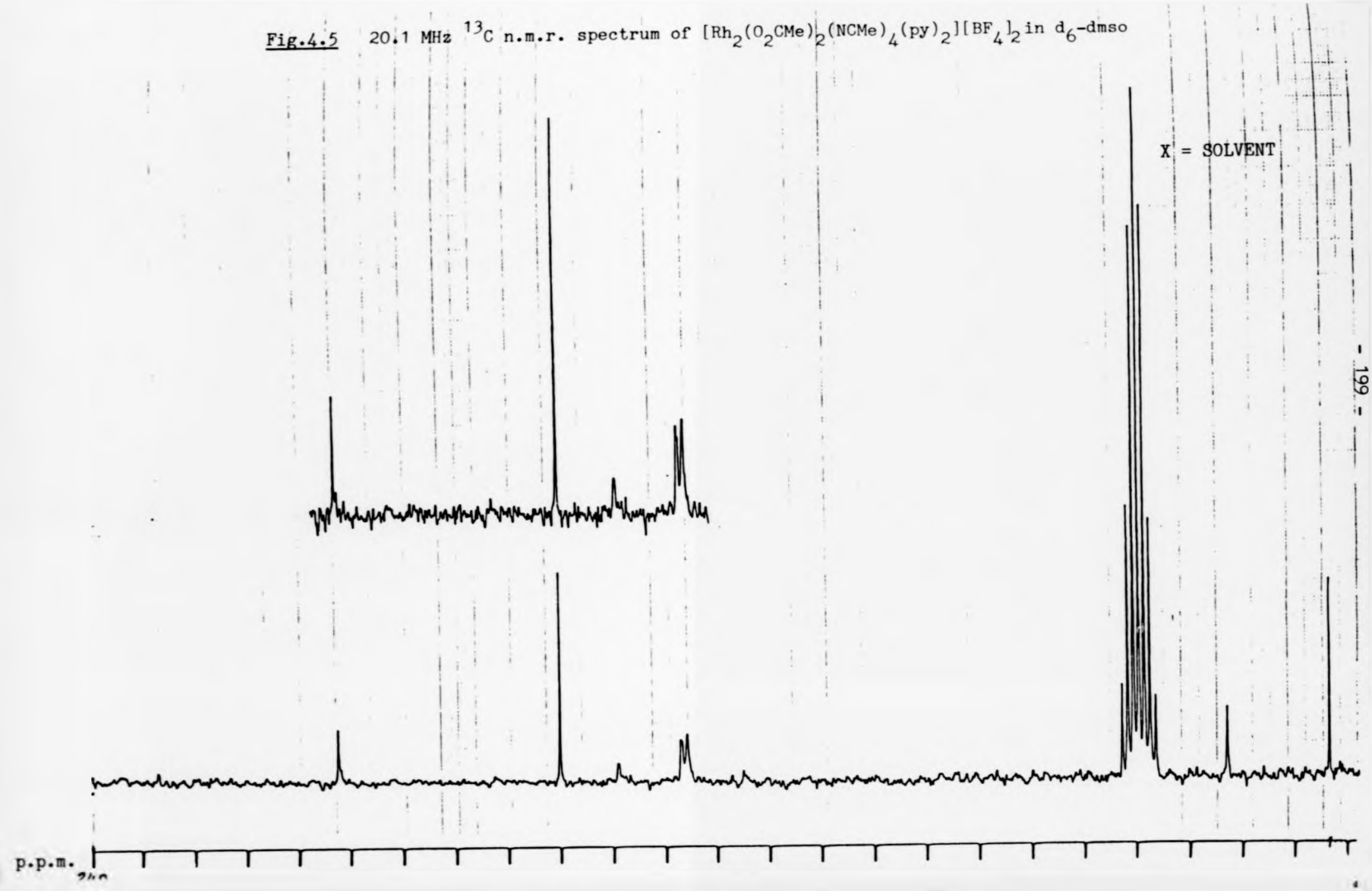

Fig.4.5 20.1 MHz ^{13}C n.m.r. spectrum of $[Rh_2(O_2CMe)_2(NCMe)_4(py)_2][BF_4]_2$ in d_6-dmso

pyridine in d_6-dmso shows signals at 7.3, 7.7, and 8.6 p.p.m. for the 3-py, 4-py, and 2-py protons, respectively. The shifts on co-ordination to the Rh_2^{4+} centre are, therefore, +0.57, +0.59, and +0.32 p.p.m., respectively, and it appears that the axial co-ordination of pyridine is retained in the molecule. The shifts of pyridine resonances on co-ordination in $[(NH_3)_5Rh(py)]^{3+}$ are +0.6, +0.67, and -0.16 p.p.m. for the 3-py, 4-py, and 2-py protons, respectively.[23]

4.3 Preparation of $[Rh_2(O_2CMe)_2(NCMe)_4(PPh_3)_2][BF_4]_2$

Triphenyl phosphine (0.13 g, 0.49 mmol) was added to a stirred solution of $[Rh_2(O_2CMe)_2(NCMe)_6][BF_4]_2$ (0.18 g, 0.24 mmol) in methanol (30 cm^3). After *ca*. 2 h, the volume of the reaction solution was reduced to *ca*. 20 cm^3 and the orange precipitate that had formed was collected by filtration, washed with diethyl ether (2 x 10 cm^3) and dried *in vacuo*. The orange powder was recrystallised from methanol. (Yield 0.22 g, *ca*. 80%)

Analyses	C	H	F	N	P	Rh
Calc. for $B_2C_{48}F_8H_{48}N_4O_4P_2Rh_2$	48.6	4.1	12.8	4.7	5.2	17.3
Found	47.5	4.4	13.3	5.1	5.3	17.2

4.3.1 Spectroscopic Studies

4.3.1(i) UV/visible spectrum

The UV/visible spectrum of $[Rh_2(O_2CMe)_2(NCMe)_4(PPh_3)_2][BF_4]_2$ in MeCN (Fig.4.6) consists of features with $\lambda_{max}(\epsilon/l\ mol^{-1}cm^{-1})$ of the following values: 460(sh)(34 498), 408(58 647), 350(sh)(3 450), 300(sh)(5 175), 260(17 249), and 226(35 233) nm. Comparison with the UV/visible spectrum of the parent compound $[Rh_2(O_2CMe)_2(NCMe)_6][BF_4]_2$

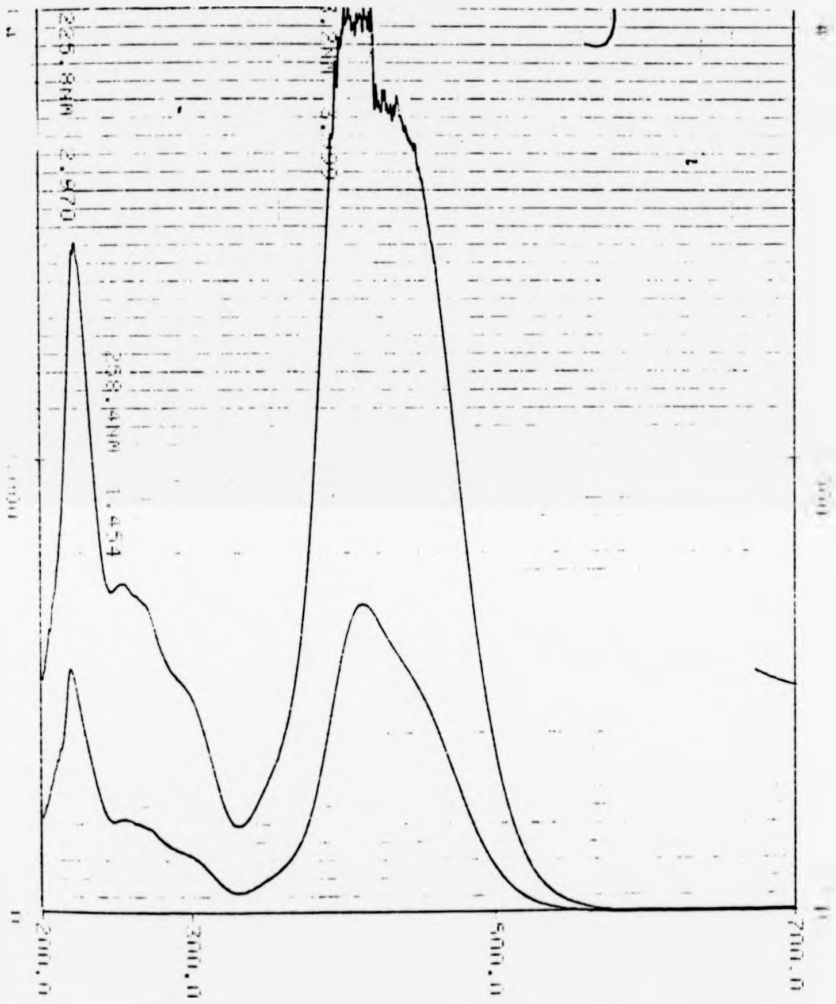

FIG. 4.6 Infrared spectrum of $[Rh_2(O_2CMe)_2(NCMe)_4(PPh_3)_2][BF_4]_2$ in MeCN

reveals that the bands in the parent compound at 520 nm has been replaced by a shoulder at 460 nm and a band at 408 nm in the PPh_3 adduct. This is very similar to that observed for $[Rh_2(O_2CCF_3)_4(PPh_3)_2]$[25] by Kawamura et al. discussed in Chapter 1.

Also, the shift in the shoulder at 350 nm in the PPh_3 adduct from the absorption in the parent compound $[Rh_2(O_2CMe)_2(NCMe)_6[BF_4]_2$ (355 nm) is only slight as discussed for axial adducts of the tetracarboxylates in Chapter 2.

4.3.1(ii) Infrared spectrum

The infrared spectrum of $[Rh_2(O_2CMe)_2(NCMe)_4(PPh_3)_2][BF_4]_2$ mulled in nujol is shown in Fig.4.7. The features at 1580 and 1530 cm^{-1} are assigned to the asymmetric O-C-O stretching vibrations of the carboxylate groups with the corresponding symmetric vibration occurring at 1460 cm^{-1}.[21] A band at 1440 cm^{-1}, close to the nujol peak, is assigned to the P-Ph vibration in PPh_3;[22] the broad band at 1050 cm^{-1} to the B-F stretching vibration in $[BF_4]^-$,[21] and the bands at 750 and 695 cm^{-1} to the out of plane C-H bending vibrations in the monosubstituted benzene rings.[22]

4.3.1(iii) N.m.r. spectroscopic studies

The ^1H, ^{13}C, and ^{31}P n.m.r. spectra of $[Rh_2(O_2CMe)_2(NCMe)_4(PPh_3)_2][BF_4]_2$ in CD_2Cl_2 solution were recorded at 300 MHz, 75 MHz, and 32.4 MHz, respectively, and these are shown in Figs. 4.8, 4.9, and 4.10.

The ^1H n.m.r. spectrum was recorded at ca. 300K and shows resonances at 1.96 and 2.07 p.p.m. and a broad resonance with features at 7.52, 7.54, and 7.65 p.p.m. The resonance at 1.96 p.p.m. is assigned to the acetate protons while that at 2.07 p.p.m. is assigned to the

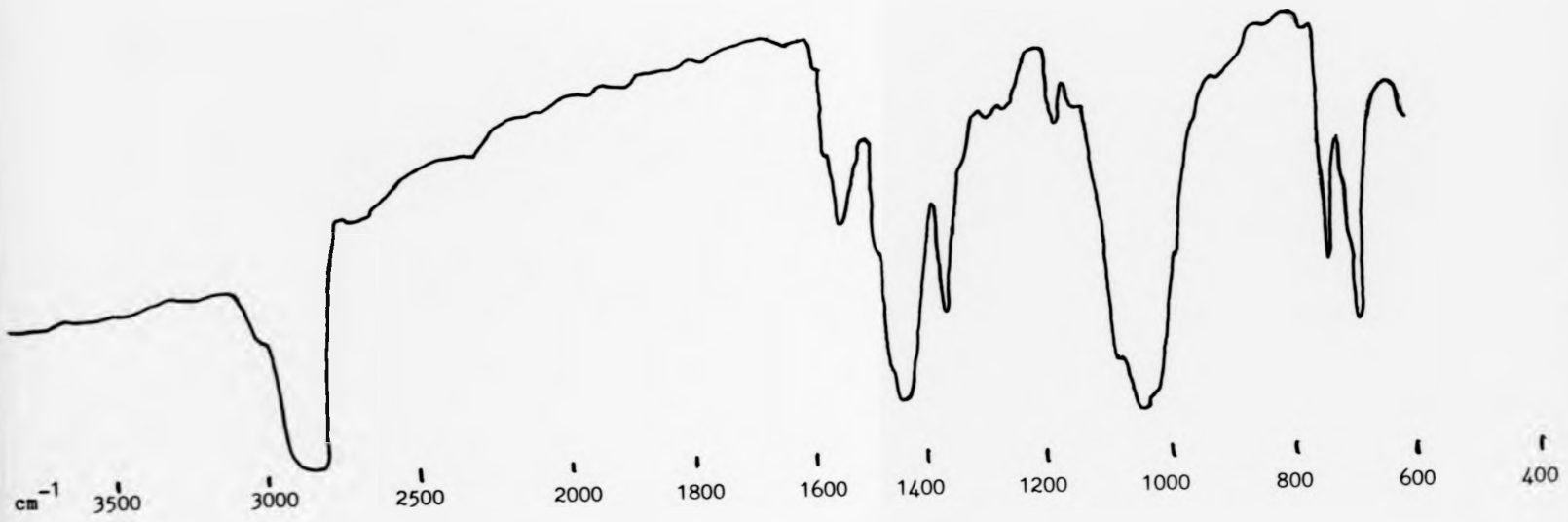

FIG. 4.7 Infrared spectrum of $[Rh_2(O_2CMe)_2(NCMe)_4(PPh_3)_2][BF_4]_2$ in nujol.

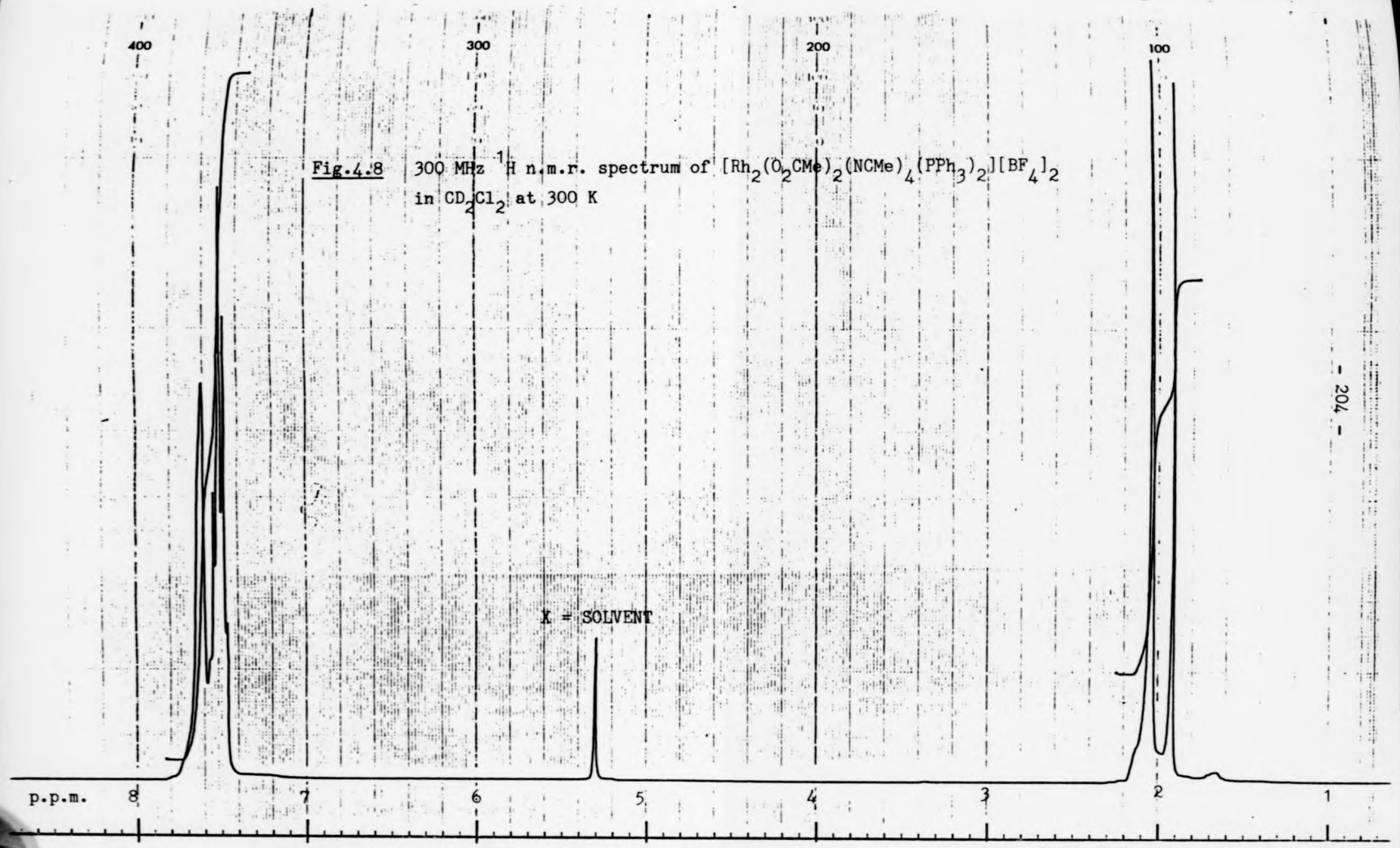

Fig.4.8 300 MHz ^{1}H n.m.r. spectrum of $[Rh_2(O_2CMe)_2(NCMe)_4(PPh_3)_2][BF_4]_2$ in CD_2Cl_2 at 300 K

acetonitrile protons. These resonances integrate in a ca. 1:2 ratio, as expected. The broad resonance is assigned to the protons of triphenylphosphine. The integrations of the peaks at 1.96, 2.07, and those around 7.5 p.p.m. are in an approximate 1:2:5 ratio, respectively, in agreement with the molecular formula. Both acetate and acetonitrile resonances have shifted from those in the parent compound; the acetate peak by 0.14 p.p.m. to lower frequency and the acetonitrile peak by 0.53 p.p.m. to lower frequency. These shifts are attributed to the effect of the ring currents of the phenyl rings of the PPh_3 ligands, some of which will be in close contact to the acetate and acetonitrile methyl protons. The PPh_3 ligands are also good σ-donors and would, therefore, be expected to affect the electronic density of the rhodium-rhodium bond.[25] This, in turn, will affect the electron density of rhodium-acetonitrile and rhodium-carboxylate bonds, and, hence, the resonance positions of these methyl protons.

The ^{13}C n.m.r. spectrum was recorded at ca. 300K (Fig.4.9) and shows resonances at 3.8, 23.6, 127.5, 129.1, 130.8, 134.1, and 193.5 p.p.m. The features at 3.8 and 127.5 p.p.m. are assigned to the methyl and cyanide carbons on the co-ordinated acetonitrile ligands, those at 23.6 and 193.5 p.p.m. to the methyl and carboxylate carbons on the acetate groups, and those at 129.1, 130.8, and 134.1 p.p.m. to the phenyl carbons on PPh_3,[26] one of the peaks containing two carbon resonances. The acetate and acetonitrile resonances are very similar to those observed for the corresponding groups of $[Rh_2(O_2CMe)_2(NCMe)_6][BF_4]_2$.

The ^{31}P n.m.r. spectrum was recorded at room temperature ca. 300K, 230K, and 200K. At room temperature and 230K, a broad triplet was observed, centred at -14 p.p.m. but, as the temperature was lowered to 200K, a sharper (linewidth 2 Hz) signal in the form of a doublet of

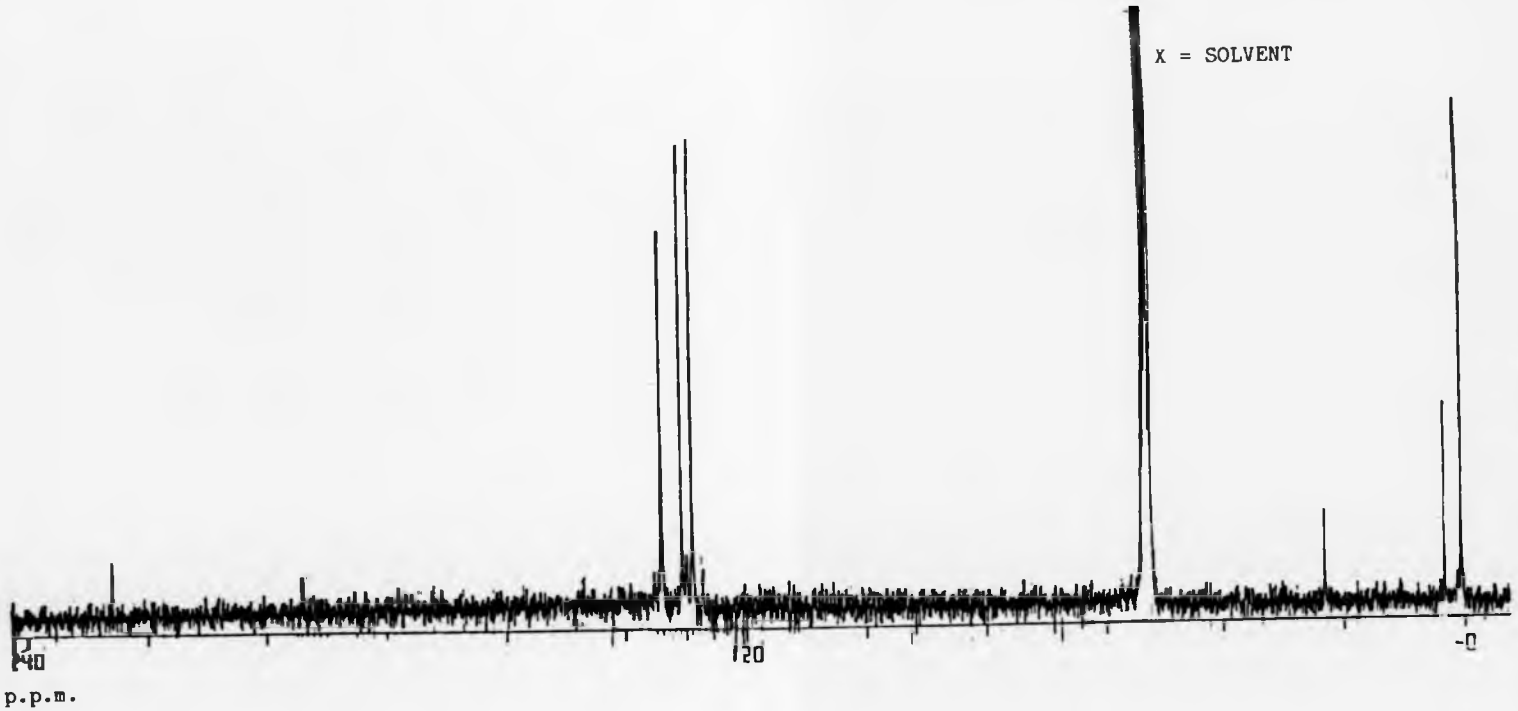

Fig.4.9 75 MHz ^{13}C n.m.r. spectrum of $[Rh_2(O_2CMe)_2(NCMe)_4(PPh_3)_2][BF_4]_2$ in CD_2Cl_2 at 300 K

doublets was obtained, centred at -14.3 p.p.m. (Fig.4.10). This consists of the XX' portion of an AA'XX' pattern [A,A' = ^{103}Rh; X,X' = ^{31}P] and is identical to the spectrum obtained for the diaxial PPh_3 adducts of $Rh_2(O_2CMe)_4$ and $Rh_2(O_2CCH_2CH_2CH_3)_4$, described later in this chapter. The pattern is also similar to a portion of the ^{31}P n.m.r. spectrum obtained by Boyar and Robinson for various bis-phosphite axial adducts.[27,28] However, on dissolution of various diaxial phosphite adducts of the dirhodium tetracarboxylates $[Rh_2(O_2CR)_4(P(OR')_3)_2]$ (R = Me, Et, Pr or Ph; R' = Me, Et or Ph) in CD_2Cl_2 at low temperature (213K), Boyar and Robinson reported the freezing out of an equilibrium mixture containing mono- and bis-adducts, plus the free phosphorus ligand, i.e.

$$[\{(R'O)_3P\}Rh(O_2CR)_4Rh\{P(OR')_3\}] \rightleftharpoons [\{(R'O)_3P\}Rh(O_2CR)_4Rh(solv)] + P(OR')_3$$

Such an equilibrium is not observed with $[Rh_2(O_2CMe)_2(NCMe)_4(PPh_3)_2][BF_4]_2$ possibly because there is an inherent lability in the phosphite donors versus phosphine donors on the dirhodium(II) centres and/or because the $[Rh_2(O_2CMe)_2(NCMe)_4]^{2+}$ core forms stronger axial bonds with phosphorus donors than does the $Rh_2(O_2CR)_4$ core.

The reaction of a greater than 2:1 stoichiometry of PPh_3 to $[Rh_2(O_2CMe)_2(NCMe)_6][BF_4]_2$ results in the formation of two products, the major one being $[Rh_2(O_2CMe)_2(NCMe)_4(PPh_3)_2][BF_4]_2$ and a minor one which has been characterised by X-ray crystallography and shown to be the rhodium(I) monomer $[Rh(PPh_3)_3(NCMe)][BF_4]$. This latter compound is discussed in Chapter 5.

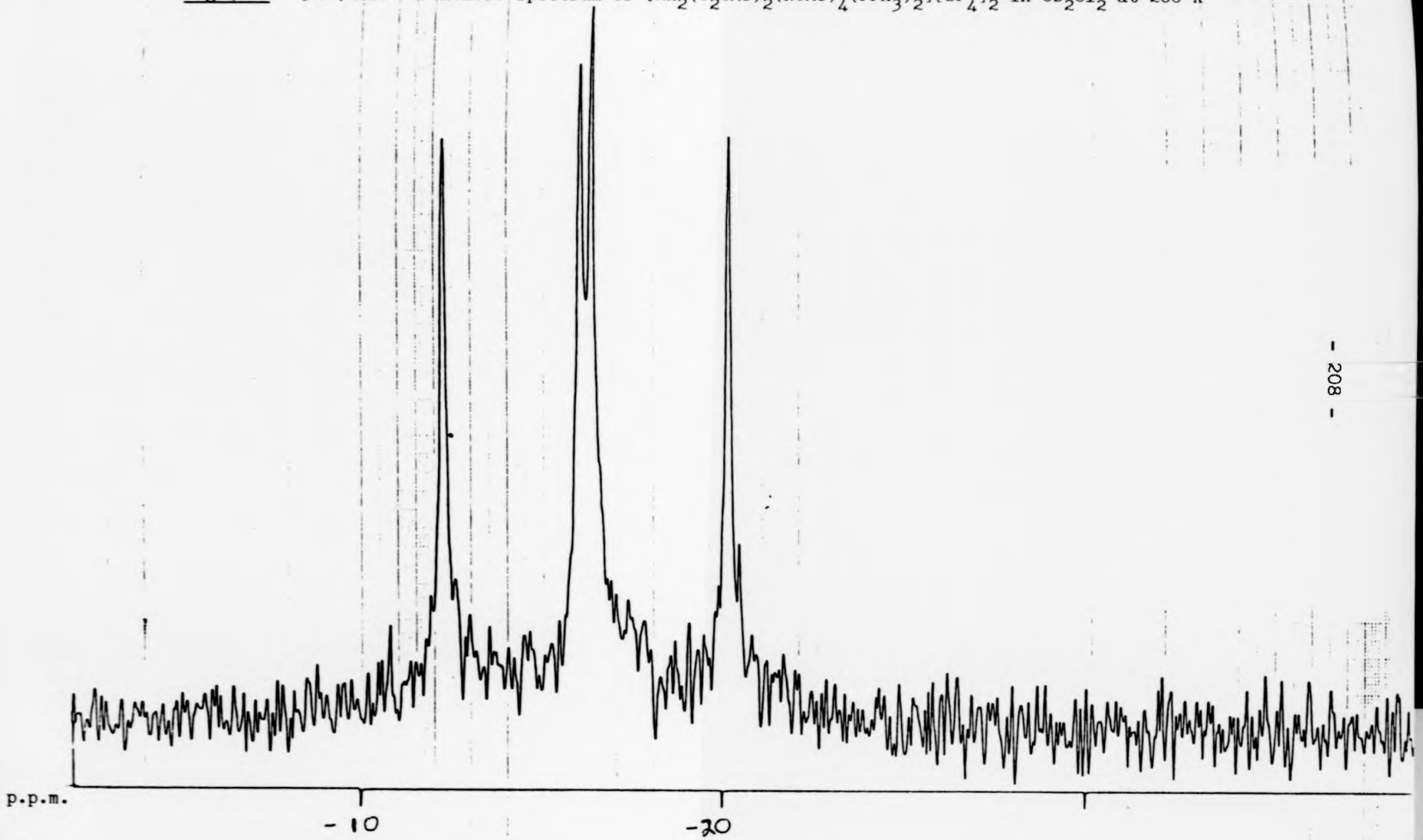

Fig.4.10 32.4 MHz ^{31}P n.m.r. spectrum of $[Rh_2(O_2CMe)_2(NCMe)_4(PPh_3)_2][BF_4]_2$ in CD_2Cl_2 at 200 K

4.4 Studies on the reaction of PPh_3 with $[Rh_2(O_2CMe)_4]$ and $[Rh_2(O_2CCH_2CH_2CH_3)_4]$ using ^{31}P n.m.r. spectroscopy

Hardly any investigation into the binding of Lewis bases to the axial positions on the dirhodium tetracarboxylates has been made using n.m.r. spectroscopy. This seems unfortunate since phosphines and phosphites, which readily bind in the axial positions provide us, via ^{31}P n.m.r. spectroscopy, with an elegant means to study mono- and bis-adduct formation. Boyar and Robinson have published low temperature ^{31}P n.m.r. studies[27,28] on the exchange processes occurring when certain bis-phosphite adducts of dirhodium tetracarboxylates $[Rh_2(O_2CR)_4(P(OR')_3)_2]$ (R = Me, Et, Pr or Ph; R' = Me, Et or Ph) are dissolved in CD_2Cl_2 solution and found that for all cases investigated at 213K the equilibrium

$$[\{(R'O)_3P\}Rh(O_2CR)_4Rh\{P(OR')_3\}] \rightleftharpoons [\{(R'O)_3P\}Rh(O_2CR)_4Rh(solv)] + P(OR')_3$$

is established. However, the process of adding a known amount of the phosphorus donor ligand to a dirhodium(II) tetracarboxylate and observing the formation of the solution species had not been investigated. Also, this study was necessary to obtain the ^{31}P n.m.r. spectra of PPh_3 axial adducts of rhodium(II) dimers to support the assignment of the spectra for $[Rh_2(O_2CMe)_2(NCMe)_4(PPh_3)_2][BF_4]_2$.

All ^{31}P n.m.r. spectra were recorded at 32.4 MHz.

Reaction of $Rh_2(O_2CMe)_4$ with PPh_3

$Rh_2(O_2CMe)_4$ (0.2 g, 0.45 mmol) was added to $\sim$1.5 cm^3 of CD_2Cl_2 in an n.m.r. tube and progressive additions of PPh_3, to produce stoichiometries of 1:1, 1:1.5, 1:2, and 1:2.5 were made. After each addition,

the ^{31}P n.m.r. spectrum was recorded for the solution at 230K. These results are displayed in Figs. 4.11a, b, c and d.

After the addition of one molar equivalent of PPh_3, a sharp doublet of doublets appeared, centred at -37 p.p.m. with coupling constants of 95 Hz and 30 Hz. The colour of the solution changed from green to deep purple but no purple solid could be isolated on work-up of this solution. Only the compounds $[Rh_2(O_2CMe)_4(PPh_3)_2]$ and $[Rh_2(O_2CMe)_4]$ could be recovered.

On further addition of PPh_3 to produce a 1:1.5 stoichiometry the feature at -37 p.p.m. disappeared and another doublet of doublets centred at -20 p.p.m. was observed. Here, second order effects were apparent as this doublet of doublets approaches a triplet and this complication makes direct measurement of coupling constants from the spectrum impossible. A sharp peak at $\sim$7 p.p.m. was also apparent.

Subsequent addition of PPh_3 to achieve a 1:2 stoichiometry produced the same features as observed for the 1:1.5 addition, but for a 1:2 ratio, as the temperature was increased from 230K to 255K the doublet of doublets feature increased in size relative to the sharp singlet.

At a ratio of 1:2.5, broadening of the features at -20 p.p.m. and -7 p.p.m. occurred, together with an increase in intensity of the peak at -7 p.p.m.

These results are interpreted as follows. At a 1:1 stoichiometric ratio the purple mono-adduct $Rh_2(O_2CMe)_4.PPh_3$ is formed. This compound gives rise to the doublet of doublets at -37 p.p.m. which comprises the X portion of an AMX pattern (A,M = ^{103}Rh; X = ^{31}P). Thus, these data allow the one bond and two bond Rh-P coupling constants to be obtained. The values, $^1J_{(Rh-P)}$ = 95 Hz and $^2J_{(Rh-P)}$ = 30 Hz are within the usual

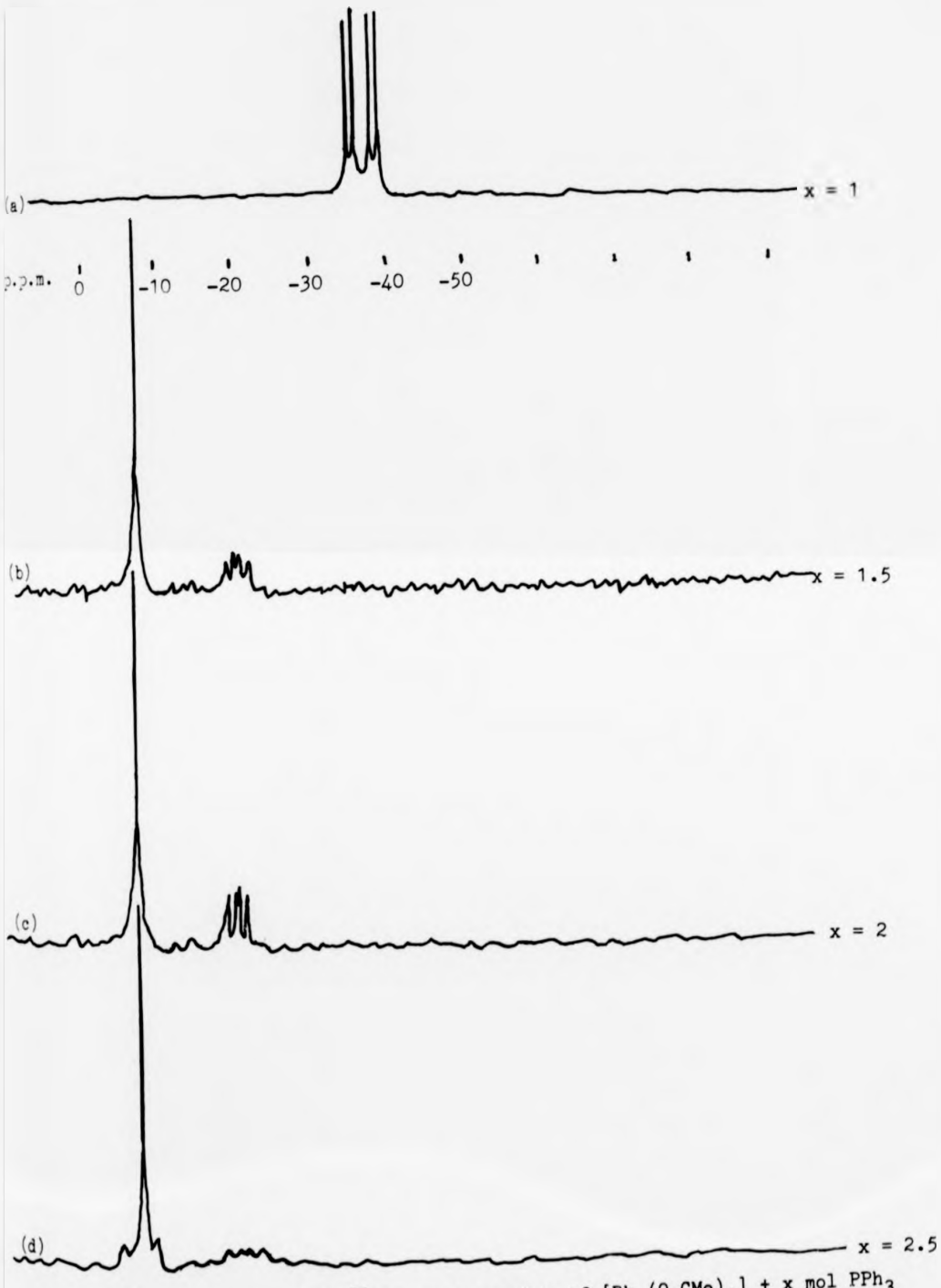

FIG. 4.11 32.4 MHz ^{31}P n.m.r. spectra of $[Rh_2(O_2CMe)_4]$ + x mol PPh_3

range of Rh-P coupling constants.[27,28] Attempted isolation of the mono-adduct resulted in the precipitation of the less soluble compounds $Rh_2(O_2CMe)_4$ and $Rh_2(O_2CMe)_4.2PPh_3$.

Increasing the relative amount of PPh_3 produced the bis-adduct which gives rise to the doublet of doublets at -20 p.p.m. Unfortunately, the bis-adduct is not very soluble in CD_2Cl_2 and begins to precipitate at such low temperatures. However, warming the solution from 230K to 255K improved the solubility and produced a clearer signal. This second doublet of doublets constitutes the XX' portion of an AA'XX' pattern (A,A' = ^{103}Rh; X,X' = ^{31}P).

The signal at -7 p.p.m. is attributed to free PPh_3. At stoichiometries of 1:1.5, 1:2, and 1:2.5 the bis-adduct appears to be in equilibrium with free PPh_3.

Changing the acetate for a longer chain alkyl carboxylate, e.g. butyrate, improves the solubility of the corresponding dirhodium complex in CH_2Cl_2. Therefore, a similar experiment was undertaken using dirhodium(II) tetra-butyrate.

$Rh_2(O_2CCH_2CH_2CH_3)_4$ (0.2 g, 0.36 mmol) was added to ≈ 1.5 cm^3 of CD_2Cl_2 in an n.m.r. tube and progressive additions of triphenyl phosphine to produce stoichiometries of 1:0.25, 1:0.5, 1:1, 1:1.25, 1:1.5, and 1:2 were made. After each addition, the ^{31}P n.m.r. spectrum was recorded at 230K and these spectra are shown in Figs. 4.12a, b, c, d, e and f.

After the addition of 0.25 molar equivalents of PPh_3, two features appeared, both doublets of doublets, centred at -20 p.p.m. and -38 p.p.m. The splitting of these doublets was identical to that observed for the

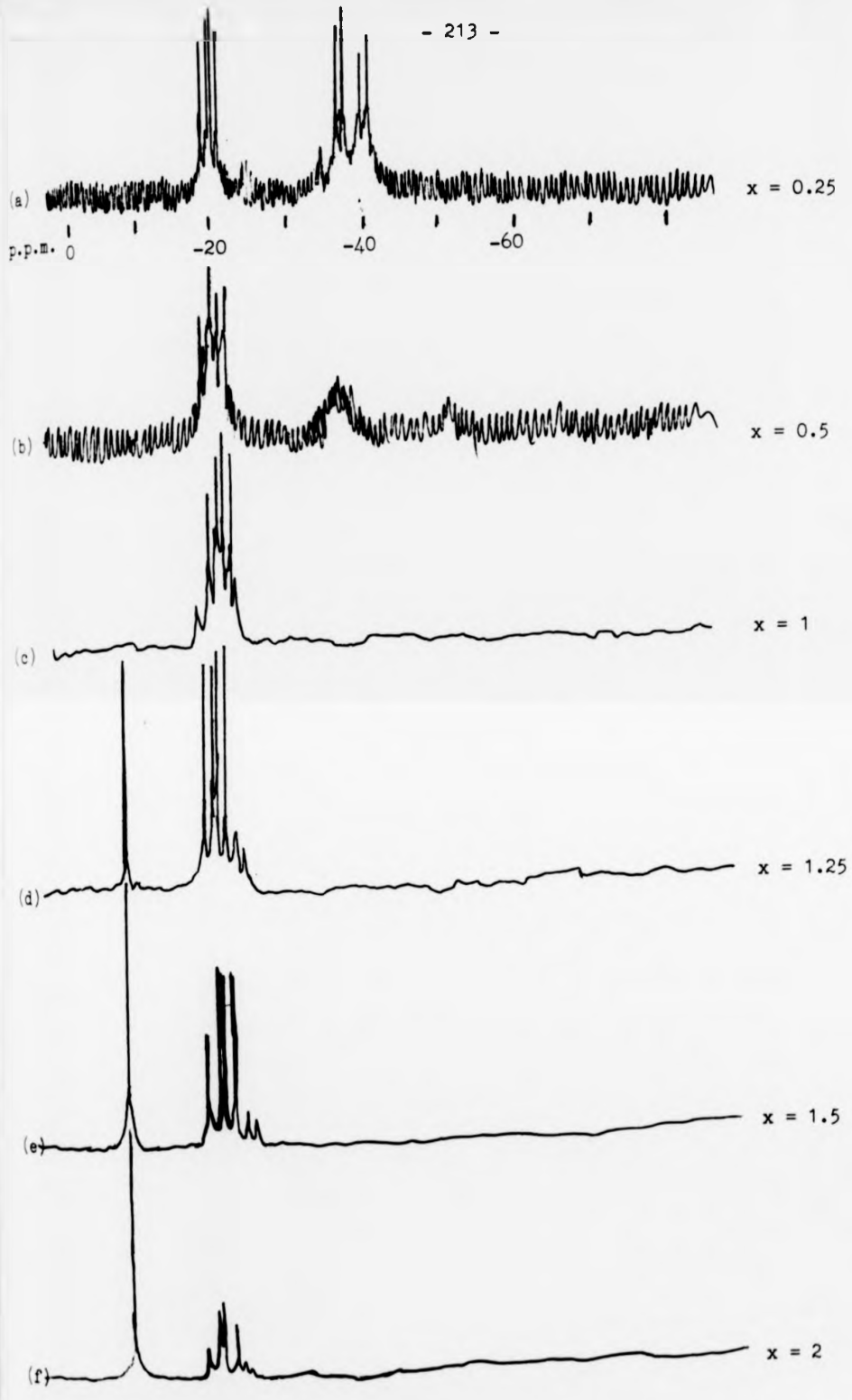

FIG. 4.12 32.4 MHz ^{31}P n.m.r. spectra of $[Rh_2(butyrate)_4]$ + x mol PPh_3

features at -20 p.p.m. and -37 p.p.m. with $Rh_2(O_2CMe)_4$. The heights of these two features are very similar, however, the integration of the -38 p.p.m. feature is approximately three times that of the second feature. On further addition of PPh_3 to give a 1:0.5 stoichiometric ratio the feature at -38 p.p.m. decreased to approximately one third the intensity of that previously and that at -20 p.p.m. increased. At a 1:1 stoichiometric ratio, the feature at -38 p.p.m. disappeared completely leaving an intense feature at -20 p.p.m. Addition of phosphine to give stoichiometric ratios of 1:1.25, 1:1.5, and 1:2 afforded an increase in the intensity of the signal at -7 p.p.m., relative to that at -20 p.p.m.

Again it appears that, as with the tetra-acetate, the mono-adduct is responsible for the doublet of doublets at -38 p.p.m., the bis-adduct for the doublet of doublets at -20 p.p.m. However, the situation is more complicated than for the tetra-acetate compound. Thus, addition of only 0.25 PPh_3 per rhodium dimer produces both the mono- and bis-adducts in solution, although the mono-adduct predominates. Therefore, the equilibrium in solution of

$$[Rh_2(\text{butyrate})_4] + [Rh_2(\text{butyrate})_4.2PPh_3] \rightleftharpoons 2[Rh_2(\text{butyrate})_4.PPh_3]$$

is proposed. Dilution of the n.m.r. sample by CD_2Cl_2 has no effect on the appearance of the spectrum and the position of the equilibrium. At 1:0.5 the ^{31}P n.m.r. data indicate that the bis-adduct predominates in solution over the mono-adduct, showing that the bis-adduct is the preferred product of the reaction of the butyrate and triphenyl phosphine, at 230K. At a 1:1 ratio, only the bis-adduct was observed and the addition of more PPh_3 leads to the presence of free phosphine, consistent with the equilibrium

$$[Rh_2(butyrate)_4.2PPh_3] \rightleftharpoons [Rh_2(butyrate)_4] + 2PPh_3$$

The ^{31}P chemical shift difference between these mono- and bis-adducts is ca. 18 p.p.m. which is less than that (ca. 60 p.p.m.) observed by Boyar and Robinson[27,28] in their studies on phosphites and dirhodium tetracarboxylates.

4.5 Preparation of $[Rh_2(O_2CMe)_2(NCMe)_4(NO_2)(MeOH)][BF_4]$

$[Rh_2(O_2CMe)_2(NCMe)_6][BF_4]_2$ (0.3 g, 0.4 mmol), prepared as described in Chapter 2, was dissolved in methanol (ca. 30 cm^3) to produce a deep blue solution. $NaNO_2$ (0.03 g, 0.4 mmol) was added with stirring and, immediately, a red-purple coloured solution formed. This was stirred for ca. 30 minutes, after which the solution was reduced in volume to ca. 10 cm^3 when small deep-red crystals formed. These were collected by filtration and recrystallised from methanol. (Yield = 0.2 g, 72%)

Analyses	C	H	F	N	Rh
Calc. for $C_{13}H_{22}N_5BF_4O_7Rh_2$	23.9	3.4	11.6	10.7	31.5 %
Found	23.9	3.6	10.2	10.5	30.0 %

The crystals had a tendency to decompose if left standing in methanol for any length of time.

4.5.1 Spectroscopic Studies

4.5.1(i) UV/visible spectrum

The UV/visible spectrum of $[Rh_2(O_2CMe)_2(NCMe)_4(NO_2)(MeOH)][BF_4]$ is shown in Fig.4.13 and the important features are summarised in Table 4.3.

FIG. 4.13 UV/visible spectrum of $[Rh_2(O_2CMe)_2(NCMe)_4(NO_2)(MeOH][BF_4]$ in H_2O.

Table 4.3 UV/visible spectrum of $[Rh_2(O_2CMe)_2(NCMe)_4(NO_2)(MeOH)][BF_4]$

λ_{max}(nm)	$\varepsilon(mol^{-1}cm^{-1}dm^3)$
506	280
380(sh)	1282
320	6072
269	16 340

The lowest energy band at 506 nm is assigned to the Rh-Rh $\pi^* \rightarrow$ Rh-Rh σ^*, the Rh-Rh $\pi^* \rightarrow$ Rh-O σ^* or the Rh-Rh $\delta^* \rightarrow$ Rh-O σ^* as in the tetracarboxylate complexes. This band has moved to higher energy from that of the parent compound, $[Rh_2(O_2CMe)_2(NCMe)_6][BF_4]_2$ (580 nm in H_2O), whilst the band at 380 nm is hardly shifted from that of the parent compound (370 nm in H_2O). This indicates that a change in axial ligation only has occurred.

4.5.1(ii) Infrared spectrum

The infrared spectrum of $[Rh_2(O_2CMe)_2(NCMe)_4(NO_2)(MeOH)][BF_4]$ as a nujol mull was recorded and is shown in Fig.4.14. Assignments of the principal absorptions are given in Table 4.4. The positions of the vibrations attributed to the nitrite group are typical of a NO_2^- ion co-ordinated via the N atom, i.e. as a nitro-complex.[21] Nitro-complexes exhibit $\nu_a(NO_2)$ and $\nu_s(NO_2)$ in the 1470-1370 and 1340-1320 cm^{-1} regions, respectively. For NO_2 bonded to the metal through one of its O atoms, (a nitrito-complex) the two $\nu(NO_2)$ vibrations are well separated, $\nu(N=O)$ and $\nu(N-O)$ being at 1485-1400 and 1110-1050 cm^{-1}, respectively.[21]

Also, the infrared spectra of nitrito-complexes lack the O-N-O wagging modes at ca. 620 cm^{-1} which appear in all nitro-complexes.[21]

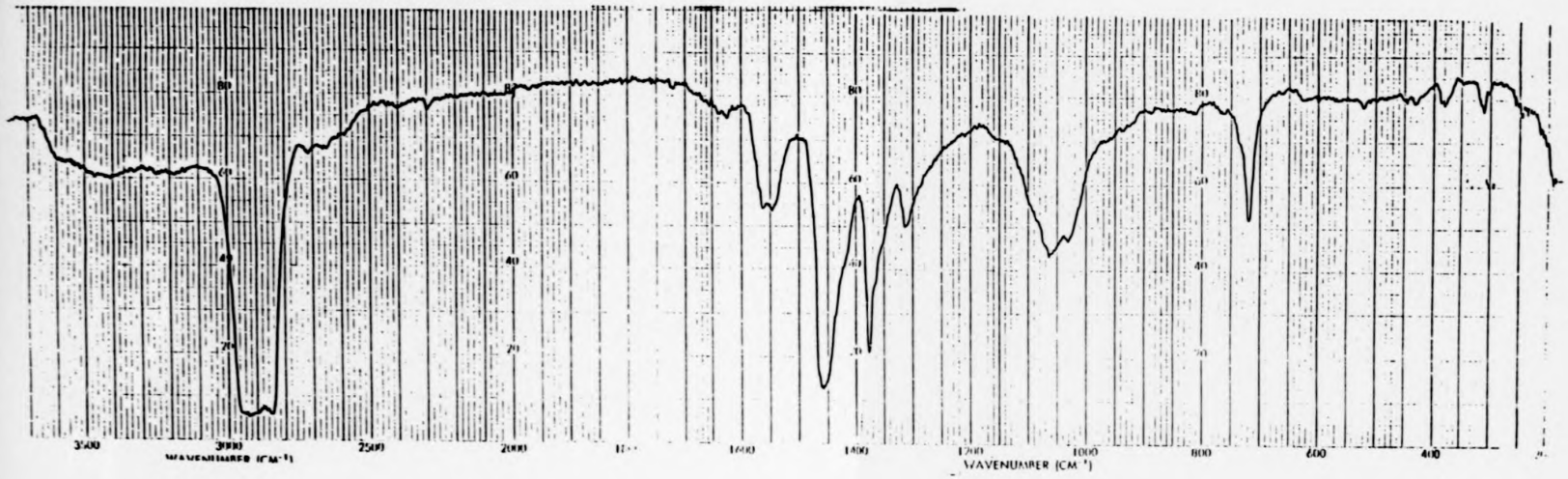

FIG. 4.14 Infrared spectrum of $[Rh_2(O_2CMe)_2(NCMe)_4(NO_2)(MeOH)][BF_4]$ as a nujol mull.

Table 4.4

Assignment of infrared spectrum of $[Rh_2(O_2CMe)_2(NCMe)_4(NO_2)(MeOH)][BF_4]$

Observed vibrations (cm^{-1})	Assignment[21]
3470	ν(OH) MeOH
2300	ν(CN)
1635	
1560	ν_{asym}(OCO) acetate
1550	
1455	Nujol
1420	$\nu_{asym}(NO_2)$
1315	$\nu_{sym}(NO_2)$
1065	ν(B-F)
1025	
825	δ(ONO)
720	
625	$\rho(NO_2)$
430	
380	ν(Rh-N)
310	

4.5.1(iii) N.m.r. spectroscopic studies

The 60 MHz ^1H n.m.r. spectrum of $[Rh_2(O_2CMe)_2(NCMe)_4(NO_2)(MeOH)][BF_4]$ in D_2O (Fig.4.15) showed, apart from a solvent peak at 4.7 p.p.m., resonances at 2.18, 2.66, and 3.4 p.p.m., which integrated in the approximate ratios 2:4:1 respectively. The resonance at 2.18 p.p.m. is assigned to the methyl protons on the acetate group, that at 2.66 p.p.m. to the methyl protons on the acetonitrile (equatorial) ligands, and that at 3.4 p.p.m. to methanol.

Structural assignments

From the analytical infrared, and ^1H n.m.r. spectroscopic data it appears that the $[Rh_2(O_2CMe)_2(NCMe)_4]^{2+}$ core is retained, with NO_2^- co-ordinated via the N atom in the axial position at one rhodium and methanol bound axially to the other rhodium, i.e.

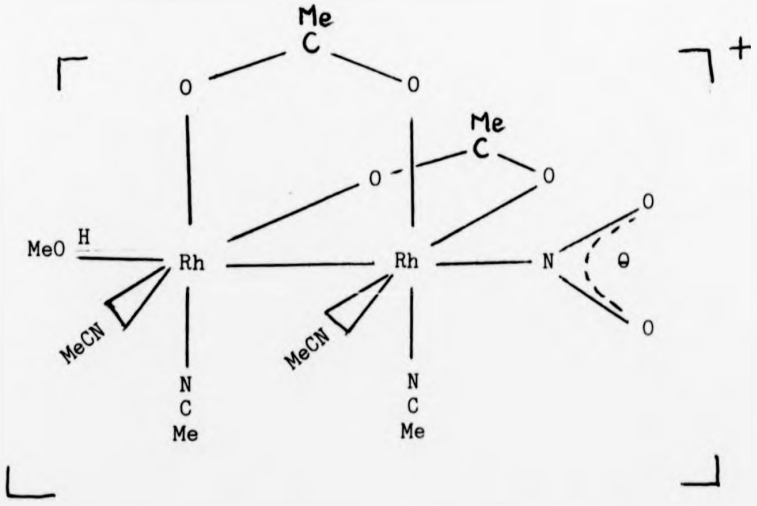

Such co-ordination of $[NO_2]^-$ is found in the complex $[Rh_2(O_2CMe)_4(NO)(NO_2)]$, which was the first diadduct of a dirhodium(II) tetracarboxylate to contain different donor molecules. The extremely short axial Rh-N bonds cause significant perturbations in the structure of

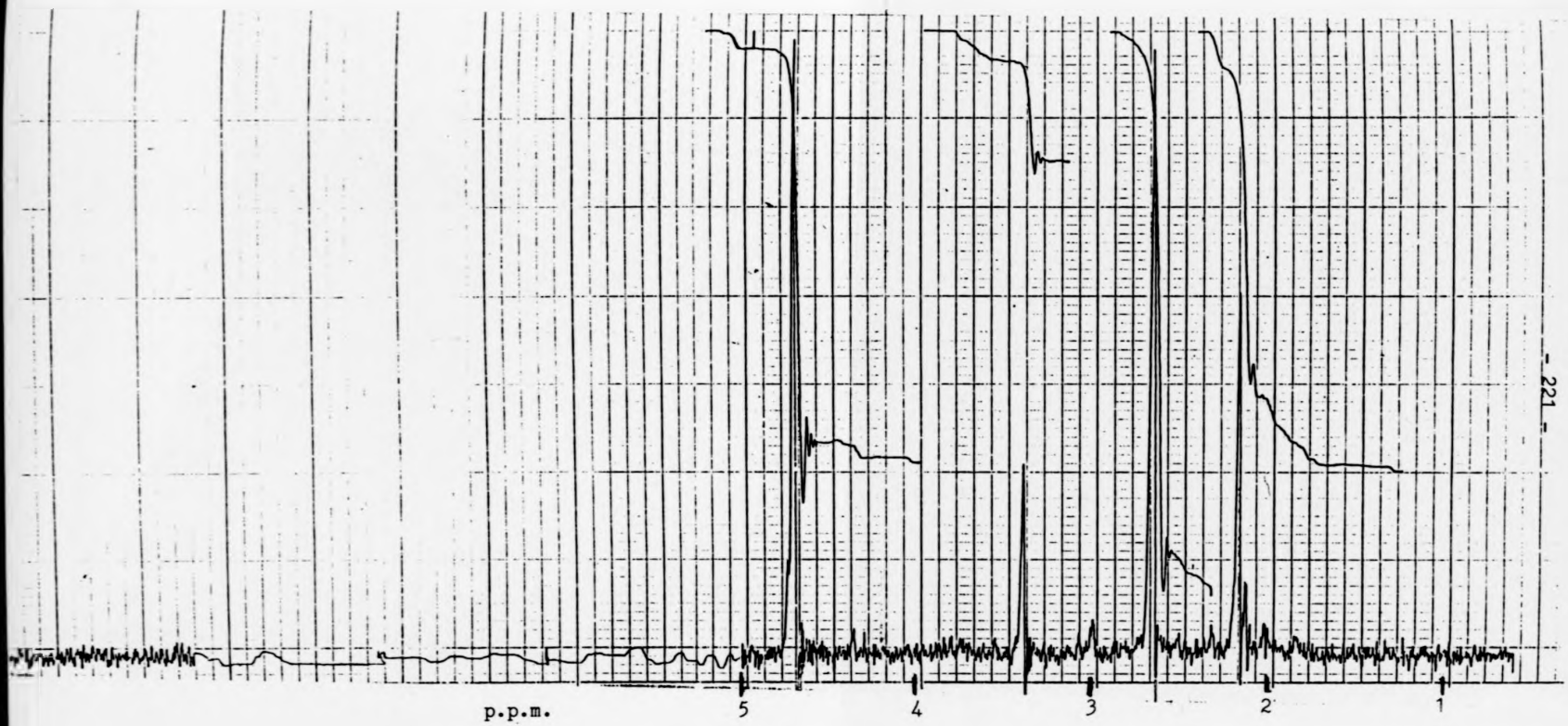

FIG. 4.15 60 MHz ^{1}H n.m.r. spectrum of $[Rh_2(O_2CMe)_2(NCMe)_4(NO_2)(MeOH)][BF_4]$ in D_2O

the $Rh_2(O_2CCH_3)_4$ framework.[11]

$[Rh_2(O_2CMe)_2(NCMe)_4(NO_2)(MeOH)][BF_4]$ shows NO_2 co-ordination in the solid state and the UV/visible spectrum in D_2O indicates a change from that of the parent compound. The ^1H n.m.r. spectrum indicates only one type of MeCN molecule is present and, thus, favours axial ligation of the nitrite group. The UV/visible spectrum and the ^1H n.m.r. spectrum indicate that axial rather than equatorial substitution has occurred, and the i.r. spectrum supports attachment through the N atom of NO_2^-, to give the complex shown above.

4.6 Preparation of $[Rh_2(O_2CMe)_2(NCMe)_4(4\text{-picoline-N-oxide})_2][BF_4]_2$

$[Rh_2(O_2CMe)_2(NCMe)_6][BF_4]_2$ (0.27 g, 0.36 mmol) (prepared as described in Chapter 2) was dissolved in methanol (30 cm^3). To this solution, 4-picoline-N-oxide (0.08 g, 0.72 mmol) was added and the reaction mixture was stirred overnight, after which time a colour change from deep blue to purple was observed. The volume of solution was reduced to ca. 15 cm^3 and diethyl ether (15 cm^3) was added to precipitate a deep purple powder. This powder was collected by filtration, washed with diethyl ether (2 x 10 cm^3) and dried in vacuo for ca. 5 hours. (Yield = 0.19 g, 60%)

Analyses	C	H	F	N	Rh
Calc. for $C_{24}H_{32}B_2F_8N_6O_6Rh_2$	32.7	3.8	17.3	9.5	23.4 %
Found	33.0	3.8	17.3	9.1	23.7 %

4.6.1 Spectroscopic Studies

4.6.1(i) UV/visible spectrum

The UV/visible spectrum of $[Rh_2(O_2CMe)_2(NCMe)_4(4\text{-picoline-N-oxide})_2][BF_4]_2$ in methanol is shown in Fig.4.16 and the important features are summarised in Table 4.5.

Table 4.5 UV/visible spectrum of $[Rh_2(O_2CMe)_2(NCMe)_4(4\text{-picoline-N-oxide})_2][BF_4]_2$ in methanol

λ_{max} (nm)	$\varepsilon(mol^{-1}cm^{-1}dm^3)$
560	284
370(sh)	600
315(sh)	4300
266	19642
215	15808

The lowest energy band at 560 nm is assigned as in the $Rh_2(O_2CR)_4$ complexes, to the Rh-Rh $\pi^* \rightarrow$ Rh-Rh σ^*,[18] the Rh-Rh $\pi^* \rightarrow$ Rh-O σ^* or the Rh-Rh $\delta^* \rightarrow$ Rh-O σ^* transition.[19] This absorption has shifted from the position (520 nm) in $[Rh_2(O_2CMe)_2(NCMe)_6][BF_4]_2$, the shift is similar to that observed in moving from $[Rh_2(butyrate)_4(NCMe)_2]$ in CH_2Cl_2 (lowest energy band 556 nm) to $[Rh_2(butyrate)_4(4\text{-picoline-N-oxide})_2]$ in CH_2Cl_2 (596 nm).[29] Drago, Long, and Cosmano have stated that dirhodium(II) dimers function as a Lewis acid, by accepting electron density from Lewis bases in the antibonding orbital Rh-Rh σ^* molecular orbital. A purely σ-bonding base, as 4-picoline-N-oxide, may raise the energy of the Rh-Rh σ^* molecular orbital, while a σ- and π-bonding base, such as MeCN, may raise the energy of the σ^* whilst lowering that of the Rh-Rh π^* orbital. Whatever the assignment of the lowest energy band,

FIG. 4.16 UV/visible spectrum of $[Rh_2(O_2CMe)_2(NCMe)_4(4\text{-picoline-N-oxide})_2][BF_4]_2$ in methanol

either Rh-Rh π^* → Rh-Rh σ^* or Rh-Rh π^* → Rh-O σ^*, the shift to lower energy of the band in going from $[Rh_2(O_2CMe)_2(NCMe)_6][BF_4]_2$ to $[Rh_2(O_2CMe)_2(NCMe)_4(4\text{-picoline-N-oxide})_2][BF_4]_2$ can be explained in terms of these σ- and π-bonding considerations.

4.6.1(ii) Infrared spectrum

The infrared spectrum of $[Rh_2(O_2CMe)_2(NCMe)_4(4\text{-picoline-N-oxide})_2][BF_4]_2$ as a nujol mull is shown in Fig.4.17 and assignments are given in Table 4.6. The band of major interest is that at 1208 cm^{-1} due to the N-O stretch of 4-picoline-N-oxide which occurs at around 1220 cm^{-1} in the free ligand. This lowering of the N-O stretching frequency is generally observed on co-ordination to transition metals.[30]

4.6.1(iii) N.m.r. spectroscopic studies

The ^1H n.m.r. spectrum of $[Rh_2(O_2CMe)_2(NCMe)_4(4\text{-picoline-N-oxide})_2][BF_4]_2$ in d_4-methanol at 220 MHz is shown in Fig.4.18. Apart from resonances due to incompletely deuterated solvent, resonances were observed at 2.04, 2.45, 2.64, 7.47 (doublet) and 8.33 (doublet) p.p.m. that integrated in a 7:7:14:5:5 ratio, respectively, in good agreement with the molecular formula. The resonances at 2.04 and 2.64 p.p.m. are assigned to the methyl protons of the acetate and equatorial MeCN groups respectively. The resonance at 2.45 p.p.m. is assigned to the 4-methyl protons on the pyridine ring, the resonance at 7.47 p.p.m. to the 3-H protons (split by coupling to the 2-H protons) and the resonance at 8.33 p.p.m. to the 2-H protons (coupled to the 3-H protons) on the pyridine ring. The ^1H n.m.r. spectrum of 4-picoline-N-oxide in d_4-methanol run at 220 MHz (Fig.4.19) contains resonances at 2.42, 7.43 (doublet) and 8.25 (doublet) p.p.m. Therefore, on co-ordination to the dirhodium(II) centre the resonances of the methyl, 3-H, and 2-H

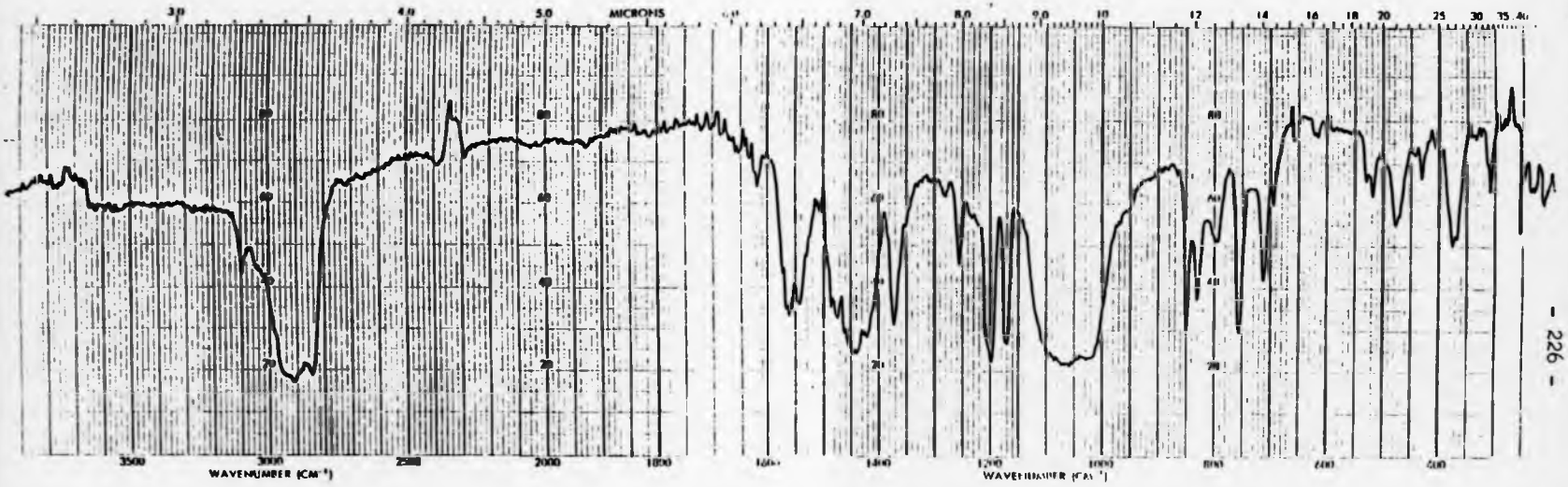

FIG. 4:17 Infrared spectrum of $[Rh_2(O_2CMe)_2(NCMe)_4(4\text{-picoline-N-oxide})_2][BF_4]_2$ as a nujol mull.

Table 4.6

Infrared spectra of $[Rh_2(O_2CMe)_2(NCMe)_4(4\text{-picoline-N-oxide})_2][BF_4]_2$

Observed vibrations (cm^{-1})	Assignment[21,30]
3120	
2305	ν(CN) MeCN
2325	
1660	
1570	ν_{asym}(OCO) acetate
1550	
1485	
1460	
1450	ν_{sym}(OCO) acetate
1430	
1380	
1265	
1208	ν(NO) picoline-N-oxide
1185	
1070	ν(BF)
860	
840	
805	
765	δ(C-H) picoline-N-oxide
722	
705	δ(C-H) picoline-N-oxide
540	δ(BF)
530	
490	
385	
375	δ(BF) BF_4 and ν(Rh-O)
320	

FIG. 4.18 220 MHz ^{1}H n.m.r. spectrum of $[Rh_2(O_2CMe)_2(NCMe)_4(4\text{-picoline-N-oxide})_2][BF_4]_2$ in d_4-methanol

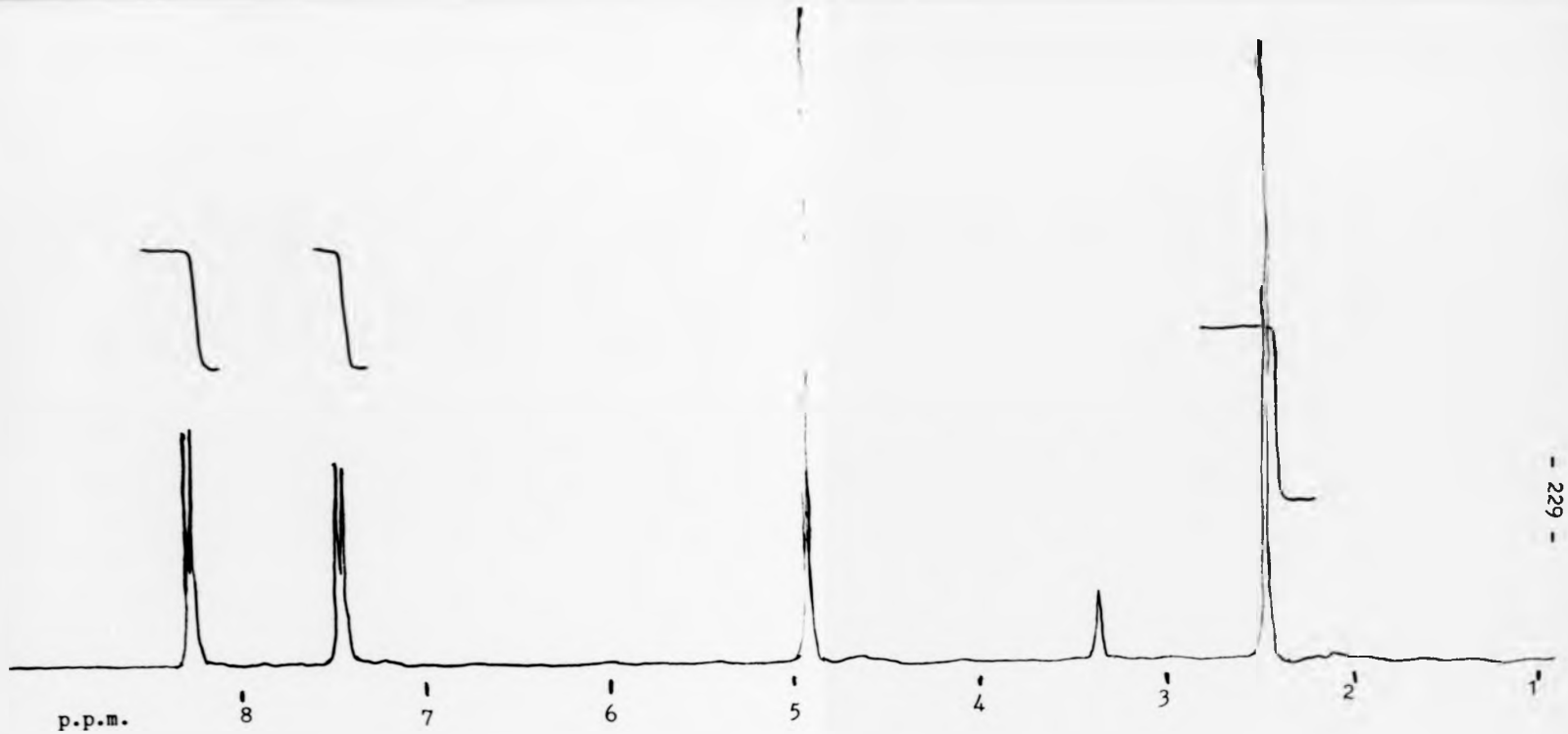

FIG. 4.19 220 MHz ^{1}H n.m.r. spectrum of 4-picoline-N-oxide in d_4-methanol.

protons shift by +0.03, +0.04, and +0.08 p.p.m., respectively.

The ^1H n.m.r. data indicate that as for the bis-pyridine adduct, the axial co-ordination of the 4-picoline-N-oxide molecules is retained in methanol.

4.7 Reaction of $[Rh_2(O_2CMe)_2(NCMe)_6][BF_4]_2$ with $Na[S_2CNEt_2]$

$[Rh_2(O_2CMe)_2(NCMe)_6][BF_4]_2$ (as prepared in Chapter 2) (0.38 g, 0.5 mmol) was dissolved in acetonitrile (20 cm^3) and to the dark purple solution, $Na[S_2CNEt_2]$ (0.46 g, 2 mmol) was added. The resultant solution was stirred for ca. 1 hour, after which the solution became dark brown in colour. The solvent was removed in vacuo to produce a yellow-brown oily solid. Washing with methanol (ca. 10 cm^3) produced a yellow powder which was recrystallised from acetonitrile.
(Yield = ca. 0.11 g, 40%)

Analyses	C	H	N	Rh	S
Calc. for $C_{15}H_{30}N_3RhS_6$	32.9	5.5	7.7	18.8	35.1 %
Found	32.9	5.6	7.8	18.8	35.2 %

4.7.1 Spectroscopic Studies

4.7.1(i) UV/visible spectrum

The UV/visible spectrum in acetonitrile (Fig.4.20) is totally free of bands assignable to a Rh-Rh dimer. It contains a shoulder at ca. 436 nm and two peaks at 314 and 247 nm.

4.7.1(ii) Infrared spectrum

The infrared spectrum of the product mulled in nujol is shown in Fig.4.21 and the infrared spectrum of NaS_2CNEt_2 mulled in nujol is

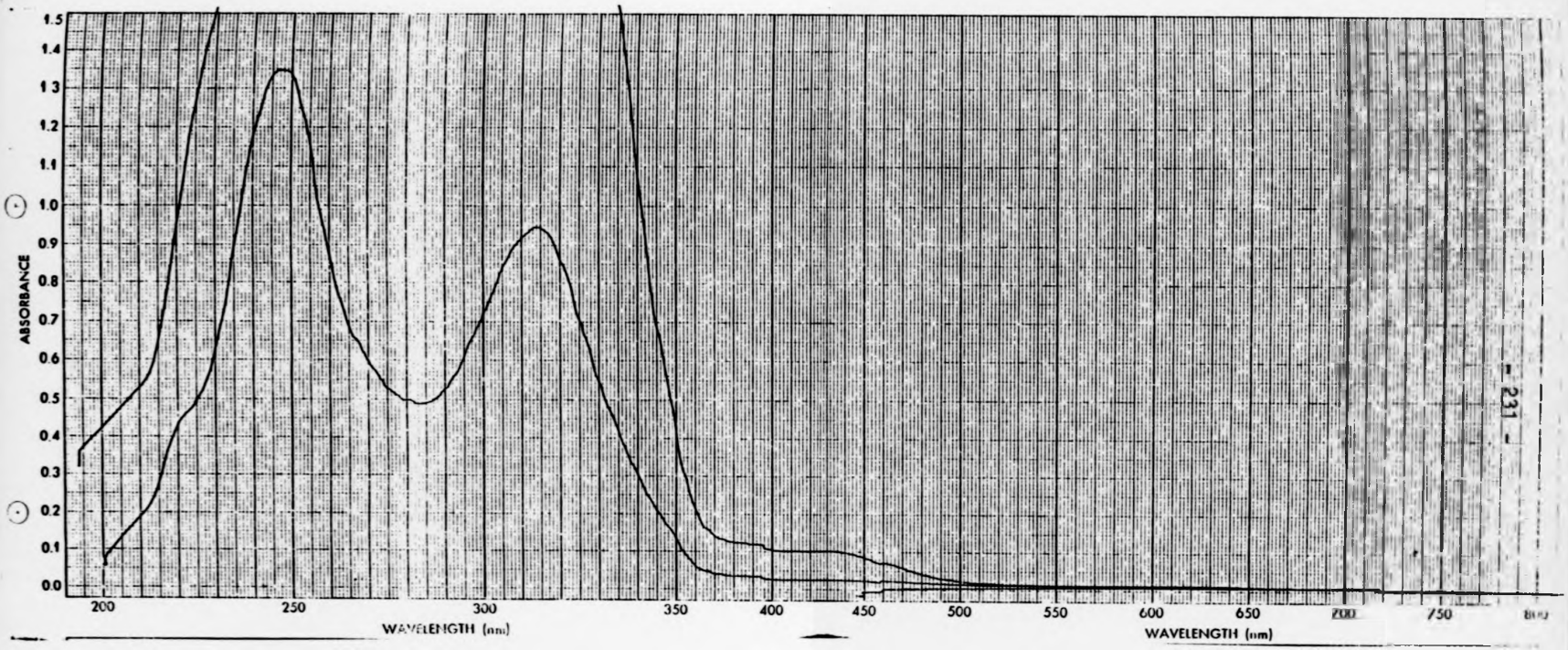

FIG. 4.20 UV/visible spectrum of $Rh(S_2CNEt_2)_3$ in MeCN

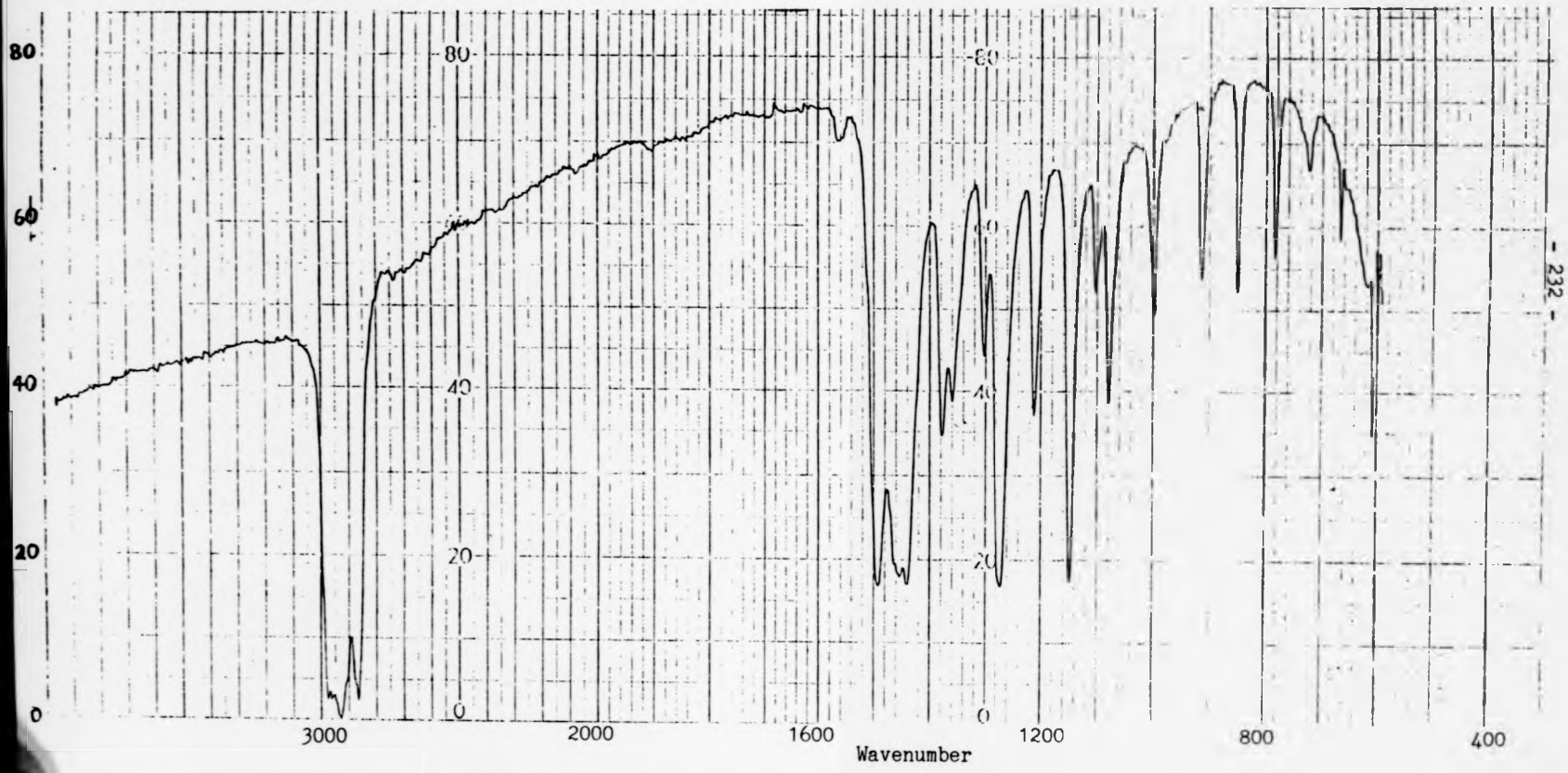

FIG. 4.21 Infrared spectrum of $Rh(S_2CNEt_2)_3$

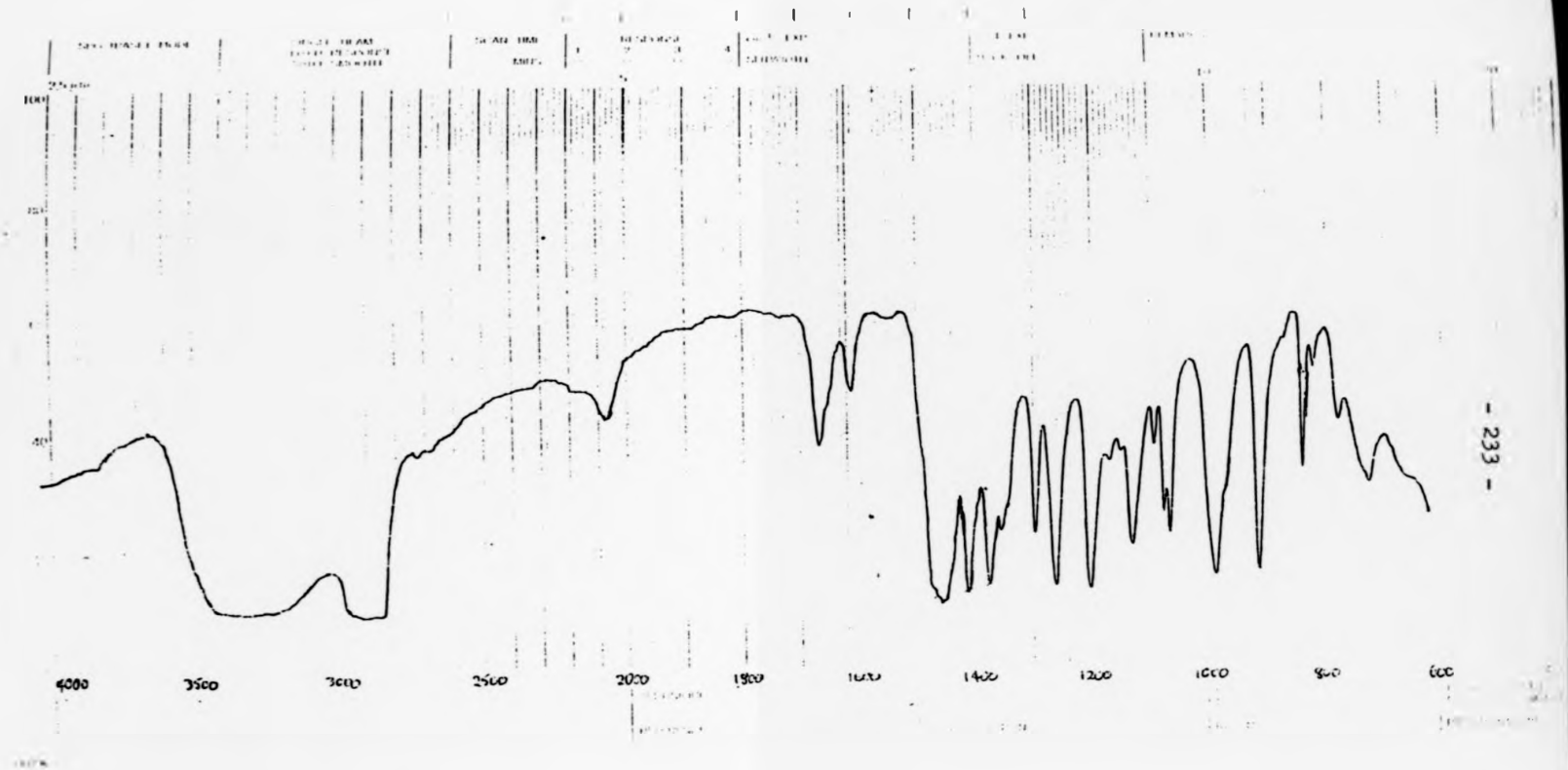

FIG. 4.22 Infrared spectrum of NaS_2CNEt_2 as a nujol mull.

shown in Fig.4.22 for comparison. From these spectra, it appears that the only ligand is dithiocarbamate present in the complex and that it bonds via a bidentate attachment to the rhodium. This is indicated by the fact that compounds with bidentate co-ordination exhibit ν(CS) near 1000 cm^{-1} as a single band whereas those with monodentate co-ordination show a doublet in the same region.[21]

4.7.1(iii) N.m.r. spectroscopic studies

The ^1H n.m.r. of $[Rh(S_2CNEt_2)_3]$ in CD_2Cl_2 at 300 MHz (Fig.4.23) shows a triplet at 1.18 p.p.m. and a multiplet at 3.63 p.p.m. On irradiating at the triplet position, the multiplet collapses to a quartet. The integration ratio of multiplet to triplet is 2:3. This spectrum is identical to that observed for $[Rh(S_2CNEt_2)_3]$.[31]

4.7.1(iv) Mass spectrum

The mass spectrum shows peaks at 546 m/e $[Rh(S_2CNEt_2)_3]^+$ and 398 m/e $[Rh(S_2CNEt_2)_2]^+$. Therefore, the product of the reaction of $[Rh_2(O_2CMe)_2(NCMe)_6][BF_4]_2$ and NaS_2CNEt_2 is the rhodium(III) monomer $[Rh(S_2CNEt_2)_3]$.

4.8 Preparation of $K_2[Fe(CO)_4]$

The procedure given in reference 32 was followed. $K(s\text{-}C_4H_9)_3BH$ (17.5 cm^3, 17.5 mmol) and thf (32.5 cm^3) were placed in a round-bottom flask and $Fe(CO)_5$ (1.1 cm^3, 8.25 mmol) added. The mixture was stirred and refluxed for ca. 4 hours, during which time a cream coloured precipitate had formed. The precipitate was collected by filtration, washed with hexane (3 x 25 cm^3), and dried in vacuo for ca. 4 hours. (Yield = ca. 1.8 g, 88%)

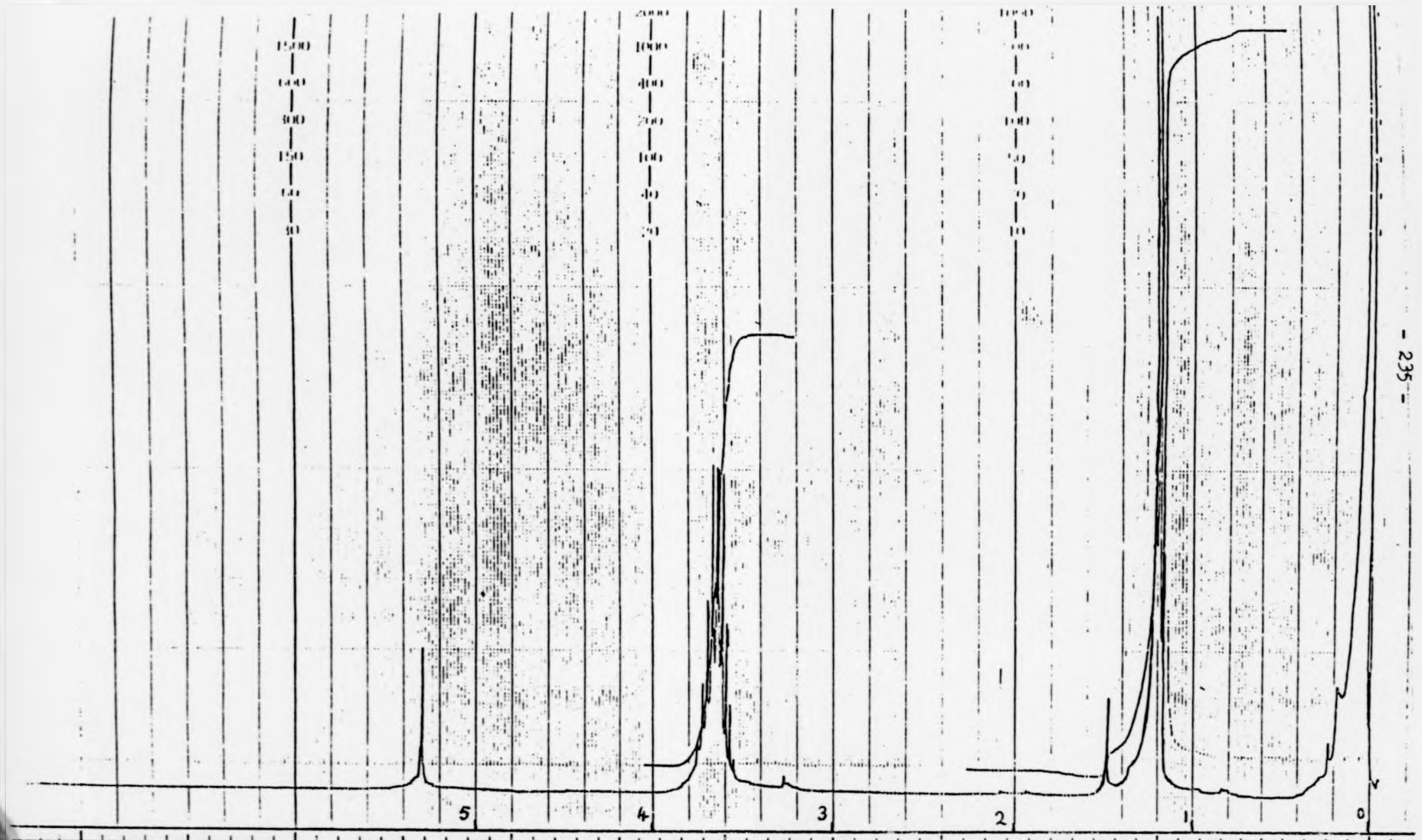

FIG. 4.23 300 MHz ^{1}H n.m.r. spectrum of $Rh(S_2CNEt_2)_3$ in CD_2Cl_2

The pale pink solid is extremely air sensitive, even more so in solution, turning to a deep red colour on exposure to the atmosphere. Also, $K_2[Fe(CO)_4]$ decomposes in protic solvents.

Analyses	C	Fe
Calc. for $C_4FeK_2O_4$	19.5	22.7
Found	19.6	23.1

4.8.1 Infrared spectrum

The infrared spectrum of $K_2Fe(CO)_4$ as a solution was recorded and shows a band at 1788 cm^{-1} in agreement with that observed in the literature.[33]

4.9 Reaction between $[Rh_2(O_2CMe)_2(NCMe)_6][BF_4]_2$ and $K_2[Fe(CO)_4]$

$[Rh_2(O_2CMe)_2(NCMe)_6][BF_4]_2$ (0.3 g, 0.4 mmol) was dissolved in thf (30 cm^3) and $K_2[Fe(CO)_4]$ (0.1 g, 0.4 mmol) added. The reaction mixture immediately became darker in colour. The mixture was stirred overnight, after which a grey/purple solid had formed under a brown solution. The grey/purple solid was shown by UV/visible spectroscopy to be $[Rh_2(O_2CMe)_2(NCMe)_6][BF_4]_2$.

The brown thf solution was filtered and the filtrate was evaporated to dryness to produce a brown oil. This oil was dissolved in CH_2Cl_2, filtered, and chromatographed on a Florosil chromatography column. Elution with hexane, followed by dichloromethane produced no movement of any coloured bands. However, on elution with a 70%/30% CH_2Cl_2/CH_3CN solution, movement of a dark brown band occurred and this band was collected. A purple band remained on the column which could not be removed, even with very polar solvents such as methanol or acetone.

The colour of this band changed from purple in MeCN to blue in acetone. Thus, this material probably was a small amount of unchanged $[Rh_2(O_2CMe)_2(NCMe)_6][BF_4]_2$.

The brown solution from the Florosil column was evaporated to dryness, dissolved in CH_2Cl_2 (15 cm^3) and the solution filtered. Diethyl ether (10 cm^3) was added to this solution and long thin black crystals slowly formed. These were collected by filtration and dried *in vacuo* for *ca*. 6 hours. (Yield = *ca*. 0.1 g)

Analyses	C	H	Fe	Rh
Found	24.1	2.3	4.1	38.6

These analyses correspond to atomic ratios of 26:30:1:5 for C:H:Fe:Rh and would be consistent with a molecular formula of $C_{26}H_{30}FeO_{26}Rh_5$. A fluorine analysis revealed no BF_4 present and a nitrogen analysis indicated the complete loss of MeCN from the product.

4.9.1 Spectroscopic Studies

4.9.1(i) UV/visible spectrum

The UV/visible spectrum of the product dissolved in CH_2Cl_2 (Fig.4.24) shows a band at 225 nm, with shoulders at 260 and 425 nm. No bands typical of $[Rh_2]^{4+}$ systems were observed.

4.9.1(ii) Infrared spectrum

The solid infrared spectrum of the product as a nujol mull (Fig.4.25) shows bands at 2030(s), 1980(s), 1940(m), 1775(s), 1750(s), 1350(w), 1245(w), 1200(w), 1135(w), 1110(m), 1085(m), 1015(w), 800(w), 720(w), 635(w), 550(w), 520(m), 435(w), and 400 (w) cm^{-1}. The infrared spectrum

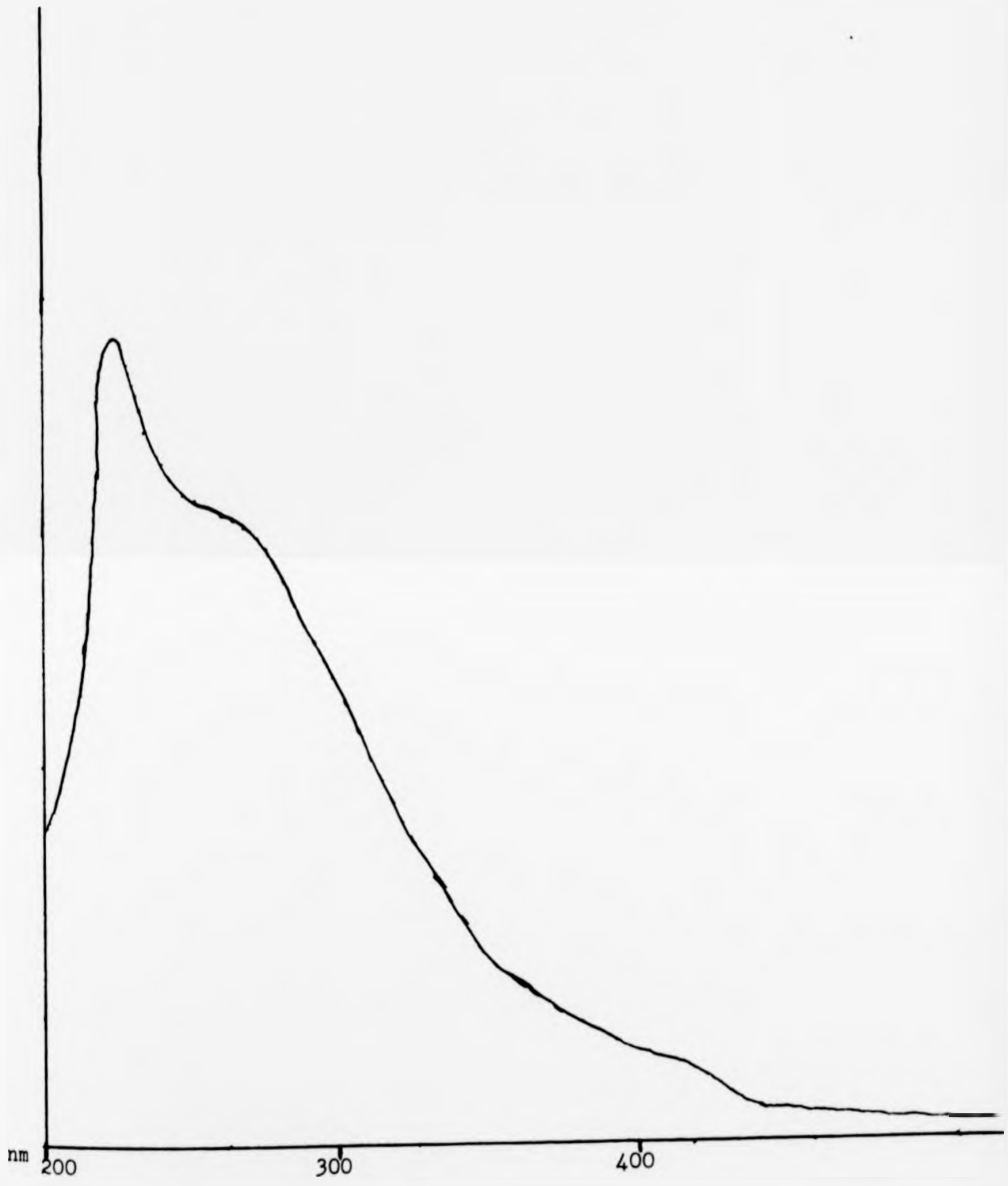

FIG. 4.24 UV/visible spectrum of product of $[Rh_2(O_2CMe)_2(NCMe)_6][BF_4]_2$ and $K_2[Fe(CO_4]$

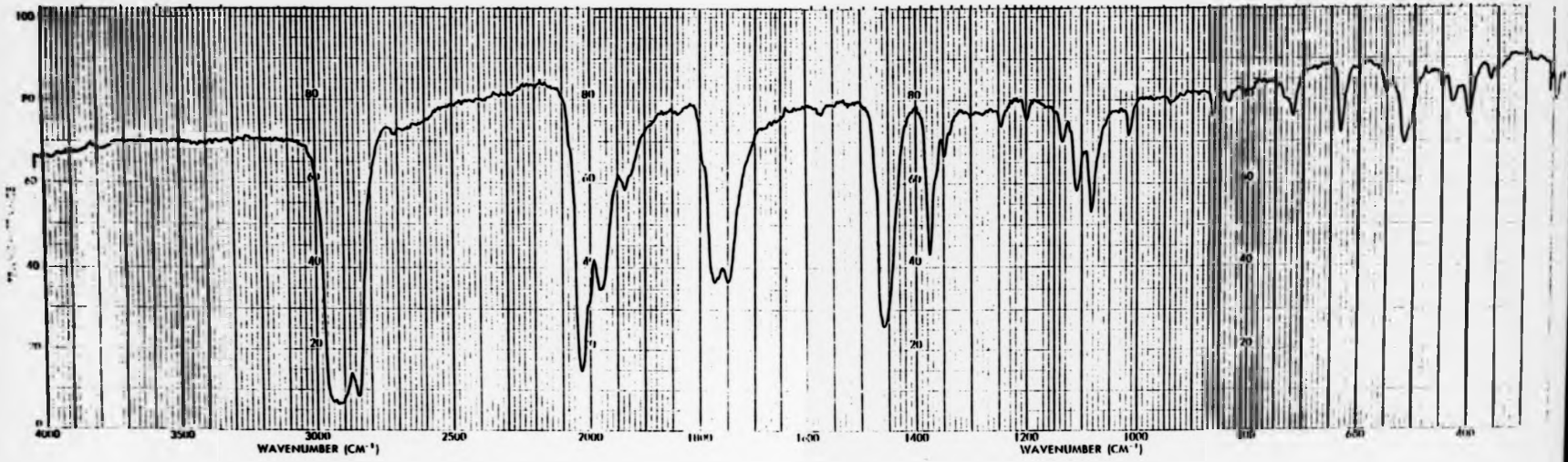

FIG. 4.25 Solid infrared spectrum of the product of $[Rh_2(O_2CMe)_2(NCMe)_6][BF_4]_2$ and $K_2[Fe(CO)_4]$ as a nujol mull.

of the product in CH_2Cl_2 solution was recorded (Fig.4.26). This showed a strong band at 2040 cm^{-1} with weaker peaks at 2005 and 1985 cm^{-1}, a broad band at 1760 cm^{-1}, and bands at 1115 and 1090 cm^{-1}.

Also, the infrared spectrum of the product in diethyl ether solution was recorded. This shows a sharp strong peak at 2035 cm^{-1}, with weaker peaks at 2010 and 1980 cm^{-1} and a somewhat broader intense band at 1790 cm^{-1}.

The sharp peaks at around 2000 cm^{-1} are attributed to CO stretching vibrations of terminal carbonyl groups. This is a shift to lower frequency from that of free CO (at 2155 cm^{-1}), an observation seen in the majority of metal carbonyl compounds.[21] The band at ca. 1760 cm^{-1} is most probably due to bridging COs between the metals, the stretching vibration of bridging carbonyls ν(CO) generally being much lower (1900-1800 cm^{-1}) than that of the terminal CO group.[21] None of these bands can be assigned to free $[Fe(CO)_4]^{2-}$ which exhibits a line in the solution infrared at 1788 cm^{-1}.[33]

The bands at ca. 1135, 1110, and 1085 cm^{-1} are possibly due to solvent absorptions. There is no evidence in the infrared spectra recorded for the presence of MeCN, BF_4 or acetate groups.

4.9.1(iii) N.m.r. spectroscopic studies

The ^1H n.m.r. spectrum of the product was recorded at 60 MHz in CD_2Cl_2 (Fig.4.27). This shows a resonance at 0.87 p.p.m. and two resonances at 3.45 and 3.65 p.p.m. These appear to be due to some aliphatic ether linkages, however, the spectrum shows that no acetate or acetonitrile is present.

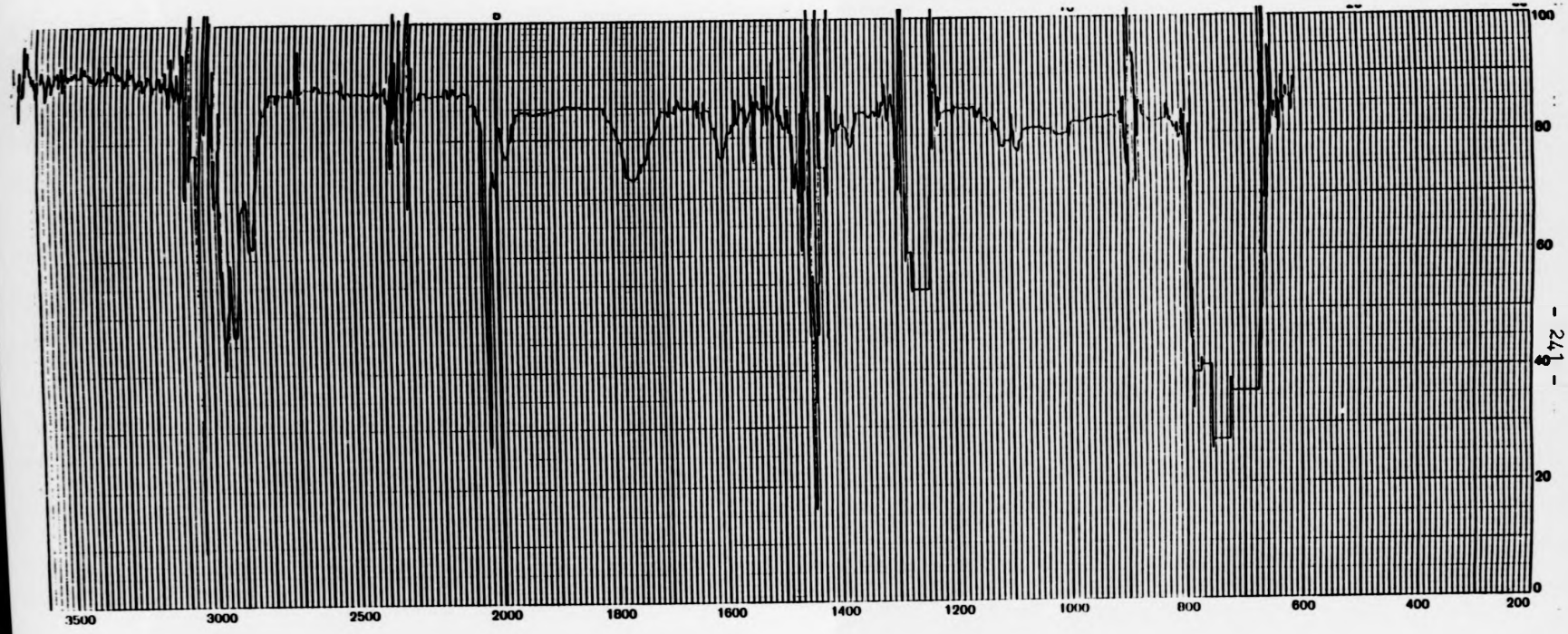

FIG. 4.26 Solution infrared spectrum of the product of $[Rh_2(O_2CMe)_2(NCMe)_6][BF_4]_2$ and $K_2[Fe(CO)_4]$ in CH_2Cl_2

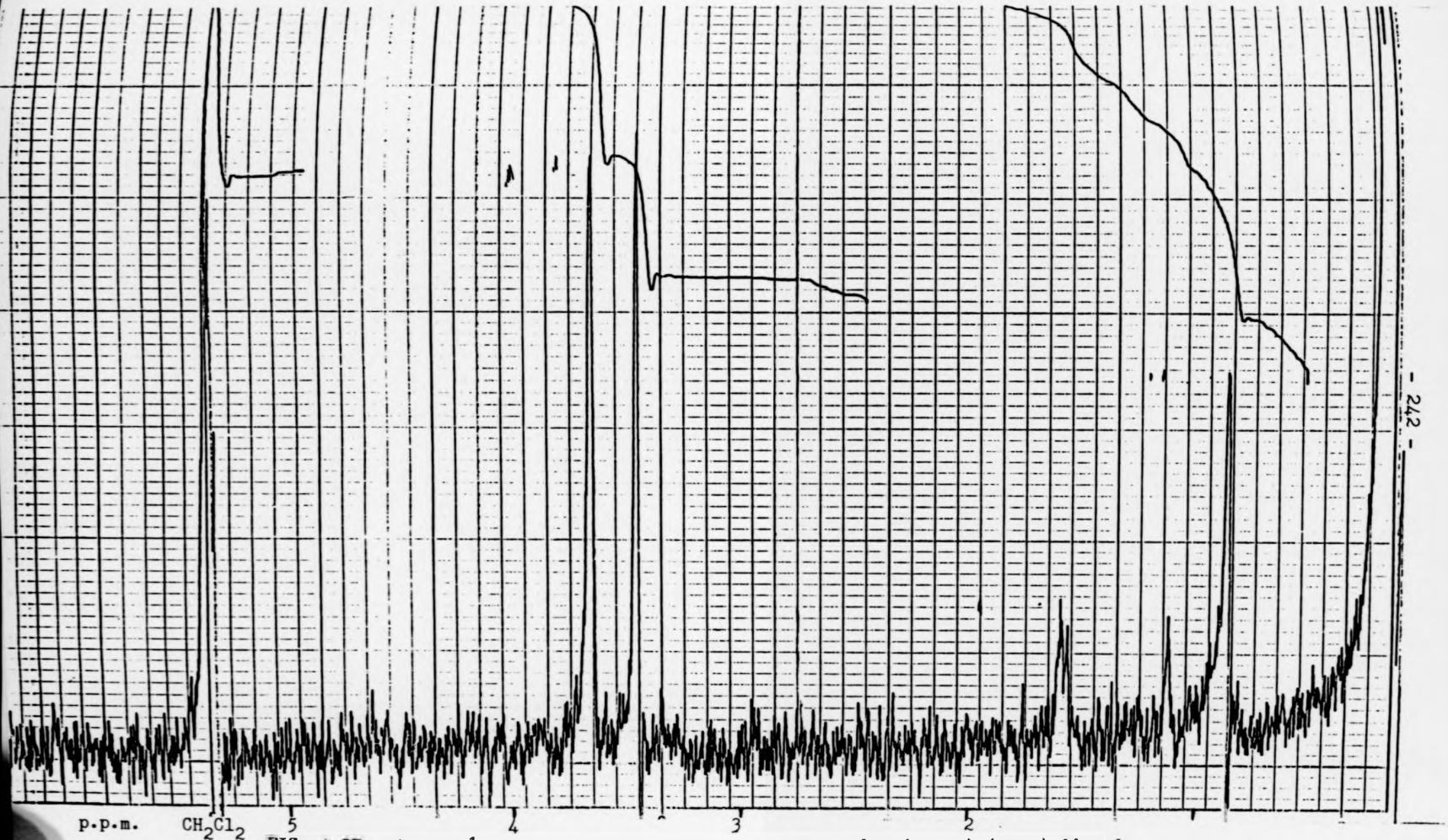

FIG. 4.27 60 MHz ^1H n.m.r. spectrum of the product of $[Rh_2(O_2CMe)_2(NCMe)_4][BF_4]_2$ and $K_2[Fe(CO)_4]$ in CD_2Cl_2

The ^{13}C n.m.r. spectrum was recorded at 75 MHz in $CDCl_3$ (Fig.4.28). This shows signals at 185.7, 184.5, 70.5, 69.0, 58.8, and 0 p.p.m. The signals at 185.7 and 184.8 p.p.m. are probably due to terminal carbonyl carbons and the splitting is probably due to Rh-C coupling; the value of the coupling constant of 71 Hz being similar to that observed in rhodium carbonyl compounds.[34] The peak at 58.8 p.p.m. is probably due to CH_2Cl_2, the solvent from which the product was obtained. The peaks at 69.0 and 70.5 p.p.m. are again in a position for aliphatic ether linkages.

Again, there is no evidence for acetate or acetonitrile groups.

Conclusions

The ratio of Fe to Rh by analysis of 1:5 is very interesting. The rhodium atoms appear to be co-ordinated to the carbonyl groups and the infrared spectrum shows evidence for bridging and terminal carbonyl groups. The other ligands of the complex appear to be organometallic in nature. However, the analytical and spectroscopic data do not lead to a molecular structure and, although crystals have been obtained, they have proved unsuitable for X-ray crystallography.

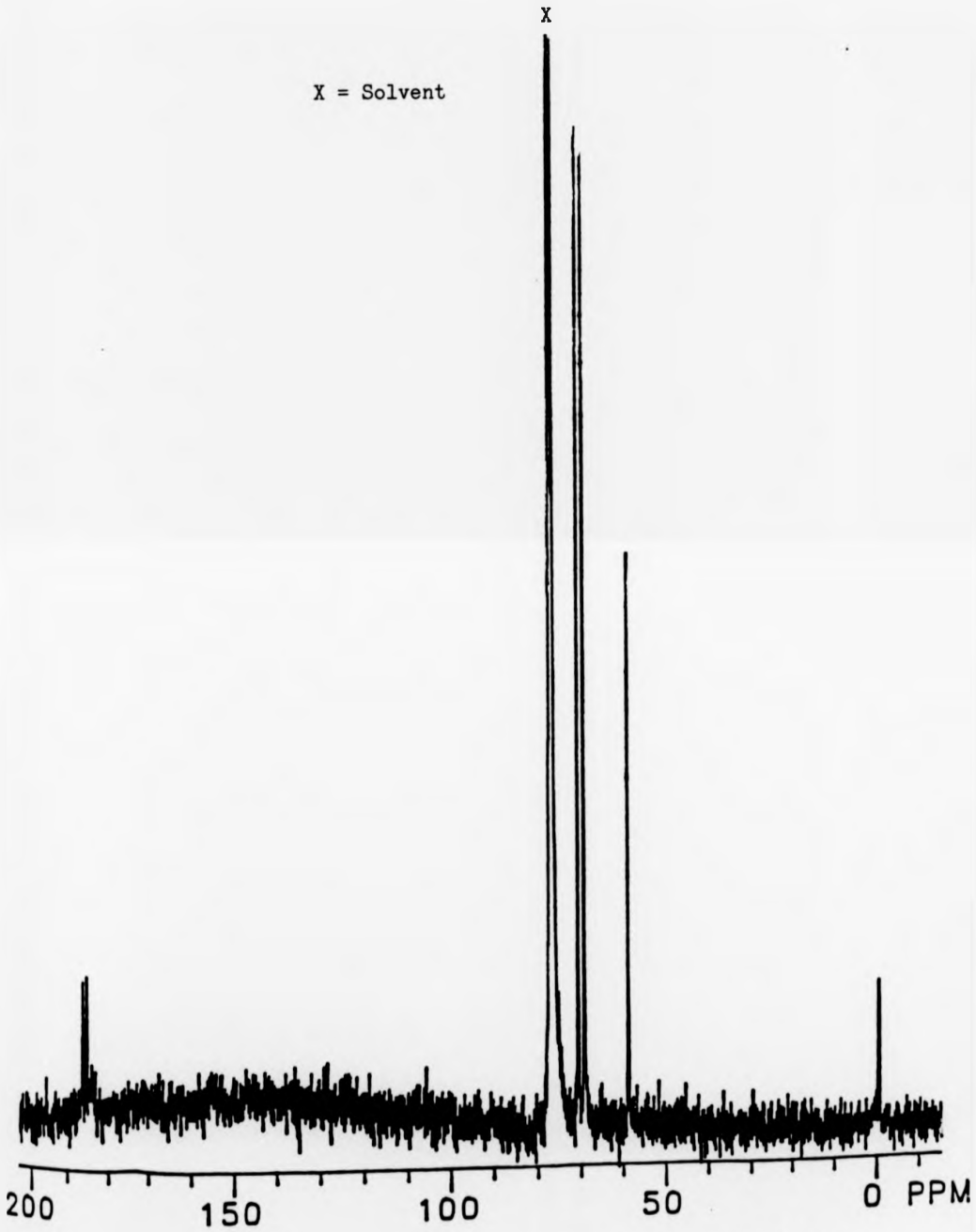

FIG. 4.28 75 MHz ^{13}C n.m.r. spectrum of product of reaction between $[Rh_2(O_2CMe)_2(NCMe)_6][BF_4]_2$ and $K_2[Fe(CO)_4]$

4.10 Reaction between $[Rh_2(O_2CMe)_2(NCMe)_6][BF_4]_2$ and $Li[PPh_2]$

$Li[PPh_2]$ (0.1 g, 0.54 mmol) was suspended in acetonitrile (40 cm^3) and $[Rh_2(O_2CMe)_2(NCMe)_6][BF_4]_2$ (0.4 g, 0.54 mmol) added slowly to the stirred suspension. A deep orange-purple solution formed which was stirred for ca. 20 hours. The volume of solution was reduced in vacuo to ca. 30 cm^3 and diethyl ether (20 cm^3) added. This precipitated a maroon-red microcrystalline solid which was collected by filtration and dried in vacuo. The material was recrystallised from acetonitrile, collected by filtration, washed with diethyl ether (2 x 10 cm^3) and dried in vacuo for ca. 3 hours. (Yield = 0.1 g)

Analyses	C	H	F	N	Rh
Found	25.2	3.3	12.8	9.5	29.9

The analyses correspond best to a composition $Rh_2(O_2CMe)_2(NCMe)_5(OH)(BF_4)$ with the calculated analyses.

Analyses	C	H	F	N	Rh
Calculated	26.6	3.5	12.0	11.0	32.5

No phosphorus is present implying that, although a reaction has occurred with $Li[PPh_2]$, the phosphide has not become ligated to the dirhodium centre.

4.10.1 Spectroscopic Studies

4.10.1(i) UV/visible spectrum

The UV/visible spectrum of the product dissolved in acetonitrile (Fig.4.29) has absorption maxima at 512, 358, 268, and 216 nm, and is very similar to that of starting material $[Rh_2(O_2CMe)_2(NCMe)_6][BF_4]_2$ (see Table 4.7). However, the UV/visible spectrum in methanol

FIG. 4.29 UV/visible spectrum of product of $[Rh_2(O_2CMe)_2(NCMe)_6][BF_4]_2$ and $LiPPh_2$ in MeCN.

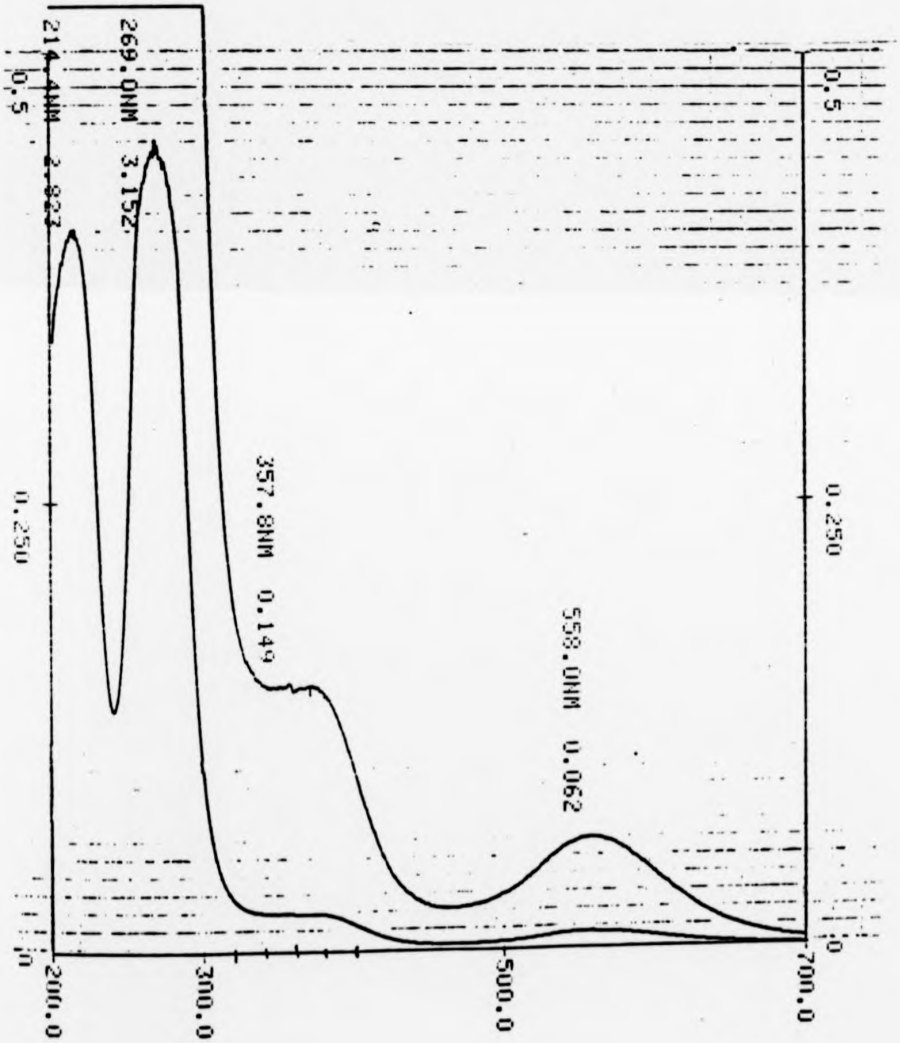

differs from that of $[Rh_2(O_2CMe)_2(NCMe)_6][BF_4]_2$ in methanol with the lowest energy absorption band occurring at 558 nm, and other absorption maxima at 370, 269, and 214 nm.

These results indicate that a dirhodium complex, very similar to the parent compound, has been prepared.

Table 4.7 UV/visible spectra of $[Rh_2(O_2CMe)_2(NCMe)_4]^{2+}$ compounds

Compound	UV/visible bands (nm)
$[Rh_2(O_2CMe)_2(NCMe)_6][BF_4]_2$	520, 355, 270, 218
$[Rh_2(O_2CMe)_2(NCMe)_4(py)_2][BF_4]_2$	470, 350, 270, 220
$[Rh_2(O_2CMe)_2(NCMe)_4$ (4-picoline-N-oxide)$_2][BF_4]_2$	560, 370, 315, 266, 215
$[Rh_2(O_2CMe)_2(NCMe)_4(MeOH)_2][BF_4]_2$	576, 374, 259, 214
Product 4.10 in MeCN	512, 358, 268, 216
Product 4.10 in MeOH	558, 370, 269, 214

4.10.1(ii) Infrared spectrum

The infrared spectrum of the product as a nujol mull (Fig.4.30) shows features at 3500 cm^{-1} (broad) which may be due to the O-H stretching vibration of some adsorbed water or of an hydroxy-group, 2310 and 2280 cm^{-1} assigned to the C≡N stretching vibration of co-ordinated acetonitrile,[21] 1630 and 1560 cm^{-1} assigned to the carboxylate asymmetric O-C-O stretching vibration, 1430 cm^{-1} (broad under the nujol peak) assigned to the symmetric carboxylate O-C-O stretching vibration and 1060 cm^{-1} assigned to the B-F stretching vibration in the $[BF_4]^-$ anion.[21]

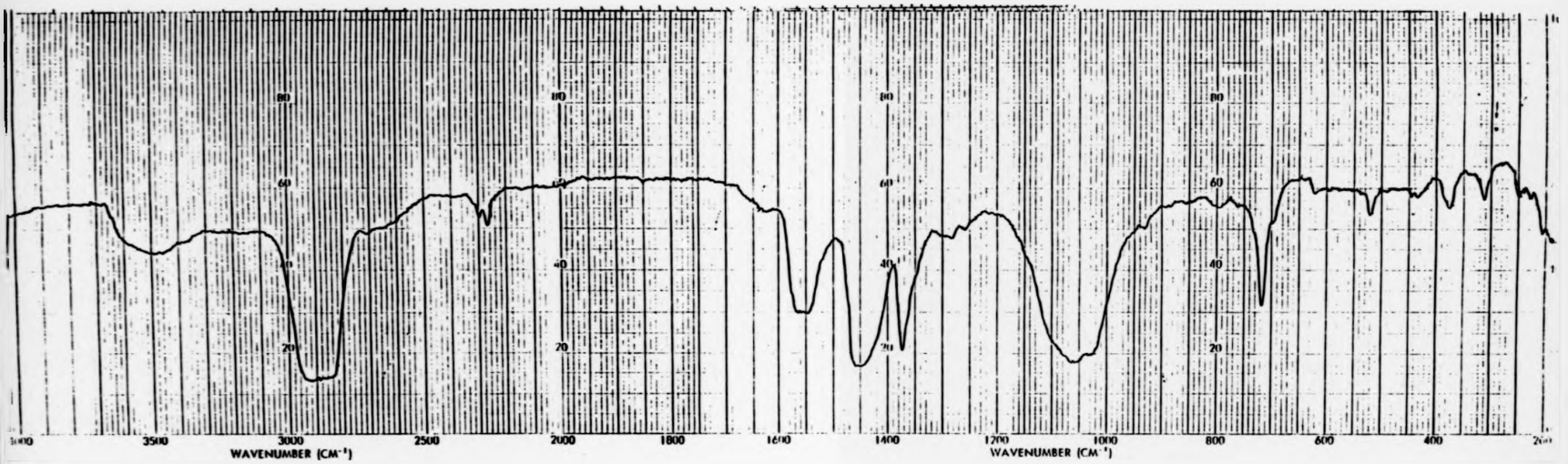

FIG. 4.30 Infrared spectrum of the product of $[Rh_2(O_2CMe)_2(NCMe)_6][BF_4]_2$ and $LiPPh_2$ as a nujol mull.

4.10.1(iii) N.m.r. spectroscopic studies

The 300 MHz ^{1}H n.m.r. spectrum of the product in d_4-methanol (Fig.4.31) shows, apart from peaks due to partially deuterated methanol and resonances due to a small amount of diethyl ether, resonances at 2.08, 2.11, and 2.67 p.p.m. These are very similar to resonances observed for $[Rh_2(O_2CMe)_2(NCMe)_6][BF_4]_2$ and are assigned as such, i.e. the resonances 2.08 and 2.67 p.p.m. are attributed to axial/free and equatorial acetonitrile groups and that at 2.11 p.p.m. to the methyl protons on the acetate groups. The integrations of equatorial to acetate to axial/free acetonitrile are ca. 2:1:1 and are the same as in the parent compound. The spectrum was scanned from +15 to -35 p.p.m., to search for any hydride or hydroxide protons that may have been present, but no other resonances were observed.

The ^{13}C n.m.r. spectrum of the product in d_4-methanol was recorded at 75 MHz (Fig.4.32) and shows resonances, apart from those of solvent, at 0, 3, 23, 128, and 193 p.p.m. That at 0 p.p.m. is assigned to the methyl carbon on free acetonitrile. Those at 193 and 23 p.p.m. are assigned to the carboxylate and methyl carbons, respectively, on the acetate group. Resonances at 128 and 3 p.p.m. are assigned to the nitrile and methyl carbons, respectively, of the equatorially co-ordinated acetonitrile. A comparison of the relative intensities for the methyl carbon of the equatorial versus the axial/free acetonitrile indicates that the peak for the nitrile carbon of the axial/free acetonitrile (which is anticipated at ca. 117 p.p.m.) would be too weak to be observed.

Summary

The complex contains only one $[BF_4]^-$ unit per dimer instead of two for the parent compound and this is the only significant difference

FIG. 4.31 300 MHz ^{1}H n.m.r. spectrum of the product of $[Rh_2(O_2CMe)_2(NCMe)_6][BF_4]_2$ and $LiPPh_2$ in d_4-MeOH.

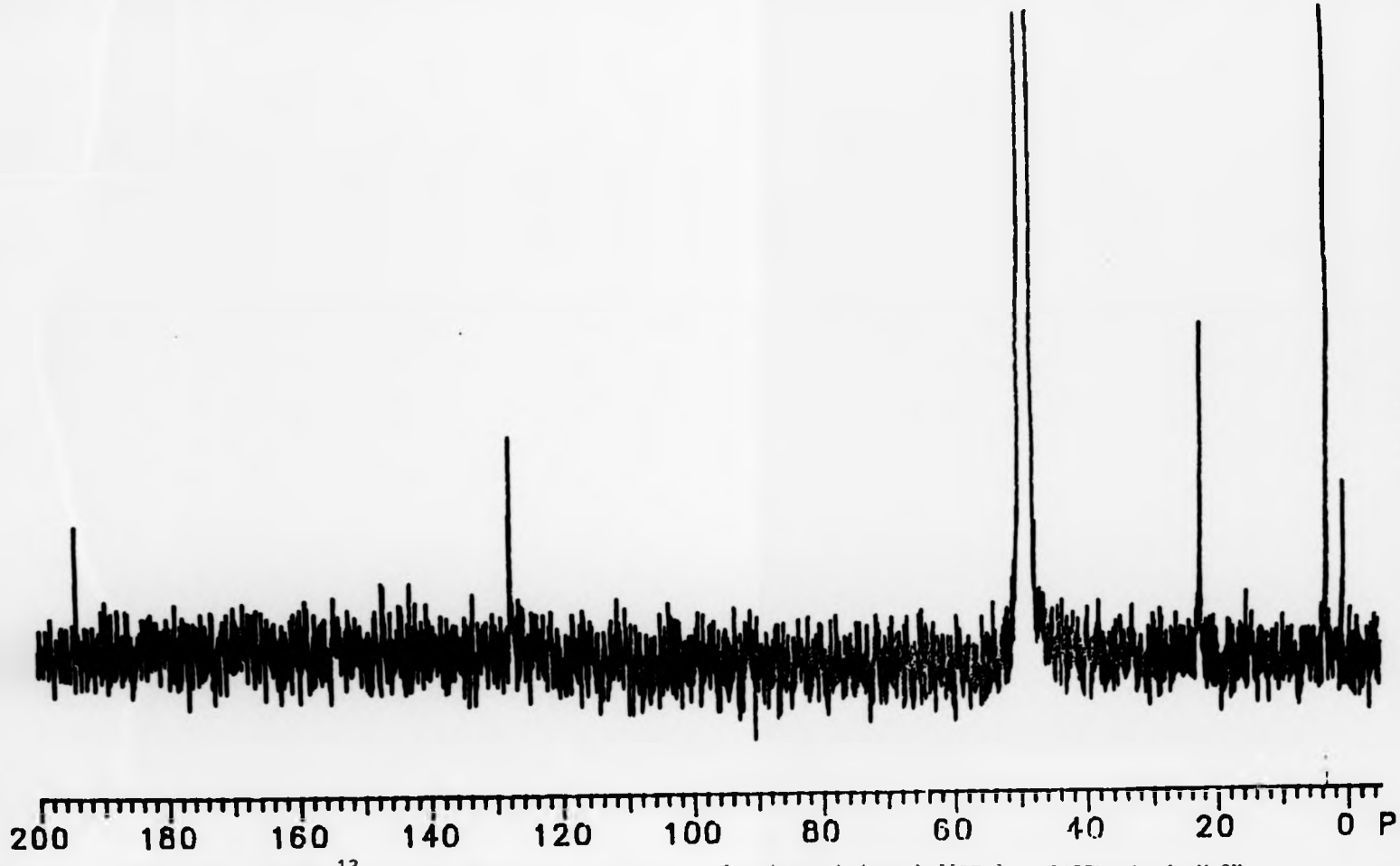

FIG. 4.32 75 MHz ^{13}C n.m.r. spectrum of product of $[Rh_2(O_2CMe)_2(NCMe)_6][BF_4]_2$ + $LiPPh_2$ in d_4-MeOH

between the two compounds. The % F is 12.8% in the product compared to 20.1% in $[Rh_2(O_2CMe)_2(NCMe)_6][BF_4]_2$ and the analyses correspond to a formula of $Rh_2(O_2CMe)_2(NCMe)_5(OH)(BF_4)$. The results could be interpreted on the basis of one of the following possibilities.

(a) The rhodium dimer has been reduced to give a mixed Rh^{II}-Rh^{I} or delocalised $Rh^{1.5}$-$Rh^{1.5}$ dimer.

(b) One $[BF_4]^-$ anion has been replaced by a free OH^- or H^- anion. Peaks due to OH^- or H^- in the n.m.r. spectrum could be too broad to be observed by ^1H n.m.r. spectroscopy. However, some evidence for the presence of OH was obtained by infrared spectroscopy. A definite conclusion would be aided by X-ray crystallography and although crystals have been so investigated, none have proved suitable. (a) is not very likely as the electronic spectrum would probably be dramatically changed on such reduction and a paramagnetic species would be produced of which there is no indication from n.m.r. spectroscopy. Also, electrochemical studies of $[Rh_2(O_2CMe)_2(NCMe)_6]^{2+}$ showed some indications of an irreversible oxidation process but no sign of any reduction process.

4.11 Summary and Conclusions

Reactions of $[Rh_2(O_2CMe)_2(NCMe)_6][BF_4]_2$ investigated in this study are shown in Fig.4.33. These illustrate the difference in lability between the equatorial and axial acetonitrile ligands. The axial acetonitriles are readily replaced by pyridine, 4-picoline-N-oxide, nitrite, and triphenylphosphine ligands. Although these products are new, such adducts of the dirhodium(II) tetracarboxylates are well known. An excess of triphenylphosphine, over the 2:1 stoichiometric ratio, produces, as well as the bis-phosphine dimer,

FIG. 4.33 Reactions of $[Rh_2(O_2CMe)_2(NCMe)_6][BF_4]_2$

a rhodium(I) monomer, indicating that triphenylphosphine can cleave the Rh-Rh bond with reduction of Rh^{II}.

Sodium dithiocarbamate also cleaves the Rh^{II}-Rh^{II} bond to produce the monomeric rhodium(III) complex $[Rh(S_2CNEt_2)_3]$. This is a further example of a sulphur donor ligand leading to a degradation of the carboxylate framework of a $Rh_2(O_2CR)_4$ compound (see Chapter 1).

The reaction with $[Fe(CO)_4]^{2-}$ appears to have produced a novel mixed-metal cluster. The reaction with diphenylphosphide did not produce a bridging phosphide dimer, rather the transfer of some anionic group (e.g. OH^-) to the Rh^{II}-Rh^{II} centre may have occurred. Therefore, investigations of the reactivity of $[Rh_2(O_2CMe)_2(NCMe)_6][BF_4]_2$ have provided examples of Rh^{II}-Rh^{II} bond retention, bond cleavage and reduction, and bond cleavage and oxidation.

REFERENCES

1. I.B. Baranovskii, M.A. Golubnichaya, L.M. Dikareva, and R.N. Shchelokov, Russ.J.Inorg.Chem., 1984, 29, 872.

2. W.R. Tikkanen, E. Binamira-Soriaga, W.C. Kaska, and P.C. Ford, Inorg.Chem., 1983, 22, 1147.

3. W.R. Tikkanen, E. Binamira-Soriaga, W.C. Kaska, and P.C. Ford, Inorg.Chem., 1984, 23, 141.

4. A.T. Baker, W.R. Tikkanen, W.C. Kaska, and P.C. Ford, Inorg. Chem., 1984, 23, 3254.

5. J. Telser and R.S. Drago, Inorg.Chem., 1984, 23, 2599.

6. G.J.-J. Chen, J.W. McDonald, D.C. Bravard, and W.E. Newton, Inorg.Chem., 1985, 24, 2327.

7. J. Kitchens and J.L. Bear, Thermochim.Acta, 1970, 1, 537.

8. R.W. Mitchell, J.D. Ruddick, and G. Wilkinson, J.Chem.Soc.A, 1971, 3224.

9. I.B. Baranovskii, M.A. Golubnichaya, G.Ya. Mazo, and R.N. Shchelokov, Russ.J.Inorg.Chem., 1977, 22, 308.

10. I.B. Baranovskii, S.S. Abdullaev, G.Ya. Mazo, and R.N. Shchelokov, Russ.J.Inorg.Chem., 1982, 27, 305.

11. T.R. Felthouse, Prog.Inorg.Chem., 1982, 29, p.73-166.

12. L.M. Dikareva, M.A. Porai-Koshits, G.G. Sadikov, I.B. Baranovskii, M.A. Golubnichaya, and R.N. Shchelokov, Russ.J.Inorg.Chem., 1978, 23, 578.

13. G.L. Geoffroy, Acc.Chem.Res., 1980, 13, 469.

14. M.H. Chisholm and I.P. Rothwell, Prog.Inorg.Chem., 1982, 29, p.13-14.

15. R.A. Jones, J.G. Lasch, N.C. Norman, B.R. Whittlesey, and T.C. Wright, J.Am.Chem.Soc., 1983, 105, 6184 (and references therein).

16. S.A. Johnson, H.R. Hunt, and H.M. Neumann, Inorg.Chem., 1963, 2, 960.

17. Y.-B. Koh and G.G. Christoph, Inorg.Chem., 1978, 17, 2590.

18. D.S. Martin, Jr., T.R. Webb, G.A. Robbins, and P.E. Fanwick, Inorg.Chem., 1979, 18, 475.

19. V.M. Miskowski, W.P. Schaefer, B. Sadeghi, B.D. Santarsiero, and H.B. Gray, Inorg.Chem., 1984, 23, 1154.

20. J.G. Norman, Jr. and H.J. Kolari, J.Am.Chem.Soc., 1978, 100, 791.

21. K. Nakamoto, "Infrared and Raman Spectra of Inorganic and Co-ordination Compounds", 3rd Edition, Wiley-Interscience. 1978.

22. D.H. Williams and I. Fleming, "Spectroscopic Methods in Organic Chemistry", 3rd Edition, McGraw Hill, 1980.

23. D.K. Lavallee, M.D. Baughman,and M.P. Phillips, J.Am.Chem.Soc., 1977, 99. 718.

24. G.C. Levy and G.L. Nelson, "Carbon-13 Nuclear Magnetic Resonance for Organic Chemists", Wiley-Interscience, 1972.

25. T. Sowa, T. Kawamura, T. Shida, and T. Yonezawa, Inorg.Chem., 1983, 22, 56.

26. L.F. Johnson and W.C. Janowski, "C-13 N.m.r. Spectra", Wiley and Sons, 1972.

27. E.B. Boyar and S.D. Robinson, Inorg.Chim.Acta, 1982, 64, L193.

28. E.B. Boyar and S.D. Robinson, J.Chem.Soc., Dalton Trans., 1985, 629.

29. R.S. Drago, J.R. Long, and R. Cosmano, Inorg.Chem., 1981, 20, 2920.

30. R.G. Garvey, J.H. Nelson, and R.O. Ragsdale, Co-ord.Chem.Rev., 1968, 3, 375.

31. M.M. Dhingra, G. Govil, and C.R. Kanekar, Chem.Phys.Letts., 1971, 12, 303.

32. J.A. Gladysz and W. Tam, J.Org.Chem., 1978, 43, 2279.

33. W.F. Edgell, J. Huff, J. Thomas, H. Lehman, C. Angell, and G. Asato, J.Am.Chem.Soc., 1960, 82, 1254.

34. V.G. Albano, P. Chini, S. Martinego, D.J.A. McCaffrey, and D. Strumolo, J.Am.Chem.Soc., 1974, 96, 8106.

CHAPTER 5

PREPARATION, CHARACTERIZATION, AND REACTIVITY AND CATALYTIC STUDIES OF THE $[Rh(PPh_3)_3(NCMe)][BF_4]$ MONOMER

5.1 Introduction

This chapter is concerned with further studies of the reaction of phosphines with the rhodium dimer $[Rh_2(O_2CMe)_2(NCMe)_6][BF_4]_2$, specifically the detailed characterisation of one product of the reaction between PPh_3 and $[Rh_2(O_2CMe)_2(NCMe)_6][BF_4]_2$ in a 4:1 stoichiometric ratio. This product $[Rh(PPh_3)_3(NCMe)][BF_4]$ is of interest not only because its mononuclear nature indicated that the preparation involved cleavage of a Rh-Rh bond but also because of the compound's similarity to the hydrogenation catalyst precursor $[Rh(PPh_3)_3Cl]$.[1-3] Furthermore a material previously reported[4] as $Rh(PPh_3)_3BF_4$ had been obtained directly from the dimeric rhodium system $[Rh_2(O_2CMe)_4]$, however, this material had not been fully characterised.

5.2 Preparation of tris(triphenylphosphine)acetonitrilerhodium (1) tetrafluoroborate, $[Rh(PPh_3)_3(NCMe)][BF_4]$

Triphenylphosphine (1.04 g, 3.96 mmol) was added to a stirred solution of $[Rh_2(O_2CMe)_2(NCMe)_6][BF_4]_2$ (prepared as described in Chapter 2) (0.49 g, 0.66 mmol) in methanol (40 cm^3). After *ca.* 2 hours, the orange solution was filtered to remove the precipitated $[Rh_2(O_2CMe)_2(NCMe)_4(PPh_3)_2][BF_4]_2$ (analytically and spectroscopically identical to that synthesised in Chapter 4). The resultant yellow filtrate was reduced in volume until a pale yellow powder precipitated. Diethyl ether (30 cm^3) was added to achieve further precipitation and the powder was collected by filtration and dried *in vacuo*. This powder was recrystallised by cooling a warm methanol solution to *ca.* 20°C. Small, yellow block-like crystals, suitable for X-ray crystallographic study, were obtained on controlled addition of diethyl ether to a concentrated solution of the material in methanol. (Yield 0.39 g, *ca.* 30%)

Analyses	C	H	N	P	Rh
Calc. for $C_{56}H_{48}BF_4NP_3Rh$	66.1	4.8	1.4	9.1	10.1 %
Found	64.6	4.6	1.3	8.9	10.3 %

Subsequently a more rational synthesis of this compound was developed from $[Rh(PPh_3)_3Cl]$.

$[Rh(PPh_3)_3Cl]$ was prepared according to the procedure described in Inorganic Syntheses.[5]

Analyses	C	H	Cl	P	Rh
Calc. for $C_{54}H_{45}ClP_3Rh$	70.1	4.9	3.8	10.0	11.1 %
Found	68.9	5.0	4.7	10.0	12.0 %

$[Rh(PPh_3)_3Cl]$ (0.4 g, 0.43 mmol) and $[Me_3O][BF_4]$ (0.19 g, 1.29 mmol) were stirred in acetonitrile (20 cm^3) for ca. 24 hours, after which time an orange solution had formed above a pale yellow precipitate. The precipitate was removed by filtration, the filtrate concentrated to ca. 10 cm^3, cooled and allowed to stand at ca. 5°C, resulting in the formation of an orange-yellow precipitate. This was collected by filtration, recrystallised from methanol and pale yellow crystals obtained. These were filtered, washed with ether and dried in vacuo. (Yield 0.22 g, 50%)

Analyses	C	H	N	P	Rh
Calc. for $C_{56}H_{48}BF_4NP_3Rh$	66.1	4.8	1.4	9.1	10.1 %
Found	65.6	4.7	1.7	8.8	10.0 %

5.3 Crystal structure determination

This study was accomplished by Dr. W. Clegg of the Institut für Anorganische Chemie der Universität, Tammannstrasse 4, Göttingen, West Germany. A yellow block crystal of dimensions 0.2 x 0.4 x 0.45 mm^3

sealed in a capillary tube was examined. The space group is Pbca with parameters a = 25.354(3), b = 21.439(1), c = 18.842(2) Å, V = 10242 Å^3 (from 2θ values of 36 reflections centred at ±ω), Z = 8, D_c = 1.320 g cm^{-3} (all atoms in general positions). M = 1017.6, T = 291K. MoK_α radiation, λ = 0.71069 Å.

The data were collected on a Stoe-Siemens AED diffractometer using a /θ scan mode with on-line profile-fitting[6] with $2\theta_{max}$ = 50° and all indices > 0. No absorption or extinction corrections were applied and an intensity decay of < 10% observed from 3 standard reflections was applied to 8994 non-extinguished reflections; 4552 of these having $I > 3\sigma(I)$ were used to solve the structure.

The structure was solved using Patterson and difference syntheses and refined using scattering factors from ref.7 by a blocked-cascade least-squares refinement on F, with a weighting $w^{-1} = \sigma^2(F) + 0.0026F^2$. The phenyl groups were treated as rigid idealised hexagons with C-C = 1.395 Å, C-H = 0.96 Å on C-C-C external bisectors and anisotropic thermal parameters were included for Rh, P, C, N, and U_{iso} (H) = 1.2U_{eq}(C); $[BF_4]^-$ was treated as a rigid, tetrahedral unit with B-F = 1.30 Å and common U_{iso} [refined to 0.309(5) Å^2]; no H atoms were included for MeCN. The refinement converged at R = 0.078, $R_w = \Sigma w^{\frac{1}{2}}|\Delta|/\Sigma w^{\frac{1}{2}}|F_o|$ = 0.084 (observed reflections only).

Atomic co-ordinates are given in Table 5.1 and selected geometrical parameters in Table 5.2.

5.3.1 Description of the structure of $[Rh(PPh_3)_3(NCMe)][BF_4]$

$[Rh(PPh_3)_3(NCMe)][BF_4]$ crystallises as discrete $[Rh(PPh_3)_3(NCMe)]^+$ and $[BF_4]^-$ ions. The anion is probably disordered, as is commonly

Table 5.1 Atomic coordinates ($\times 10^4$) for $[Rh(Ph_3P)_3(NCMe)][BF_4]$

	x	y	z
Rh	1336(1)	6200(1)	7265(1)
P(1)	1720(1)	7176(1)	7209(2)
C(112)	933(3)	8111(3)	7305(3)
C(113)	630	8554	7663
C(114)	721	8672	8381
C(115)	1116	8347	8741
C(116)	1419	7905	8383
C(111)	1328	7787	7665
C(122)	2245(2)	7858(3)	6111(4)
C(123)	2256	8147	5448
C(124)	1826	8094	4991
C(125)	1384	7751	5197
C(126)	1373	7461	5860
C(121)	1803	7514	6317
C(132)	2623(3)	7788(3)	7775(4)
C(133)	3089	7798	8166
C(134)	3274	7253	8486
C(135)	2992	6698	8413
C(136)	2525	6688	8021
C(131)	2341	7233	7702
P(2)	1900(1)	5755(1)	6487(2)
C(212)	2305(3)	6386(4)	5288(4)
C(213)	2681	6738	4925
C(214)	3150	6907	5262
C(215)	3243	6724	5961
C(216)	2867	6372	6324
C(211)	2398	6203	5988
C(222)	2330(3)	5063(3)	7598(4)
C(223)	2689	4655	7913
C(224)	3063	4349	7497
C(225)	3079	4451	6766
C(226)	2720	4859	6451
C(221)	2346	5165	6867
C(232)	1663(3)	4868(3)	5394(5)
C(233)	1347	4644	4844
C(234)	885	4960	4660
C(235)	741	5499	5026
C(236)	1057	5722	5576
C(231)	1518	5407	5760
P(3)	886(1)	5257(1)	7512(2)
C(312)	1309(4)	5380(3)	8871(5)
C(313)	1442	5184	9554
C(314)	1311	4584	9778
C(315)	1048	4179	9319
C(316)	915	4375	8636
C(311)	1045	4976	8412
C(322)	1332(2)	4116(3)	7073(4)
C(323)	1366	3582	6653
C(324)	990	3473	6127
C(325)	580	3897	6022
C(326)	547	4431	6442
C(321)	923	4541	6968
C(332)	-155(3)	5155(4)	8048(4)
C(333)	-694	5290	8053
C(334)	-907	5680	7535
C(335)	-583	5936	7012

Table 5.1 (continued)....

C(336)	-45	580i	7007
C(33i)	i69	54ii	7525
N(4)	783(4)	6575(4)	7904(5)
C(4i)	433(6)	6808(6)	8169(9)
C(42)	-50(6)	7089(8)	8519(14)
B	-28i(5)	7235(6)	5572(7)
F(i)	i34	6996	5271
F(2)	-473	7672	5169
F(3)	-634	6803	5663
F(4)	-i5i	7470	6183

Table 5.2 Unconstrained bond lengths (Å) and selected bond angles (°) for $[Rh(Ph_3P)_3(NCMe)][BF_4]$.

Rh-P(i)	2.3ii(3)	Rh-P(2)	2.26i(3)
Rh-P(3)	2.367(3)	Rh-N(4)	2.015(10)
P(i)-C(iii)	1.855(7)	P(i)-C(12i)	1.843(8)
P(i)-C(i3i)	1.830(8)	P(2)-C(2ii)	1.845(7)
P(2)-C(22i)	1.840(8)	P(2)-C(23i)	1.836(9)
P(3)-C(3ii)	1.845(9)	P(3)-C(32i)	1.848(7)
P(3)-C(33i)	1.848(8)	N(4)-C(4i)	1.134(17)
C(4i)-C(42)	1.5i6(23)		
P(i)-Rh-P(2)	94.9(i)	P(i)-Rh-P(3)	170.3(i)
P(2)-Rh-P(3)	94.1(i)	P(i)-Rh-N(4)	87.7(3)
P(2)-Rh-N(4)	175.2(3)	P(3)-Rh-N(4)	83.6(3)
Rh-N(4)-C(4i)	169.5(ii)	N(4)-C(4i)-C(42)	177.2(14)

observed for such small, highly symmetrical counterions; neither individual atomic co-ordinates nor anisotropic thermal parameters could be successfully refined. This disorder and the high thermal motion of some of the cation phenyl ring carbon atoms are considered to be responsible for the high proportion of unobserved reflections.

The structure of the cation is shown in Figure 5.1. In this cation the Rh(I) atom has an essentially square planar P_3N co-ordination. In-plane deviations from ideal square planar co-ordination (Table 5.2) consist of P-Rh-P angles greater than, and P-Rh-N angles less than 90°, as a result of the disparate steric bulk of the PPh_3 and MeCN ligands. However, any out-of-plane distortion towards tetrahedral co-ordination is very slight; the deviations of the atoms from the mean RhP_3N plane are Rh-0.002(2), P(1) 0.079(3), P(2) - 0.067(3), P(3) 0.080(3), N(4) - 0.090(10) Å. All three Rh-P bond lengths are significantly different; the shortest lies <u>trans</u> to the acetonitrile ligand, which forms an essentially linear Rh-N-C-C arrangement.

Wilkinson's catalyst, $[Rh(PPh_3)_3Cl]$, may be obtained in a red or an orange form, depending on the method of synthesis,[1,8] and the crystal structures of both have been determined.[3] The two forms differ in their packing arrangements, in the orientations of the phenyl rings, in the degree of distortion of the square planar co-ordination towards tetrahedral, and in the Rh...H intramolecular closest contacts. Important features of the co-ordination in both forms and in $[Rh(PPh_3)_3(NCMe)]^+$ are compared in Table 5.3. The $[Rh(PPh_3)_3(NCMe)]^+$ cation shows much less out-of-plane distortion than either form of $[Rh(PPh_3)_3Cl]$, and a more orderly 'paddle-wheel' arrangement of the PPh_3 ligands; thus the three bonds P(1)-C(111), P(2)-C(211) and P(3)-C(321) lie approximately in the RhP_3N mean plane [subtending angles

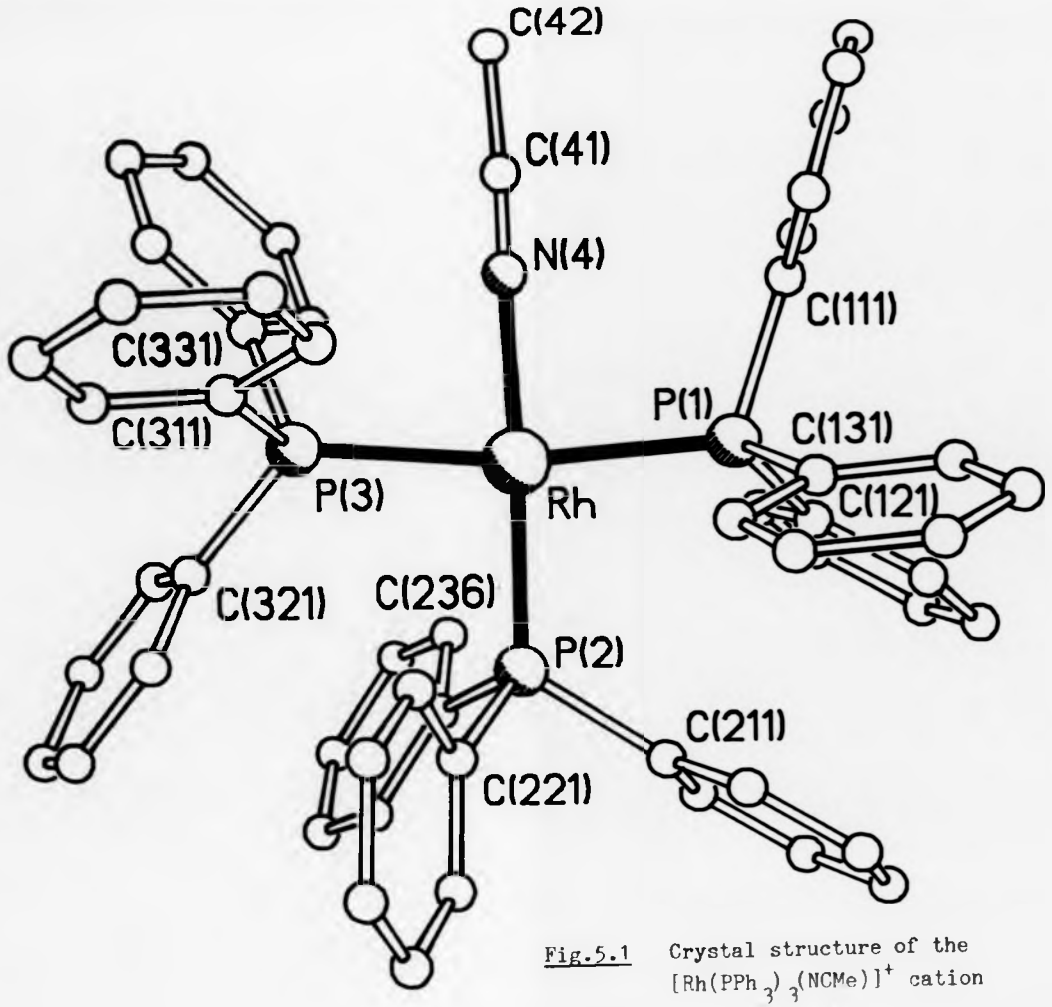

Fig.5.1 Crystal structure of the $[Rh(PPh_3)_3(NCMe)]^+$ cation

Table 5.3 Comparison of selected dimensions (Å, degrees) for the coordination of Rh in $[Rh(PPh_3)_3(NCMe)][BF_4]$ and the red and orange forms of $[Rh(PPh_3)_3Cl]$.

Dimension	$[Rh(PPh_3)_3(NCMe)][BF_4]$	$[Rh(PPh_3)_3Cl]$	
		orange	red
Rh-X[a]	2.015(10)	2.404(4)	2.376(4)
Rh-P *cis* to X	2.367(3)	2.338(4)	2.332(4)
	2.311(3)	2.304(4)	2.334(3)
Rh-P *trans* to X	2.261(3)	2.225(4)	2.214(4)
P-Rh-P *cis*	94.9(1)	97.7(1)	97.9(2)
	94.1(1)	96.4(2)	100.4(1)
P-Rh-P *trans*	170.3(1)	159.1(2)	152.8(1)
X-Rh-P *cis*	83.6(3)	84.5(1)	86.1(2)
	87.7(3)	85.3(1)	85.2(2)
X-Rh-P *trans*	175.2(3)	166.7(2)	156.2(2)
r.m.s. Δ[b]	0.071	0.272	0.426

[a] X = MeCN or Cl [b] r.m.s. deviation (unweighted) of the RhP_3N atoms from their mean plane.

of 6.5(2), 4.9(2), and 13.0(2)° respectively with it], and the phenyl rings mesh together around the co-ordination plane (Fig.5.1). The difference in the P(1)-Rh-N(4) and P(3)-Rh-N(4) angles can also be ascribed to this arrangement of the ligand substituents.

The phenyl ring arrangement in $[Rh(PPh_3)_3(NCMe)]^+$ brings several hydrogen atoms into close proximity with the Rh atom. Each PPh_3 ligand has one ortho-H atom within 2.85 Å of Rh: H(136) 2.80, H(236) 2.83, H(312) 2.81 Å (for the purpose of these calculations the C-H bonds were extended to 1.08 Å). All other Rh...H distances are > 2.9 Å. This contrasts with the two forms of $[Rh(PPh_3)_3Cl]$, for each of which one particularly short ortho-H...Rh distance was observed.[3,9] Since an idealised geometry for phenyl rings was assumed in all three structure determinations, the significance of the hydrogen atom position is, however, questionable.

Despite these secondary differences, the overall co-ordination geometry in all three compounds is very similar.

5.4 Conductivity and spectroscopic measurements

5.4.1 Conductivity measurements

Conductivity measurements for 0.0043, 0.00215 and 0.00108 M solutions of $[Rh(PPh_3)_3(NCMe)][BF_4]$ in dry, freshly distilled, degassed acetonitrile were accomplished using a Phillips PW9504/00 conductivity bridge and platinum electrodes. Measurements were also made for 0.00552, 0.00276 and 0.00138 M solutions of $[CH_3(CH_2)_6]_4NI$ and 0.00516, 0.00258 and 0.00129 M solutions of $[Rh_2(O_2CMe)_2(NCMe)_6][BF_4]_2$ in this solvent. All measurements were performed at ca. 298K. The data are summarised in Table 5.4 and a plot of conductivity against concentration

shown in Fig.5.2 and these indicate that $[Rh(PPh_3)_3(NCMe)][BF_4]$ behaves as a 1:1 electrolyte in acetonitrile.

Table 5.4 Conductivity measurements of $[Rh(PPh_3)_3(NCMe)][BF_4]$, $[CH_3(CH_2)_6]_4NI$ and $[Rh_2(O_2CMe)_2(NCMe)_6][BF_4]_2$ in acetonitrile

Compound	Concentration ($x10^{-3}$ mol l^{-1})	Resistivity[a] ($x10^4\Omega$)	Molar Conductivity ($\Omega^{-1}mol^{-1}cm^2$)
$[Rh(PPh_3)_3(NCMe)][BF_4]$	4.32	0.15	108.0
	2.15	0.262	124.3
	1.08	0.572	113.3
$[CH_3(CH_2)_6]_4NI$	5.52	0.128	99.07
	2.76	0.215	117.96
	1.38	0.395	128.42
$[Rh_2(O_2CMe)_2(NCMe)_6][BF_4]_2$	5.16	0.073	185.83
	2.58	0.119	228.0
	1.29	0.194	279.7

a. Cell constant = 0.70 cm^{-1}

5.4.2 UV/visible spectrum

The UV/visible spectrum of $[Rh(PPh_3)_3(NCMe)[BF_4]$ in acetonitrile solution (Fig.5.3) consists of absorption bands with molar extinction coefficients as shown in Table 5.5.

- A= [Rh (PPh$_3$)$_3$ (NCMe)] [BF$_4$]
- B= [(Me (CH$_2$)$_6$)$_4$ N] I
- C= [Rh$_2$ (O$_2$ CMe)$_2$ (NCMe)$_6$] [BF$_4$]$_2$

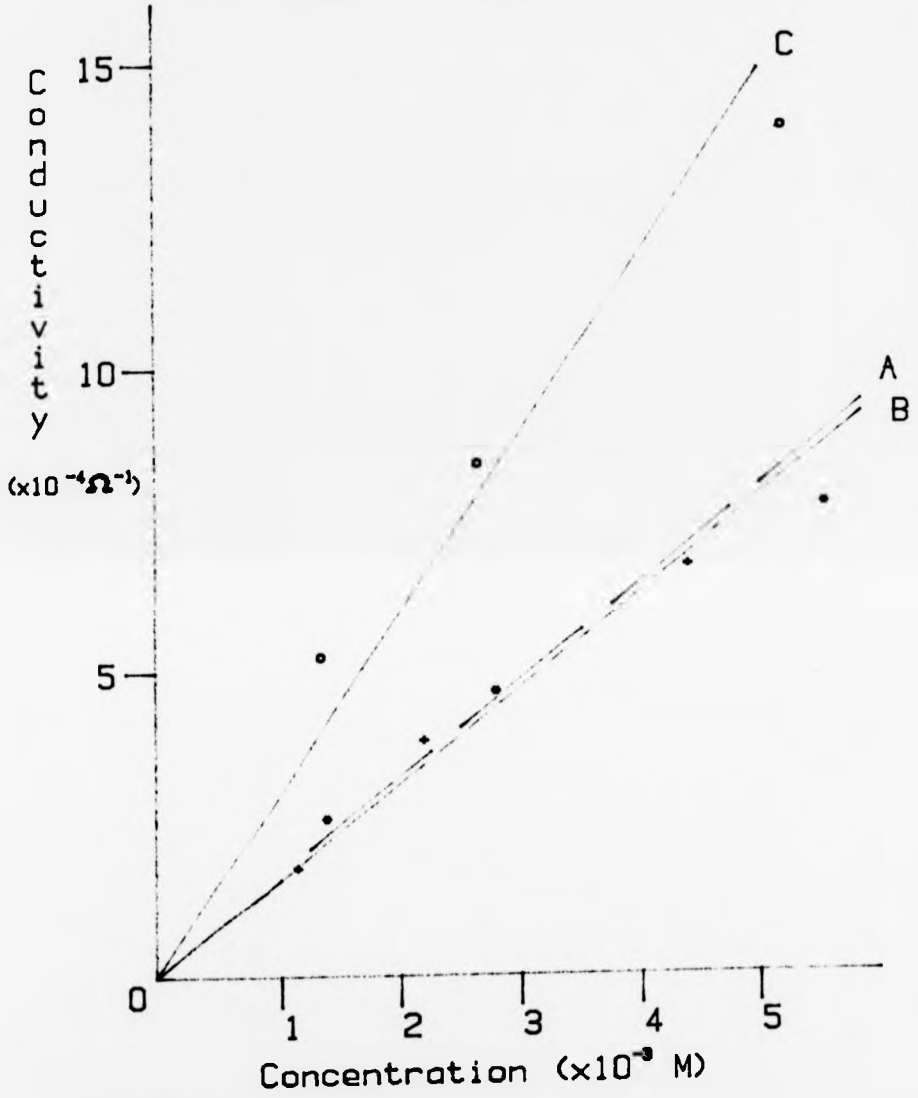

Fig 5.2
Plot of Conductivity against Concentration for solutions A, B and C in acetonitrile

Table 5.5 UV/visible absorption bands for $[Rh(PPh_3)_3(NCMe)][BF_4]$

λ_{max}(nm)	$\varepsilon(mol^{-1}cm^{-1}l^{-1})$
400	1433
350	3604
300	9000
260	16000
226	60300

This profile is very similar to that observed for $[Rh(PPh_3)_3Cl]$ in acetonitrile (Fig.5.4) and the absorption bands are shown in Table 5.6.

Table 5.6 UV/visible absorption bands for $[Rh(PPh_3)_3Cl]$

λ_{max}(nm)	$\varepsilon(mol^{-1}cm^{-1}l^{-1})$
400	1239
364	2656
302	8852
273	17705
265	18413
226	86311

5.4.3 Infrared spectrum

The infrared spectrum of $[Rh(PPh_3)_3(NCMe)][BF_4]$ (Fig.5.5) mulled in nujol shows absorptions very similar to that for $[Rh(PPh_3)_3Cl]$ (Fig.5.6) except the former contains a band at 1055 cm^{-2} assigned to the B-F stretching vibration[10] of the $[BF_4]^-$ ion and the latter contains a band at 296 cm^{-1} assigned to the Rh-Cl stretching vibration.[11]

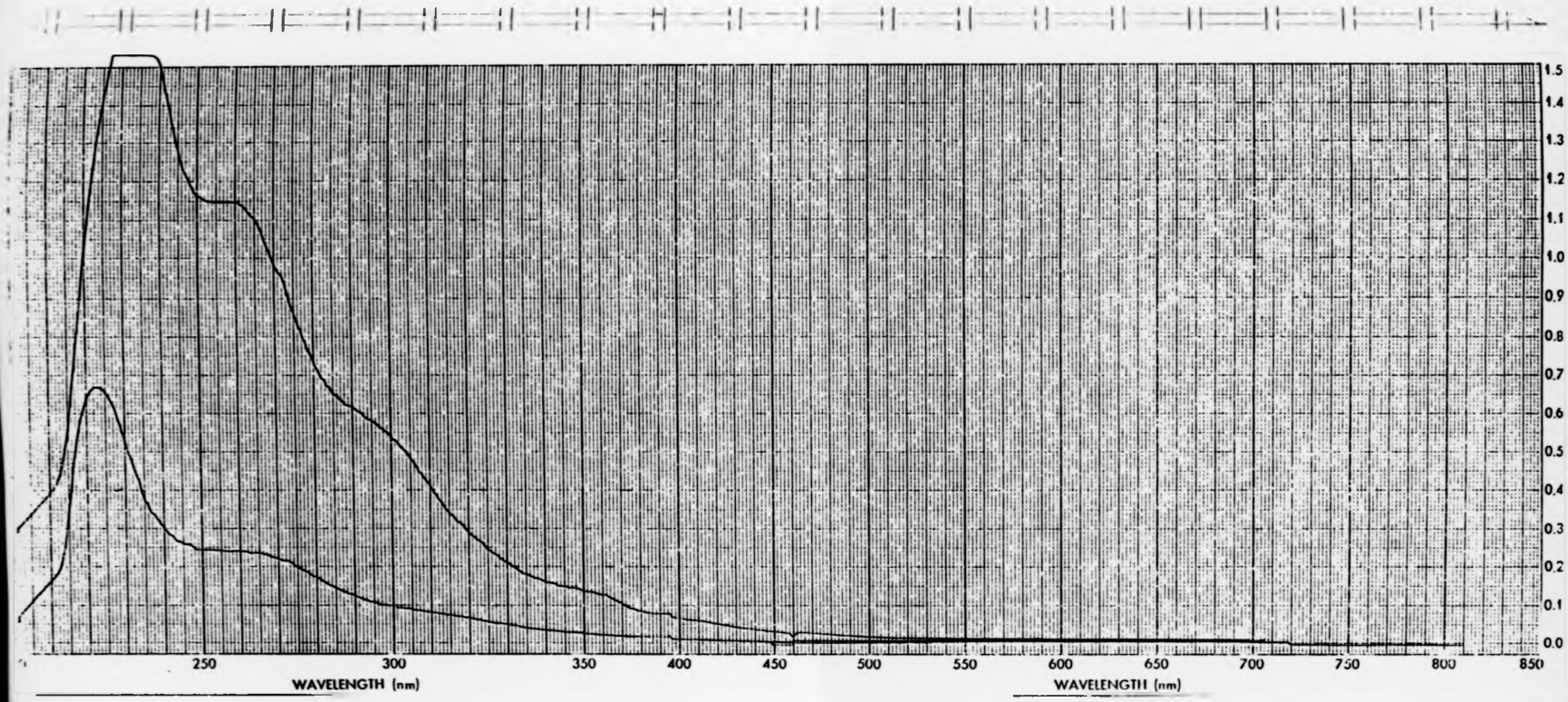

Fig.5.3 UV/visible spectrum of $[Rh(PPh_3)_3(NCMe)][BF_4]$ in acetonitrile

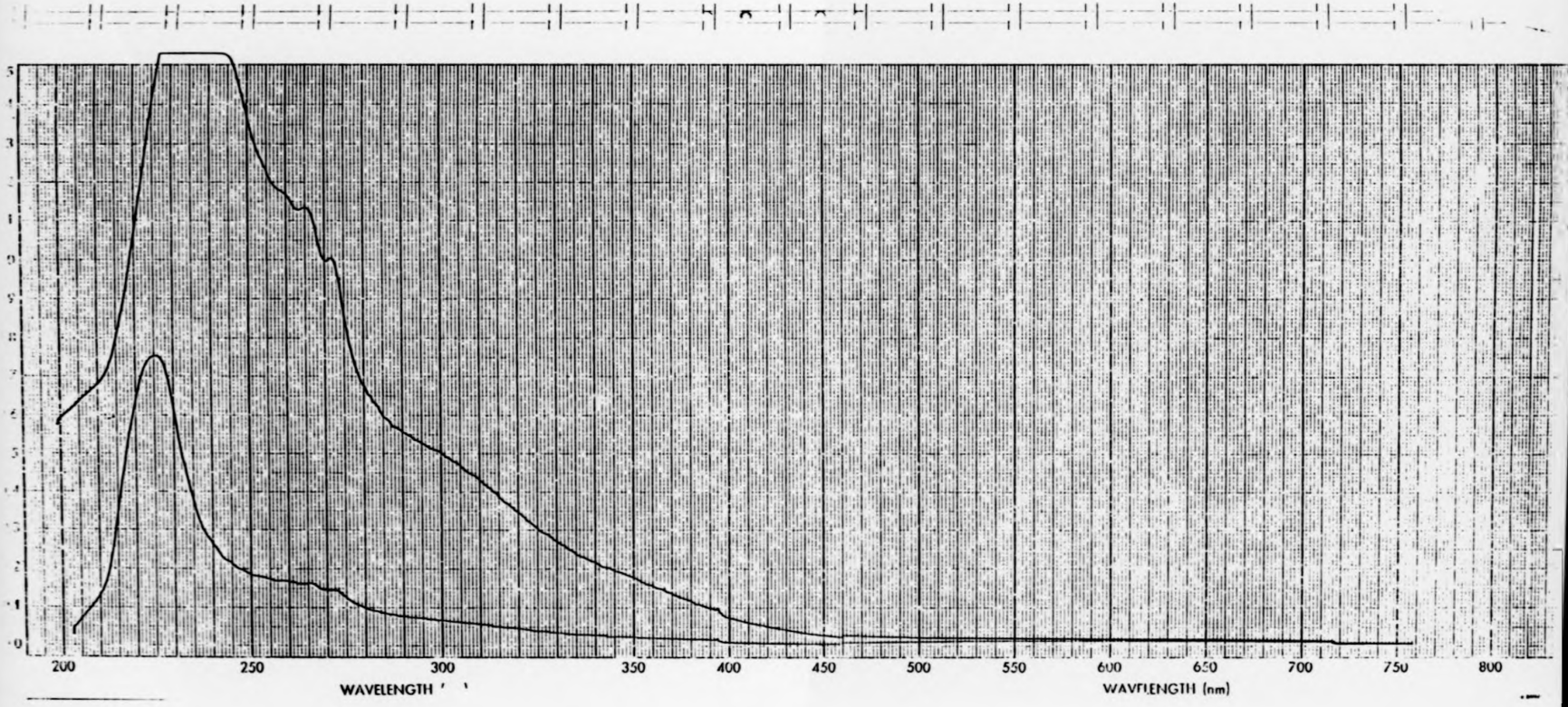

Fig.5.4 UV/visible spectrum of $[Rh(PPh_3)_3Cl]$ in acetonitrile

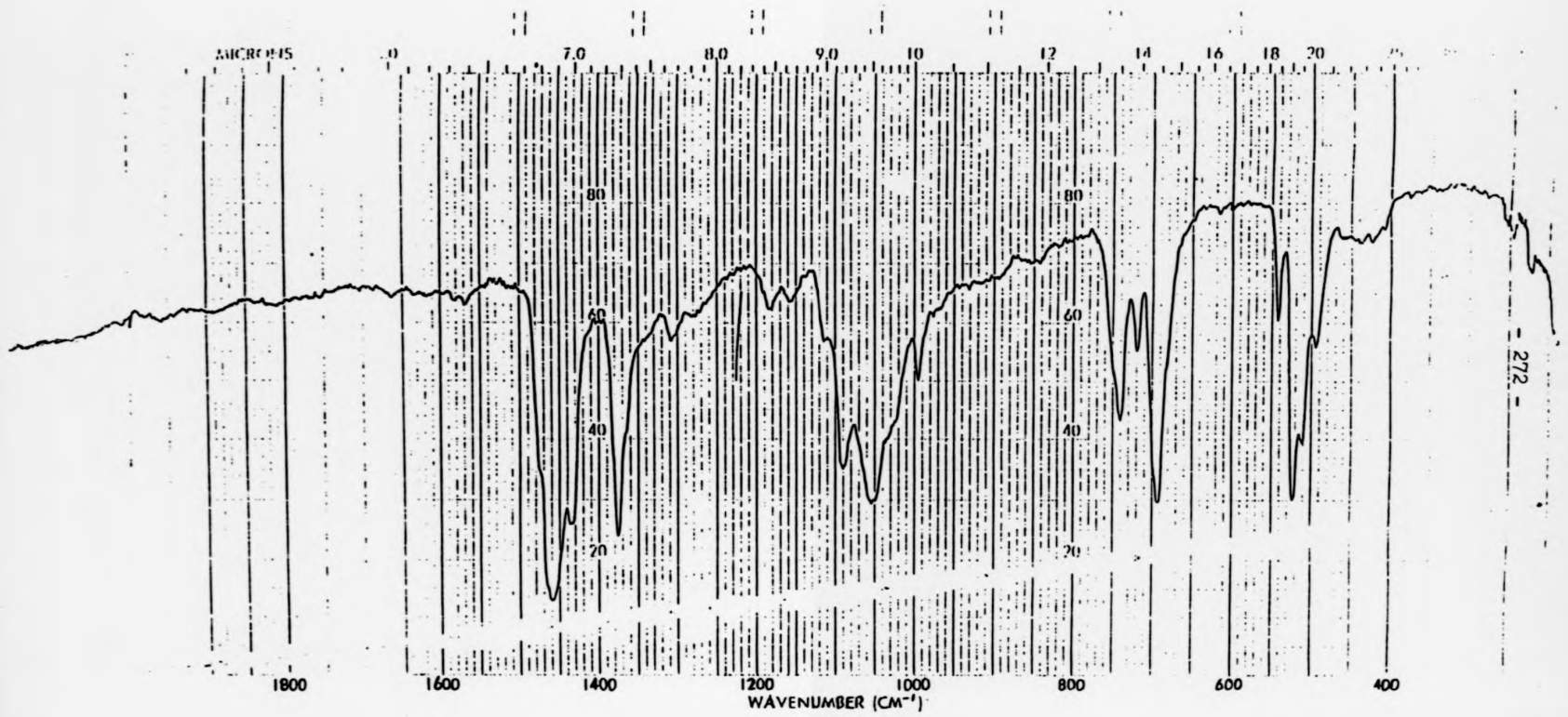

Fig.5.5 Infrared spectrum of $[Rh(PPh_3)_3(NCMe)][BF_4]$

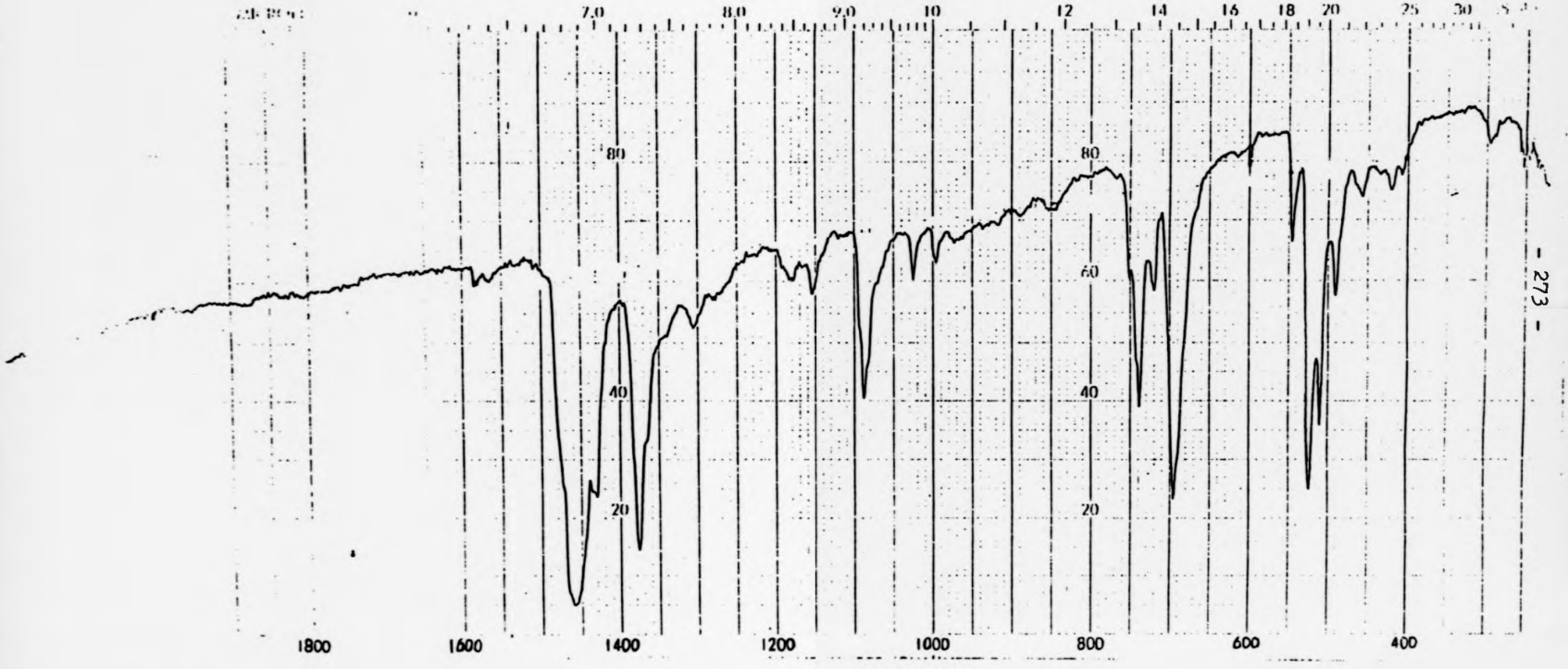

Fig.5.6 Infrared spectrum of $[Rh(PPh_3)_3Cl]$

Common bands are seen at 1430 cm^{-1}(s) (P-Ph), 740 cm^{-1} and 690 cm^{-1} (both out-of-place C-H bending vibrations for a mono-substituted benzene ring).[12]

5.4.4 N.m.r. spectroscopic studies

The ^{1}H, ^{13}C, ^{19}F and ^{31}P n.m.r. spectra (Figs. 5.7, 5.8, 5.9, 5.10) recorded for the title compound in CD_2Cl_2 solution were consistent with the solid state structure of cation and anion being retained in solution. The ^{1}H n.m.r. data recorded at 80 MHz and 260K (Fig.5.7) consist of two peaks of relative intensity 2:1 at 7.5 and 7.3 p.p.m., which are assigned to the phenyl hydrogens of the inequivalent PPh_3 groups, and a sharp resonance at 2.11 p.p.m., which is attributed to the hydrogens of the ligated acetonitrile molecule - the resonance being slightly shifted from that (1.96 p.p.m.) of free acetonitrile. The relative integrations agree with the formulation. The ^{13}C n.m.r. spectrum (Fig.5.8) run at 20.1 MHz and 230K shows signals at {128.3, 129.9}, {130.1, 131.7}, {132.2, 134.0}, {134.3, and 134.5} p.p.m., which are assigned to the four inequivalent carbons on each phenyl ring,[13] the doubling (as indicated) being a consequence of the two inequivalent PPh_3 groups. Also, the ^{13}C resonances at 127.8 and 0.87 p.p.m. are assigned to the nitrile and methyl carbon, respectively, the former resonance showing a significant shift from that (119 p.p.m.) of the free ligand, in a sense also observed (Chapter 2) for $[Rh_2(O_2CMe)_2(NCMe)_6][BF_4]_2$. The ^{19}F n.m.r. spectrum (Fig.5.9), run at 75 MHz and 290K comprised a single resonance 38 Hz in width at -74 p.p.m. (referenced to CF_3CO_2H), consistent with the presence of $[BF_4]^-$.[14]

The ^{31}P n.m.r. spectrum (Fig.5.10), at 32 MHz and 200K consists of a doublet of doublets centred at 32.1 p.p.m. and a doublet of triplets

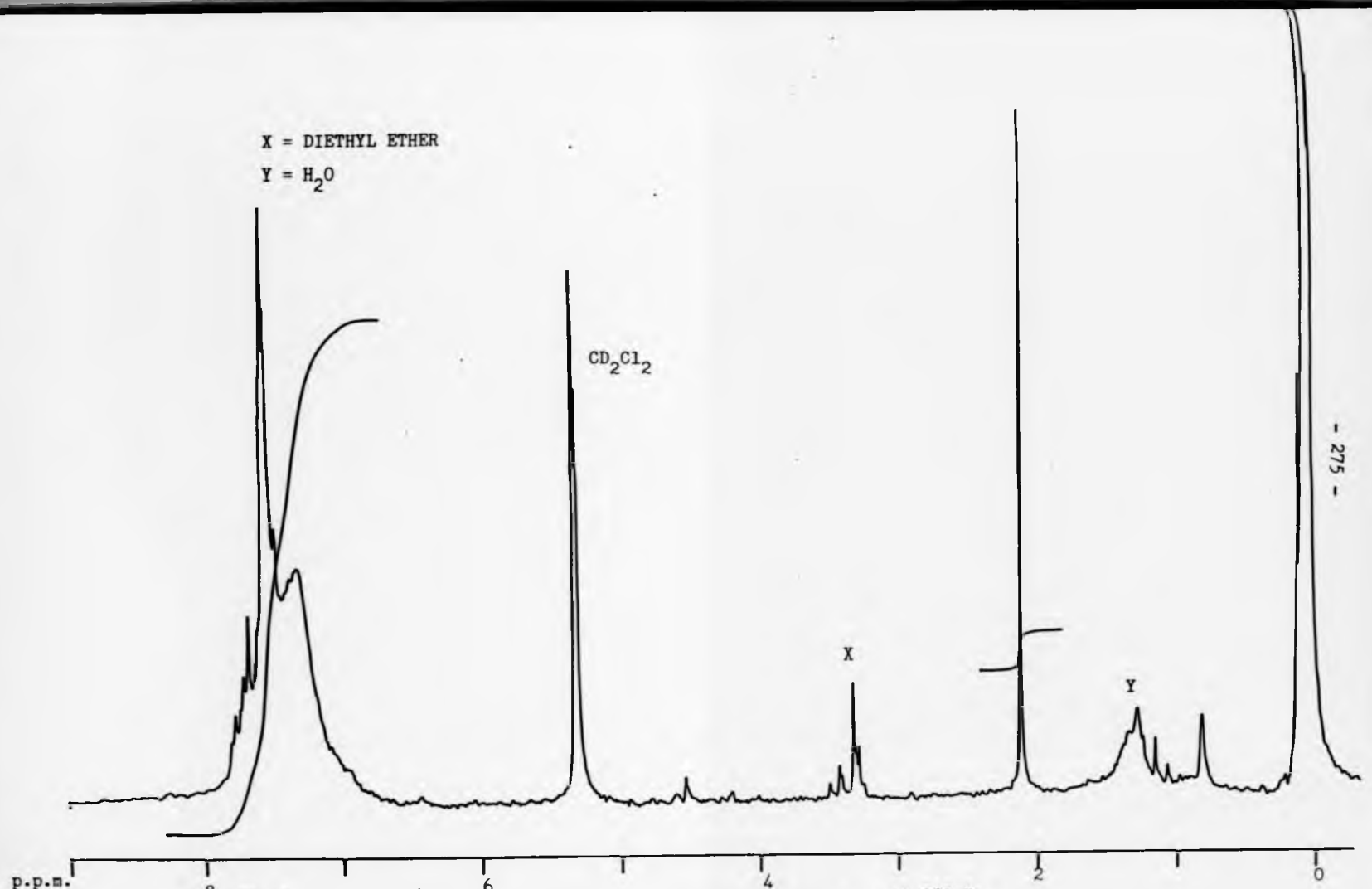

Fig.5.7 80 MHz ^1H n.m.r. of $[Rh(PPh_3)_3(NCMe)][BF_4]$ in CD_2Cl_2 at 260 K

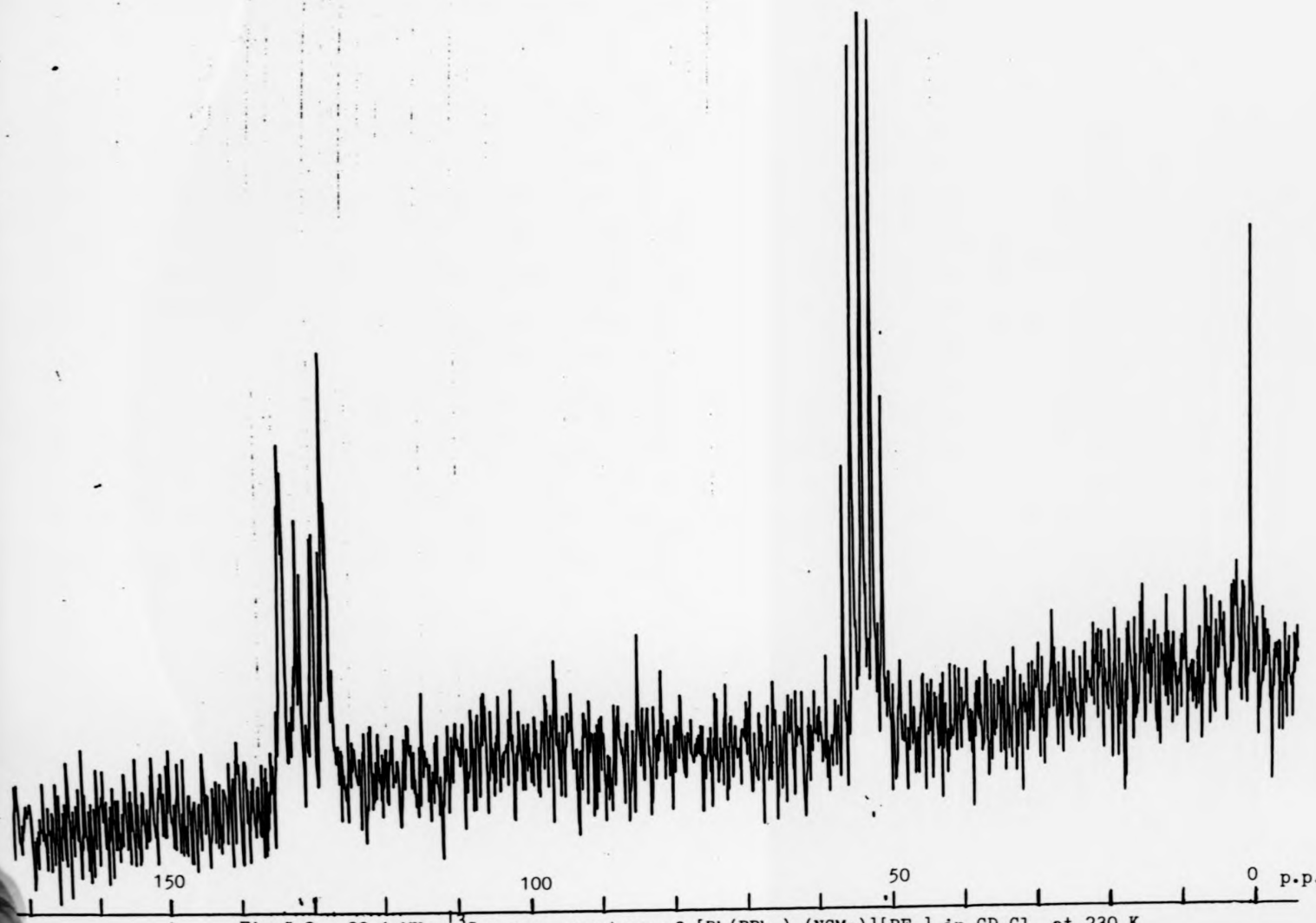

Fig.5.8 20.1 MHz ^{13}C n.m.r. spectrum of $[Rh(PPh_2)_2(NCMe)][BF_4]$ in CD_2Cl_2 at 230 K

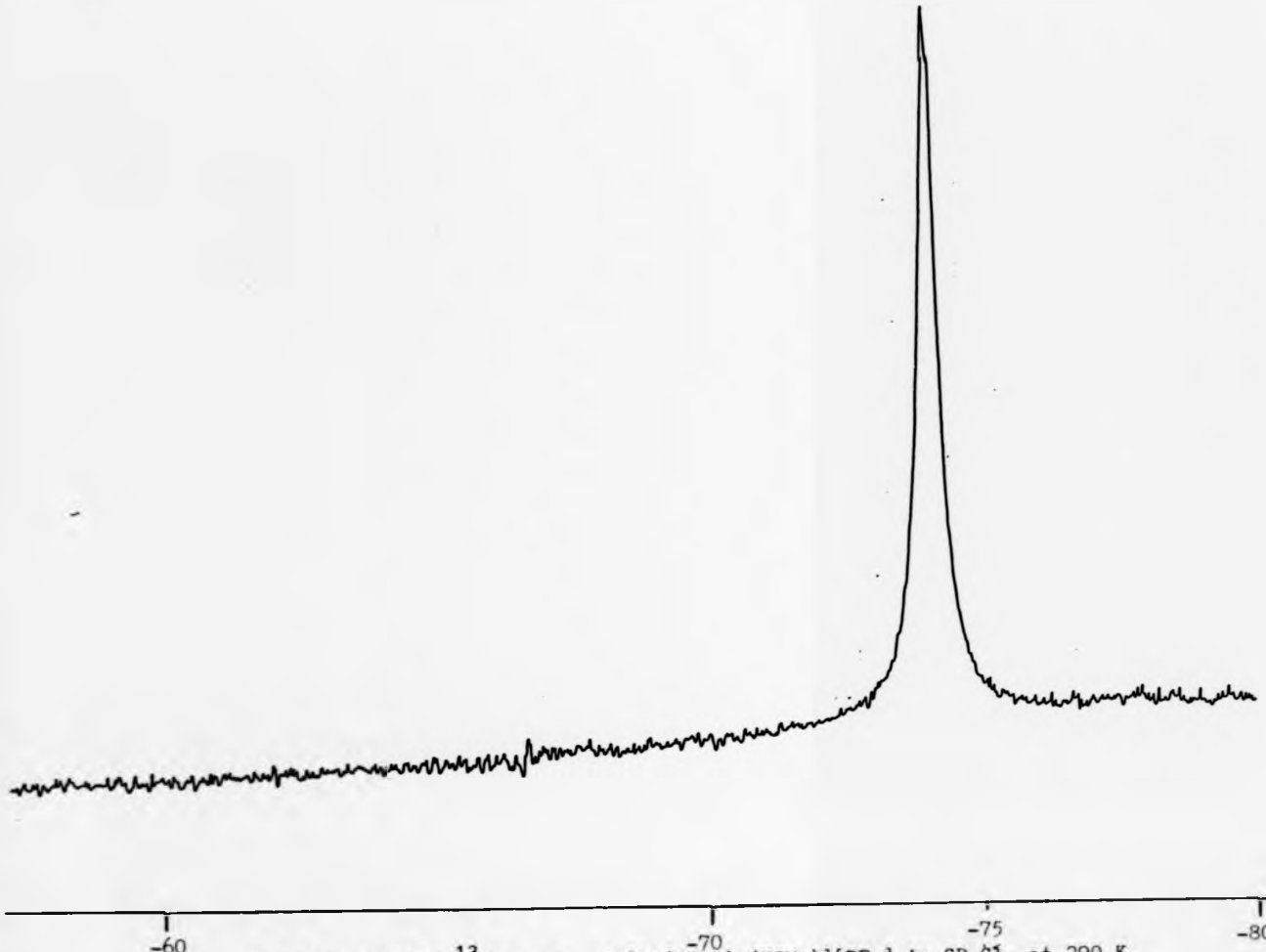

Fig.5.9 75 MHz ^{13}F n.m.r. of $[Rh(PPh_3)_3(NCMe)][BF_4]$ in CD_2Cl_2 at 290 K

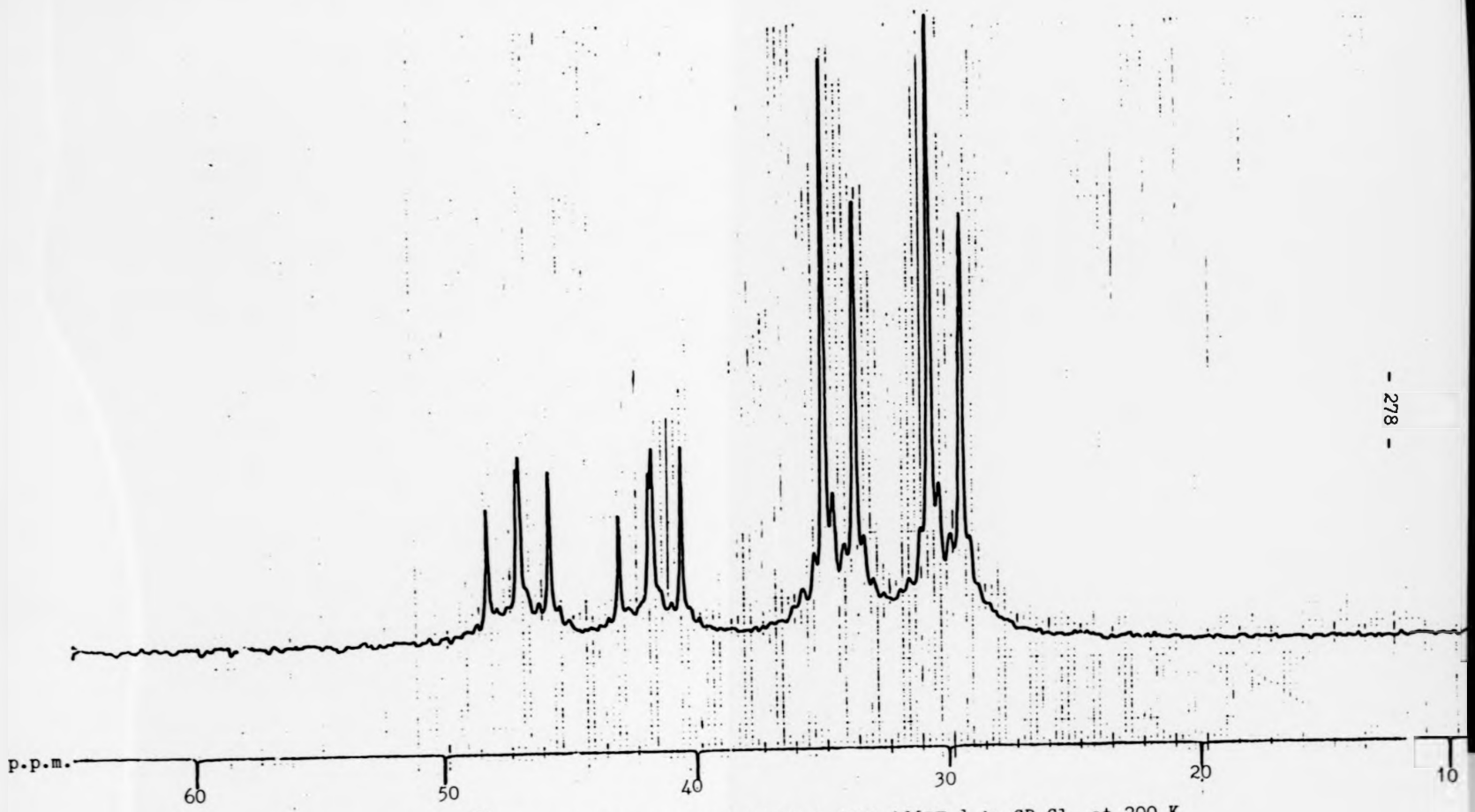

Fig.5.10 32 MHz ^{31}P n.m.r. spectrum of $[Rh(PPh_3)_3(NCMe)][BF_4]$ in CD_2Cl_2 at 200 K

(with the central peak of each triplet split by second-order effects[15]) centred at 44.3 p.p.m. This pattern is typical of an A_2BX system;[16,17] here, A are the mutually *trans* P atoms, B is the P atom *trans* to acetonitrile, and X = Rh, with $\delta P_{\underline{A}}$ = 32.1 p.p.m. and $\delta P_{\underline{B}}$ = 44.3 p.p.m. The coupling constants are: $J(Rh-P_{\underline{A}})$ = 136 Hz; $J(Rh-P_{\underline{B}})$ = 170 Hz; $J(P_{\underline{A}}-P_{\underline{B}})$ = 39 Hz. The ^{31}P chemical shifts and Rh-P coupling constants observed here closely resemble the corresponding data obtained for $[Rh(PPh_3)_3X]$ (X = Cl, Br or I).[17] Taking the ^{31}P chemical shifts and the Rh-P coupling constants for this A_2BX system a computer simulated ^{31}P n.m.r. spectrum was produced (Fig.5.11) by means of the program SPIN on the Varian XL-300 n.m.r. spectrometer host computer. This agrees well with the spectrum shown in Fig.5.10. Thus, it can be seen that second-order effects caused splitting of the central triplet peaks, however the simulation shows some smaller splittings in the doublets which were not detected experimentally.

5.5 ^{31}P n.m.r. study of the reaction of $[Rh(PPh_3)_3(NCMe)][BF_4]$ with $P(OMe)_3$

Much attention has been given to determining the degree of dissociation of PPh_3 from $[Rh(PPh_3)_3Cl]$ in solution.[1,8,18,19] This concern reflects the postulation that the nominally three co-ordinate species $[Rh(PPh_3)_2Cl]$ formed in the reaction

$$[Rh(PPh_3)_3Cl] \rightleftharpoons [Rh(PPh_3)_2Cl] + PPh_3$$

may be a key intermediate in catalytic hydrogenation schemes.[8] It is now certain that in the absence of all reagents save the solvent, of low co-ordinating power, the dissociation of a PPh_3 ligand occurs only to a small extent (*ca.* 5%) at room temperature[16] or below.[18,19]

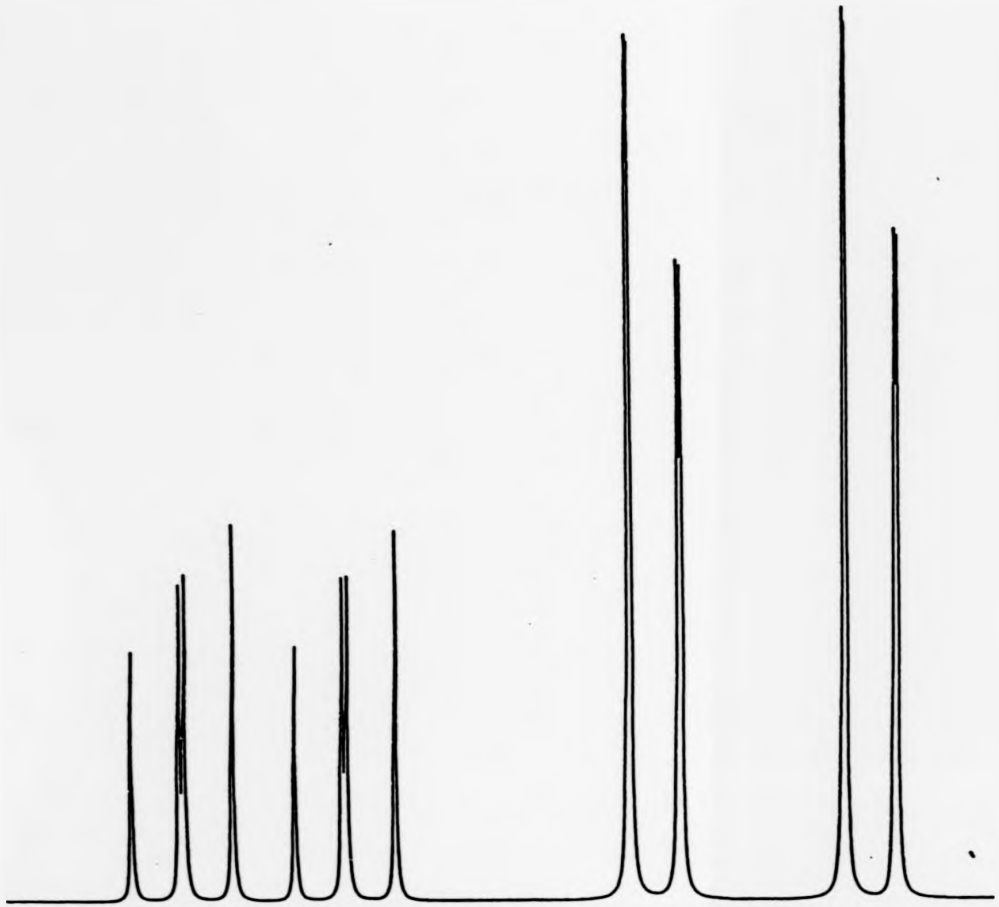

FIG. 5.11 Computer simulated ^{31}P n.m.r. spectrum for the A_2BX system

The $[Rh(PPh_3)_3Cl]$ portion of the ^1H n.m.r. spectra of decimolar solutions in deuterochloroform shows no change when free PPh_3 is added.[16] However, n.m.r. studies have shown that the PPh_3 ligands equilibrate with added tri(p-tolyl)phosphine $P(C_7H_7)_3$. The rate of exchange is less than that of cis/trans isomerisation and it has been postulated that a structure is involved in which one of the phosphine ligands is more loosely bound than the other two.[16]

A ^{31}P n.m.r. study of the effect of adding excess PPh_3 to a CD_2Cl_2 solution of $[Rh(PPh_3)_3(NCMe)][BF_4]$ at 200K shows no broadening due to exchange. However, at 303K line broadening of about 30% is observed and the signals due to $[Rh(PPh_3)_3(NCMe)][BF_4]$ and free PPh_3 begin to move towards coalescence. Phosphine exchange is proposed to be involved in the homogeneous hydrogenation catalytic cycle[8,20] (Fig.5.12). This cycle depends entirely on the formation, concentration, and fate of the three-co-ordinate intermediate $Rh(PPh_3)_2Cl$.[20] It has been proposed by Tolman that this species must be solvated, since the unsolvated compound violates the 16-electron rule.[21] Violation of the rule, however, is positively advantageous for catalytic intermediates. Proof of whether $Rh(PPh_3)_2Cl$ is solvated is difficult but a solvated species is proposed in one mechanistic scheme, and a solvent concentration term is incorporated in the kinetic equation.[20] However, phosphine exchange, generating a free co-ordination site for catalysis, followed by hydrogenation of alkenes via the hydride route, is thought to be important. Furthering the studies on phosphine exchange with $[Rh(PPh_3)_3(NCMe)][BF_4]$ as preliminary investigations into the catalytic activity of the complex, a study of its reaction with a different phosphorus donor was carried out. Study of such a reaction via ^{31}P n.m.r. was performed to indicate if phosphine exchange was occurring and whether any selectivity was being

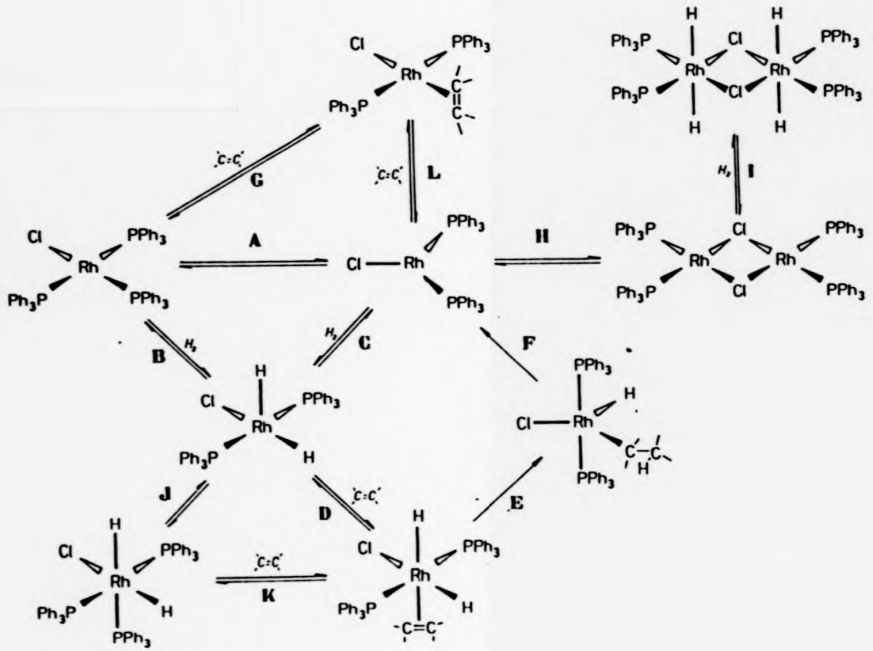

FIG. 5.12 Homogeneous hydrogenation reaction scheme for $Rh(PPh_3)_3Cl$

exercised. Trimethyl phosphite $P(OMe)_3$ was chosen as a marker to study this reaction.

Upon addition of $P(OMe)_3$ to a solution of $[Rh(PPh_3)_3(NCMe)][BF_4]$ in deuteroacetonitrile at 303K, the intensity of the doublet of triplets centred at 44.3 p.p.m. decreased and the peaks were completely removed for a 1:1 molar ratio of the reagents (Fig.5.13). Concomitantly, two peaks centres at 135 p.p.m. appeared and, at the 1:1 ratio, took on the appearance of a doublet of triplets. Therefore, it is concluded that $P(OMe)_3$ selectively replaces the PPh_3 group <u>trans</u> to MeCN in $[Rh(PPh_3)_3(NCMe)]^+$, i.e.

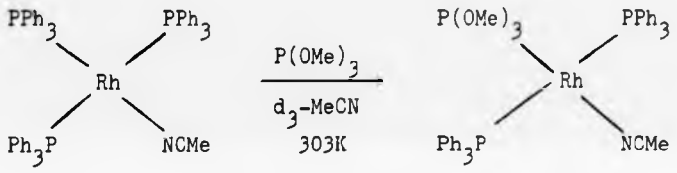

This same stabilisation of the <u>trans</u> product of the reaction is seen in the reactions between $[Rh(PPh_3)_3Cl]$ and both PF_3 and $PF_2(NMe_2)$ where the products are <u>trans</u>$[Rh(PPh_3)_2(PF_3)Cl]$ and <u>trans</u>$[Rh(PPh_3)_2(PF_2(NMe_2))Cl]$ respectively.[23,24] On consideration of the <u>trans</u> effect order of ligands,[25] phosphines exert more of a <u>trans</u> effect, i.e. a labilising effect, on <u>trans</u> ligands in square planar systems than do chloride and most probably acetonitrile. Thus exchange of a <u>cis</u> phosphine would be expected to occur preferentially. However, the final products have <u>trans</u> geometries. This leads to the conclusion that a thermodynamic rather than a kinetic effect is influencing this reaction.

The MeCN ligand itself does not provide a further labile site, as might be expected with co-ordination of a solvent molecule. In CD_2Cl_2 the solid state structure is retained in solution and the ^{13}C n.m.r. study indicates a shift to higher frequency in the position of

exercised. Trimethyl phosphite $P(OMe)_3$ was chosen as a marker to study this reaction.

Upon addition of $P(OMe)_3$ to a solution of $[Rh(PPh_3)_3(NCMe)][BF_4]$ in deuteroacetonitrile at 303K, the intensity of the doublet of triplets centred at 44.3 p.p.m. decreased and the peaks were completely removed for a 1:1 molar ratio of the reagents (Fig.5.13). Concomitantly, two peaks centres at 135 p.p.m. appeared and, at the 1:1 ratio, took on the appearance of a doublet of triplets. Therefore, it is concluded that $P(OMe)_3$ selectively replaces the PPh_3 group *trans* to MeCN in $[Rh(PPh_3)_3(NCMe)]^+$, i.e.

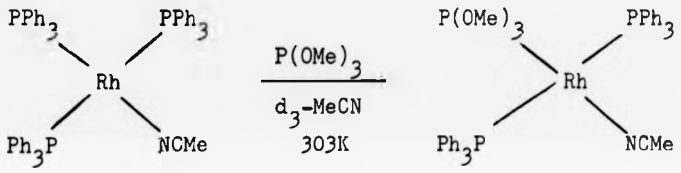

This same stabilisation of the *trans* product of the reaction is seen in the reactions between $[Rh(PPh_3)_3Cl]$ and both PF_3 and $PF_2(NMe_2)$ where the products are *trans*$[Rh(PPh_3)_2(PF_3)Cl]$ and *trans*$[Rh(PPh_3)_2(PF_2(NMe_2))Cl]$ respectively.[23,24] On consideration of the *trans* effect order of ligands,[25] phosphines exert more of a *trans* effect, i.e. a labilising effect, on *trans* ligands in square planar systems than do chloride and most probably acetonitrile. Thus exchange of a *cis* phosphine would be expected to occur preferentially. However, the final products have *trans* geometries. This leads to the conclusion that a thermodynamic rather than a kinetic effect is influencing this reaction.

The MeCN ligand itself does not provide a further labile site, as might be expected with co-ordination of a solvent molecule. In CD_2Cl_2 the solid state structure is retained in solution and the ^{13}C n.m.r. study indicates a shift to higher frequency in the position of

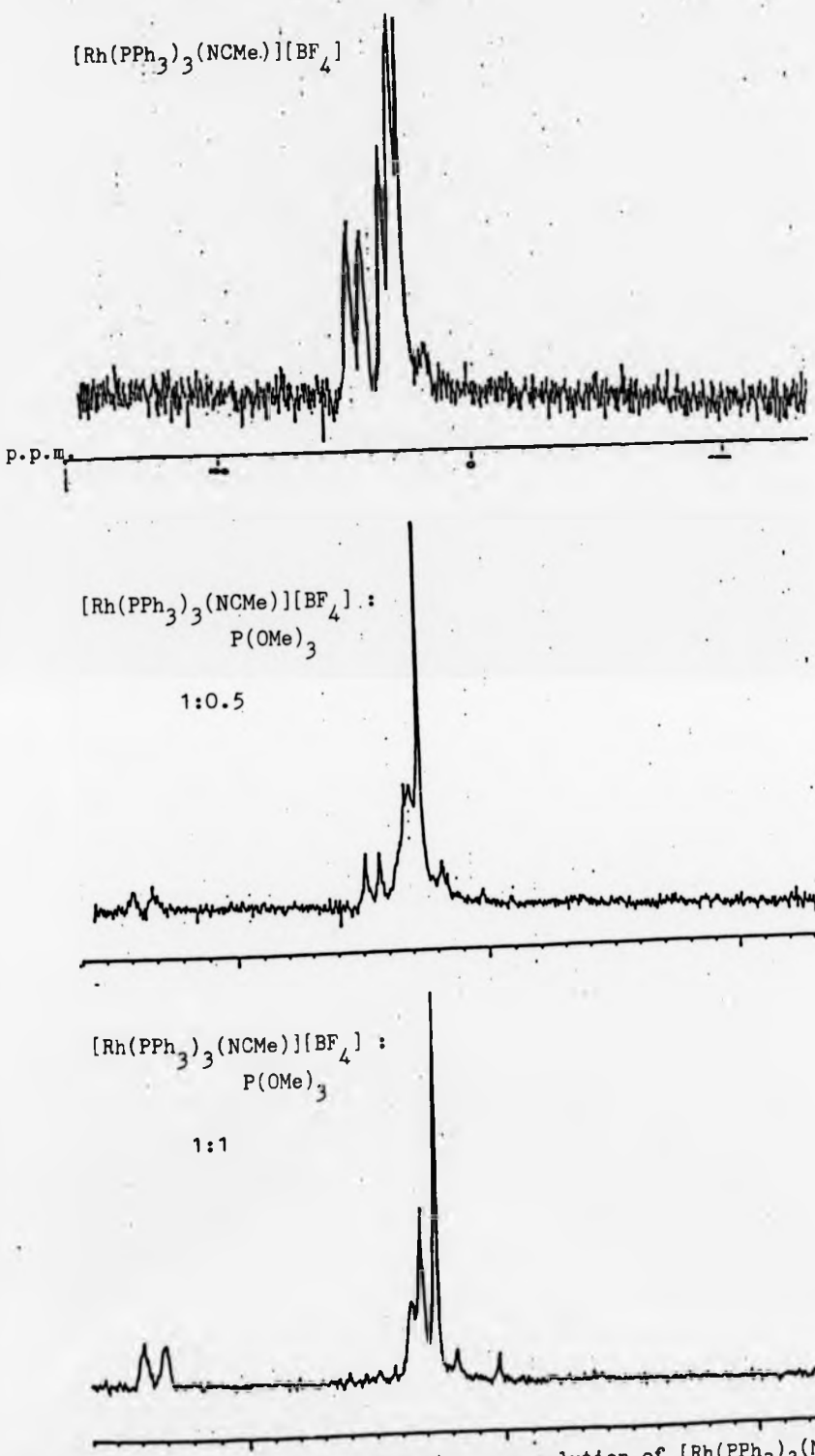

Fig.5.13 Addition of $P(OMe)_3$ to a solution of $[Rh(PPh_3)_3(NCMe)][BF_4]$ in CD_3CN

the nitrile carbon of the co-ordinated MeCN from that of free MeCN (127 p.p.m. versus 119 p.p.m. respectively), a similar shift to that observed for equatorially co-ordinated MeCN in $[Rh_2(O_2CMe)_2(NCMe)_6][BF_4]_2$ (Chapter 2). The somewhat stronger binding properties of MeCN to rhodium over other solvents has also been noted by Schrock and Osborn in studies on cationic rhodium dihydrides $[RhH_2(PPh_3)_2S_2]^+$ (S = acetone, ethanol and acetonitrile).[26] N.m.r. spectroscopic studies indicated that acetone and ethanol are significantly more labile than acetonitrile and that this could be a reason for the lack of olefin hydrogenation of the catalyst precursor $[Rh(NBD)(PPh_3)_2]^+$ in acetonitrile.[26]

5.6 Investigation of $[Rh(PPh_3)_3(NCMe)][BF_4]$ as a Catalytic Precursor

The first rapid and practical system for the homogeneous reduction of alkenes, alkynes and other unsaturated substances at 25°C and 1 atmosphere pressure used $[Rh(PPh_3)_3Cl]$.[27,8,28] It owes its efficacy to the ease with which it will add molecular hydrogen oxidatively to give the five co-ordinate rhodium(III) complex $[RhCl(H)_2(PPh_3)_2]$.[8,21] This species, being co-ordinatively unsaturated, can complex further with alkenes or alkynes. The hydrogen ligands are rapidly transferred from rhodium to carbon, a step that is followed by elimination of the hydrocarbon.

Because of this mechanism of hydrogenation, it shows many advantages over conventional heterogeneous hydrogenation catalysts, which are usually finely divided late transition metals. The most obvious advantage is realised in the change to a homogeneous system; at once all problems associated with the reproducible production of catalyst

particle size and surface properties are eliminated. Furthermore, a selectivity can be achieved in that hydrogenation will occur only at the C=C or C≡C bond co-ordinated to the vacant sixth co-ordination site leaving other reducible groups, or more sterically hindered olefinic groups free from hydrogenation.[20] In the catalytic cycle (Fig.5.12), although only a small fraction of the parent complex is converted into the bis(triphenylphosphine) complex, equilibrium A is perturbed by the equilibria B and C (because of the presence of hydrogen) and by equilibria G and L (because of the presence of alkene).

The removal of $[Rh(PPh_3)_3Cl]$ by reaction with alkene (equilibrium L) is parasitic if hydrogenation is considered to take place by the hydride route C→D→E→F. It has been shown that incorrect conclusions have been drawn from several experiments purporting to demonstrate this route to alkanes.[20]

The addition of alkene to form an octahedral dihydro alkene complex requires the alkene to be <u>cis</u> to at least one hydride ligand. The most recent view is that the complex formed has the geometry shown in Fig.5.12: that is, the alkene is added <u>trans</u> to one hydride ligand and inevitably <u>cis</u> to the second.[20]

Sequential addition of two hydrido ligands to alkenes occurs and regenerates $Rh(PPh_3)_2Cl$ which can then react in the catalytic cycle to give the dihydro complex $RhCl(H)_2(PPh_3)_2$ and so the cycle continues.

Another important process in catalysis is the Fischer-Tropsch synthesis which initially involved heterogeneous catalysis leading to production of alkanes, alkenes, alcohols, aldehydes, carboxylic acids, esters and arenes from hydrogenation of carbon monoxide.[29] The thermodynamically favoured product is methane but partial reduction of CO by

H_2 to give alcohols has been shown to be feasible. The reduction of CO to give methanol

$$CO + 2H_2 \longrightarrow CH_3OH \qquad \Delta H = -92 \text{ kJ mol}^{-1}$$

over copper-promoted ZnO catalyst at ca. 250°C and 50 atmospheres is used commercially.

Recently a search for soluble liquid phase counterparts to classical Fischer-Tropsch catalysts has been made due to the fact that a high and often manipulable selectivity is the hallmark of a successful homogeneous catalyst.[30] Typical catalyst systems for alcohol production have involved ruthenium "melt" catalysis[31] where the ruthenium source, such as ruthenium(IV) oxide or ruthenium(III) acetylacetonate, is dispersed in molten quaternary phosphonium or ammonium salt with run conditions of 220°C, 430 atmospheres pressure and a 1:1 $CO:H_2$ ratio; ruthenium carbonyls in run conditions of 225-275°C, 1300 atmospheres pressure and a 2:3 $CO:H_2$ ratio;[30] and cobalt and rhodium carbonyls run at 200°C, 300 atmospheres pressure and a 1:1 $CO:H_2$ ratio.[32]

High selectivity is a reversal of the initial goal of the Fischer-Tropsch synthesis as the oil crisis in the seventies necessitated the development of economically profitable alternative sources of chemical raw materials. The efficiency of a catalyst was previously measured in terms of the "degree of liquefaction", resulting from the production of liquid fuels from synthetic gas, whereas nowadays the achievement of as narrow as possible a product distribution is of particular interest.[29]

Selectivity is therefore desirable and has been shown to be attainable with homogeneous catalysts.[29-32]

In view of these two important catalytic processes, the catalytic properties of the rhodium monomer $[Rh(PPh_3)_3(NCMe)][BF_4]$ versus hydrogenation of heptene and reduction of carbon monoxide were investigated. The author wishes to thank Dr. D. Waddan for his valued assistance and helpful discussions in the following catalytic studies.

Hydrogenation of hept-1-ene using $[Rh(PPh_3)_3(NCMe)][BF_4]$

$[Rh(PPh_3)_3(NCMe)][BF_4]$ (0.01 g, 9.8×10^{-3} mmol) was dissolved in methanol (1 cm^3). Hept-1-ene (1 cm^3) was added and the flask was degassed and filled with dihydrogen to atmospheric pressure. This mixture was stirred at room temperature for 1 week. On subsequent gas chromatography analysis of the stirred solution the amount of heptane present was in an approximate 1:1 stoichiometric ratio with the rhodium monomer. This observation contrasts with the results of a corresponding experiment using $[Rh(PPh_3)_3Cl]$, where an approximate 90% + hydrogenation of hept-1-ene to heptane was observed via gas chromatography. A rapid hydrogenation of hept-1-ene, along with a wide variety of other olefins, has been observed in the literature.[8,20]

Since $[Rh(PPh_3)_3(NCMe)][BF_4]$ does not appear to be an active catalyst for the mild hydrogenation of olefins, it was considered important to investigate the catalytic activity of this compound with dihydrogen under pressure. $[Rh(PPh_3)_3(NCMe)][BF_4]$ (0.05 g, 4.9×10^{-2} mmol) was dissolved in methanol (2 cm^3). Hept-1-ene (1 cm^3) was added and this solution was shaken for 2 days under dihydrogen at 6.8 atmospheres. Again subsequent gas chromatographic analysis of the solution provided no indication that hept-1-ene had been hydrogenated to heptane to any significant extent.

Despite this lack of encouragement, the reactivity of $[Rh(PPh_3)_3(NCMe)][BF_4]$ with dihydrogen under pressure was investigated in case a stable

hydride was being formed which in some way blocked catalysis.

$[Rh(PPh_3)_3(NCMe)][BF_4]$ (0.01 g, 9.8×10^{-3} mmol) was dissolved in acetonitrile (1 cm^3) and this solution was stirred under 6.8 atmospheres of dihydrogen for 2 days. No change in the UV/visible spectrum was observed after this time. The yellow solution was then taken and its 60 MHz ^1H n.m.r. spectrum recorded, scanning closely the region 0 to -30 p.p.m. to identify any hydride resonances. The spectrum showed peaks due to $[Rh(PPh_3)_3(NCMe)][BF_4]$ and to solvent but no hydride resonances were present. This is in direct contrast to $[Rh(PPh_3)_3Cl]$ where, in solvents as chloroform and benzene, three broad lines at ca. -17, -11 and -8 p.p.m. and in pyridine and acetonitrile, two broad lines at -18 and -17 p.p.m. are observed, indicating the presence of rhodium dihydrides.[8]

Therefore, not only does $[Rh(PPh_3)_3(NCMe)][BF_4]$ show no catalytic activity for the hydrogenation of hept-1-ene but also no indication of the formation of a stable hydride was obtained. It has been shown that $[Rh(PPh_3)_3Cl]$ is a very efficient catalyst for hept-1-ene hydrogenation at ambient temperature and pressures of 1 atmosphere or below.[8] Our experiment here also shows that $[Rh(PPh_3)_3Cl]$ will catalyse almost a total conversion of hept-1-ene to heptane, yet under the same conditions $[Rh(PPh_3)_3(NCMe)][BF_4]$ shows almost no noticeable amount of heptane production even at higher pressures. $[Rh(PPh_3)_3Cl]$ will also form stable hydrides on reaction with dihydrogen at ambient temperature and pressures of 1 atmosphere, that can be detected by ^1H n.m.r. spectroscopy.[8] $[Rh(PPh_3)_3(NCMe)][BF_4]$ shows no such hydride formation even when stirred under 6.8 atmospheres of dihydrogen. This lack of reaction with dihydrogen may be advantageous for alternative homogeneous catalyses. $[Rh(PPh_3)_3(NCMe)][BF_4]$ could be capable of catalysing the reduction of

CO by H_2, for example, co-ordinating and activating the former molecule for attack by the latter molecule.

$[Rh(PPh_3)_3(NCMe)][BF_4]$ (0.02 g, 1.96 x 10^{-2} mmol) was dissolved in acetonitrile (3 cm^3) and this solution was stirred under an atmosphere of 2.72 atmospheres CO and 2.72 atmospheres H_2 at 80°C for ca. 2 hours. This solution was then stirred at room temperature for ca. 24 hours prior to analysis by gas chromatography. No decomposition of the monomer to metallic rhodium was indicated, despite heating to 80°C. Methanol was observed by gas chromatography, in an amount determined to be approximately 0.025 g. This provides some evidence that the reduction of CO to methanol could be being catalysed by $[Rh(PPh_3)_3(NCMe)][BF_4]$. The small quantity of methanol produced possibly results from the fact that very low pressures of CO and H_2 were employed compared to those recorded in the literature.[30-32] However, these were the highest able to be obtained with the system in use. The temperature of the reaction was also somewhat low. In the near future a much more efficient system is to be obtained which will allow higher pressures and temperatures. It will be connected directly to a gas chromatographic/mass spectroscopic instrument to analyse all the products in the reaction, whether in the gas or liquid phase. Further work concerning the effect of this rhodium monomer on the CO/H_2 reaction will then be continued.

5.7 Conclusions

The initial synthesis of $[Rh(PPh_3)_3(NCMe)][BF_4]$ involves the cleavage of the Rh-Rh single bond of $[Rh_2(O_2CMe)_2(NCMe)_6][BF_4]_2$ and the reduction of Rh^{II} to Rh^{I} upon reaction with PPh_3. It is likely that the corresponding oxidation involves phosphine to phosphine oxide, the oxygen being supplied by traces of water, and use of excess phosphine does not dramatically improve the yield of $[Rh(PPh_3)_3(NCMe)][BF_4]$. This reaction

resembles the synthesis of a material of composition $Rh(PPh_3)_3BF_4$,[4] which was isolated as a product of the protonation of $[Rh_2(O_2CMe)_4]$ by $H[BF_4]$, followed by reaction with PPh_3. The conductivity of solutions of this material in $MeNO_2$ solution was significantly less than expected for a 1:1 electrolyte and, therefore, co-ordination of the tetrafluoroborate anion to the metal was postulated. This contrasts with $[Rh(PPh_3)_3(NCMe)][BF_4]$ which behaves as a 1:1 electrolyte. An important difference in the two syntheses is that the route reported here commences with MeCN co-ordinated to the rhodium of the dimeric starting material and this clearly clings tenaciously through the subsequent reaction and the recrystallisation from methanol. The more rational synthesis of $[Rh(PPh_3)_3(NCMe)][BF_4]$ involves the removal of the chloro ligand from $[Rh(PPh_3)_3Cl]$ by $[Me_3O][BF_4]$ and replacement by an MeCN solvent molecule. A similar reaction has been observed between $[Rh(PPh_4)_3Cl]$ and $Tl[ClO_4]$.[33] Initially the solvated complex is produced

$$[Rh(PPh_3)_3Cl] \xrightarrow[Tl[ClO_4]]{Me_2CO} [Rh(PPh_3)_3(Me_2CO)][ClO_4].$$

However on recrystallisation from CH_2Cl_2, the T-shaped cation $[Rh(PPh_3)_3]^+$ is obtained as its $[ClO_4]^-$ salt. Thus, it is clear that MeCN is more strongly bound to rhodium than Me_2CO, a fact which has been noted by Schrock and Osborn in respect of the cationic rhodium dihydrides $[RhH_2(PPh_3)_2S_2]^+$ (S = acetone, ethanol, or acetonitrile).[26]

Although phosphine exchange is possible for $[Rh(PPh_3)_3(NCMe)]^+$, unlike $[Rh(PPh_3)_3Cl]$ this does not result in the complex being a good catalyst for the homogeneous hydrogenation of olefins. Some encouragement has been obtained, however, in respect of $[Rh(PPh_3)_3(NCMe)]^+$ acting as a catalyst for the conversion of CO to CH_3OH.

REFERENCES

1. M.A. Bennett and P.A. Longstaff, Chem.Ind.(London), 1965, 846.

2. F.H. Jardine, J.A. Osborn, G. Wilkinson, and J.F. Young, Chem.Ind.(London), 1965, 560.

3. M.J. Bennett and P.B. Donaldson, Inorg.Chem., 1977, 16, 655.

4. P. Legzdins, R.W. Mitchell, G.L. Rempel, J.D. Ruddick, and G. Wilkinson, J.Chem.Soc.(A), 1970, 3322.

5. J.A. Osborn and G. Wilkinson, Inorg.Synth., 1967, 10, 67.

6. W. Clegg, Acta Crystallogr., Sect.A, 1981, 37, 22.

7. International Tables for X-Ray Crystallography, Vol.IV, Kynoch Press, 1974, pp.99, 149.

8. J.A. Osborn, F.H. Jardine, J.F. Young, and G. Wilkinson, J.Chem.Soc.(A), 1966, 1711.

9. M.J. Bennett, P.B. Donaldson, P.B. Hitchcock, and R. Mason, Inorg.Chim.Acta, 1975, 12, L9.

10. Infrared and Raman Spectra of Inorganic and Co-ordination Compounds, 3rd Edition, 1977, Wiley-Interscience, K. Nakamoto.

11. M.A. Bennett, R.J.H. Clark, and D.L. Milner, Inorg.Chem., 1967, 6, 1647.

12. Spectroscopic methods in organic chemistry, 3rd Edition, 1980, McGraw-Hill, D.H. Williams and I. Fleming.

13. L.F. Johnson and W.C. Janowski, C-13 N.m.r. Spectra, Wiley and Sons, 1972.

14. J.W. Emsley, J. Feeney, and L.H. Sutcliffe, High Resolution N.m.r. Spectroscopy, Vol.2, Pergamon Press, 1966.

15. P.L. Corio, Structure of High-Resolution N.m.r. Spectra, Academic Press, 1966, N.Y. London.

16. D.R. Eaton and S.R. Suart, J.Am.Chem.Soc., 1968, 90, 4170.

17. T.H. Brown and P.J. Green, J.Am.Chem.Soc., 1970, 92, 2359.

18. R.W. Mitchell, J.D. Ruddick, and G. Wilkinson, J.Chem.Soc.(A), 1971, 3224.

19. D.F. Shriver, D.D. Lehman, and I. Wharf, J.Chem.Soc., Chem.Comm. 1970, 1486.

20. F.H. Jardine, Prog.Inorg.Chem., 1981, 28, 63.

21. C.A. Tolman, P.Z. Meakin, D.L. Lindner, and J.P. Jesson, J.Am.Chem.Soc., 1974, 96, 2762.

22. M.A. Bennett and T.W. Turney, Aust.J.Chem., 1973, 26, 2321.

23. M.A. Bennett and T.W. Turney, Aust.J.Chem., 1973, 26, 2335.

24. D.A. Clement and J.F. Nixon, J.Chem.Soc., Dalton Trans., 1973, 195.

25. K.F. Purcell and J.C. Kotz, Inorganic Chemistry, Holt-Saunders, International Edition, 1977, p.702-706.

26. R.R. Schrock and J.A. Osborn, J.Am.Chem.Soc., 1976, 98, 2134.

27. J.F. Young, J.A. Osborn, F.H. Jardine, and G. Wilkinson, J.Chem.Soc., Chem.Comm., 1965, 131.

28. F.H. Jardine, J.A. Osborn, and G. Wilkinson, J.Chem.Soc.(A), 1967, 1574.

29. W.A. Herrmann, Angew.Chemie, 1982, 21, 117.

30. J.S. Bradley, J.Am.Chem.Soc., 1979, 101, 7419.

31. J.F. Knifton, J.Am.Chem.Soc., 1981, 103, 3959.

32. J.W. Rathke and H.M. Feder, J.Am.Chem.Soc., 1978, 100, 3623.

33. Y.W. Yared, S.L. Miles, R. Bau, and C.A. Reed, J.Am.Chem.Soc., 1977, 99, 7076.

APPENDIX A

All reactions were carried out under an atmosphere of dinitrogen and using standard Schlenk techniques. The dinitrogen used was BOC, white spot grade and was not purified further. All solvents were dried and freshly distilled under a dinitrogen atmosphere.

Microanalyses were carried out by Mr. M. Hart and his staff in the Microanalytical Department of this University.

UV/visible spectra were recorded on either a Shimadzu UV-260 or a Perkin-Elmer 402 spectrometer.

Infrared spectra were recorded either on a Perkin-Elmer 577 grating spectrometer (4,000-200 cm^{-1}) or a Pye-Unicam SP3-200 spectrometer.

Proton n.m.r. spectra were recorded at 60 MHz on a Perkin-Elmer R-12B spectrometer, at 300 MHz on a Varian SC-300 spectrometer and at 300 MHz on a Varian XL-300 spectrometer.

^{13}C n.m.r. spectra were recorded at 20 MHz and 75 MHz using Bruker WP-80 and Varian XL-300 instruments respectively.

^{31}P n.m.r. spectra were recorded at 32.4 Hz on a Bruker WP-80 spectrometer.

APPENDIX A

All reactions were carried out under an atmosphere of dinitrogen and using standard Schlenk techniques. The dinitrogen used was BOC, white spot grade and was not purified further. All solvents were dried and freshly distilled under a dinitrogen atmosphere.

Microanalyses were carried out by Mr. M. Hart and his staff in the Microanalytical Department of this University.

UV/visible spectra were recorded on either a Shimadzu UV-260 or a Perkin-Elmer 402 spectrometer.

Infrared spectra were recorded either on a Perkin-Elmer 577 grating spectrometer (4,000-200 cm^{-1}) or a Pye-Unicam SP3-200 spectrometer.

Proton n.m.r. spectra were recorded at 60 MHz on a Perkin-Elmer R-12B spectrometer, at 300 MHz on a Varian SC-300 spectrometer and at 300 MHz on a Varian XL-300 spectrometer.

^{13}C n.m.r. spectra were recorded at 20 MHz and 75 MHz using Bruker WP-80 and Varian XL-300 instruments respectively.

^{31}P n.m.r. spectra were recorded at 32.4 Hz on a Bruker WP-80 spectrometer.

APPENDIX B

Suppliers of Chemicals

The chemicals used in the syntheses described in this thesis were purchased from a variety of suppliers.

dppe	Ventron
dppm	Ventron
$Fe(CO)_5$	Aldrich
FLORISIL 60-100 mesh	BDH
Hmhp	Aldrich
$KB[CHMeC_2H_5]_3H$	Aldrich
$LiPPh_2$	Alfa Products
Me_3OBF_4	Lancaster
$NaNO_2$	Aldrich
picoline-N-oxide	Aldrich
$P(OMe)_3$	Aldrich
PPh_3	Aldrich
NaS_2CNEt_2	BDH

APPENDIX C

Abbreviations

acac	=	acetylacetonate
Ar	=	aryl
arphos	=	1-diphenylphosphino-2-diphenylarsinoethane
biph	=	2-phenylphenyl
bipy	=	2,2'-bipyridyl
2-BPC	=	2-biphenylcarboxylate
bpnp	=	2,7-bis(2-pyridyl)-1,8-naphthyridine
Bu^i	=	iso butyl
Bu^n	=	neo butyl
Bu^t	=	tert butyl
CD	=	Circular Dichroism
dinp	=	5,6-dihydrodipyrido[2,3-b:3',2'-j]-[1,10]phenanthroline
diphos	=	bis(diphenylphosphino)ethane
dmg	=	dimethylglyoximate
dmpe	=	bis(dimethylphosphino)ethane
DMSO	=	dimethylsulphoxide
DNA	=	deoxyribonucleic acid
dppe	=	bis(diphenylphosphino)ethane
dppm	=	bis(diphenylphosphino)methane
en	=	ethylenediamine
Et	=	ethyl
e.p.r.	=	electron paramagnetic resonance
EXAFS	=	extended X-ray absorption fine structure
fhp	=	2-fluoro-6-hydroxypyridine
Hchp	=	2-hydroxy-6-chloropyridine

Hdmhp	=	2,4-dimethyl-6-hydroxypyrimidine
HF	=	Hartree-Fock
HFS	=	Hartree-Fock-Slater
Hmap	=	2-amino-6-methylpyridine
Hmhp	=	2-hydroxy-6-methylpyridine
HOMO	=	Highest Occupied Molecular Orbital
LCAO	=	Linear Combination of Atomic Orbitals
LUMO	=	Lowest Unoccupied Molecular Orbital
Me	=	methyl
MO	=	Molecular Orbital
NHE	=	Normal Hydrogen Electrode
n.m.r.	=	nuclear magnetic resonance
np	=	1,8-naphthyridine
ORD	=	Optical Rotatory Dispersion
Ph	=	phenyl
phen	=	1,10-phenanthroline
p.p.m.	=	parts per million
Pr	=	propyl
Pr^i	=	iso-propyl
Pr^n	=	neo-propyl
py	=	pyridine
pynp	=	2-(2-pyridyl)-1,8-naphthyridine
RHF	=	Restricted Hartree-Fock
RNA	=	Ribonucleic acid
R-pn	=	(R)-1,2-diaminopropane
SCE	=	Standard Calomel Electrode

SCF-HF	=	Self Consistent Field-Hartree-Fock
SCF-Xα-SW	=	Self Consistent Field-Xα-Scattered Wave
sh	=	shoulder
TFMS	=	trifluoromethanesulphonate
THF	=	tetrahydrofuran
TMS	=	tetramethylsilane
UHF	=	Unrestricted Hartree-Fock